UNIVERSITY OF SOUTHAMPTON

Faculty of Environmental and Life Sciences
School of Ocean and Earth Science

# Variation in the field metabolic rate of wild living plaice (*Pleuronectes platessa*) from the North Sea: constraining influences of body size, temperature, seasonal cycle, individual level growth rate and year of sampling

*By*
**Joseph William Jones**
MSci

*A thesis for the degree of Doctor of Philosophy*

For Examination

# Acknowledgments

I firstly want to thank Dr Clive Trueman, my primary supervisor, for your unwavering enthusiasm and ability to see the positive in any and every situation. During times when I have been frustrated with analysis or unsure what direction to pursue, Clive's collaborative manner has been amazing to work with, and has made undertaking a PhD project exciting at every turn. I honestly can't thank you enough for this opportunity, it has been so much more fun than I ever imagined.

CEFAS partially funded this project and provided samples. I want to thank Dr Ewan Hunter for his guidance throughout the project. Ewan's Plaice knowledge has been brilliant, and allowed us to develop the project in multiple directions.

Thank you to Dan Doran, the rock man! This PhD would have not been possible without you, you're an amazing teacher and really going to miss not being able to just run downstairs to say hello!

Megan and Bastian have been so much help, trusting me to run samples independently, and during the last 6 months when I broke the Keil pretty much every time.. we always laughed about it. I'm sorry if I was a pain, but hopefully now I'm gone it might work properly…… but somehow I doubt it.

My sister, Dr Helen Jones, has been an inspirational figure in my life. We were never very good at school (being very dyslexic), I couldn't spell my name till I was 9 (called myself Jow), but whenever a teacher told Helen to lower her academic aspirations she wouldn't listen. Without Helen to look up to in this manner I would never have believed I could do a PhD, and I promise I didn't apply just because you already had one!

Dr Bede Davies has been a massive pain throughout this project, and for that I thank him. Your unique brand of character and annoying habit of usually being right has helped me so much. Bede is an excellent statistician and whenever I have had any questions he has always been there, providing information which I usually don't understand.

My parents Graham and Claire Jones, have always had the ability to provide a good distraction, after 29 years I'm still not sure if this is intentional, but it's very helpful nether the less. Your extensive side projects have been a lot of fun, and provided a contrast to the PhD, which has made it so much easier.

Thank all the PhD friends I've made, your all amazing and I count myself lucky to have met you. Millie, your sense of adventure and enthusiasm for life is amazing, I know we are gonna have so much fun in the future and I cant wait to see what we get up to next, so happy I met you! Elisa, you were the first friend I made here and I dono what id do without you, thank you so much! Andrea, you're the cleverest person I know, your gonna do great things and I cant think of anyone more deserved. Thomas, you're a terrible belay. Sandy, stop wasting money on art. Pablo, I don't think your ever gonna age. Lewis, London aint that great. Spencer, stop stealing my clothes. Maartine, Stayce, Nathan, Jack, Mark, Africa, Ben, Will, Harry; your all the best!

Last I want to thank Sarah Alewijnse, you might be the strongest person I know. Having you in the office and doing very similar topics has been so much fun, you've helped me so much more than I've helped you cant thank you enough!

University of Southampton

Abstract

Faculty of Environmental and Life Sciences School of Ocean and Earth Science

Doctor of Philosophy

**Variation in the field metabolic rate of wild living plaice (*Pleuronectes platessa*) from the North Sea: constraining influences of body size, temperature, seasonal cycle, individual level growth rate and year of sampling**

by Joseph William Jones

Field metabolic rate (the combined energetic cost of performance when exposed to natural conditions) represents how an individual with a particular expressed genotypical and phenotypic respiratory potential reacts to the experienced environment. Population-scale measurements of field metabolic rate (FMR) can potentially identify the sensitivity of populations to environmental drivers such as temperature, and the capacity for climatic resilience through behavioural adaptation. To date, from a fisheries perspective, FMR is largely inferred or assumed from the relationship between environmental conditions and distribution, coupled with laboratory based respiratory potential experiments. Such studies have broad and untested assumptions, and as a result the accuracy of their findings has been questioned.

In this thesis I apply a newly emerging proxy for estimating field metabolic rate in marine fishes, drawing on stable isotope values from otolith aragonite. Stable carbon isotope compositions are used to estimate the proportion of respiratory $CO_2$ within the blood (and, therefore, the rate of oxidation of dietary carbon), while stable oxygen isotope values are used to infer experienced temperature. I apply the otolith metabolic rate proxy to otoliths recovered from a population of European plaice from the North Sea sampled during a period of rapid warming between the 1980s to the mid 2000s. I estimate time averaged FMR, experienced temperature and growth rate in 558 fish during various life stages and test three main hypotheses: 1) FMR covaries with environmental drivers influencing standard metabolic rate (body size and temperature), in a comparable manner to established metabolic theories of ecology: 2) variations in FMR over a seasonal cycle covary with seasonal bioenergetics rather than extrinsic thermal variability: and 3) individual level growth rate varies predictably with FMR.

Within the sampled data set, FMR did not covary systematically with body size and temperature for adult populations. Temperature was shown to positively covary with FMR during juvenile life stages of the same individuals, suggesting that the energetic drivers forming FMR expression are not consistent throughout individual life history. Individual variation in FMR was conserved between juvenile and adult samples, and metabolic phenotype explained a greater proportion of among-individual variation in adult FMR than either body size or temperature. Seasonal variations in among-individual FMR appear to correlated to the

migratory, feeding and breeding cycles of plaice, suggesting that FMR expression is a complex relationship between a combination of behavioural and physiological drivers. The inclusion of intrinsic factors, such as condition, explain a greater proportion of growth rate deviance within this data when compared to extrinsic factors. These findings imply that FMR trends are more complex than previously believed, and highlights the importance of incorporating individual behavioural patterns into predictive biogeographical and population output models.

Stable isotope-derived estimates of field metabolic rate have great potential to expand our understanding of ecophysiology in general and especially mechanisms underpinning the relationships between animal performance and changing environmental and ecological conditions.

# 1 Introduction

## 1.1 Climate change effects on fisheries

Commercial and recreational fisheries are a key source of food and economic stability for populations on global and regional scales, and changes in fisheries production and distribution related to climate change have large implications for local and regional economies (Brugère and Young 2015). According to the United Nations intergovernmental panel on climate change (IPCC) fifth assessment report, a third of Africa's total animal protein intake comes from fisheries (Pachauri and Reisinger 2008) with a 21% potential decline by 2050 resulting in a US$331 million economic loss (Stocker et al., 2013). Due to Asia's high fisheries output, producing more than half of the global marine catch in 2008 (Pachauri and Reisinger 2008), the predicted northly shift of fish populations has severe implications for local rural communities (Stocker et al., 2014), potentially causing wealth and population redistribution. The combination of over fishing and climate change is predicted to have dramatic economic consequences for Australasia due to the ecosystem service they provide (Field and Barros 2014) and the southerly shift of shell fish farming grounds. Similar ecological and social patterns are expressed throughout all continents (Field and Barros 2014), however it is suggested that areas of high poverty and unequal wealth distribution are at greater risk (Stocker et al., 2014). As fisheries are such a crucial resource on a global scale it is important we improve our understanding of how climate change and fishing pressure are likely to impact fish populations.

The overarching aim of this PhD project has been to explore a newly emerging isotopic proxy for estimating individual level field metabolic rate and experienced temperature. The context for this work is the belief that bioenergetics are key to developing mechanistic predictions of fish responses to climate change. Developing an *in-situ* measure of energetic demand of individual fish, and associated relationships with both intrinsic and extrinsic potential co-variates, could improve fishery predictions in response to modelled future climate scenarios. Below I outline the findings from recent observational studies looking into how current fish populations are believed to be responding to current and past environmental gradients, examples of when anthropogenic exploitation has pushed fisheries to its critical limits, current methods used to predict future population distributions and how laboratory based metabolic rate measurements have been used to identify the critical thermal limits of physiological

performance. I then attempt to identify how field metabolic rate studies can be used to test metabolic theories of ecology and aid with fisheries biogeographical and population output models.

## 1.2 Fisheries, overfishing and sustainability

Fisheries ecosystem functionality and fluctuations in abundance have historically been unpredictable, with multiple examples where over fishing has reduced stock sizes to critical limits (Myers et al., 1997), in such cases even if biomass recovers this may be a long and delicate process with economic and anthropogenic consequences (Myers and Worm 2005). Here we use a specific case study, where a population of Atlantic cod (*Gadus morhua*) was over exploited, with documented resulting impacts on ecosystem functionality and fishery recovery. We also point out that the process of fisheries recovery is more complex during a period of pronounced climatic change, as it is difficult to statistically separate effects of climate and fishing on population trends, due to the similar impact the two sources of variability have on ecosystem functionality.

When an overexploited east cost of America cod population, which crashed in 1954, was analysed in terms of allele frequency there was little increase in genetic diversity until 1970, and full recovery was not achieved until 1998 (Hutchinson et al., 2003). Furthermore, there was a significant degree of genetic divergence, as the population in 1998 is genetically distinct from the earlier community. During the 1940s it was a thriving fishery, supporting a large anthropogenic community and representing a significant input to the American economy (Hutchinson et al., 2003). In 1954 the catch per unit effort fell significantly indicating a reduction of population abundance and stock spawning biomass, however the human response was to increase fishing effort with more sophisticated exploitation techniques, larger vessels and a more expansive geographical range (Hutchinson et al., 2003). This unsustainable exploitation rate lead to a collapse of the fish stock, with the anthropogenic economic consequences leading to a geographical wealth redistribution with many people out of work and needing to change their way of living. The fishing stock took multiple generations to recover, with evidence phenotypical differences and some physiologists arguing that the fishing stock is far more vulnerable to environmental change post the anthropogenic disturbance (Hutchinson et al., 2003). Reduced population size also has been shown to impact genetic diversity (Jørgensen et al., 2007; Natugonza et al., 2022). Long term biomass recovery has been shown to vary between fish groups (Fogarty et al.,

1991). For gadids (cod, haddock) and non-cupids (flat fish) there is little if any recovery as much as 15 years after a 45-99% reduction in reproductive biomass (Hutchings 2000). This is not the case for all fish populations, for example herring reach maturity at a young age and express high fecundity rates (Hutchings 2000), therefore fishing can cause varied community restructuring across different species. Fishing is also likely to have a selective impact on phenotype variability. There are also many secondary ecological consequences of the removal of a high trophic level predator, such as food web restructuring and trophic cascade (Daskalov et al., 2007), indicating that the collapse of a fish stock can have more severe consequences than simply the reduced population size of a single species. This ecological restructuring potentially explains why some Atlantic cod stocks have collapsed without recovery (Myers et al., 1996; Myers et al., 1997;), due to increased predation pressure (Frank et al., 2005), such as jellyfish density which may impair cod biomass recovery (Lynam et al., 2006) as individuals experience increased predation pressure as larvae and competition as juveniles. Jackson et al., 2001 shows that once a population is over exploited recovery is difficult even if there is a breeding population (Jackson et al., 2001). Again, due to similar fish species of a comparable trophic level filling the missing niches and performing similar ecological roles. This indicates that we do not know the full impact of over fishing on population dynamics and ecology. Fishing is also likely to have a selective impact on phenotype variability. Differences in individual swimming behavior have been shown to impact the likelihood of an individual being caught via trawling techniques (Winger 2004), and it is possible that this will narrow individual variability of the population; as it is thought that swimming speed is linked to physiology, with higher metabolic rates relating to increased swimming speed capacity (Killen et al., 2007). It is suggested that differences in swimming speed can be explained by variations in metabolic rate (Plaut 2001), with higher metabolic rates resulting in higher swimming speeds. Therefore, it is possible that fishing has a selective impact on metabolism. There is also evidence that bottom trawling adapts the benthic ecosystem, further reducing the recovery capacity of a ground fish population (Thurstan et al., 2010). It is argued that bottom trawling reduces the prey biomass, as well as the amount of shelter for fished species. An important message from the experiences described above is that genetic and phenotypic diversity within an exploited population may influence the potential for that stock to rebound following over-exploitation or its resilience to climate change.

## 1.3 Climate change

Climate change effects on fisheries are well documented (Burrows et al., 2011; Poloczanska et al., 2013; Bates et al., 2014). Adaptive behavior, including migration and deepening of populations to colder more natural water conditions is already apparent (Murawski 1993). From 1980 to 2004 the whole demersal fish assembly of the North Sea is reported to have deepened by 3.6m a decade, a pattern expressed across most assemblages (Dulvy et al., 2008). There is a reported northerly re distribution of mean latitude abundance for widespread thermal specialists, coupled with a southerly shift of species with a small body size and high abundance (Perry et al., 2005) and evidence of species expressing distributional changes having faster life cycles and smaller body sizes than non-shifting species (Perry et al., 2005). From a genetic perspective it is difficult to suggest how climate change is impacting populations, as most studies which report a genetic change do not have enough evidence to link their findings to climatic variation (Merilä and Hendry 2014); there are too many unknown factors, such as plastic change. Some studies have successfully identified shifts in phenotypes and genetic basis (Cruz-Neto and Bozinovic 2004; Chown and Gaston 1999; Nussey et al., 2007; Gienapp et al., 2008), but under laboratory conditions and usually looking into allele frequencies. This information is useful from a modelling perspective but does not provide data about how climate change is impacting whole populations, suggesting that we still require more information to predict how populations will be impacted. Recent studies investigating community assembly theories and related assembly rules (Weiher et al., 2011) have focused on interspecific differences between co-occurring species to predict community shifts; however, the importance of intraspecific variance within a population is ignored. The same can be said for community phylogenetics, where assemblages are studied from a phylogenetic view point (Cavender-Bares et al., 2009), again ignoring individual variance. The flaws of these studies have been pointed out by Violle (2012), where its stated that several studies report low intraspecific variation for both individual organism traits (Buckley et al., 2010) and at a population level. With contradictory studies reporting high trait variation for all individuals within a community (Messier et al., 2010) and for populations along environmental gradients (Albert et al., 2010). This contradiction implies that measuring the mean of a population potentially does not provide enough information to assess population dynamics, as it does not account for how variance is important for ecosystem functionally or stability.

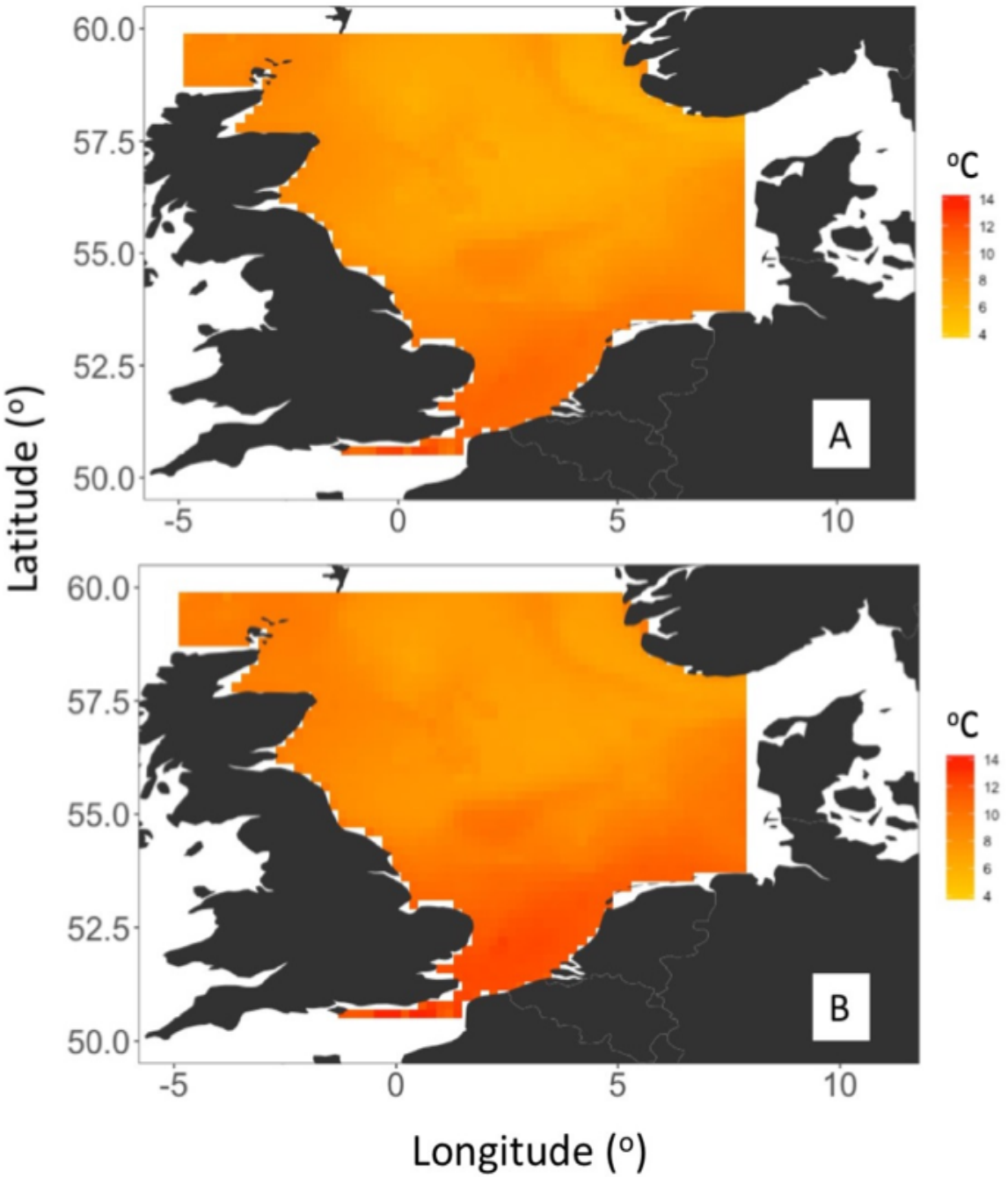


***Figure 1**: AHOI model benthic North Sea temperature estimates outputs for 1980-1990 (A) and 1990-2002 (B) (Núñez-Riboni and Akimova 2015). This is displaying the bottom 5 meters, as that is the smallest resolution available from the model and represents the likely habitat the individuals used within this study experienced.*

As well as anthropogenic exploitation, fishing communities are thought to be significantly impacted by a recent rise in winter and summer sea temperatures (Kushnir 1994), which is a consistent trend across oceanic gradients. Figure **1** shows extracted benthic layer and of North Sea temperature

distribution from 1980 to 2002, highlighting the average increase in benthic temperatures over southern and northerly regions during 1990-2002 when compared to 1980-1990 (Núñez-Riboni and Akimova 2015). Furthermore, future model scenarios suggest further shifts in climatic conditions, such as salinity, habitat distribution, oxygen availability and many more (Baudron et al., 2014; Hiddink et al., 2015; Schrum et al., 2016;). Changes in habitat density and distribution, such as coral and sea grass removal, which both act as key nursing grounds for marine communities, is predicted to have a dramatic impact on ecosystem functionality (Tagliapietra and Sigovini 2010; Wood et al., 2012; Rengstorf et al., 2013; Reiss et al., 2015). This abnormally rapid evolution of environmental conditions brings into question the adaptive capacity of natural marine communities (Bernhardt and Leslie 2013), especially as the majority of marine populations are ectothermic and therefore their physiological needs are directly related to the environmental variables they are exposed to (Johnston and Dunn 1987; Treberg et al., 2016).

## 1.4 Measures of population performance

From observational studies, suggesting that fishing does not only reduce population size but has severe ecological, trophic, genetic, phenotypic and environmental consequences, (Last et al., 2011) potentially the inclusion of more detailed ecological parameters, such as phenotypic variability, will provide a greater understanding of the full impact of fishing and improve the capacity of fisheries management strategies. Historical fishery-induced population crashes have stimulated development of many methods for assessing the health of a fish community. As of yet the only measures of population health commonly used in management are means and averages calculated from models and catch data (Ono et al., 2015), which provide useful information regarding population size and reproductivity. These data are used to produce quotas for what biomass of fish is safe to catch (Sanchirico et al., 2006), however using this information it is difficult to predict how populations will react to climate change and the full effect that fishing has on ecosystem functionality. If we could measure population health and diversity it would significantly improve our ability to sustainable fish a population.

### 1.4.1 Growth

Spawning stock biomass (SSB) is the total estimated weight of all sexually mature fish in a stock (McAngus et al., 2018). Since 1999 ICES advice has identified what catch options will keep SSB within a precautionary criteria, aiming to keep SSB at a sustainable limit above a minimum precautionary level (Bpa) (Roach et al., 2018). Bpa is set high enough to allow for a margin of error, keeping SSB above the lower limit level (Blim), which is the minimum SSB said to maintain a sustainable harvest (figure **2**). This data provides little information about the flexibility and diversity of the community, and does not tell us how close individuals are to their limits of survival. SSB is closely linked to growth rate, as a population expressing high individual and population growth rates is more likely to recover the proportion of the stock capable of spawning at a faster rate (Armstrong and Witthames 2012). Population growth rate (both total and unique size class abundance) is also a common factor used to assess the health of a fishery, as a reduction in growth potentially indicates less favourable conditions, that the stock is more vulnerable to environmental instability and also reduces the commercial value as the level of sustainable exploitation is lowered (Cury et al., 2014). Individual growth rates are less commonly used as a physiological measurement of performance, as it describes the rate of growth of an individual in response to both intrinsic and extrinsic factors (Van Winkle et al., 1993). The level of uncertainty around individual growth is greater as it is difficult to link unique environmental conditions to growth rate trends. Factors like individual phenotypic variation, which currently are not accounted for, can potentially provide information about population stability (Loreau et al., 2001). Furthermore, fishing legislation does not account for the combined impact of fishing and climate change (Brander 2010). ICES state that fisheries advice is constantly evolving, suggesting that potentially their measure of maximum sustainable yield may not be correct, and ecosystem limitations on fisheries have typically not yet been identified in management policies (McAngus et al., 2018). There are EU plans to implement a new set of management measures, the Marine Strategy Framework Directive (MSFD), which recognises limits such as biodiversity, sea floor integrity and food webs (McAngus et al., 2018); which, as previously discussed, are all variables fishing activity impacts. The MSFD does not however account for changing climatic conditions or phenotypic diversity, which has been argued to be one of the most important ecological indicators for population stability (Long 2011).

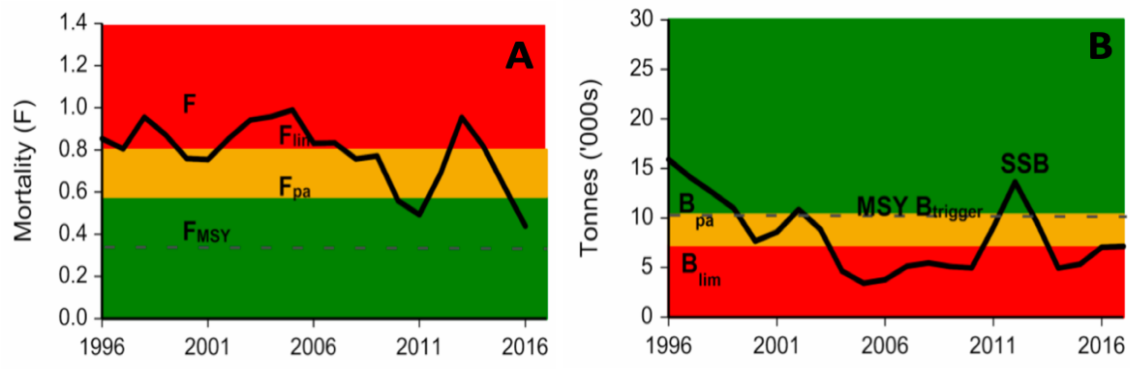


***Figure 2**: Graphical representation the fluctuation in both fishing mortality (A) and stock spawning biomass (B) from 1969 to 2016. Fishing mortality and stock spawning biomass are described in the text and are estimated measures of population stability used to form fishing quotas (McAngus et al., 2018). Figure adapted from the Marine Management Organisations' UK sea fisheries annual statistics report 2018, for Atlantic cod*

### 1.4.2 Physiology

Other forms of measurable population performance draw on aspects of individual physiological fitness, such as condition, (e.g. mass per unit length), metabolism, individual somatic growth rate, parasite load and forms of anthropogenic pollution load (Tonn et al., 1990; Perry et al., 2005; Killen et al., 2007; Nicholson et al., 2008; Rijnsdorp et al., 2009; Crozier and Hutchings 2014; Komoroske et al., 2014; Lõhmus and Björklund 2015). Population condition has been proven to vary in response to simulated environmental stressors under laboratory conditions, with lower condition factors commonly expressed at higher temperatures under fixed feeding levels (Cui and Wootton 1988; Morita et al., 2010). In natural settings, however, condition has been proven to react to multiple forms of behavioral and environmental variable's (Rätz and Lloret 2003; Keyombe et al., 2015; Thorson 2015). Species with complex migratory and breeding cycles express predictable variation in condition throughout the annual cycle, increasing during feeding periods as energy reserves and gonad tissues are grown and reducing during spawning periods (when individuals expend gametes and draw on fat supplies to meet energetic demand) (Hunter et al., 2004; Darnaude et al., 2014).

The issue with using condition (or other indirect measures of energy use) to predict fitness is that multiple variables and behavioral influences make forming correlation to extrinsic environmental factors difficult. Direct measures of metabolic rate or energy expenditure have been extremely difficult to obtain (Chung et al., 2021), with only small archivable sample sizes and large associated uncertainty.

Therefore, metabolic rate measurements have previously been used in theoretical and laboratory settings (Brown et al., 2004; Deutsch et al., 2020), with no meaningful *in situ* observations. Isotopically derived metabolic rate, as it is averaged over a time period when an individual is within its natural environment accounts for behavior and environmental factors.

## 1.5 Individual variance

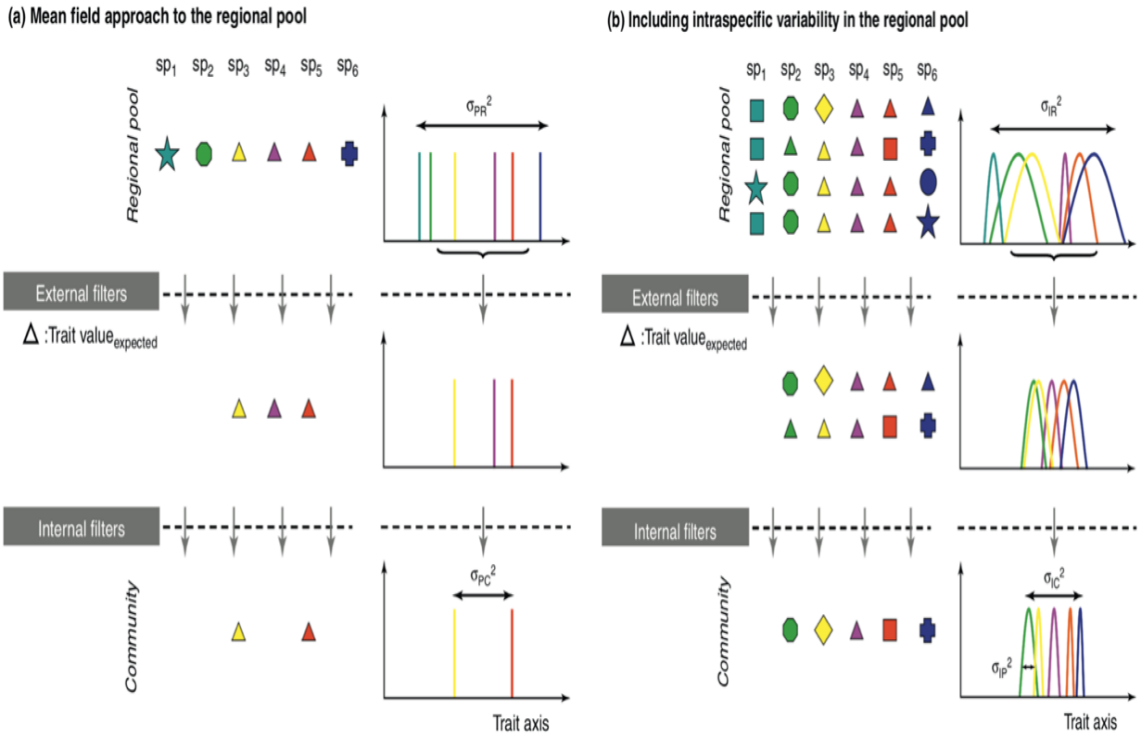


***Figure 3**: A comparison between the mean field approach (A), which estimates the health of a population using average expression, such as average distribution, stock spawning biomass and fishing mortality. Graph B represents the individual variance approach, which aims to assess the health of a population by measuring all the expressed phenotypes presented. Individual variance suggests that the greater number of phenotypes present in the population results in a more stable population. For example, there is more change a population can withstand to environmental instability with more phenotypes present. This graphical representation shows how means only capture part of the ecology and phenotypic reactions of a community. Suggesting that populations are more adaptable to biotic and abiotic factors than previously thought. Figure adapted from Violle et al., 2012*

The accuracy of process-based models used to predict the future of fisheries stocks has come into question, as they rely on averages and means (F and SSB, referred to as the "mean field approach") (Cheung et al., 2008). However there have been efforts made to increase the accuracy of these models, by including the recently renewed ecological theory of individual variance (Rutterford et al., 2015). As described by figure **3** individual variance theory aims to measure the total distribution of phenotypes expressed within a population, where measuring the mean only represent some individuals of the total population, and only individuals which express the most common phenotypes (Nussey et al., 2007). A population with a high number of individuals and low phenotypic diversity might be more susceptible to environmental change when compared to a smaller population with greater phenotypic diversity, as there are less phenotypes present which can withstand anomalous environmental events (Figure **3**). To fully understand community dynamics, all individual phenotypes of a community should be considered. Individual variance theories argue that only by representing all phenotypes can you understand how they interact to form inter and intraspecific relationships along geographical boundaries, environmental gradients and other ecological patterns (Violle et al., 2012). Individual variability, if accounted for, also can potentially improve our ability to model and predict how natural populations are likely to be impacted by climate change and fishing activity. Simply examining the averages of a population ignores natural flexibility and the adaptive capacity of a community (Violle et al., 2012). As a result, it is unlikely that the full nature of how a population will respond to abiotic and biotic factors can be captured using population trait averages. It has been argued that including individual variation captures, if not fully, natural population variability and therefore improves our understanding of ecosystem functionality (Ivandic et al., 2003).

Our capacity for including trait variation into models is improving, with promising results. Jung (2010) uses a null model approach to investigate the role of inter and intraspecific variation in habitat filtering and niche differentiation of plant communities along a flooding gradient (Jung et al., 2010). The model reveals a miss match of variability, with some individual traits accounting for as much as 44% of variance and some remaining unchanged over environmental gradients (Jung et al., 2010). Furthermore, intraspecific variation has a significant impact on both habitat filtering and niche differentiation, and when the data is applied to a model which does not account for intraspecific variation no niche differentiation was detected (Jung et al., 2010). Similarly, when models which incorporate individual variability are compared with the commonly used mean field approach (focusing on averages), results show that the community diversity is higher, and consequently more stable when variability is

accounted for (Bolnick et al., 2011). These studies provide evidence for the strong role of intraspecific trait variation in community assemblies, suggesting that variability enables species to adapt in relation to biotic and abiotic factors; which cannot be detected by simply looking into population means. These examples along with many other studies (Violle et al., 2012) highlight the importance of individual variance, and raise questions whether community ecology should focus on species or individuals. If we are able to incorporate trait analysis, at both an individual and population level, into fisheries estimates this could potentially provide more information as to how fish communities have been impacted, are being impacted and how they are likely to respond.

Attempts have been made to improve the predictive capacity of process-based fisheries distribution models (Cheung et al., 2008). By including examples of intraspecific variation and environmental selection, not accounted for by previous model predictions, Rutterford (2015) uses GAMs to investigates future distributions (Rutterford et al., 2015). An example of the intraspecific variation examined by this study is non-thermal habitat selection. When studying summer and winter North Sea Cod individuals tagged movements compared to metabolically predicted preferable habitats, there is evidence to suggest that individuals occupy sub optimal thermal habitats for extended periods of time regardless of metabolic costs (Neat and Righton 2007) with northerly migrations to colder conditions than the optimum for aerobic scope of performance (Perry et al., 2005). This data potentially implies that either current studies predicting aerobic scope of performance do not fully capture the environmental drivers behind population distribution. It is suggested that the strong association between individuals with specific habitats may prevent further poleward migrations of species, a contradictory prediction to previous studies (Cheung et al., 2010). Using data showing spatially-contrasting local changes in response to warming (Simpson et al., 2011) to explain why mean latitudinal range shifts are only apparent in some species (Perry et al., 2005), they produce estimates where present and future changes in latitude and depth distributions are more similar than previously anticipated. However, this study still does not account for natural variability in thermal tolerance or metabolic constraints, which it is pointed out will ultimately determine population distributions (Donelson et al., 2012; Crozier and Hutchings 2014). The in-cooperation of in-situ metabolic rate variability will likely improve upon predictions.

Another advantage of measuring individual variability is in the application of *in situ* data studies to laboratory derived data. Controlled energetic demand laboratory data is calculated from an individual

physiology baseline perspective, with a proportional increase measured over an environment gradient (Clark et al., 2013). When measured from an average perspective there is a high degree of individual variance over the total population, making identifying trends over extrinsic gradients difficult (Killen et al., 2007). As we cannot control the experienced parameters of wild individual, potentially measuring the degree of deviance from a mean population value might produce more relatable findings, making it easier to apply metabolic theories to natural populations (Violle et al., 2012).

## 1.6 Moving forward: direct observation of individual level metabolic rate

Field-based observational data is key for developing predictions of potential responses of fish populations to future climate scenarios as natural field-based data include potential behavioral responses of individuals to interacting conditions (Treberg et al., 2016; Chung et al., 2021). Using observations to model biological responses to extrinsic variability however does present some issues, with uncertainty regarding the exact cause of any ecological trends as we are unable to isolate unique environmental parameters or measure the impact of multiple extrinsic sources of variability on natural community physiology (Nisbet et al., 2000; Nisbet et al., 2012). Identifying a common measure of individual metabolic performance, representing the cumulative impact of multiple competing extrinsic and intrinsic variables on the realised energy demand (or energy budget) would provide a direct link between field-based observation and bioenergetic fishery models.

## 1.7 Metabolic rate Introduction

In recent years the metabolic expression of fish populations has been attracting interest as a variable used to predict how populations are likely to be impacted by environmental changes (Farrell et al., 2009; Marras et al., 2015) and increased anthropogenic stressors (Leach and Taylor 1980; Redpath et al., 2010). Metabolic rate is a measure of physiological performance (Metcalfe et al., 2016; Chung et al., 2019; Alewijnse et al., 2021; Chung et al., 2021), representing the sum of the total energy consuming processes of an organism (Treberg et al., 2016). Metabolic rate therefore describes the energetic input required to maintain physiological maintenance and ecological performance (Treberg

et al., 2016). Metabolic rate is a measure of energy and therefore should be expressed in units of joules. However, most measures of animal physiology draw on indirect calorimetry and express energy use in units of oxygen consumption rate (Brown et al., 2004; Clark et al., 2013). The link between oxygen consumption and energetic production is defined in equation (1.1).

$$C_6H_{12}O_6 + 6O_2 -> 6CO_2 + 6H_2O + ATP \qquad (1.1)$$

Thus, oxygen consumption (and $CO_2$ production) rate is directly limited to the rate of respiration of food and the production of energy (Brown et al., 2004). The amount of energy produced (measured using the volume of carbon dioxide released divided by the volume of oxygen absorbed during respiration) per unit of food (in grammes for example) consumed varies with the energetic content of food. This is describing how the respiratory quotient varies between food groups, respiratory quotient is a dimensionless number describing the ratio between carbon dioxide production to oxygen absorption, and describes the amount of energy (in oxygen consumption rate) produced per food group consumed (Brown et al., 2004). For carnivorous fishes consuming protein and lipids with minimal carbohydrates we assume a common respiratory quotient and thus that the relationship between oxygen consumption rate and energy is effectively independent of variations in diet (Brown et al., 2004). By assuming a common respiratory quotient, we assume the food groups consumed between individuals is similar, which is a potential source of inaccuracy, and one we planned to address with further laboratory analysis.

### 1.7.1 Measurements of metabolic rate

An animal's metabolic rate is the sum of all energy consuming processes operating over a period of time (total energetic budget represented by figure **4**) (Treberg et al., 2016). As animals may be performing a range of different functions, differing measures of metabolism have been adopted in an attempt to standardise measures (Clark et al., 2013). Most of these metabolic definitions represent manipulations possible in the laboratory and may have limited meaning under field conditions (Nisbet et al., 2012; Chung et al., 2019). Under laboratory conditions studies attempt to isolate metabolic costs with extrinsic variability, removing the energetic costs of growth, digestion, excretion and reproduction; isolating basal metabolic costs (Clark et al., 2013), represented in figure **5**).

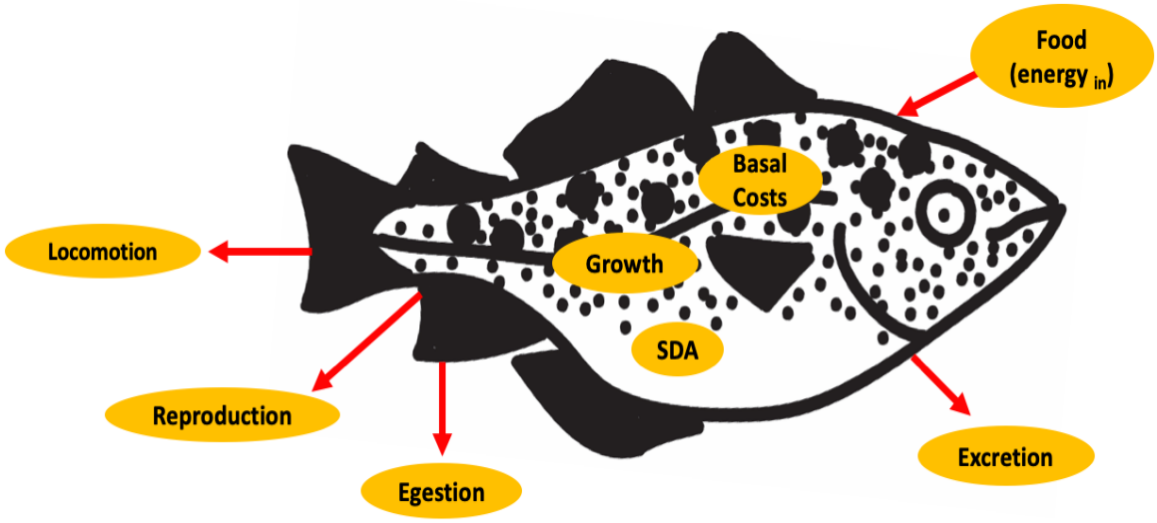


***Figure 4**: Conceptual diagram of the components contributing towards an individual's total energetic budget. SDA represents the specific dynamic action, which is the amount of energy expenditure above the basal metabolic rate due to the cost of processing food for use and storage. Egestion is the removal of undigested food, while excretion is the removal of metabolic waste products. Diagram adapted from Treberg et al., (2016).*

The lowest rate of metabolism is either called basal or standard metabolic rate (SMR) (Chabot et al., 2016), within this study we refer to SMR. In theory, basal metabolism defines the energetic cost of cellular maintenance alone (Sloman et al., 2000). In practice it is difficult to exclude all energy demanding activities, especially in fishes where some degree of active motion is needed to maintain swimming position (Beauregard et al., 2013). SMR describes the metabolic rate when under resting conditions, with no digestion costs, and is designed to measure the metabolic rate the individual needs to perform base level physiological functionality without growth, feeding, digestion, movement or any other behavioral process such as avoiding predators (Cutts et al., 1998a).

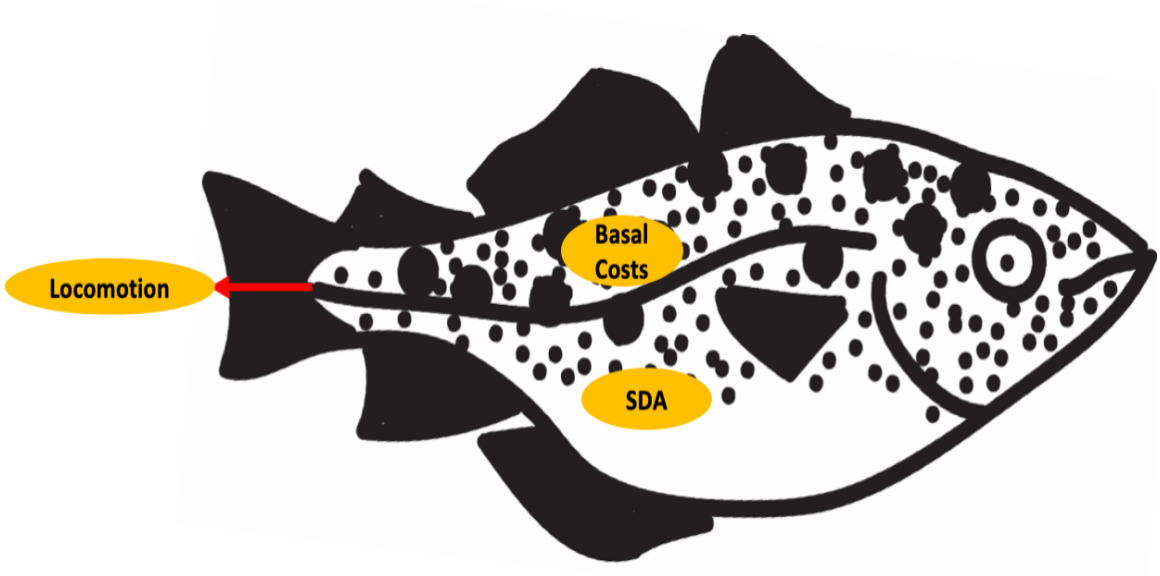


***Figure 5**: Conceptual diagram of the components contributing towards the metabolic rate expression represented by standard and maximum metabolic rates. Standard metabolic rate (SMR) is measured under resting condition, maximum metabolic rate (MMR) is measured under full exertion. SMR and MMR are measured under laboratory conditions, where it is possible to isolate metabolic rate responses with extrinsic variability, without every metabolic component contributing towards an individual total energetic budget.*

Resting metabolism is when the individual is at rest after feeding, so describes more physiological processes than SMR, as the individual is fed and digesting, therefore should be slightly elevated when compared to SMR, and is described by specific dynamic action (SDA) (Treberg et al., 2016).

Maximum metabolic rate (MMR) is generally determined as the peak metabolic performance following acute activity challenge such as swimming to exhaustion (Killen and Halsey 2017). MMR, therefore estimates an individual's maximum physiological capacity (Little et al., 2020).

Standard and maximum metabolic rate therefore define an organism's respiratory capacity at a given temperature and body size. The difference between maximum and standard metabolic rate is termed the aerobic scope (Farrell 2016), and is considered to reflect the metabolic potential available to sustain all additional energetic costs (e.g. digestion, feeding, muscle activity, growth, reproduction, defense from disease or parasite infection) (Clark et al., 2013).

Field metabolic rate (FMR) is defined as the average energy expenditure over a given period of time in the natural environment, and is the sum of three metabolic components: SMR, specific dynamic action (the post prandial increase in metabolism) and activity metabolism (Chung et al., 2019).

## 1.8 Metabolic scaling

An organisms' metabolic rate (can be MMR or SMR depending on measurement conditions) is the sum of all cellular activity – therefore total metabolic rate must increase with increasing body size (number of cells) (Treberg et al., 2016). Furthermore, metabolism is an ectothermic process, and reaction rates will be influenced by temperature (at least within a thermal range at which enzymes function). Consequently, the scaling of metabolic rate with body size and temperature is a critical consideration both to compare measurements across individuals and to understand the evolutionary and ecological significance of variation in organism metabolic rate (Von Herbging 2006; Killen et al., 2007; Bruno et al., 2015; Jerde et al., 2019).

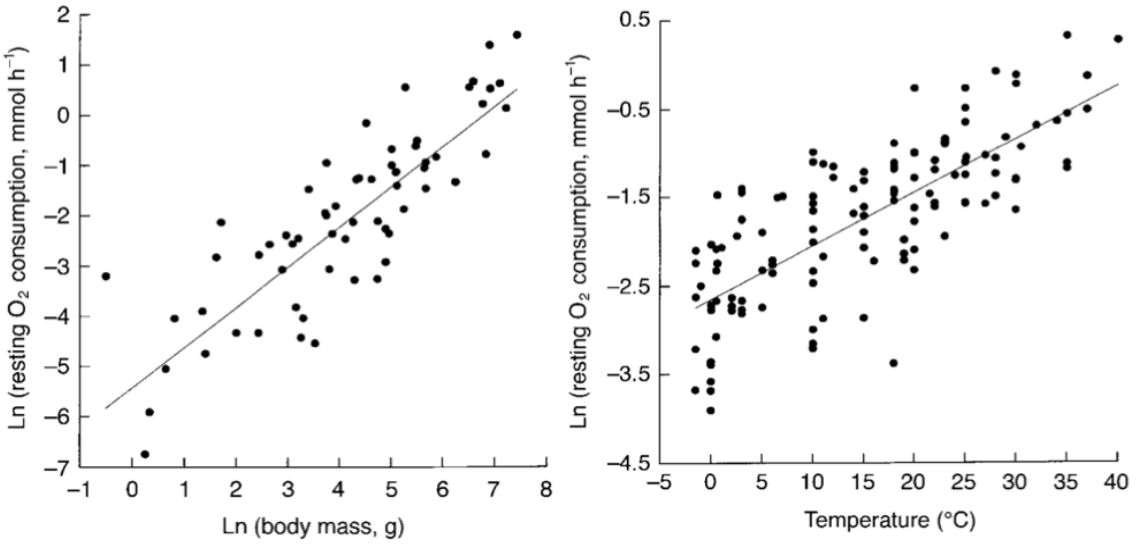


***Figure 6**: Between-species scaling relationship between SMR (measured in resulting oxygen consumption (Resting metabolic rate, mmol h±1)) temperature (Log/log plot with fitted least-squares regression line) and wet body mass (M, g) in teleost fish. Each species is represented by a single data point (ONESTUDY data set). Adapted from Clarke (1999)*

The metabolic theory of ecology attempts to describe the predictable mass and temperature scaling relationship of standard metabolic rate (figure **6**) using equation (1.2) (Clarke and Johnston 1999a). However, there is a large degree of debate about the applicability of this equation to natural populations due to the uncertain nature of the applicability of SMR to wild fish, and the nature or precise values which should be used for the scaling terms (Glazier 2010). Despite these debates, metabolic theory of ecology scaling equations are a powerful tool used to form biogeographical and population output models in response to climate change scenarios (Clarke and Johnston 1999a).

$$B = B_0 M^{\alpha} e^{-E/Kt} \qquad (1.2)$$

where B represents mass specific metabolic rate, $B_0$ is a normalization constant that is independent of body size and temperature, $M^{\alpha}$ is how body mass, M , scales with $\alpha$, an allometric scaling exponent, and $e^{-E/Kt}$ is the exponential Arrhenius function, where E is an "activation energy", k is Boltzmann's constant ($8.62 \times 10^{-5}$ $_eV$ K − 1 ), and T is body temperature in Kelvin (Gillooly et al., 2001; Brown et al., 2004; Kozlowski and Konarzewski 2005).

$B_0$ is a normalization constant independent of body size, and aims to describe the variance in metabolic 'level' between species from different environmental niches (Clarke and Johnston 1999a), for example a pelagic species is believed to have a higher metabolic level than a benthic species even at the same body size and temp, therefore we cannot directly compare individual metabolism between species (Clarke and Johnston 1999a). The normalization constant describes the species-specific relationship between basal metabolic rate, field metabolic rate, and maximal metabolic rate.

Alpha describes the mass scaling exponent, which aims to standardise metabolic rate across individuals and species of varying sizes. As larger animals have a greater mass requiring a higher energetic input for a greater quantity of cells, therefore they express higher absolute metabolic rates when compared to smaller species. However, when compared on a mass specific basis, smaller animals usually express higher rates of energetic expenditure (Kleiber et al., 1932; Schmidt-Nielsen and Knut 1984). Metabolic rate therefore changes allometrically with body mass. The scaling coefficient is species specific, but the scaling exponent has long been believed to be relatively fixed and has been found to be c. 0.75 (3/4) (Kleiber et al., 1932; Schmidt-Nielsen and Knut 1984; Von Herbging 2006). The existence of a fixed scaling "law" has been challenged on multiple occasions, and remains a highly debated topic in biology

(Darveau et al., 2002; Bokma 2004; Duncan et al., 2007; Glazier 2010; Kearney and White 2012). As variations have been found in scaling exponents amongst species have been linked to differences in their ecology, physiology and life-style (Glazier 2005; Killen et al., 2007; Killen et al., 2010). Furthermore, the maximum aerobic metabolic rate of animals often scales with body mass with an exponent significantly higher than 0.75, usually between 0.8 and 1 (Brett 1971; Weibel et al., 2004; Darveau et al., 2002; Killen et al., 2007). This variation between SMR and MMR within the same population does not support the existence of a single universal scaling relationship for metabolic rate.

The universal temperature dependence hypothesis, estimates temperature scaling parameters to express an average value of between 0.6 and 0.7 eV, which is the average activation energy of respiration (Gillooly et al., 2001; Brown et al., 2004), which has been observed under experimental settings measuring metabolic potential. This suggest that Arrhenius relationships may describe enzyme thermodynamics, however relationships may not scale up when considering the temperature effects on the metabolic rates of a whole organism (Tilman et al., 2004; Clarke 2006). The effect of temperature on metabolic rate may vary depending upon the range of temperatures over which an organism is adapted (Clarke 2006), and under natural condition organisms may not conform to temperature scaling relationships due to the multiple extrinsic factors impacting FMR (Richards et al., 2010; Clark, et al., 2013; Norin and Clark 2017; Jutfelt 2020).

Understanding how the growth rates of various species is likely to change also is important for biogeographical models, as with migratory behavior some areas are going to experience increased ecological competition for habitat and prey selection. The causes for metabolic rate body mass scaling relationships is a heavily debated and unresolved topic. Some potential explanations include the individuals needs to dissipate internally-produced metabolic heat across the body surface (Hirst et al., 2014) in accordance with “Kleiber’s law”, and scaling relationships being shaped by a suite of physiological, ecological, and evolutionary factors (Glazier 2010, 2014, 2005; Killen et al., 2010; Harrison 2017; Hatton et al., 2019).

## 1.9 Applying metabolic rate data

There are currently two main schools of thought regarding measuring how individual level metabolic rate variability translates into population distribution and abundance shifts, being aerobic scope (Clark

et al., 2013) and individual variability (Cutts et al., 1998b) (discussed in section 1.5). Aerobic scope focuses on predicting the available energetic resources of an individual, defined as the difference between SMR and MMR of an individual (Killen et al., 2007). According to metabolic theory (Brown et al., 2004) every individual has a limit to MMR, therefore as an individual's standard or resting metabolic rate is increased, closer to the MMR, the energy available for that individual's physiological performance in reduced (Brown et al., 2004). Aerobic scope has been used to predict the temperatures at which fish populations reproductive output will begin to reduce and the limits of physiological tolerances, based on standard metabolic rate thermal response curves (Pörtner 2010). Surveys have suggested that aerobic scope thermal response curves successfully explain the effects of rising temperatures on species abundance in the field (Pörtner 2010); with hypotheses such as the oxygen and capacity limited thermal tolerance (OCLTT) and gill-oxygen limitation theory (GOLT), which state that the combined impact of a greater energetic demands (as a result of an elevated metabolic rate) and lower oxygen levels at higher thermal ranges explain metabolic suppression at higher temperatures, and temperature limited cellular reactions lowering metabolic rate at cooler conditions (Ejbye-Ernst et al., 2016; Pauly 2021). The GOLT and OCLTT attempt to explain the Arrhenius relationship maximum metabolic rate expresses with temperature, where at thermal conditions beyond the optimum thermal range of performance MMR is reduced (figure **7**). The GOLT suggests that at higher temperatures the environmental factor limiting metabolism is oxygen transport into the blood through the gills, therefore oxygen demand is greater than the supply, resulting in reduced respiration and metabolic rates (Pauly 2021). The OCLTT explains metabolic suppression at high temperatures through enzymatic reactions, suggesting that at high thermal ranges the chemical bonds maintaining enzyme substrate structure denature, therefore reducing enzyme abundance and consequently the rate of chemical reactions required for respiration (Jutfelt et al., 2014; Pörtner 2021).

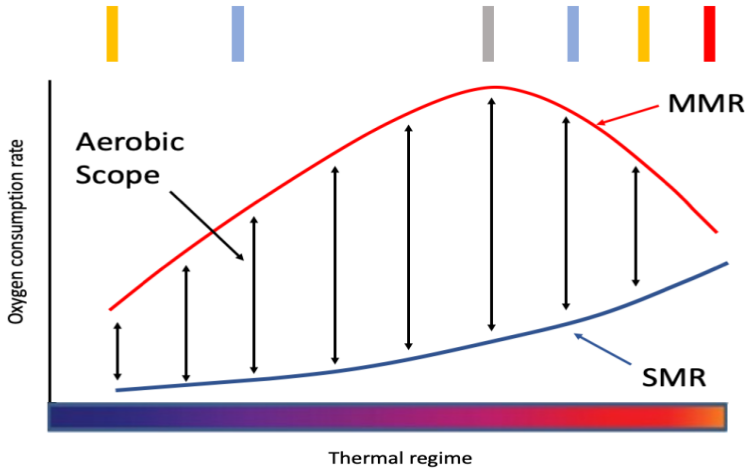


***Figure 7**: TAheoretical representation of the calculation of aerobic scope, adapted from Clark (2013). The red line represents the maximum metabolic rate of the individual, the blue line being the minimum metabolic rate. The X axis is a theoretical thermal gradient, with warmer temperatures represented by red and orange colours. The difference between MMR and SMR is thought to represent the available energetic capacity of the individual, being the Aerobic scope (Clark 2013). At lower temperatures SMR and MMR are thought to be limited by temperature, and increase to a maximum value with higher temperatures, and represented by the grey colour rectangle. Beyond this maximum aerobic scope value, MMR is limited yet SMR continues to increase, reducing aerobic scope (Clark 2013).*

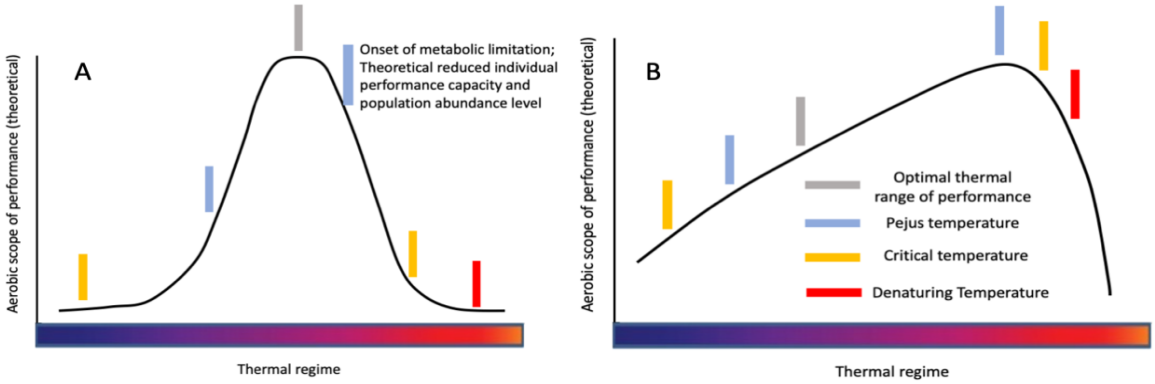


***Figure 8**: hypothetical interaction between aerobic scope and temperature in fishes, both excluding (A) and including (B) population performance. A, assumes that the optimal (preferred) temperature of the species coincides with maximal aerobic scope, while B assumes the optimal temperature is below that which elicits maximal aerobic scope and instead aerobic scope increases until close to the upper critical temperature. Adapted from Clark (2013)*

There are multiple examples where the metabolic theories can be successfully applied to wild invertebrate populations throughout various life cycles (larval to mature adult), such as limited oxygen consumption rates in larval kelp crab *Taliepus dentatus* and small zooplankton species *Daphnia magna*

above and below their optimum thermal range (Seidl et al., 2005; Storch et al., 2009). Similar physiological and temperature related performance trends in invertebrate species have been identified using proxies such as a reduced maximum body size, with reduced growth at elevated temperatures correlated to oxygen solubility (Chapelle and Peck 1999). There are however very few examples where such correlations between population physiological performance and temperature variability can be formed for wild fish populations. These include a period of unusually high-water temperatures within the Fraser River in 2004, which is claimed to be linked to elevated sockeye salmon *Oncorhynchus nerka* mortality when migrating from marine to freshwater habitats (Farrell et al., 2008).

It has been suggested that in this example water temperatures were above the optimal thermal range (Farrell et al., 2008), leading to an increase in basal oxygen demand beyond cardiac pumping capacity (Brett 1971; Lee et al., 2003; Farrell et al., 2008). This increase in oxygen demand (due to elevated temperature) is said to have been greater than the individual energetic supply leading to a reduced aerobic scope resulting in anaerobic metabolism, exhaustion and higher population mortality (Pörtner and Knust 2007). Another example where it is suggested that the OCLTT hypothesis is applicable to wild fish populations is the north and Baltic sea eelpout, *Zoraces viviparous*. This non-migratory species expressed a reduction in relative population size during warmer time periods between 1954 to 1989 within the North Sea, with higher summer water temperatures correlating to increased individual mortality (Pörtner and Knust 2007). Such studies attempt to form conclusions regarding population physiological performance by comparing environmental data with laboratory derived eelpout aerobic scope temperature relationships (Zakhartsev et al., 2003) from the same population, with results re adjusted for yearly variations in salinity and body mass. Using this method, they conclude the higher temperature result in reduced aerobic scope in wild populations, explaining both reduced abundance and individual body size and suggesting that lower aerobic scope likely leads to reduced fertility. There has also been an effort to model population temperature responses, with suggested future depth preference compression (Raye and Weng 2015) and latitudinal population shifts (Craig and Crowder 2005).

However, there are potential issues with applying laboratory derived metabolic measurements to wild populations (Jutfelt et al., 2018), including inconsistencies in interpreting the optimal thermal range from laboratory derived aerobic scope studies and uncertainties regarding the physiological inputs to field metabolic rate. The OCLTT and GOLT defines the optimal thermal range for physiological

performance where aerobic scope expresses a maximum value and population performance is limited at higher and lower temperatures (Pörtner 2010). This assumption has been debated in recent years, with some findings indicating that temperatures optimal for physiological performance occur below maximum aerobic scope (figure **8**).

Tropical fish species, when presented with a range of thermal conditions spanning the temperatures they would naturally be exposed to consistently chose to inhabit cooler waters than that of expressed maximum aerobic scope (for the same individuals) (Norin et al., 2014). This suggests that maximum aerobic scope does not translate to optimal physiological conditions and aerobic scope constantly increases until lethal temperature ranges (Norin et al., 2014). When examining Atlantic cod (*Gadus morhua*) models predict that optimal temperatures for growth and fitness lies below that for aerobic scope; aerobic scope is therefore said to be a poor predictor of fitness at high temperature (Holt and Jørgensen 2015). This implies that higher temperature initially expands aerobic scope, increasing growth rate and reproductive output, however when aerobic scope is at a maximum the increased metabolic requirements intensify foraging demand and reduce survival; therefore, increased oxygen demand increases competition (Holt and Jørgensen 2015). Other studies attempt to constrain the relationship between aerobic scope and physiological performance through bioenergetic modelling. These results indicate that aerobic scope is not a controlling factor for physiological performance, indicating that other ecological factors control metabolism (Clark et al., 2013).

Another contentious issue with applying laboratory based aerobic scope findings to wild populations is the adaptive capacity of aerobic scope with time and temperature. Aerobic acclimatisation, meaning the restoration of aerobic scope to normal levels over time after experiencing thermal changes, is expressed in both tropical (Donelson et al., 2010; Donelson et al., 2012) and temperate species (Sandblom et al., 2014) within a single generation (Angilletta and Angilletta 2009). There is also evidence that parental effects (influences on offspring phenotype) can facilitate acclimation to temperature variability between generations, termed transgenerational effects (Angilletta and Angilletta 2009; Mousseau and Fox 1998). Currently we have a limited understanding of how aquatic organisms adapt their physiology over generational time scales (Hofmann and Todgham 2010; Skelly et al., 2007), however there is still enough evidence to question how we apply lab based aerobic scope measurements to wild populations (Healy and Schulte 2012). Environmental variables aside from temperature also impact aerobic scope, such as elevated carbon dioxide concentration enhancing

aerobic scope throughout temperature range (Rummer et al., 2013). Due to these uncertainties it is arguable that to model and predict how fish population are likely going to respond to environmental changes we need more information in the form of temperature integrated real time metabolic responses of wild populations.

Metabolic rate has been shown to vary between feeding regimes, as expected given that metabolism is dependent upon energy supply (Killen 2014; Herbing and White 2002). Individuals treated to varying thermal conditions yet a standardised feeding regime express suppressed metabolism with higher temperatures (Gingerich et al., 2010). This trend is likely explained by an increased energetic requirement, therefore impacting the energetic supply demand ratio (Clark et al., 2013), allowing greater energetic partitioning towards growth and condition as standard energetic requirements take up less of the total energy budget.

## 1.10 Field Metabolic rate

Field metabolic rate (FMR) is an attractive variable, as it describes the energetic response of the entire organism to the physical and ecological environment as described by figure **4**) (Sinnatamby et al., 2015; Chung et al., 2019; Alewijnse et al., 2021; Chung et al., 2021). Field-based measurements of FMR also reflect specific conditions each population is adapted to, thereby circumventing some problems associated with removing individuals from natural settings and exposing them to new laboratory conditions (Chung et al., 2019; Alewijnse et al., 2021; Chung et al., 2021). There have been many attempts to quantify total FMR or components of FMR in marine organisms, mostly focusing on activity proxies such as accelerometry (Yasuda et al., 2012), otolith growth ring increment width (Wright et al., 1992), behavior characteristics such as tail beat frequencies (Ohlberger et al., 2007), enzyme activity (Yang and Somero 1993) and many more (Treberg et al., 2016). All such methods have advantages and drawbacks; accelerometry gives accurate movement data, however it is expensive, difficult to recover and does not readily convert to oxygen consumption rate. Otolith increment growth again does not supply oxygen consumption data and assumes that growth rate and metabolism in the field form a linear relationship.

FMR paired with standard and maximum metabolic rate measurements provides an understanding of the physiological performance of the individual, as with all measures of metabolic rate we are able to

tell if an individual is in the upper or lower parts of its aerobic scope, therefore how close an individual is to its maximum energetic demand. An individual FMR value, without supporting laboratory or mathematically derived minimum and maximum metabolic rate measurements does not tell us how close an individual is to its maximum metabolic rate of performance, as individual metabolism varies on a threefold basis between individuals of the same population. There are also many unknown sources of deviance and random factors within field metabolic rate measurements, making the interpretation of FMR data difficult, and it is difficult to identify the drivers of population shifts in energetic demand.

In this study I apply a newly emerging metabolic proxy which allows comparisons of field metabolic rates between individuals within their natural environment.

## 1.11 Otolith-derived field metabolic rate proxy

Here termed otolith derived field metabolic rate ($FMR_{oto}$), the otolith FMR proxy recovers the rate of production of respired $CO_2$, by estimating the proportion of respired compared to external (dissolved inorganic) carbon present in the blood and therefore the otolith, determined by laboratory metabolic rate studies paired with blood carbon dioxide concentration and otolith carbonate measurements (Chung et al., 2019; Chung et al., 2019b) represented by figure **9**).

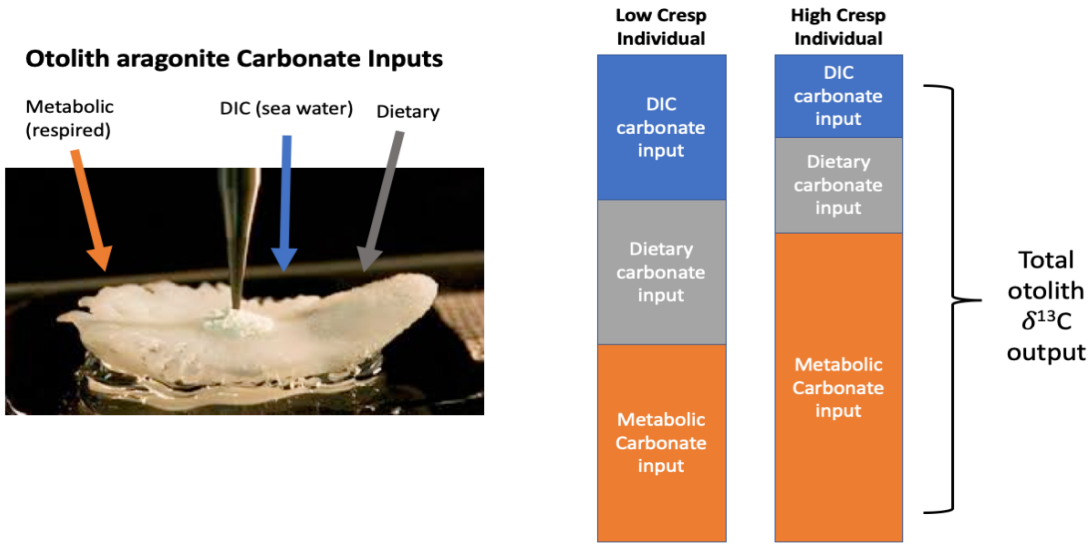


***Figure 9**: Theoretical representation of the different sources of carbonates contributing to otolith aragonite, including dissolved inorganic, dietary and metabolically derived carbonate and how the different proportions contribute towards total otolith aragonite carbonate values (Chung et al., 2019). Cresp is a measure of the proportion of total otolith aragonite isotopic values derived from metabolic sources. Therefore, we have to measure the proportion of each source of carbonate contributing to total otolith aragonite carbonate values. The low metabolic rate individuals total otolith aragonite carbonate values are proportionally made up of less metabolically derived aragonite than the high metabolic rate individual (Chung et al., 2019).*

$FMR_{oto}$ measurements exploit the fact that otolith mineral is formed from multiple carbonate sources with distinct isotopic compositions, incorporated into the metabolically inert aragonite (Degens et al., 1969). The isotopic composition of otolith carbon is not in equilibrium with dissolved inorganic carbon (DIC) from surrounding water, this is explained by the contribution of carbon within the blood (Wurster and Patterson 2003; Solomon et al., 2006). Otolith aragonite is a product of $CO_2$ within the blood which is transported to the fluid surrounding the otolith (McConnaughey et al., 1997; Wurster and Patterson 2003) and DIC from surrounding sea water. There are therefore two main sources of dissolved $CO_2$ within the blood. An external source, being the product of dissolved carbon from gas exchange in the gills or digestion via the stomach (McConnaughey et al., 1997) and an internal source produced through cellular respiration. Due to pH regulation of the blood, as the individual experiences an increase in respiration, the proportion of the respired carbon source within the blood increases relative to the external source of $CO_2$. This is useful from an isotopic perspective, as the isotopic composition of respired carbon expresses approximately 15-20‰ more negative values than carbon from external dissolved inorganic sources. Therefore, as the proportion of respired $CO_2$ in the blood increases, due to higher metabolic rate, the isotopic values of otolith carbon becomes more negative. The sources of isotopic carbon are described by (Tohse and Mugiya 2008; Grønkjær et al., 2013). External dissolved inorganic carbonate sources are not assumed to be constant and where possible is modelled, but if possible is measured.

Recently, two studies have attempted to calibrate the proportion of total otolith aragonite isotopic values derived from of metabolic carbonate (Cresp) values against oxygen consumption rates in laboratory conditions, manipulating metabolic rates through heating. Chung (2019) describes the relationship between $\delta^{13}C$ and oxygen consumption, reporting individual oxygen consumption rates paired with otolith derived FMR for Atlantic cod (Chung et al., 2019). Providing a correlation between temperature and $\delta^{13}C$, showing that otolith aragonite varies predictably with temperature. Chung argues that this methodology provides a tool to investigate and compare the metabolic expression of behavioral response to environmental changes among individuals, species and populations (Chung et al., 2019). Martino et al., 2018 exposed four groups of Australian snapper (*Pagrus auratus*) to varying temperature levels for two months, determining $\delta^{13}C$ values in the otolith, liver and muscle. Temperature treatment significantly altered the $\delta^{13}C$ values of all tissues (Martino et al., 2020). This study concludes that otolith aragonite can provide a valuable insight into FMR, as the proportion of

metabolically derived otolith carbon contribution significantly increases with temperature (Martino et al., 2020).

Other examples where $FMR_{oto}$ has been applied to natural settings include testing metabolic scaling relationships within myctophid species from the Scotia Sea, finding that Cresp ranges between 0.123 to 0.248 (unit less) and that ecological and physiological differences among species are better predictors of variation in Cresp values than body mass and temperature (Alewijnse et al., 2021). When myctophid Cresp values are compared to estimates of metabolic rates derived from scaling relationships, estimates of oxygen consumption rates derived from different methods are broadly similar, however, there are considerable discrepancies at the species level (Alewijnse et al., 2021). Chung et al., 2021 examines the extrinsic dependability of FMR within genetically distinct ecotypes of juvenile Atlantic cod from the Skagerrak coast of southern Norway (Chung et al., 2021). The distinct ecotypes expressed different thermal performance curves for field metabolic rate, revealing that the cold-adapted fjord ecotype maintained higher field metabolic rates at cooler temperatures than the warm-adapted North Sea ecotype, which showed clear preference for warmer waters around the thermal optimum (Chung et al., 2021). This data suggests that there is a genetic component to metabolic expression and that physiological conditions in the field should be considered in the evaluation of the effect of climatic variables on fish population dynamics (Chung et al., 2021).

## 1.12 Model species: European Plaice *Pleuronectes platessa*

The aims of this project are to use the otolith FMR proxy to explore the extent and causes of variation in FMR expressed in a population of wild marine fishes across seasons and years. The model species and population chosen is the North Sea European Plaice (*Pleuronectes platessa*). North Sea Plaice are a benthic flat fish species, with three sub populations within the central and southern North Sea basin (the southerly, easterly and westerly (Hunter et al., 2009; Darnaude et al., 2014;)), with complex life cycles including an annual breeding and feeding cycles accompanied with southerly and northerly migrations (Hunter et al., 2004). During winter months each individual sub population inhabits their separated feeding grounds, during the spring there is a simultaneous migration to the breeding grounds of the southern North Sea, and juveniles move to nursery areas for the first summer of life then join their sub populations annual cycle (Hunter et al., 2009; Darnaude et al., 2014).

A key element of European Plaice biology is seasonal migrations between feeding and spawning grounds. To explore these movements, (investigating the reasons for selected locational and the timings of movements) studies have employed tagging methods (Hunter et al., 2009), revealing a seasonal migration split between sup-population winter feeding grounds and spawning areas, as described by figure **10** (Hunter et al., 2009).

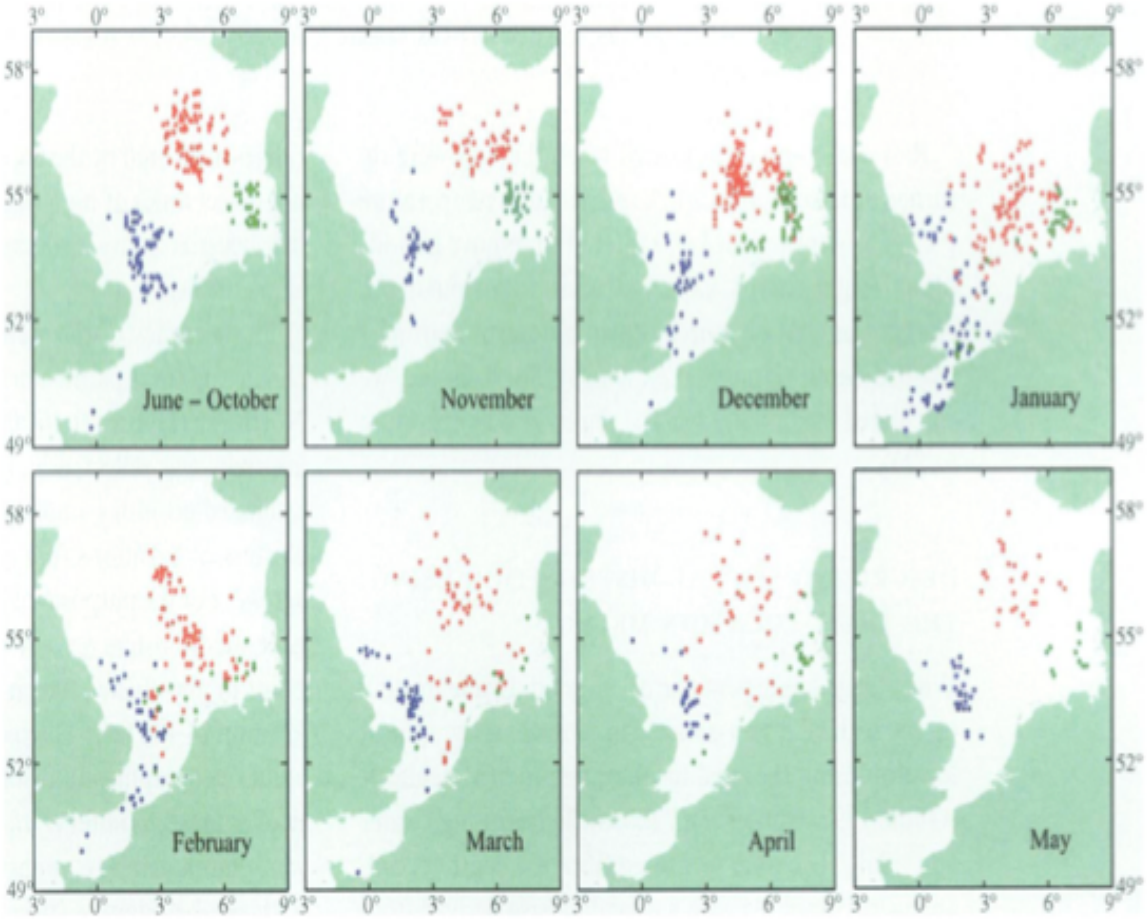


***Figure 10**: Tagged Plaice data showing distribution of the Northern North Sea sub-population (Red), Eastern North Sea sub-population (Blue) and Western North Sea sub-population (Green) throughout the year. With seasonal migrations, including the feeding and spawning seasons. This figure is adapted from Hunter et al., 2009).*

There are three distinct sub groups of plaice which remain geographically distinct from May-October; the northern North Sea (NNS), eastern North Sea (ENS) and western North Sea (WNS) (Hunter et al., 2004). Figure 10 shows plaice distribution, measured with electronic tags, though a yearly cycle. This indicates there is a southerly shift of all populations, to established spawning grounds from December

to March. However, during the vast majority of the year there is distinct separation between the sub populations (figure **10**.) (Hunter et al., 2009). When populations inhabit their separate distinct sub population habitats, this is suggested to be due to feeding and growing activity.

Males predominate on the spawning grounds and are thought to spend several months there - in contrast to female plaice which remain for a few weeks (Hefford 1916; Rijnsdorp 1989), although a precise estimate of the duration of spawning is not available. During the spawning period plaice almost cease feeding (Lande 1973; Rijnsdorp 1989), but it is not known whether this is caused by the absence of food or by behavioral changes associated with spawning.

The relative importance of the different spawning groups is indicated by their total egg production and has previously been calculated in the 1960s (Rijnsdorp 1989; Harding 1978). The total production of fertilised eggs in the North Sea and English Channel was estimated at $25xlO^{12}$ (Rijnsdorp 1989); of this total, 65% occurred in the central and eastern North Sea, 20 % in the Southern Bight, less than 5 % in the western English Channel, and 10% in the eastern English Channel (Harding 1978). This is useful information, as it informs us about the relative fecundity of each sub population, and the implications of over fishing.

Individuals tend not to feed during spawning time periods, relying on fat reserves built up over growing time periods. The diet of individuals varies from juveniles inhabiting nursery grounds and adults inhabiting feeding grounds. On nursery ground the diet has been measured to predominantly be made up of polychaetes, crustacean and mollusks of all sizes (Amara et al., 2001), with growth rates on nursery grounds ranging between 0.55 to 0.81 mm per day (Amara et al., 2001).

One topic of interest is the migratory behavior of North Sea European Plaice, and the causes of specific timings. Adult plaice are known to adopt activity patterns in phase with the tidal currents (Hunter et al., 2004). During autumn and winter for example, southward-migrating plaice in the southern North Sea leave the seabed during south flowing tides, matching their periods of swimming with flowing and slack water time periods (Buckley and Arnold 2001). This potentially is to reduce the energetic impact of migration, however currently we have very little information regarding the energetic demand of migration in natural settings.

When measuring activity levels of Irish sea plaice over the annual cycle the highest rate of swimming occurred during expected times of migration and spawning (October to March) and plaice infrequently spent >5 h in mid-water. Tidal patterns of activity occurred in all studied sub-stocks, but predominantly during the migratory period. Within North Sea feeding and spawning grounds, plaice often swim only at night (Jones et al., 1979; Arnold and Cook 1984; Hunter et al., 2004).

The benthic habitat which individuals choose to inhabit also varies between feeding and spawning periods, with a shallow warmer environment during summer spawning periods to the more northerly latitudes associated with deeper, colder water conditions. Tagging study results show that some individuals returned to within 20km of their previous season's spawning location. Juvenile plaice generally migrate in to deeper water as they get larger (Gibson et al., 2002) although some older/larger individuals may overwinter in shallow water, with the reasons for this variance in migratory behavior being unclear (Nash et al.,1994; Nash and Geffen 1999).

Juvenile movements are unpredictable as there are often sudden "pulses" where a large number of individuals arrive in a short space of time (which the exact timings and reasons we are unable to predict); these sudden unpredictable peaks in population movements are features of many flatfish populations (Rauck and Zijlstra 1976; Hovenkamp 1992; Allen et al., 2008). It has been suggested that periodic migration behavior may be caused by periodicity in spawning or hatching pulses (Allen et al., 2008), or differential transport from different spawning locations (Al-Hossaini et al., 1989) or selective tidal transport (Creutzberg et al., 1978; Rijnsdorp et al., 1985).

Developing juvenile fish then maintain their position in the inter-tidal zone by adopting a system of tidal transport, allowing individuals to make feeding excursions onto the mud flats during times of high water (Kuipers 1973), then retreating below the low water mark before the expected time of low tide (Hunter et al., 2004).

## 1.13 Plaice metabolism

Plaice daily oxygen consumption, food consumption and growth rates have been measured over varying feeding and temperature regimes finding that oxygen consumption was related to body weight of the fish as a power function, with a weight exponent of between 0.71 and 0.85 (Fonds et al., 1992).

Oxygen consumption was found to be influenced by oxygen concentrations below a critical level of 45-60 mmHg. Rates of oxygen uptake were also affected by fish size, temperature and nutritional status. The problems presented by such laboratory derived data are the applicability to wild fish situations (Jobling 1982).

### 1.13.1 European Plaice, Relationship Between Oxygen Concentration and Metabolism

An experiment was carried out to find out the impact of low levels of oxygen concentration on plaice oxygen consumption rate, the fish used in this tests weighted between 10-15g (Jobling 1982). Some fish species (conformers) express oxygen consumption rates directly dependent upon ambient oxygen tension. However, the majority (nonconformers) have rates of oxygen consumption independent of environmental oxygen tension. In this experiment, plaice were found to have a relatively constant rate of oxygen uptake as the oxygen tension decreased from 150 to 45-60 mmHg; as a result, plaice can be classified as non-conformers (Jobling 1982). At 45-60mmHg (critical oxygen tension) there was a drop in the rate of oxygen consumption which continued until the tests were terminated at an oxygen tension of 20-25 mmHg (Jobling 1982). Previous but similar experiments found that plaice were capable of recovery even after exposure to waters having oxygen tensions as low as 5 mmHg (Edwards et al., 1970; Woods and Weber 1975).

### 1.13.2 European Plaice Body, Relationship Between Size and Metabolism

In general oxygen consumption rate increases with body mass, due to higher number of cells, requiring a higher concentration of oxygen for physiological performance. There is a high level of debate regarding the scaling coefficient of body mass with oxygen consumption. Figure **11** describes the body mass oxygen consumption rate relationship with plaice.

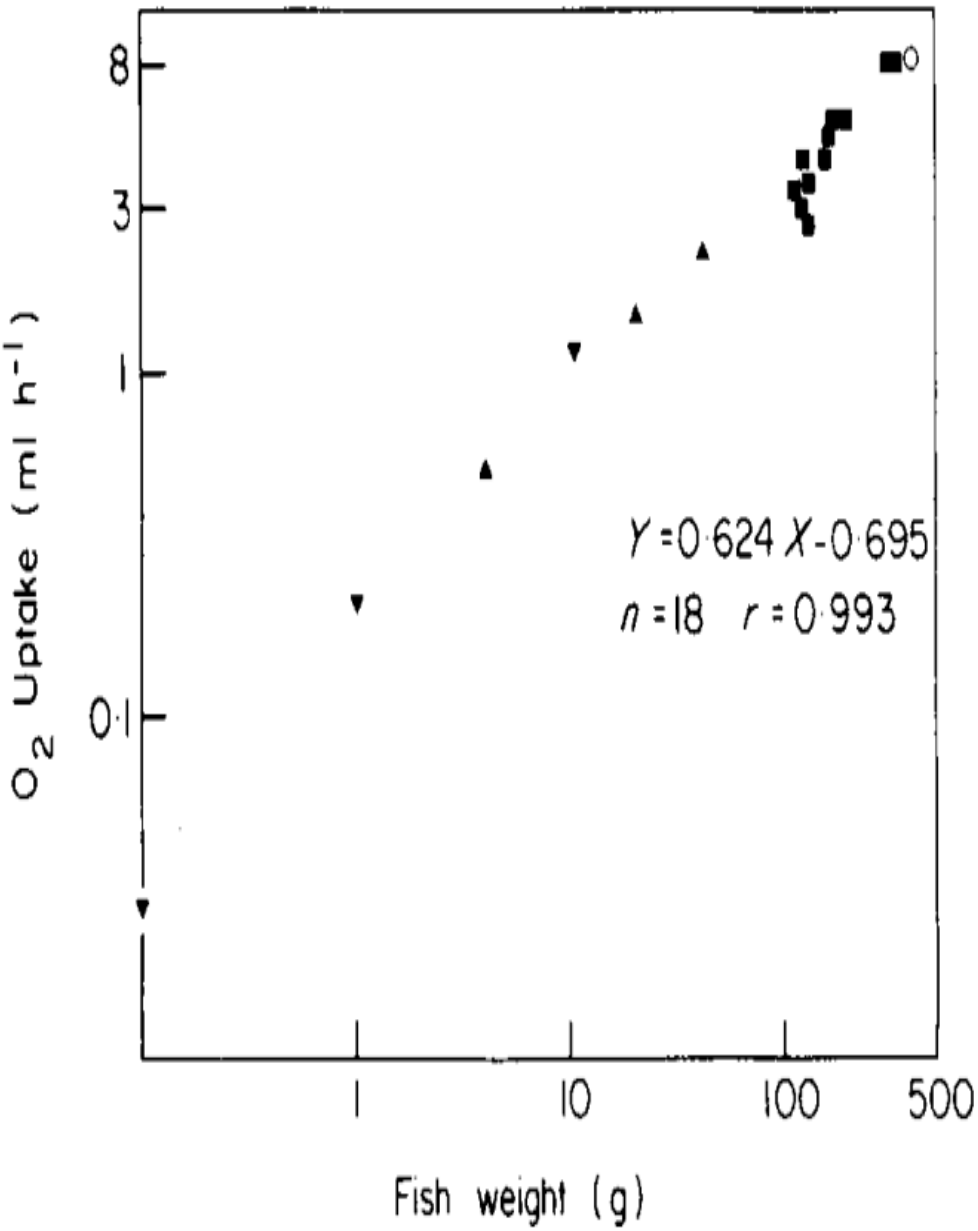


***Figure 11**: Effects of body size on oxygen consumption by plaice at 10 degrees. This figure is adapted from Jobling (1982). Displaying the increased oxygen consumption rate with body mass.*

The analysis this data presented in figure **11** revealed a common regression coefficient of 0.626. There has been much discussion with regard to metabolism-body size relationships, suggesting that metabolism was related to body size to the power 0.75 (Brody and Lardy 1946; Kleiber et al., 1961; Jobling 1982). Theoretical considerations suggest that metabolism should be proportional to surface area (the surface law) or body size to the power 0.67 (Jobling 1982). When reviewing the published data for fish species, Winberg (1956) suggested a weight exponent of 0.81 to be appropriate. Since that time, a vast amount of information has been published relating to fish size-metabolism interactions and, whilst the majority of the values for the weight exponent fall between 0.65 and 0.9, reported values range from 0.4 to in excess of unity (Winberg 1956; Jobling 1982).

### 1.13.3 European Plaice, Relationship Between Temperature and Metabolism

Oxygen consumption under laboratory conditions, as previously mentioned, scales predictably with temperature (Jobling 1982). Figure **12** shows the impact of increased thermal regime on plaice, measuring fish of varying mass (figure **12**) and metabolic measurements (figure **13** MMR being labelled as “active”, SMR being labelled as “rest” and routine metabolism in this case is SMR whilst the individual is “fed”.

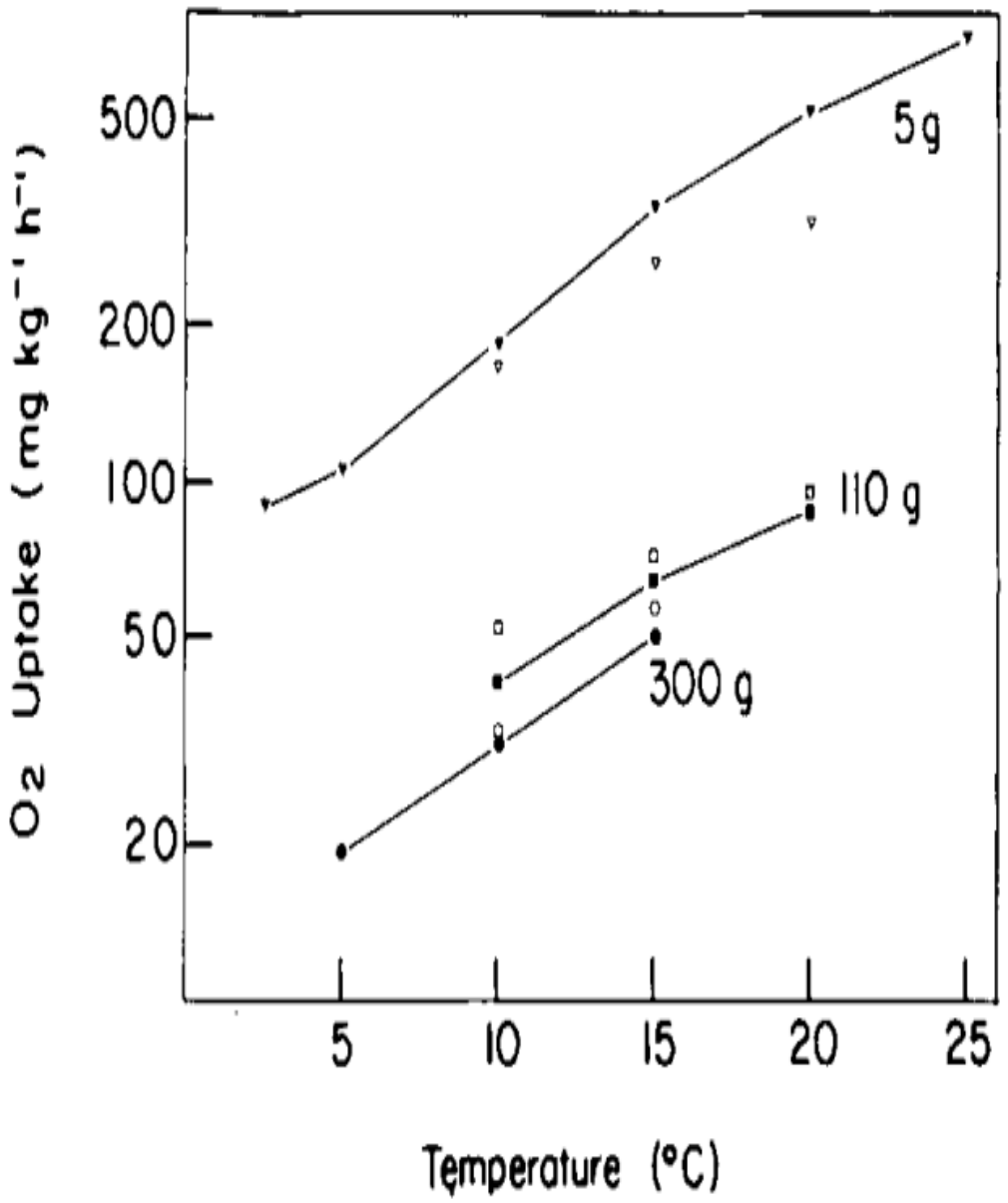


***Figure 12**: Plaice temperature oxygen consumption (SMR) relationship. This figure is adapted from Jobling (1982). Displaying the increased oxygen consumption rate temperature, over varying body sizes. (Jobling 1982).*

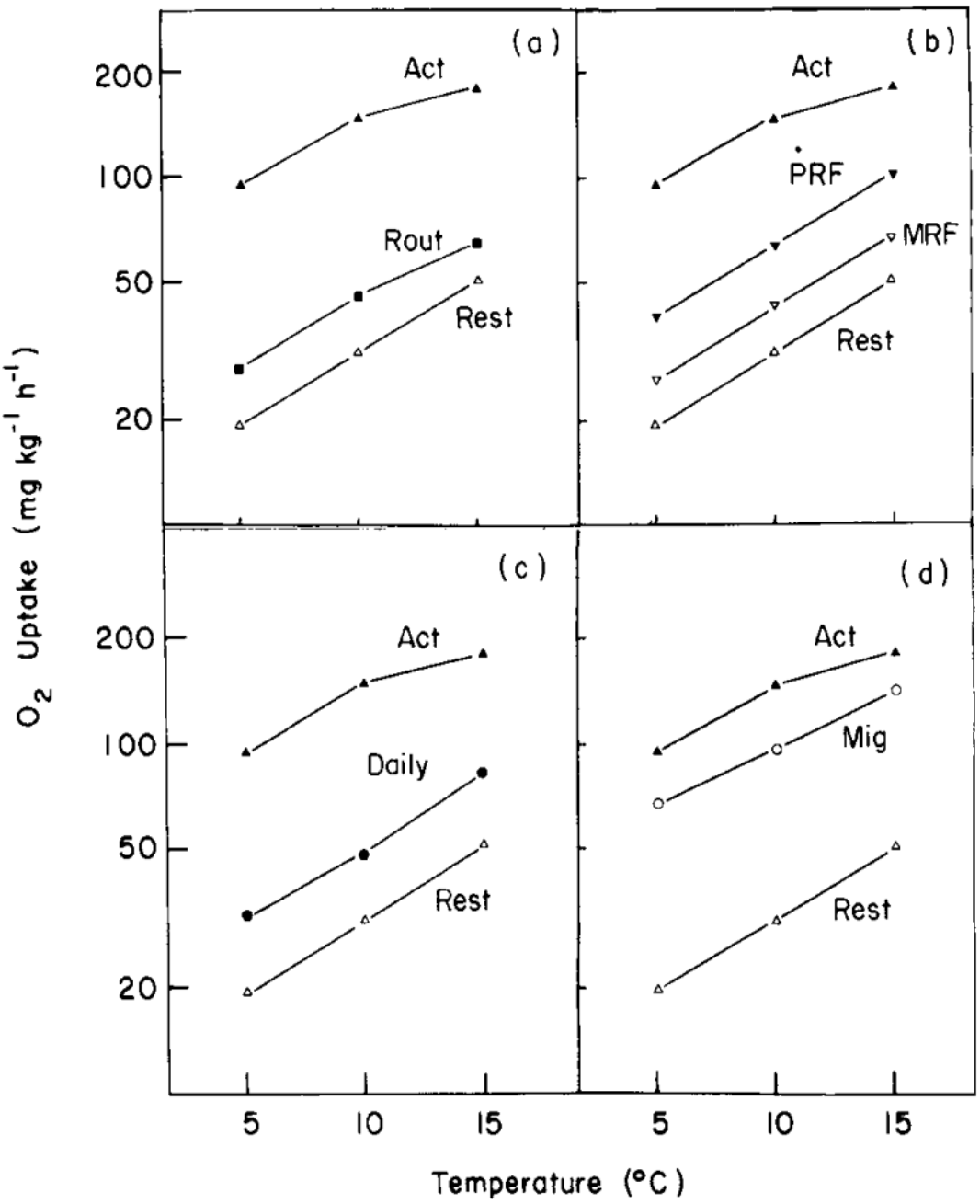


***Figure 13**: Plaice temperature and SMR (listed as resting), MMR (listed as active) and routine metabolic rate (labeled as daily, representing the inclusion of digestion) relationship. This figure is adapted from Jobling (1982). Displaying the increased oxygen consumption rate temperature, with varying metabolic measurements (Jobling 1982). Requirements calculated for a standard 300 g fish. Figure A is Oxygen requirement for swimming activity. Figure B is Oxygen uptake associated with food processing. Figure C Oxygen requirement of fish under conditions of routine activity and feeding. Figure D is Oxygen requirement of migrating fish (Jobling 1982).*

In this experiment (performed by Jobling (1982)) the fish have become acclimated to the new thermal regime. When respiratory rates of fish acclimated to different temperatures ($10^oC$, $15^oC$ or $20^oC$) were compared at the same temperature ($10^oC$ or $20^oC$), the fish acclimated to the higher temperature had a lower oxygen consumption (Jobling 1982). These results suggest that the fish display a thermal acclimation response. When rates of oxygen consumption were measured at acclimation temperatures, fish acclimated to $20^oC$ and $15^oC$ had higher rates than those acclimated to $10^oC$ (Jobling 1982). This shows that the thermal acclimation response was partial. The acclimation response was further investigated using groups of fish which had been acclimated to either $10^oC$ or $20^oC$ (Jobling 1982).

In an attempt to relate SMR and MMR to wild fish previous studies have examined the behavior of wild juvenile plaice and gave estimates of the time spent in swimming activity, relating resting activity to SMR, and active swimming to MMR (Gibson 1980). Gibson recorded two types of swimming movements; the fish either' shuffles' slowly over the bottom propelling itself forward on the tips of the median fin rays or lifts the whole of the body off the substratum and propels itself forward by vertical strokes of the caudal fin and posterior part of the body (Gibson 1980). The oxygen consumption associated with daily activity were calculated to be 30 to 45% of resting rates depending upon temperature (Gibson 1980).

## 1.14 Plaice growth

Previous studies attempting to explain European plaice growth rate variation have focused on temperature, prey conditions, intraspecific competition and interspecific competition (Ciotti et al., 2013; Ciotti et al., 2014). However, previous studies have found interactive effects, for example links between temperature and food availability. In this review I am to briefly describe previous knowledge on the impact of temperature, pray availability, spatial variability and potential metabolic growth rate relationships.

Studies have attempted to linking benthic fauna and the growth and abundance of plaice populations (Edwards and Steele 1968; Macer 1967), as a proximation for food availability, to test if fish operating in areas with more prey express higher growth rates. Laboratory and field estimates of food intake, density and growth provided evidence for food competition and compensatory density-dependence

(Macer 1967; Edwards and Steele 1968). The findings of such studies have suggested that food availability limits natural growth rate, and was supported by observations of juvenile plaice stomach content analysis (Edwards and Steele 1968). However, contrasting stomach content analysis have found that prey abundance was more than sufficient to meet food requirements of plaice, within the Dutch Wadden Sea (Kuipers 1977) and Swedish coastlines (Evans 1983). As a result, investigations of growth dynamics in plaice became focused on testing the 'maximum growth/optimal food condition' hypothesis which states that food is always in excess and that temperature alone controls growth rate (Ciotti et al., 2014).

Plaice growth rates during juvenile life stages have been shown to vary between feeding and temperature treatments, with lower feeding levels resulting in suppressed somatic growth (Ciotti 2012). Individuals which experience starvation lost mass, while "half rationed" fish grew slower but still gained mass, however at a lower rate than fully fed fish (Fonds et al., 1992). However, under natural conditions there have been studies reporting no correlation with temperature and growth rate, attributing shifts in population growth rate to plaice density, eutrophication, and seabed disturbance by beam trawling (Rijnsdorp and Van Leeuwen 1996). During the 1960s-1970s a major increase in growth rate was reported for both plaice and sole in the North Sea (Rijnsdorp and Van Leeuwen 1996). This increase could not be related to changes in temperature, but coincided with an increase in both eutrophication and intensity of beam trawling (Rijnsdorp and Van Leeuwen 1996). However, contrasting studies within the North Sea found the juvenile growth was positively correlated with bottom temperature, whereas growth of adults was negatively correlated with bottom temperature; concluding that for juveniles, the temperature–growth relationship likely reflects a response to growing season length while for adults it could reflect temperature-dependent changes to metabolic rate or food availability (Sleen et al., 2018).

In order to study juvenile plaice *in situ* growth trends studies utilised RNA quantities in muscle fibers to explain underlying causes, including maximum growth, temperature, prey conditions and competition (Ciotti et al., 2010). RNA-based estimates of the individual level daily growth rates (G, day−1, measured using white muscle RNA and DNA concentration), coupled with experienced water temperatures (calculated at the time of capture), and fresh body mass have been used to examine the extrinsic parameters impacting *in situ* plaice growth rates (Ciotti et al., 2010); aiming to test the effects of temperature on growth over small scale (25km) gradients (Ciotti et al., 2010). The findings of this

study report no predictable relationship between temperature and growth rate, unable to predicted *in situ* growth trends from extrinsic variables alone (Ciotti et al., 2010). The same studies find that growth is predictable from total growth, food availability and condition, suggesting that plaice growth might be closely linked to growth phenology and individual physiology. However, with the inclusion of intrinsic energetic demand and experienced temperature we hope to aid with explaining more of the deviance within the data (Ciotti et al., 2010).

From these studies, it is apparent that we do not fully understand the mechanisms controlling fish growth. Potentially the incorporation of field metabolic rate measurements might help with reducing some of the unexplained variability within growth rate studies. Such data would potentially improve our understanding of the level of energetic resources partitioning (amount of resources diverter towards growth, predation and other behavioral practices), performed by individuals.

## 1.15 Questions tackled in this thesis

In this thesis I draw on otolith-based estimates of FMR in plaice to explore three principle questions: In chapter 2 I explore how relationships between *in situ* FMR, body mass and temperature can be related to established metabolic theories of ecology, in an attempt to test the basic assumptions, such as metabolic scaling relationships, are applicable to natural data.

Chapter 3 explores how individual FMR varies across seasons. Feeding and seasonal cycles influence energy needs and energy budgets. Such seasonal variations may result in time periods when the population is more vulnerable to environmental instability, and could potentially identify which extrinsic variables are important for community performance over the monthly cycle. Here I aim to identify the controlling factors of metabolic variability over the annual cycle.

Chapter 4 explores relationships between experienced temperature, growth and FMR. Growth rate is a key response variable commonly used by fisheries scientists and ecologists to assess the health of a population. Growth rate has been observed to vary with environmental stressors, such as decadal shifts in climatic conditions, fishing pressure and many more. Fishing quotas are formed by measuring the abundance of different size classes of individuals within the population, in an attempt to predict the stock spawning biomass and the associated economic value. However, studies looking into *in situ*

growth rate and dynamic energy budgets point out that observations do not always agree with predicted population trends, and that at this stage we are unable to explain the intrinsic and extrinsic factors responsible for wild population growth rate. The same studies suggest that a measure of *in situ* energetic demand, and how field metabolic rate interacts with both physiological and environmental factors will potentially aid with explaining and consequently modelling growth rate trends. Here we combine FMR, experienced temperature and otolith increment width measurements over the life history of the individual, in attempt to explore the intrinsic and extrinsic factors responsible for growth rate trends.

Finally, my results and their implications are synthesised in a discussion chapter.

# 2 European Plaice Otolith derived Field Metabolic rate Thermal Dependence – Published with a special issue of Frontiers in Marine Science on Stable isotope applications in ecology

## 2.1 Abstract

In recent years fish metabolism has been identified as a key variable used to explain shifts in population distribution and output. Under laboratory conditions oxygen consumption rates scale predictably with both body mass and temperature. Such observations have led to the formation of several theoretical metabolic frameworks attempting to explain the relationship between energetic demand and shifts in population geographical distributions, abundance and individual-level physiological characteristics (such as size and growth rate).

Laboratory-derived respiratory potential data (meaning the maximum and minimum respiration rate an individual can sustain in a controlled environment) paired with theoretical frameworks have been used to model fish responses in terms of biogeography and population abundance to future climate scenarios; with results suggesting northerly shifts in distribution (within the northern hemispheres) to environmental conditions which better suit their physiology, coupled with a reduction of individual length and age of maturity.

In recent years the applicability of a study framework that builds on observations of independent interactions between environmental conditions and metabolism under laboratory conditions, to wild fish populations has been questioned. *In situ* individual-level data of fish metabolic expression is needed to quantify the realised sensitivity of fish energetics to combinations of intrinsic and extrinsic factors, such as prey availability, individual behaviour, natural phenotypic expression and the adaptive (generational and individual levels) capacity of wild fish.

Here we apply a newly emerging proxy for estimating field metabolic rate (FMR) in marine fishes, drawing on $\delta^{13}C$ values from otolith aragonite to estimate the proportion of respiratory $CO_2$ within the blood (and, therefore, the rate of oxidation of dietary carbon), alongside with otolith derived experienced temperature. We apply the otolith FMR proxy to a population of European plaice from the North Sea during a period of rapid warming between the 1980s to the early 2000s and throughout individual life history (juvenile and adult) stages. Using a time-integrated *in situ* measurement of energetic demand we quantify among individual variations in FMR and the relationship to extrinsic and intrinsic parameters such as body size and temperature.

Realised FMR expressed either a very small degree of covariance with both body size and temperature for adult life stages, suggesting that temperature and body size-dependent sources of among-individual variation in FMR outweigh commonly assumed drivers of individual metabolic rate variability. During juvenile life stages, FMR does covary positively with experienced temperature, suggesting that the environmental, behavioral and physiological variables which impact energetic demand, consequently forming FMR expression, are not consistent throughout individual life history.

We also find evidence of metabolic phenotypic expression within this data set. Within a single otolith, relative individual level FMR scaling among individuals is conserved between juvenile and adult life stages, despite absolute metabolic expression differing between time periods. Individual metabolic phenotype explains a greater proportion of among-individual variation in FMR at year 4 than either body size or temperature. We are unable however to determine whether conditions experienced during early life stage impact adult metabolic expression or if differences in physiological energetic demand are inherited genetic effects.

Stable isotope-derived estimates of field metabolic rate have great potential to expand our understanding of ecophysiology in general and especially mechanisms underpinning the relationships between animal performance and changing environmental and ecological conditions.

# 2.2 Introduction

## 2.2.1 Effects of Temperature on Fish Performance

The physiological performance of wild fishes reflects the interaction between the individual phenotype and the availability of resources (Seebacher 2005; Binning et al., 2015; Metcalfe et al., 2016; Killen et al., 2017; Duncan et al., 2019; Devlin et al., 2020; Scott and Dalziel 2021). The relationship between fish physiology and environmental conditions is inherently complex (Fablet et al., 2009; Agüera et al., 2017; Monaco and McQuaid 2018), drawing on multiple interactive internal and external processes (such as predation, prey availability, habitat selection preference, reproduction and many more) (Hoar et al.,1983), which are difficult to simulate in laboratory conditions (Nussey et al., 2007; Nisbet et al., 2000'; Nisbet et al., 2012). Consequently, how to produce field-relevant predictions of how fish performance will respond to environmental change has been a contentiously debated topic within the field of fisheries sciences for several decades (Mieszkowska et al., 2009; Albouy et al., 2013; Chung et al., 2020). Population growth, size and distribution (and consequently fisheries production) depends on the energetic efficiency with which individuals can acquire and assimilate the available resources (Forster et al., 2012; Pinsky et al., 2013; McCauley et al., 2015; Lindmark et al., 2022). In a changing climate, fish production also depends on the ability of a population to either adapt their physiology to changing conditions or migrate towards more favourable habitats (Perry et al., 2005; Dulvy et al., 2008; Forster et al., 2012; Violle et al., 2012; Killen et al., 2013; Lindmark et al., 2022). Predicting the responses of fishes (either as individuals or populations) to climate change requires consideration of the mechanistic effects of external drivers on physiology (Neuheimer et al., 2011; Baudron et al., 2014; Huss et al., 2019).

External water temperature is one of the most commonly measured environmental drivers in fish ecophysiology (Deutsch et al., 2015a). The body temperature of ectothermic fishes closely matches that of the external water, so temperature influences fish physiology directly (Brander 2010), as well as through the inverse relationship between temperature and oxygen solubility. Changes in water temperature may produce multiple complex biological responses, including behavioral (such as large- or small-scale migratory responses), changes in feeding intensity, activity levels (Murawski 1993) or physiological effects (such as metabolic responses or changes allocation of energy resources) (Tonn

1990; Roessig et al., 2004; Rijnsdorp et al., 2009; Little et al., 2020). Furthermore, responses are likely to vary depending on the magnitude and rate of experienced temperature variation relative to the long-term average climate in the population's home range (Volkoff and Rønnestad 2020; Hazel 1984; Gandar et al., 2017), and are likely to vary with local context such as availability of resources (Vinton and Vasseur 2022). From a physiological perspective, metabolic effects of temperature have received the most attention in terms of attempting to explain fish distributions and predict changes to fish production and distributions in future climatic conditions (Sinnatamby et al., 2015; Chung et al., 2019; Martino et al., 2019; Chung et al., 2021).

### 2.2.2 Metabolic Rate as a Thermally-Sensitive Performance Trait

Metabolic rate represents the sum of all energetic activity in an organism. Metabolic rate therefore integrates multiple physiological and potentially behavioral responses, and is a useful trait as a proxy for whole animal performance (Treberg et al., 2016). Metabolic rate reflects the rates of chemical reactions (enzyme-mediated oxidation of food resources), and is therefore directly influenced by temperature (Bruno et al., 2015). At temperatures below the range of optimum performance, basal (standard) metabolism is thought to be limited by the thermodynamics of enzyme kinetic reactions (Reid et al., 2011; Clark et al., 2013). Consequently, metabolic rates are expected to follow Arrhenius-type thermal response curves, with the thermal sensitivity of whole organism metabolic rates similar to the activation energy of enzyme reactions, close to 0.65eV (Brown et al., 2004; Pauly 2021). However, in many cases thermal response curves for (maximum) metabolic rates are parabolic, with a thermal optimum and a decline in metabolic rates where (sub-lethal) temperatures exceed the thermal optimum (Neubauer and Andersen 2019; Andersen and Beyer 2006). There are two principle theoretical frameworks aiming to explain metabolic limitation. Thermal limitation may occur due to declining performance of enzyme proteins due to structural effects associated with denaturing (limiting enzymatic reaction rate) (Clark et al., 2013), or due to limitations on the capacity to acquire, process and distribute resources (especially oxygen) through the body (Clark et al., 2013).

The gill oxygen limitation theory (GOLT), and associated Oxygen and Capacity Limited Thermal Tolerance (OCLTT) framework, explain parabolic thermal performance curves by suggesting that oxygen supply concentration at high temperature is below the demand concentration (Pauly 2021), and that population performance is maximised at temperatures providing maximum optimum aerobic scope

(Pörtner 2010; Pörtnerr and Knust 2007). Mobile animals such as fishes are expected to avoid limiting (chronic) temperatures, and thus thermal limitation of metabolic performance may be limited to populations at range edges, or under acute heat wave / cold shock conditions (Neubauer and Andersen 2019).

Despite uncertainty remaining over the applicability of laboratory-derived thermal response curves to wild conditions (Fablet et al., 2009; Nisbet et al., 2012), thermal response curves have been used to predict population and species biogeography by mapping how the distribution of habitat optimum for population functionality (derived from aerobic scope measurements) is likely to expand, reduce or shift in latitude according to future climate model scenarios (Rutterford et al., 2015). This approach suggests wide scale population shifts, to higher latitudes, with dramatic changes in population assemblages and ecosystem functionality (Nisbet et al., 2012; Comte and Grenouillet 2013; Thomas et al., 2019).

As stressed above, however, in natural settings, behavioral and physiological responses of fishes to temperature are likely to vary depending on the magnitude and rate of experienced temperature variation relative to the long-term average climate in the population's home range. Predictions of fish community responses to temperature gradients based on laboratory-determined metabolic performance curves may not be directly applicable to *in situ* fish communities due to the adaptive capacity of natural populations, (Skelly et al., 2007; Hofmann and Todgham 2010; Donelson et al., 2012; Healy and Schulte 2012; Norin et al 2014; Holt and Jørgensen 2015; Wootton, Audzijonyte, 2021; Wootton et al., 2022;) and energetic trade-offs for animals operating within aerobic scope (Neubauer and Andersen 2019). The assumption that populations centralise around optimum conditions for physiology (Daan 1973; Daan et al., 1990; Van der Veer and Witte 1993; Rijnsdorp and Vingerhoed 2001; Hiddink et al., 2008; Van der Veer et al., 2009; Wootton et al., 2022) have also been questioned (Del Raye and Weng 2015).

### 2.2.3 Variation in Thermal Sensitivity of Metabolic Rate

The realised thermal sensitivity of fish performance under wild conditions reflects a combination of direct thermodynamic effects on reaction rates, limitations to performance from capacity to supply oxygen and nutrients, and behavioral energetic trade-offs, all moderated through the phenotypic and genotypic adaptive capacity of the population (Van Denderen et al., 2021; Vinton and Vasseur 2022).

Purely thermodynamic effects of temperature are expected to increase reaction rates through Arrhenius-type responses with an activation energy of 0.65 eV (Kozlowski and Konarzewski 2005). This therefore provides an end member prediction of thermal sensitivity for performance against which field performance can be compared. Fish growth rates for instance show lower thermal sensitivity to average temperature expressed as a $Q_{10}$ of c. 1.1-1.5 compared to c. 2-2.6 predicted from activation energies of $0.65_eV$ (Van Denderen et al., 2021).

Teleost fish typically increase body size over orders of magnitude during growth, with strong selection pressure acting to maximise growth in early life, but less in later life. Changes in energy allocation across life stages could potentially induce differences in the thermal sensitivity of field metabolic rate across life history stages in an individual fish (Metcalfe et al., 1995; Dahlke et al., 2020). Laboratory studies have suggested higher thermal sensitivity for standard metabolic rates in early juvenile life stages of fishes (reviewed in Dahlke et al., 2020), due to a number of factors, including smaller body sizes. If so, attempts to predict fish performance and distribution through bioenergetic models should consider life stages separately. If varying life stages do differ in metabolic thermal response the impact of environmental shifts will vary within a population, potentially with an increased juvenile mortality compared to adult life stages, or rapid environmental metabolic phenotypic selection. Similarly, for a population operating within its aerobic scope, the thermal sensitivity of field metabolic rate may vary systematically across seasons, reflecting variations in availability of food resources and life cycle variations in energy partitioning associated with feeding, migration and reproduction.

In order to further our understanding of population dynamics, with an aim to improve the predictions of sustainable harvest levels for fisheries, we need to understand how *in situ* energetic demand varies with temperature (Nisbet et al., 2000; Freitas et al., 2010), across seasonal cycles and with life stage (Nisbet et al., 2000; Dahlke et al., 2020). Understanding how requirements of an individual, such as how energetic partitioning towards growth or reproduction, are impacted by environmental and physiological variables will aid with ecological models and policy formation. We also need to identify if field metabolic rate (the energetic response of the entire organism to the physical and ecological environment) acts in a similar manner to laboratory-based measurements of standard metabolic rate, as predictive models use respiratory potential data to estimate biogeography (Nisbet et al., 2000). Models predicting fisheries population dynamics over the seasonal cycle use mass and temperature scaling relationships to estimate population level energetic demand, with little data supporting the relevance

of these measurements (Freitas et al., 2010). By identifying energetic trends in wild populations over the seasonal cycle, over thermal ranges and across life stages we potentially can improve model predictions and reduce the uncertainty of biogeographical estimates.

### 2.2.4 Stable Isotope Based Estimation of Field Metabolic Rate

Here we apply a newly emerging method for deriving *in situ* FMR, termed otolith-derived FMR (Chung et al., 2019; Alewijnse et al., 2021). The otolith-derived FMR method is based on using stable isotope compositions of carbon sources recorded in otolith carbonate as a natural tracer for the rate of production of respiratory carbon. This method draws on the observation that carbon in biogenic carbonates is derived from two isotopically-distinct sources of carbon: dissolved inorganic carbon (DIC) from seawater, and metabolic carbon released from the respiration of diet (Chung et al., 2019; Alewijnse et al., 2021). As fish regulate blood carbonate concentrations to maintain optimum blood pH, when metabolic rate increases (with respiration) the proportion of respired carbon contributing to the blood carbonate (and consequently otolith aragonite) increases relative to the other sources (Chung et al., 2019; Alewijnse et al., 2021). In marine fishes, dietary derived carbon has a $\delta^{13}C$ value typically in the range (c. -12 ~ -25‰) (Trueman et al., 2017; Trueman and St. John Glew 2019; St. John Glew et al., 2019), while the isotopic composition of DIC in surface seawater averages around 1‰ (Tagliabue and Bopp 2008; Schmittner et al., 2013). Increasing the proportion of respiratory carbon in the blood therefore results in lower $\delta^{13}C$ values in the otolith. The proportion of respiratory carbon contributing to otolith aragonite ($C_{resp}$) can then be estimated by isotopic mass balance given measurements of otolith $\delta^{13}C$ values and measurements or estimates of $\delta^{13}C$ values of diet and DIC.

Many studies have demonstrated relationships between $\delta^{13}C$ values of otoliths and relative metabolic rates (Kalish 1991; Sherwood and Rose 2003; Shephard et al., 2007; Niloshini et al., 2015; Sinnatamby et al., 2015; Chung et al., 2021; Alewijnse et al., 2021;). The relationship between $C_{resp}$ values and oxygen consumption rates can be estimated in laboratory experiments, using temperature to manipulate metabolic rates. Such experiments suggest an exponential limited relationship between $C_{resp}$ values and oxygen consumption rates (Chung et al., 2019; Chung et al., 2019b; Martino et al., 2020), meaning a linear relationship at lower FMRs, but at energetic demand increases the linear relationship breaks down due to unknown factors. It is possible that the non-linear portion of the relationship is influenced

by metabolic demands other than SMR contributing to oxygen consumption at high temperatures, these metabolic demands at this stage in FMR research is unknown, however we hypothesis it is due to oxygen limitation, digestion rate and potentially the rate of acclimation to higher temperatures requiring longer than allowed to fully capture MMR and SMR measurements. We are at present designing statistical models and laboratory experiments to test the reasons for this nonlinear component of the FMR thermal response curve.

Otolith derived field metabolic rate has been tested in wild populations and in laboratory settings against SMR and MMR measurements, expressing predictable variability in $C_{resp}$ values with oxygen consumption rates, suggesting that otolith aragonite $\delta^{13}C$ values detect enough variability in wild populations to identify broad scale *in situ* metabolic trends (Chung et al., 2019; Chung et al., 2021).

Other examples where otolith derived FMR (otoFMR, defined separately as there are other methods used to derive FMR which have previously been described) has been applied to natural settings include testing metabolic scaling relationships within myctophid species from the Scotia Sea (Alewijnse et al., 2021), finding that $C_{resp}$ values range between 0.123 to 0.248 and that ecological and physiological differences among species are better predictors of variation in Cresp values than body mass and temperature (Alewijnse et al., 2021). When myctophid Cresp results are compared to estimates of metabolic rates derived from scaling relationships, they find estimates of oxygen consumption from different methods are broadly similar, however, there are considerable discrepancies at the species level (Alewijnse et al., 2021). Chung et al., 2021 showed that genetically distinct ecotypes of juvenile Atlantic cod from the Skagerrak coast of southern Norway expressed different thermal performance curves for field metabolic rate; cold-adapted fjord ecotypes maintaining higher field metabolic rates at cooler temperatures than the warm-adapted North Sea ecotype, which showed clear preference for warmer waters around the thermal optimum (Chung et al., 2021). This data suggests that there is a genetic component to metabolic expression and that physiological conditions in the field should be considered in the evaluation of the effect of climatic variables on fish population dynamics (Chung et al., 2021).

European plaice *Pleuronectes platessa* (henceforth, plaice) are a commercially exploited species, with an associated North Sea benthic trawling fishery that supports fishing industries over a relatively wide geographical range (Hunter et al., 2009; Ciotti 2012; Ciotti et al., 2014; Darnaude et al., 2014). The

fishery has existed in some form for hundreds of years (Ciotti et al., 2014), but commercially monitored from the 1800s. Otoliths are routinely removed from North Sea plaice for age and growth studies, and the UK fisheries laboratory Cefas have maintained an otolith archive with (incomplete) sampling dating to the early 1900s. Due to their commercial value, plaice have been a highly studied species, with annual fisheries population dynamic reports measuring mortality, stock spawning biomass and many more fisheries monitoring techniques in attempts to predict the maximum sustainable yield (Hunter et al., 2009; Ciotti 2012; Darnaude et al., 2014). It is because of these factors why we have chosen North Sea plaice as a model species within this study, as the North Sea meta data is readily available, with regular Cefas otolith sampling, and the economic importance of the species.

In this study we use otolith isotope-derived estimates of field metabolic rate to quantify the relationship between experienced temperature and expressed field metabolic rate across seasons and life stages in a wild fish (plaice).

## 2.3 Methods

### 2.3.1 Sample Selection

Plaice otoliths were obtained from Cefas archived otolith collections taken from research fishery cruises conducted as part of ICES coordinated bottom trawling surveys in the North Sea. From the 1970s to recent time periods within the North Sea system there have been multiple observed shifts in fish population distribution and physiology (Clark et al., 2003), including species extending their geographical range to higher latitudes and greater depths with environmental conditions believed to better suited to their physiological capacity, as well as quickening life cycles and reduced body length when reaching maturity (Murawski 1993; Perry et al., 2005; Dulvy et al., 2008). These observational shifts within the North-Sea system have been correlated to increased summer and winter average water temperatures (Perry et al., 2005), and it has been suggested that the findings pose a significant threat to the future of ecosystem functionality (Pörtner and Farrell 2008). Sampling therefore aimed to capture seasonal variations together with potential historical differences between years with warm and cold mean water temperatures.

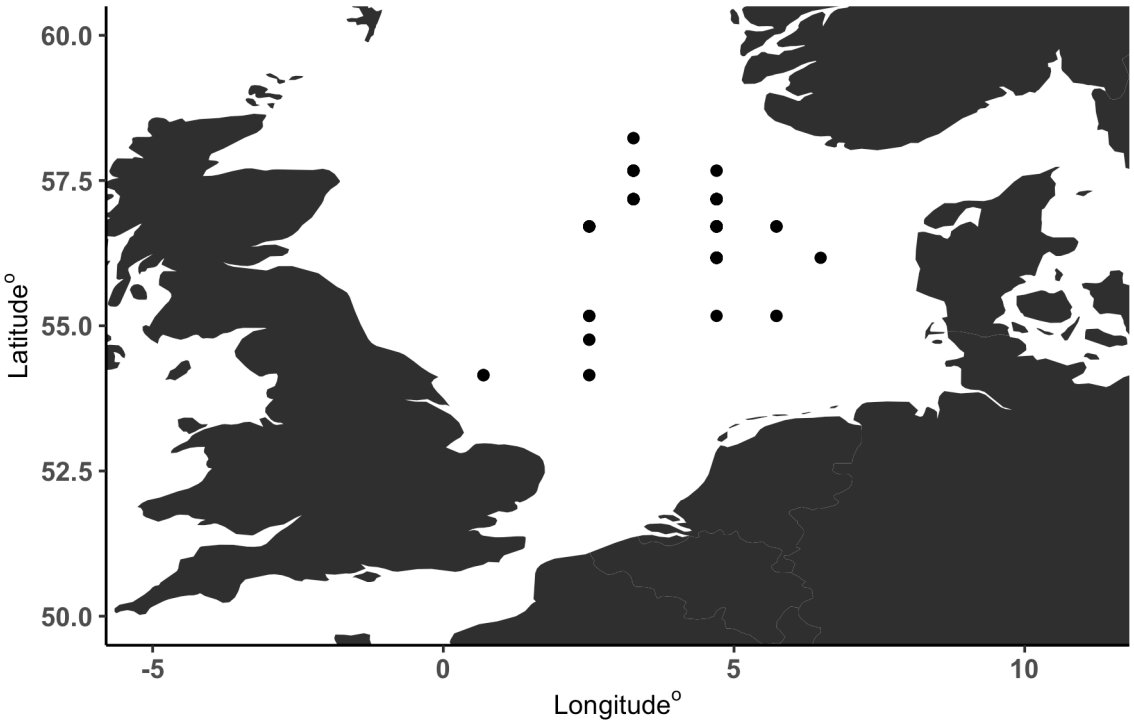


***Figure 14**: Representing the sample capture locations for individuals analysed within this chapter. Samples were taken from the Cefas groundfish surveys, and are trawling locations, therefore each point is a trawling site and multiple fish come from each point. They aim to cover all ICES rectangles within the North Sea, however we could only find plaice from these locations, and samples taken for analysis was reduced due to COVID.*

558 individual otolith samples analysed within this study were collected during Cefas beam trawl surveys, spanning all four fishing monthly quarters (1 = January-March, 2 = April-June, 3 = July-September, 4= October-December) and North Sea ICES areas IVB and IVC. We chose to only include these areas to minimise potential geographical dependent metabolic variability, arising from evolutionary differences between separate populations and different average environmental conditions (Figure **14**), we are currently designing a study to investigate the impact of genetic separation and evolutionary development of FMR between populations. All otoliths were pre-aged by Cefas sclerochronologists (Carbonara and Follesa 2019). To minimise age-dependent metabolic variability and sample fish with a relatively high growth rate (for larger volumes of otolith available for sampling), sample selection targeted individuals assessed to have been spawned 4 years prior to capture. Otoliths were selected from survey years with high sample coverage and specific biological regimes (Table **1**). North Sea annual average water temperature experienced a significant period of warming within ICES areas IVB and IVC from 1980s-2010 (Núñez-Riboni and Akimova 2015), otoliths were therefore selected from years reflecting colder (pre-1990) and warmer (post- 1990) periods as well as periods with relatively high and low place abundance. We attempted to produce a systematic time series, but were unable due to COVID restrictions reducing visits to Cefas otolith archive. The full list of ICES rectangles sampled and individual distribution across each quarter is provided within the supplementary material. The sample years selected were 1984, 1985, 1986, 1987, 1990 1993, 1995, 1997, 1998, 1999, 2001 and 2002; The distribution of data throughout sexes and years is presented in (Table **1**).

***Table 1**: Representing the distribution of Samples selected for analysis throughout years, sub populations and sexes, used within this chapter. Otolith samples were collected form CEFAS otolith archive, specifically the ground fish survey. The data is split by North Sea plaice sub-populations, which individuals have been assigned to using previous tagging, isotopic analysis and experienced extrinsic variability studies (Hunter et al., 2009; Darnaude at al., 2014). Year Regime represents the reason why this year was selected for analysis.*

| | | **Males (n)** | | | **Females (n)** | | |
|---|---|---|---|---|---|---|---|
| **Year** | **Year Regime** | **A** $_{\text{sub population}}$ | **B** $_{\text{sub population}}$ | **C** $_{\text{sub population}}$ | **A** $_{\text{sub population}}$ | **B** $_{\text{sub population}}$ | **C** $_{\text{sub population}}$ |
| 1984 | Cold Year | - | 2 | 1 | - | 1 | 3 |
| 1985 | Cold Year | 13 | 10 | 9 | 11 | 4 | 3 |
| 1986 | High recruitment | 10 | 7 | 8 | 7 | 11 | 8 |
| 1987 | Cold Year | 6 | 4 | 7 | 20 | 6 | 7 |
| 1990 | Warm Year | 13 | 2 | 8 | 13 | 4 | 10 |
| 1993 | Low SSB | 12 | 3 | 7 | 19 | 3 | 6 |
| 1995 | Low SSB | 12 | 2 | 4 | 17 | 5 | 10 |
| 1997 | High recruitment | 12 | 5 | 1 | 26 | 3 | 3 |
| 1998 | Warm Year | 14 | - | 2 | 28 | - | 6 |
| 1999 | Warm Year | 18 | 1 | - | 31 | - | - |
| 2001 | High recruitment | 12 | 6 | 4 | 8 | 11 | 9 |
| 2002 | Warm Year | 10 | 9 | 2 | 19 | 6 | 4 |
| **total** | | **132** | **51** | **53** | **199** | **54** | **69** |

### 2.3.2 Sample Preparation

The otolith preparation protocol followed previous work (Chung et al., 2019; Chung et al., 2021). Initially otoliths were cleaned with fresh water to remove any residue tissue, and fixed to an epoxy (Struers Eopfix resin) mount with the proximal (sulcus) surface uppermost. Otolith sampling was designed to provide sufficient powder while averaging over the smallest time interval possible. The external otolith surface area representing the most recent period of aragonite deposition was then sampled, using a Dremel 4000 rotary engraving tool, with straight sided, cylindrical diamond-encrusted bits. Sampling was performed at low rotation speed, with the shaft of the drill bit touching at an incident angle to the otolith surface allowing the most efficient recovery of powder. Aragonite powder was collected from the surface of the resin block containing otoliths by tapping powder into a weigh paper. Following external edge sampling, a subset of the otoliths was sectioned (to approximately 20$\mu m$ thickness) at the University of Southampton thin sectioning laboratories. Otolith sections were used to visually estimate the depth of external milling and therefore the time period of sampled otolith growth (and the time period which FMR and temperature is integrated), and to provide access to the first year of growth for analyses of FMR and temperature during juvenile life stages. Otolith thin sections were photographed and the time period represented by the milled sample (described in chapter 4), individual age, growth and marginal otolith condition (opaque or translucent) was estimated from digital images using ImageJ (Schneider et al., 2012) in combination with the ObjectJ plug-in. Otolith growth representing the second half of the first year of life was sampled using an ESI New Wave Micromill either by milling trenches and/or from multiple drill holes (described in Growth rate chapter). Otoliths were independently read by two otolith readers to check data quality.

### 2.3.3 Mass spectrometry

The stable isotope compositions of carbon and oxygen in otolith aragonite were measured at the Stable Isotope Ratio Mass Spectrometry Laboratory (SEAPORT Laboratory, Southampton, UK), with a Kiel IV Carbonate device coupled with a MAT253 isotope ratio mass spectrometer. Approximately 20-70 $\mu g$ of aragonite powder was accurately weighed into borosilicate glass reaction vessels prior to evolution of $CO_2$ through reaction with phosphoric acid. The calibration standards used were NBS 19 and NBS 18, as well as a quality control GS1 (Carrara marble produced by the SEAPORT laboratory).

Results are reported in permil (‰) (as $\delta^{13}C$ and $\delta^{18}O$ values) relative to Vienna Pee Dee Belemnite. Accuracy and precision determined from long-term analyses of internal standards of known composition is 0.01 ‰ for both $\delta^{13}C$ and $\delta^{18}O$ of otolith aragonite. The standard deviations determined from repeated measures of internal standards in each run are presented in the supplementary materials.

### 2.3.4 Estimation of the Proportion of Metabolic Carbon in Otolith Aragonite

We estimated the proportion of respiratory carbon in otolith aragonite ($C_{resp}$) from a two-component mixing model as described by (Chung et al., 2019; Chung et al., 2019b):

$$C_{resp} = \frac{(\delta^{13}C_{oto} - \delta^{13}C_{DIC-sw})}{(\delta^{13}C_{diet} - \delta^{13}C_{DIC-sw})} + \epsilon_{total} \qquad (2.1)$$

Where $\delta^{13}C_{oto}$ represents the $\delta^{13}C$ values of the sampled otolith aragonite, $\delta^{13}C_{DIC-sw}$ represents the $\delta^{13}C$ value of dissolved inorganic carbon (DIC), $\delta^{13}C_{diet}$ represents the $\delta^{13}C$ value of individual diet (Chung et al., 2019) which is collected from the mussel of an individual or in this case from a previous study by Jenning and Cogan (2015) that measured the $\delta^{13}C_{diet}$ of multiple Plaice throughout the North Sea. $\epsilon_{total}$ is the total isotopic fractionation from DIC and diet to blood, blood to endolymph and endolymph to otolith (Chung et al., 2019; Chung et al., 2019b). The absolute value of $\epsilon_{total}$ may vary among species, and requires further laboratory experimentation to calculate. Within this study, we assume that $\epsilon_{total}$ does not vary systematically among individuals of the same species and is set to 0 (Chung et al., 2021). Without more laboratory experiments we are unable to tell is the fractionation of from DIC and diet to blood changes between species, so we have set it to 0 in this study, meaning there is unlikely to be a source of error introduced between individuals, but between species it is likely to change, however as we are looking into one species this is unlikely to affect the results. $\delta^{13}C_{diet}$ values were estimated based on a compilation of stable isotope data from plaice from the North Sea provided by Jenning and Cogan (2015), ranging from -19.4‰ to -14.5‰ (varying due to geographical distribution), averaging -16.8‰. $\delta^{13}C_{DIC-sw}$ values were estimated from Burt et al., 2016, who presented spatially-explicit $\delta^{13}C_{DIC}$ values from across the North Sea collected in September 2011 by (Burt et al., 2016) (ranging from 0.5‰-0.8‰ averaging 0.613), and adjusted for the Suess effect (the decrease in $\delta^{13}C_{DIC-sw}$ over time due to anthropogenic carbon emissions since the industrial revolution) (Tagliabue and Bopp 2008). Confidence limits upon model estimates are presented in

model output tables (Table **3**). Standard errors for Cresp and temperature values are caulculated using Monte Carlo resampling and presented in table **3**. In subsequent analyses we take the median of the posterior distribution for Cresp values.

### 2.3.5 Estimating Oxygen Consumption Rates

To assist with comparisons with alternative measures of metabolic rate (such as aerobic scope), Cresp was converted into oxygen consumption rate using a previously calculated statistical calibration, based on juvenile cod individuals (Chung et al., 2019; Chung et al., 2019b). This statistical conversation subjected cod to various temperature-controlled laboratory conditions accompanied with SMR and MMR measurements, to defined variables for equations **2.2** and **2.3**. The relationship between Cresp values and oxygen consumption rates are best estimated as an exponential model with an upper limit ('C') reflecting the maximum proportion of respired carbon that the fish can maintain in the otolith (and thus endolymph and blood). A similar calibration experiment applying a statistical calibration with the temperate Australian snapper *Pagrus auratus*, returned a calibration with a similar exponential form, but different parameters (Martino et al., 2018), reflecting likely species-specific variations in the proportions of respiratory carbon tolerated in the blood. Here we apply both published statistical calibration models to the plaice data, recognising that the estimated mass-specific oxygen consumption rates may require re-assessment as and when calibration experiments are performed for plaice. The use of Cod parameters to predict Plaice oxygen consumption is unlikely to affect intraspecific trends, which is what we are focusing on within this study. It is likely to impact inter specific trends, making it difficult to compare metabolic trends to other species here. This means the data is

$$C_{resp} = C\left(1 - e^{-k(\text{Oxygen Consumption Rate})}\right) \qquad (2.2)$$

$$\text{Oxygen Consumption Rate} = \frac{\ln\left(1 - \frac{C_{resp}}{C}\right)}{-k} \qquad (2.3)$$

Equations **2.3** and **2.2** represent the calculation of Cresp and oxygen concentration rate. C represents an upper boundary nominally reflecting the maximum proportion of respiratory carbon that the fish can accommodate in blood (and therefore otolith aragonite) fitted as 0.243 and k is a decay constant

with a fitted value of $8.88 \times 10^{-3}$. The derived oxygen consumption from equation 2.3 is in the units of mg $O_2 kg^{-1} h^{-1}$.

### 2.3.6 Estimating Experienced Temperature

Time averaged experienced temperature was reconstructed using a species-specific otolith isotope temperature equation (Geffen 2012).

$$\delta^{18}O_C - \delta^{18}O_W = 3.72 - 0.19T(^oC) \qquad (2.4)$$

$\delta^{18}O$ values of the ambient sea water ($\delta^{18}O_w$) vary largely according to salinity, as freshwater inputs have lower $\delta^{18}O$ values than seawater. In the North Sea salinity varies considerably in space and time, complicating the use of oxygen isotope thermometry (see below). $\delta^{18}O_w$ values of the ambient sea water were initially estimated from the national aeronautical space administration's (NASA) "global seawater oxygen-18 Database" (LeGrande and Schmidt 2006), with model outputs presented in figure **15**. $\delta^{18}O_c$ represents the otolith aragoinite $\delta^{18}O$ values.

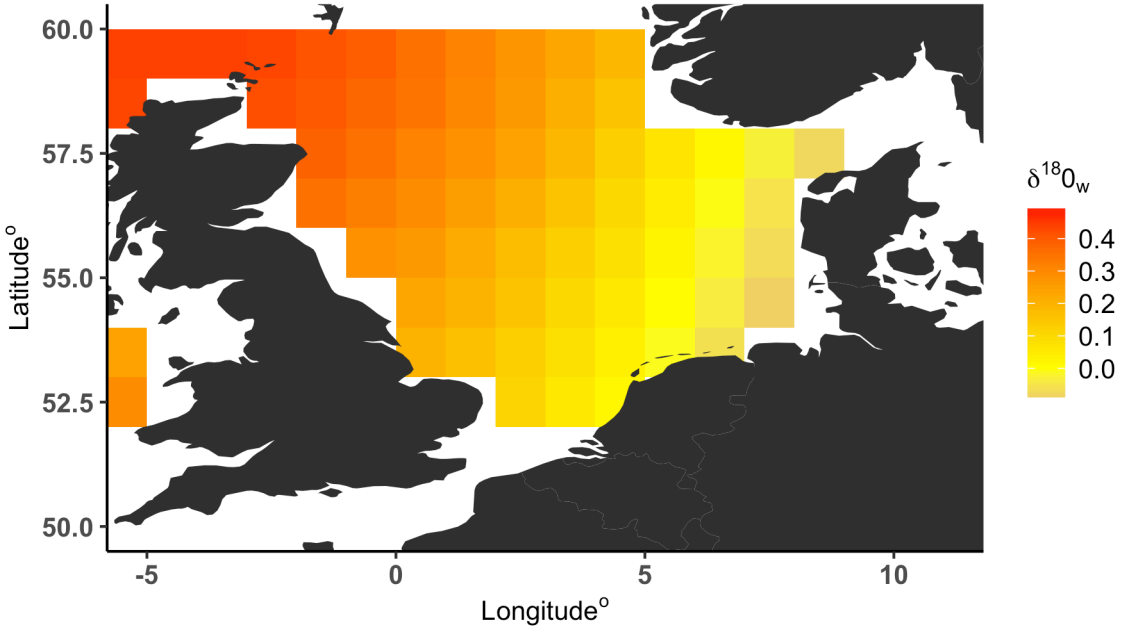


***Figure 15**: NASA global seawater oxygen-18 Database model outputs (LeGrande and Schmidt 2006). Subsetted to include only include benthic environments (bottom 5m) over the total 17-year range of data collection. Individual specific values were calculated from sample locations during adult life stages*

***Table 2**: The values used for each parameter of every equation and calculation used within this chapter, and sources of data used to calculate appropriate parameter values.*

## Adult Populations

| parameter | value | source | sD | source |
|---|---|---|---|---|
| $\delta^{18}O_w$ | 0.0135 (minimum) 0.294 (maximum) | (LeGrande and Schmidt 2006) | 0.1 | 95% CI range = 0.4 per mill (Trueman 2019) |
| $\delta^{18}O_{oto}$ | 0.0122 (minimum) 3.297 (maximum) | (SEAPORT Laboratory, Southampton, UK) | 0.05 | 95% CI range = 0.2 per mill (Trueman 2019) |
| $\delta^{13}C_{diet}$ | -16.82 (average) | (Jennings and Cogan 2015) | 0.25 | 95% CI range = 1 per mill (Trueman 2019) |
| $\delta^{13}C_{DIC}$ | 0.623 (average) | (Burt et al., 2016) | 0.1 | 95% CI range = 0.4 per mill (Trueman 2019) |
| $\delta^{13}C_{oto}$ | -2.45 (minimum) 0.7 (maximum) | (SEAPORT Laboratory, Southampton, UK) | 0.1 | 95% CI range = 0.4 per mill (Trueman 2019) |
| $Temp^{Slope}$ | -0.190 (average) | - | 0.01 | (Geffen 2012). |
| $Temp^{INT}$ | 3.72 (average) | - | 0.01 | (Geffen 2012). |

## Juvenile Populations

| | | | | |
|---|---|---|---|---|
| $\delta^{18}O_w$ | 0.1 (singular estimation) | (LeGrande and Schmidt 2006) | 0.15 | estimation from likely location (Hunter 2009) |
| $\delta^{18}O_{oto}$ | 2.081 (maximum) -0.917 (minimum) | (SEAPORT Laboratory, Southampton, UK) | 0.08 | estimation from likely location (Hunter 2009) |
| $\delta^{13}C_{diet}$ | -16.82 (average) | (Jennings and Cogan 2015) | 0.8 | estimation from likely location (Hunter 2009) |
| $\delta^{13}C_{DIC}$ | 0.623 (average) | (Burt et al., 2016) | 0.15 | estimation from likely location (Hunter 2009) |
| $\delta^{13}C_{oto}$ | -2.877 (minimum) 0.468 (maximum) | (SEAPORT Laboratory, Southampton, UK) | 0.15 | estimation from likely location (Hunter 2009) |

### 2.3.7 Assigning Individuals to Population

Plaice in the North Sea are divided into three sub-populations based primarily on spawning locations, which experience differing salinity environments (Darnaude et al., 2014). Sub-population B in particular experiences low salinity waters in the German Bight. As oxygen-isotope based temperature estimates require assumptions about the isotopic composition of oxygen in water (linked to salinity), we restricted estimates of temperature to individuals from sub-population A which experiences the least variable salinity conditions (Darnaude et al., 2014). As the population distributions potentially overlap, particularly during spawning migrations in winter (figure **16**, Darnaude et al., 2014), it is not possible to infer population membership simply from location at capture. We therefore drew on spatial distributions and isotopic data presented in Darnaude et al., 2014, to develop the following identification pipeline to assign individuals into most likely sub populations: Initially we drew on otolith $\delta^{18}O$ compositions and inferred experienced water temperatures using equation (**2.4**) and individual specific water $\delta^{18}O_w$ (figure **15**) based on sample location (figure **16**), representing full marine salinity.

- Individuals captured north of latitude $56^oN$ are assigned to group A. (Darnaude et al., 2014)
- Individuals with $\delta^{18}O$ otolith values in excess of 2.3‰ (indicating cold water temperatures and high salinity) are assigned to group A. (Darnaude et al., 2014)
- Individuals sampled north of latitude $56^oN$ but showing apparent experienced temperature higher than $14^oC$ (i.e. indicating low salinity and low $\delta^{18}O_W$ water values), are assigned to group B. (Darnaude et al., 2014)
- Individuals sampled in winter months east of $4^oE$ where apparent experienced temperature exceeds $11^oC$ (unrealistically warm inferred temperatures indicating low salinity) are assigned to group B. (Darnaude et al., 2014)
- Individuals captured west of longitude $2^oE$ are assigned to group C. (Darnaude et al., 2014)

- Individuals sampled in winter months sampled west of $4^{o}E$ showing apparent individual experienced temperatures $> 11^{o}C$ are assigned to group C (Darnaude et al., 2014).

The resulting otolith derived experienced temperatures were then compared to seawater temperature estimates from physical ocean modes described by (Núñez-Riboni and Akimova 2015) over the time integrated period and likely geographical range of movement (Darnaude et al., 2014). Subsequent analyses involving individual estimated temperatures were restricted to population A where experienced salinity fluctuations are limited to less than $1.5\%_{o}$ (between $36\%_{o}$-$34.5\%_{o}$) (Darnaude et al., 2014). This was used within this chapter to assign an individual to a likely sub population.

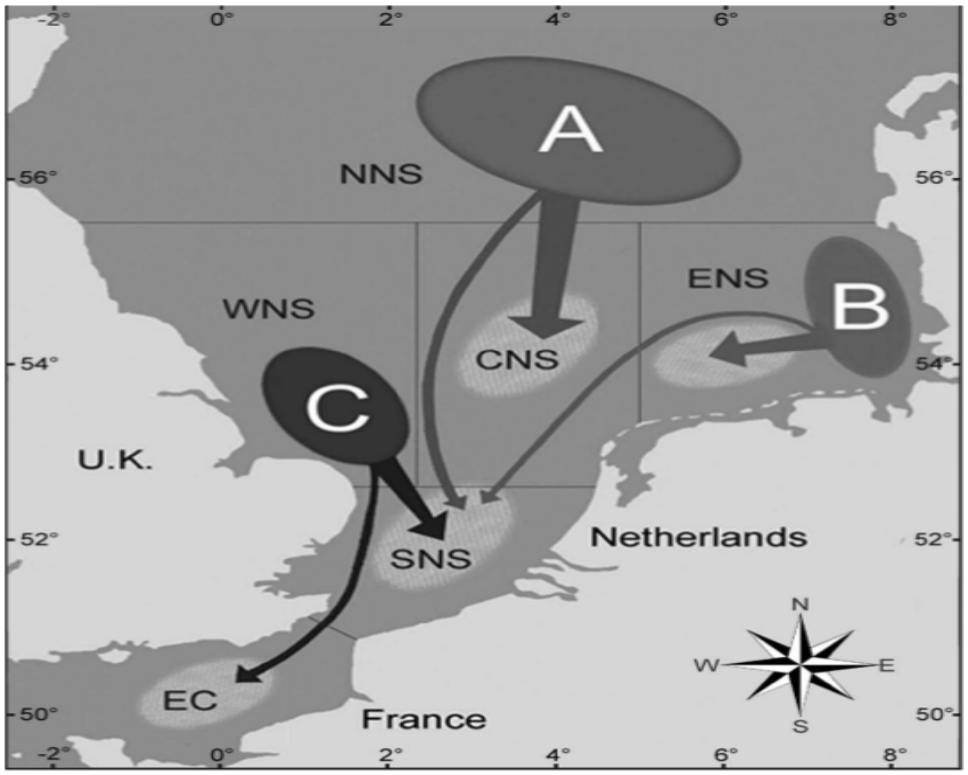


***Figure 16****: North Sea plaice sub population movements, representing separate feeding and common spawning locations. Adapted from Darnaude (2014). EC, meaning English Channel. SNS, meaning southern North Sea. WNS, meaning western North Sea. CNS, meaning central North Sea. ENS, meaning eastern North Sea. NNS, meaning northern North Sea.*

### 2.3.8 Condition

$$\text{Condition (g cm}^{-3}) = \frac{Weight(g)}{Length^3(cm)} \qquad (2.5)$$

We estimated condition to identify seasonal variations in energy storage and use, and potentially among-individual variations in performance (Bervoets and Blust 2003). Condition is defined in equation **2.5** (Bervoets and Blust 2003), where weight is in g and length is in cm. Cefas measure weight to the nearest 5g (giving a standard deviation of 2.5g), and measure length to the nearest cm (giving a standard deviation of 0.5). Condition standard deviations are calculated using Monte Carlo models and presented in Table **3**.

### 2.3.9 SMR Calculation

Variations in standard metabolic rate (SMR, in the units of mg $O_2 kg^{-1} h^{-1}$), based on body mass (in grammes) and temperature were estimated based on metabolic scaling relationships with body mass and temperature (here using otolith derived time averaged temperature $^oC$) across fish species (Clarke and Johnston 1999b; Gauldie 1996) described in equation **2.6**.

$$SMR = B_o \times BM^{\alpha} \times e^{\frac{-0.65}{8.62\times10^{-5}\times(T)}} \qquad (2.6)$$

$B_o$ is a normalisation constant, here taken as an average across multiple fish taxa (Chung et al., 2019; Chung et al., 2019b) and $\alpha$ is the allometric scaling exponent of body mass (BM), approximated here as a 3/4-power (i.e −0.25 (as the exponent) for mass-specific metabolism) (Brown et al., 2004) but is found to be 0.79 for teleost fishes (Clarke and Johnston 1999b; Clarke 2006).

### 2.3.10 Statistical Treatment of Data

Initially population ranges of Cresp values and experienced temperature were summarised and displayed graphically (figures **17**, **18**, **19** and **21**). A combination of linear models and Wilcoxon signed-rank test were used to compare the relationship between $C_{resp}$ values and experienced

temperature, sex, life stage and time period. A combination of mixed effect's models were then used to explore the interactions between environmental and physiological factors on Cresp expression. Due to this data set containing multiple continuous variables and no assumption of linearity GLMER models were selected. Sex, year and month are applied as factors within the GLMER structure, other terms such as Cresp, temperature and body mass are applied as predictor variables. REML structure was applied to all GLMER models. Model structures for adult Cresp, juvenile Cresp and the relationship between adult and juvenile Cresp expression (phenotypic expression) are all summarised in model outputs tables **4**, **5**, **6** and **7** as well as equations **2.7** and **2.8**. GLMER models were applied using the 'mgcv' (Wood 2011; Wood 2003; Wood 2004; Wood et al., 2016; Wood 2017) package and linear models using 'lmne4' (Bates et al., 2015) and 'ordinal' (Christensen 2019) packages with base R and optimised using AIC values.

## 2.4 Results

### 2.4.1 Population Assignment

From the overall sampled population (totaling 558), 281 samples were assigned to population A, 100 to population B and 73 to population C. $\delta^{18}O_{oto}$ values range between 0.0122‰ and 3.45‰ for population A averaging 2.38‰. For population B the range is between 0.892‰-2.29‰ averaging 1.63‰, and for population C the range was 0.991‰-2.76‰ averaging 1.93‰ (figure **17**). The results discussed below draw only on the individuals from population A, in an attempt to limit effects on uncertain $\delta^{18}O_w$ values in low salinity waters on inferred experienced temperatures. Juvenile samples represented here are a further random sub set of otoliths already sampled and assigned to population A. We are unable to model estimated temperature for juvenile life stages as we do not know the exact capture locations, but population A spawns in the central North Sea, with juveniles potentially experiencing higher salinity conditions at least compared to population B juveniles. To infer otolith derived experienced temperatures during juvenile life stages we assume a $\delta^{18}O_w$ value of $0.1‰_o$ presented in table **2**. We are unable to estimate model temperature estimates because they are based on time period and specific location, which we are unable accurately estimate from otolith increments alone. We are able to estimate otolith derived experienced temperature using a broad scale average of the southern North Sea $\delta^{18}O_w$ values, however this does produce a larger degree of associated error

with otolith derived temperature than in adults. This has since been validated by the publication of this chapter (Jones et al 2023).

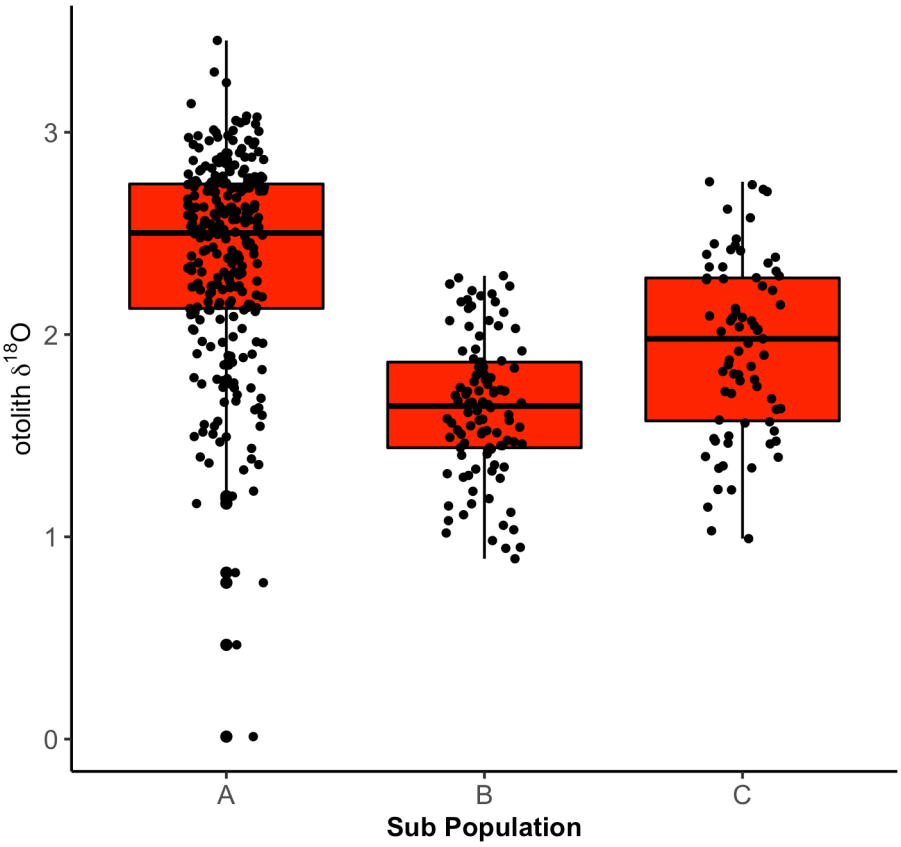


***Figure 17**: Otolith derived oxygen isotopic expression between separate adult life stage North-Sea Plaice sub-populations represented within this data set. Sub populations are estimated using Hunter (2003) tagging surveys, and Darnaude (2014) previously measured experienced temperature and oxygen isotopic values. Sub-population distributions are fully described Darnaude (2014).*

### 2.4.2 Estimating the Time Integration Window

The $\delta^{13}C$ and $\delta^{18}O$ values from population A (totalling 281 otoliths) used within this study are a combination of outer edge time of capture sampled (the outer edge of the otolith, aragonite deposited just before capture) isotopic values representing adult life stages and juvenile (otolith aragonite deposited one year post spawning) life stages of each individual; as a result each otolith is sampled twice to capture the metabolic rates at two points within the life history of the individual. For otoliths where the outer edge sampling area is visible within the thin sectioned slide, the time period over which isotopic values are averaged over was calculated to the nearest month, and for the remaining otoliths

where the outer edge sampling is not visible the time integration period was estimated from the total average over the month of capture (meaning the average time integration period, calculated from thin section measurements, over that individual specific month of capture). Otoliths selected within this study are pre-aged by Cefas to be of 4 years old, however we find age to vary between 3 and 8 (described in detail in chapter **4**). Juvenile sampling targeted the first translucent band of the first year of life (representing the first summer post hatch), and the time integration period is estimated to be one month.

The final number of samples reflects the number of intact otoliths available of sufficient quality to sample each life stage without increasing the time integration area, and subsequently assigned to sub-population A; the number was reduced due to sample access over the pandemic, as the Cefas archive was closed to visitors. Each model and form of statistical analysis within this study was performed with the same number of samples, to avoid unpredictable sources of uncertainty. The samples used within each form of model iteration are detailed in Table.**1**.

### 2.4.3 Experienced Temperature: Adults

Time averaged experienced temperature reconstructed from otolith outer edge $\delta^{18}O_{oto}$ values (which varied between 1.19‰ and 3.3‰) for the samples presented within the study ranged between 1.38 $^{0}C$ to 17.29 $^{0}C$ with an average of 8.02 $^{0}C$ (table **3**). Previous studies analysing sub population A predicted temperature (based on location at time of capture) between approximately $4^{o}C$ to $14^{o}C$ over the annual cycle, therefore the results which we report are comparable with previous works (Darnaude et al., 2014). There is no significant difference in temperature between sexes (with a Kruskal Wallace p-value of 0.413) with males recording a slightly higher average temperature ($7.2^{o}C$ +/- 2.6) than females ($6.24^{o}C$ +/-2.53). There is no expressed covariance with experienced temperature and location within this data set, largely because individuals were sorted into sub populations partially based upon capture locations. There is no significant difference expressed between years (with a Kruskal Wallace tests p-value of 0.122), with relatively consistent temperatures between 1987-1999 and significantly higher experienced temperatures during 2002.

### 2.4.4 Experienced Temperature: Age 0 Fish

The time integrated experienced temperature of individuals estimated during juvenile life stages (within the second half of the first year of life) was reconstructed using $\delta^{18}O_{oto}$ values (figure **18**) which range between -0.917 to 2.42. Assuming constant assumed $\delta^{18}O_w$ values of 0.1 (estimated from model extracted values (figure **15**) and likely juvenile distribution areas), otolith inferred temperatures ranged between $6.82^oC$ and $24.4^oC$ with an average of $13.7^oC$ (+-3.1). The time integrated period for juvenile otolith sampling was kept to a minimum, estimated to represent a maximum period of a month, the individual measured time integration period is presented in the supplementary materials. There is no significant difference in experienced temperature expressed between sexes, with a Kruskal Wallace tests p-value of 0.481. There is no significant difference in experienced temperature expressed between sample years, with a Kruskal Wallace tests p-value of 0.481.

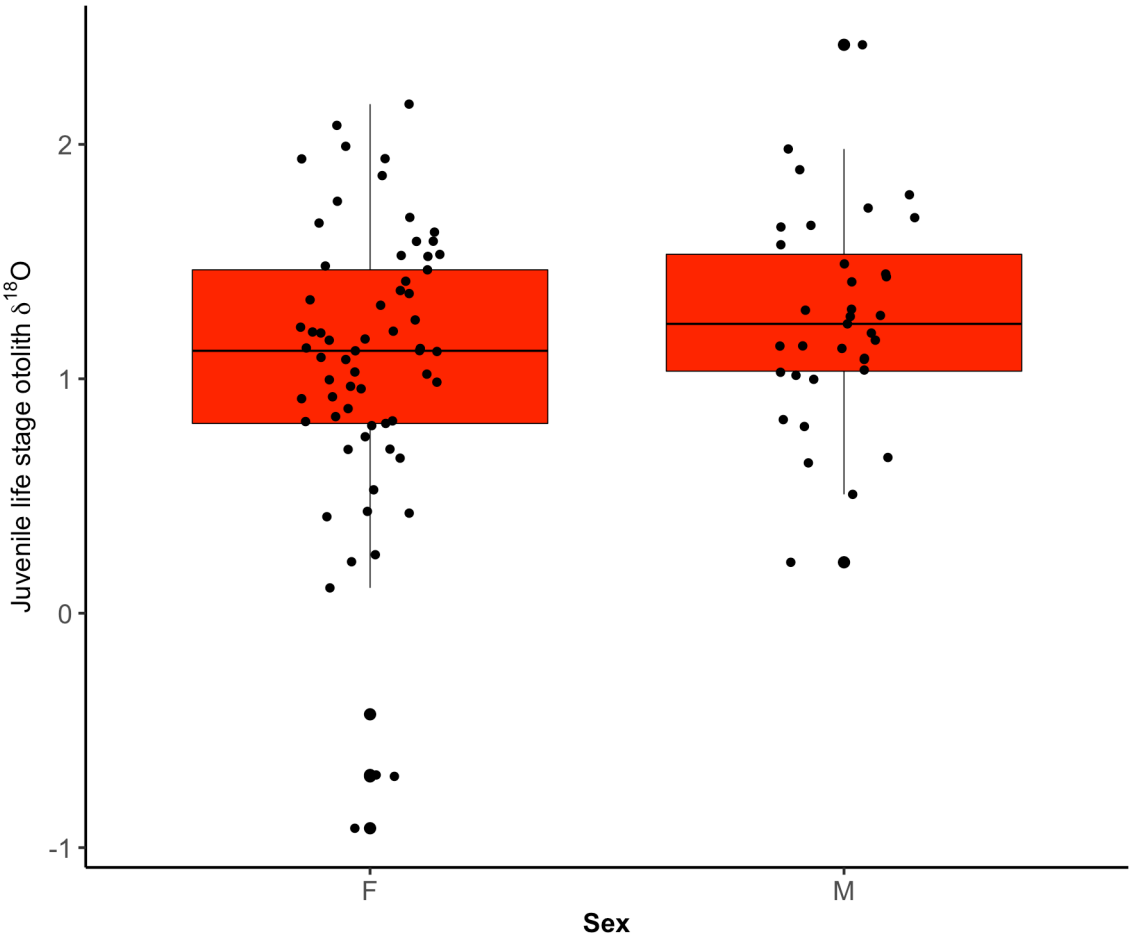


***Figure 18**: Displaying the otolith derived oxygen isotopic expression of individual North-Sea Plaice presented within this study during their juvenile life stage, split by sex.*

### 2.4.5 Cresp Values: Adults

Adult Cresp values range between 0.0367% - 0.218 % for sub-population A with an average of 0.12%, between 0.095 % - 0.119% with an average of 0.107 for B and between 0.095- 0.119 with an average of 0.122 for population C. There is no significant difference between adult $C_{resp}$ values by sex, with a Kruskal Wallace tests p-value of 0.481, or between sample years, with a Kruskal Wallace test p-value of 0.134. inferred mass-specific oxygen consumption rates ranged between 19.4 $mgO_2kg^{-1}h^{-1}$ to 236 $mgO_2kg^{-1}h^{-1}$ averaging 83.3 $mgO_2kg^{-1}h^{-1}$.

The predicted energetic demand rates (in oxygen consumption units) presented within this study are lower than expected based on laboratory respirometry, however we are unsure of the appropriate

parameters used to convert Cresp values to oxygen consumption (equation **2.3**) for plaice without prior experimentation, therefore we are drawing on calibration parameters derived for Atlantic cod. Fish Base measured Plaice SMR varies between 13 $mgO_2kg^{-1}h^{-1}$ - 202 $mgO_2kg^{-1}h^{-1}$ over comparable temperatures (between $5^oC$- $20^oC$) and body masses (between 27g - 632g), therefore similar to the samples presented within this study. Without further investigation we are unable to compare the reported oxygen consumption rates within this study to other intra specific or inter specific populations as we expect these values to be precise but inaccurate; therefore, the trends within this data set are unlikely to be affected but are un-comparable to realised oxygen consumption rates. This means that trends from fish from the same population and species (as this study does) are likely to be unaffected, as the same error is present within each individual, however comparing between species introduces an unknown level of error we are unable to account for, however within this study we do not attempt to do this. We are currently looking into designing an experiment to measure the relationship between Cresp and oxygen consumption rate for multiple species, which will resolve this issue.

### 2.4.6 Cresp Values: Age 0 Fish

Cresp values for the juvenile portions of otoliths recovered from individuals from sub-population A range between 0.0505 - 0.239 with an average of 0.141 (figure **21**). There is no expressed significant difference in Cresp values between sexes during juvenile life stages (Kruskal-Wallis p-value = 0.481, figure **22**). When comparing years there is a significant difference, with a Kruskal-Wallis p-value of 0.0161, and years with warmer average temperatures resulting in higher Cresp averages for juvenile populations. These results are described within the model below (equation **2.8** and table **5**).

### 2.4.7 Condition

We are unable to predict the condition during juvenile life stages, as it is impossible to estimate mass and length from otolith diameter alone. During adult life stages the total range in condition is between 6.72 g $cm^{-3}$ to 18.8 g $cm^{-3}$, 6.72 g $cm^{-3}$ to 14.7 g $cm^{-3}$ for males (averaging 10.4 g $cm^{-3}$) and 7.04 g $cm^{-3}$ to 18.8 g $cm^{-3}$ for females (averaging 12.6 g $cm^{-3}$). There is a significant difference between sexes (Kruskal-Wallis p-value = $7.05 \times 10^{-4}$), with females on average expressing higher values. Condition also varies significantly depending on year of sample (Kruskal-Wallis p-value = 0.0221).

Condition values expressed here are relatively higher than expected as the equation is designed for tubular fish, when we are applying it to a benthic flat fish species, however intra specific trends are unlikely to be affected.

***Table 3**: A description of fixed variables used within varying model structure iterations, with (where appropriate/possible) mean, minimum, maximum values and the standard deviation. The description of how each variable is calculated is provided in the text above.*

| | Juveniles | | | | Adults | | | |
|---|---|---|---|---|---|---|---|---|
| | **Min** | **Max** | **Mean** | **SD** | **Min** | **Max** | **Mean** | **SD** |
| **Cresp** | 0.02 | 0.23 | 0.1 | 0.04 | 0.03 | 0.20 | 0.08 | 0.04 |
| **Temperature ($^oC$)$_{otolith}$** | 6.14 | 24.17 | 15.14 | 3.68 | 1.38 | 17.29 | 8.02 | 3.19 |
| **$O_2$Consumption (mg $O_2kg^{-1}hr^{-1}$)** | - | - | - | - | 19.42 | 236.45 | 83.29 | 36.52 |
| **SMR (mg $O_2kg^{-1}hr^{-1}$)** | - | - | - | - | 24.26 | 79.89 | 40.26 | 12.08 |
| **Length (cm)** | - | - | - | - | 27.00 | 41.00 | 33.97 | 0.50 |
| **Body Mass (g)** | - | - | - | - | 190.00 | 750.00 | 411.74 | 5.00 |
| **Condition (g $cm^{-3)}$** | - | - | - | - | 6.73 | 18.75 | 11.87 | 2.89 |
| **$\delta^{18}O_{oto}$** | -0.92 | 2.43 | 1.13 | 0.59 | 1.19 | 3.30 | 2.48 | 0.49 |
| **$\delta^{13}C_{oto}$** | -2.88 | 0.47 | -1.01 | 0.64 | -2.46 | 0.71 | -0.63 | 0.60 |

## 2.4.8 Relationship between Cresp, Body Mass and Experienced Temperature

### 2.4.8.1 Adults

Table **3** shows summary statistics for all variables included in GLMER modelling. The full GLMER model structure used to explore adult Cresp intrinsic and extrinsic interactions was:

$$\text{Adult } C_{resp} \sim Temperature + \text{Body Mass} + (1 \mid Sex) + (1 \mid Year) + (1 \mid Month) \qquad (2.7)$$

Sex, year and month are treated as random factors (figure **20**) as we are using data from multiple years and months, but we are attempting to explain individual thermal Cresp interactions which are potentially impacted by these variables. Individual thermal metabolic interactions potential change over monthly and yearly cycles, as well as between sexes (due to behavioral influences), therefore we are treating them as random factors, to attempt to predict thermal interactions independently as in laboratory studies.

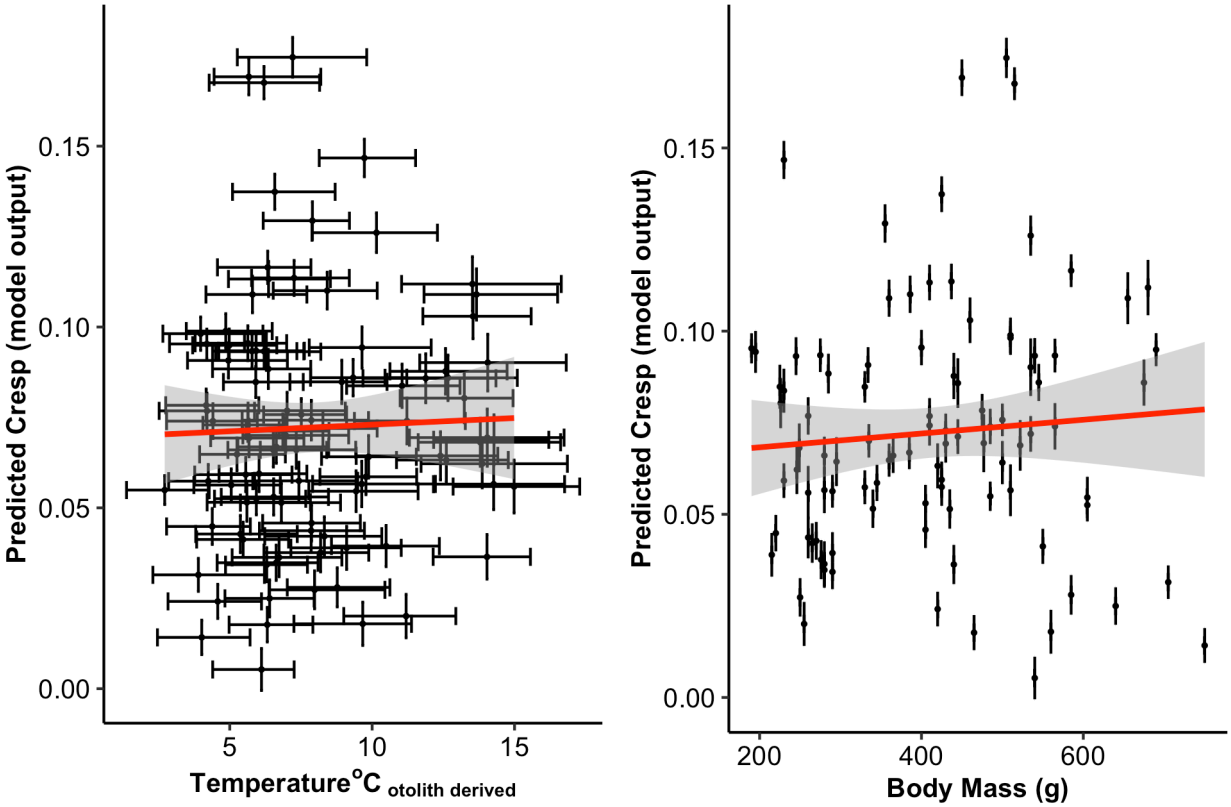


***Figure 19****: Model predicted output data, extracted from best fitted mixed effects models used to explore Cresp variability with predictor variables (full model structure described above). Here the model predicted Cresp response variable and predictor variables, including temperature and body mass, are presented. Error bars are calculated using Monte Carlo simulation analysis.*

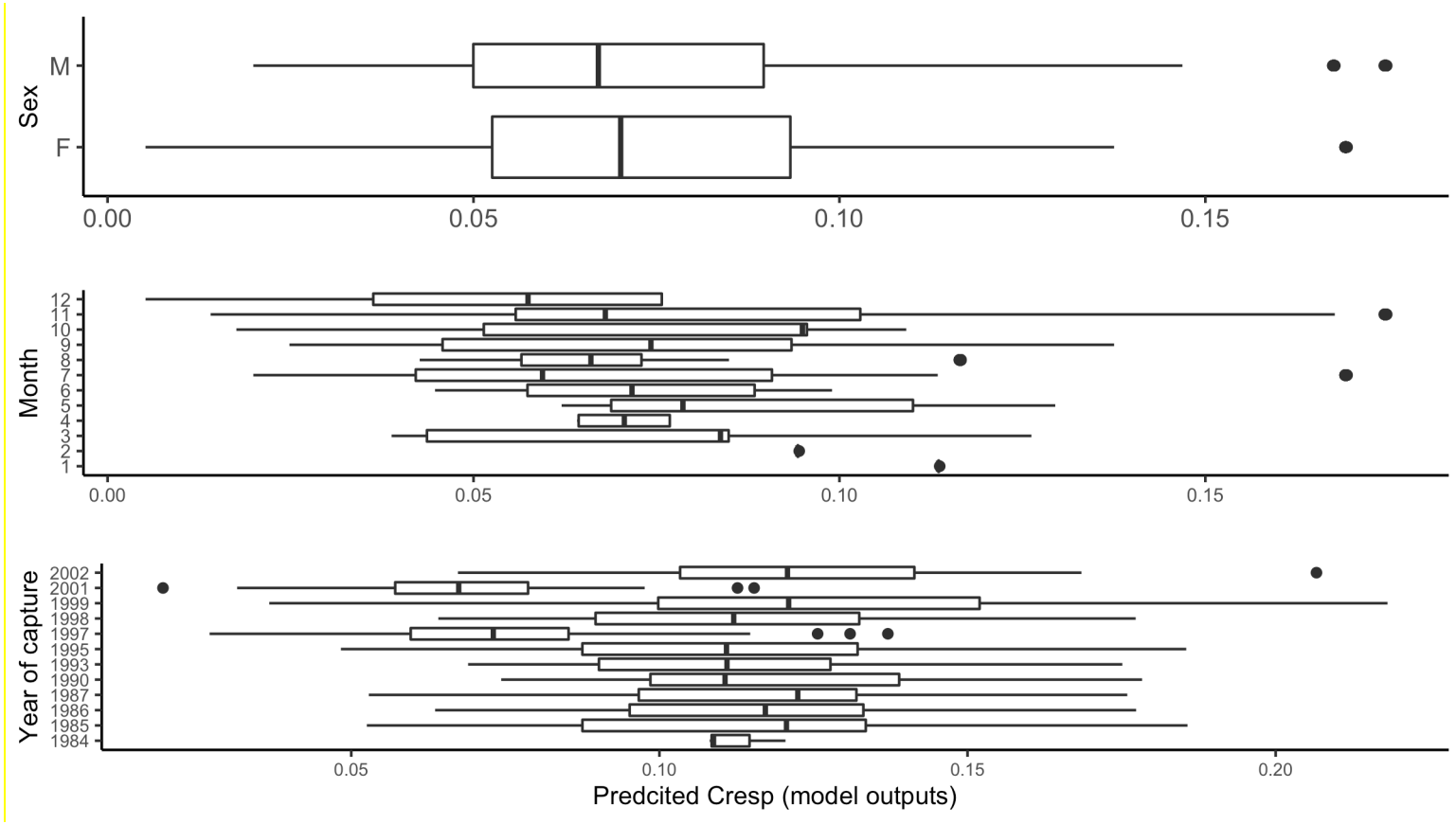


***Figure 20***: *Representing mixed effects model random effects plots, with extracted model predicted Cresp values compared with random effects included within model structure (model described in text above).*

***Table 4**: Adult GLMER model output table. Model structure (equation 2.7) is described above.*

| Variable | Coefficient | standard error | p values | effect type | group |
|---|---|---|---|---|---|
| **intercept** | -2.158262120467 | 0.10228818 | **<0.0001*** ** | fixed | |
| **Temperature** | 0.013744624498 | 0.03275326 | 0.68 | fixed | |
| **body mass** | 0.051598605307 | 0.03138082 | 0.1 | fixed | |
| **intercept** | 0.092984668755 | | - | random | month |
| **intercept** | 0.073723460800 | | - | random | year |
| **intercept** | 0.000005397797 | | - | random | sex |
| **observation** | 0.264009891213 | | - | random | Residual |

Bold values denote significant p values (<0.05) and asterick's define level of significance: p<0.0001 = '<0.0001***'; p< 0.001 = '***'; p < 0.01 = '**'; p<0.05 = '*'

We see no predictable relationship between body mass and Cresp during adult life stages within this data set (figure **19**, figure **20**), as predicted from best fitted mixed effects models. If aerobic scope findinngs can be applied to this data set body mass must covary positively with SMR, therefore this finding suggests that additional variables overwhelm the effect of body mass on realised metabolic expression (at least within the body size range sampled in this study of similarly aged fish). SMR and temperature dependence data may therefore not capture FMR trends. Mass and temperature do have a significant impact on model fit. The AIC value for the model described in equation **2.7** and table **4** is -65242.95, when body mass is removed the AIC value is -65253.60, and when temperature is removed the AIC value is -65258.62. As the AIC are more negative with the inclusion of mass and temperature they improve model fit. However, the predicted values by the model described in equation **2.7** and table **4** expresses a non-significant relationship between $C_{resp}$ and both mass and temperature. As shown from (Figure **219**) model predicted values do not significantly vary over the metabolic gradient presented within this data set.

### 2.4.8.2 Juveniles

Below is the GLMER model structure used to explore juvenile Cresp intrinsic and extrinsic interactions. Otolith radius is not used as a proxy for body mass as not every otolith from this study (collected from Cefas otolith archive) is a complete otolith. Some have been used previously for aging and are cracked, leaving half an otolith, enough for aragonite sampling but not an accurate radius calculation:

$$\text{Juvenile Cresp} \sim temperature_{otolith} + (1 \mid Sex) + (1 \mid Year) \qquad (2.8)$$

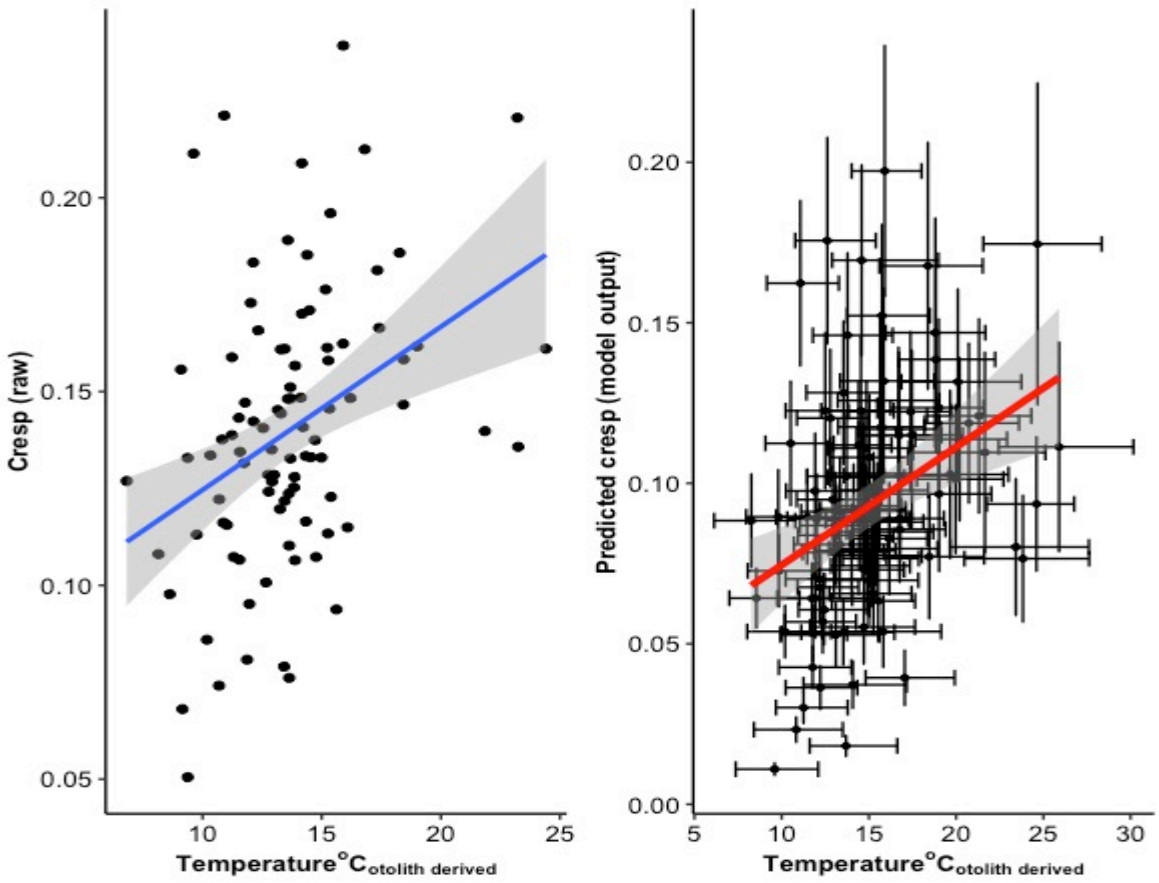


***Figure 21**: Comparison between raw and model predicted juvenile metabolic thermal response curve, using otolith derived experienced temperature, as we are unable estimate modelled temperature as we do not know the location at time of sampling for juveniles. The error bars for the extracted model predicted Cresp and calculated using Monte Carlo simulation analysis.*

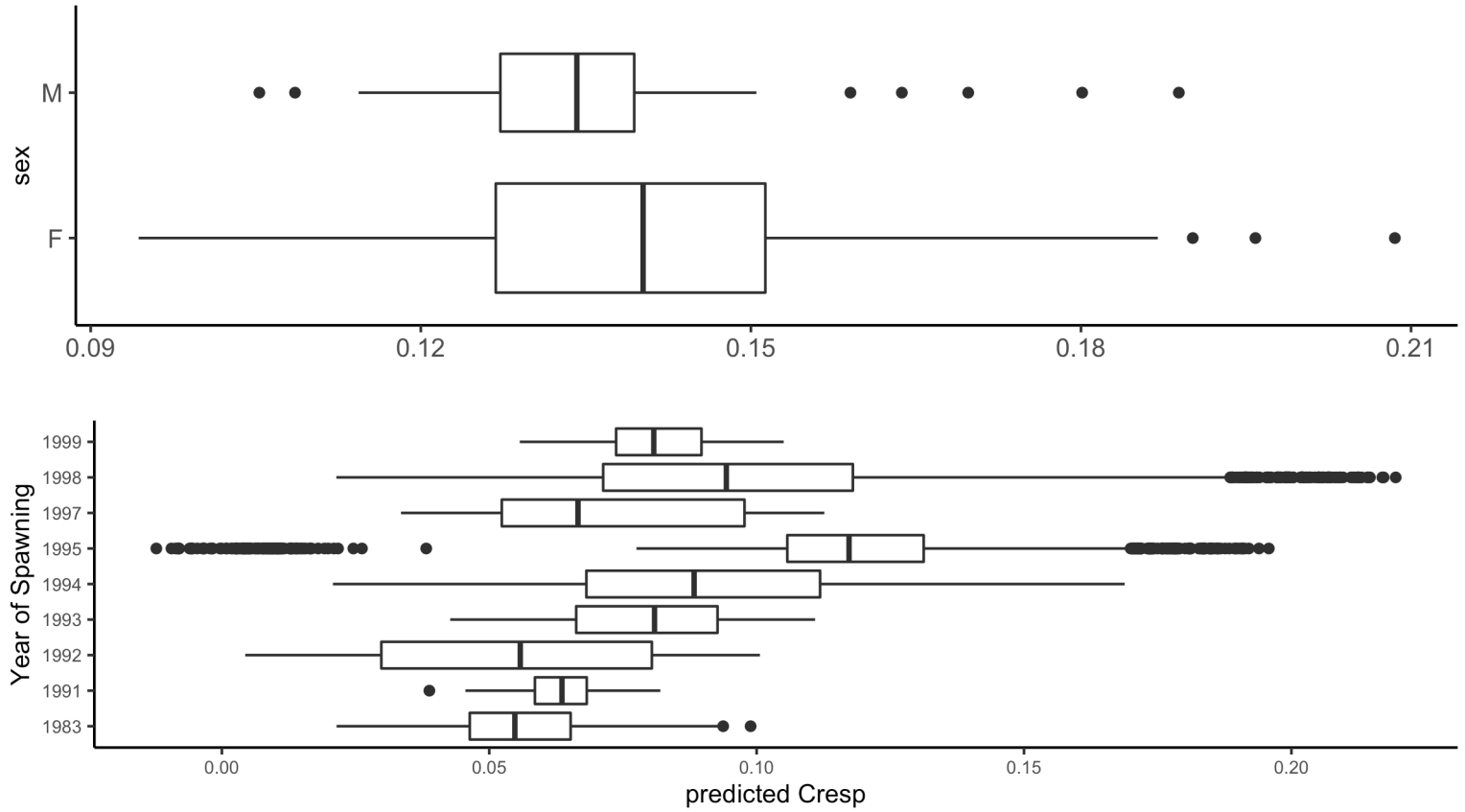


***Figure 22**: Representing mixed effects model random effects plots used to explore metabolic variability in juvenile populations, with extracted model predicted Cresp values compared with random effects included within model structure (model described in text above).*

***Table 5**: Mixed effects model output table for the model used to explore variability in juvenile life stages. Model structure (equation 2.8) is described above.*

| Variable | Coefficient | standard error | p values | effect type | group |
|---|---|---|---|---|---|
| **intercept** | -2.36413288 | 0.120122280 | **<0.0001*** ** | fixed | |
| **Temperature** | 0.02859222 | 0.008176748 | **<0.0001*** ** | fixed | |
| **Year** | 0.04298718 | | - | random | year |
| **intercept** | 0.00000000 | | - | random | sex |
| **observation** | 0.23470536 | | - | random | Residual |

Bold values denote significant p values (<0.05) and asterick's define level of significance: p<0.0001 = '<0.0001***'; p< 0.001 = '***'; p < 0.01 = '**'; p<0.05 = '*'

### 2.4.9 Thermal sensitivity of FMR in Juvenile and Adult Stages

Over the range in sample experienced temperature ($11.1^{o}C$ total range for adult life stages) across the expressed body mass variability, adult Cresp, does not co-vary significantly vary with temperature (Figures **19** and **23**). The total spread of Cresp values varies over the experienced thermal range, with maximum variability occurring between $4^{o}C$ to $7^{o}C$. The highest absolute (but not median) Cresp values occur at $15^{o}C$, again this is likely due to the larger sample size.

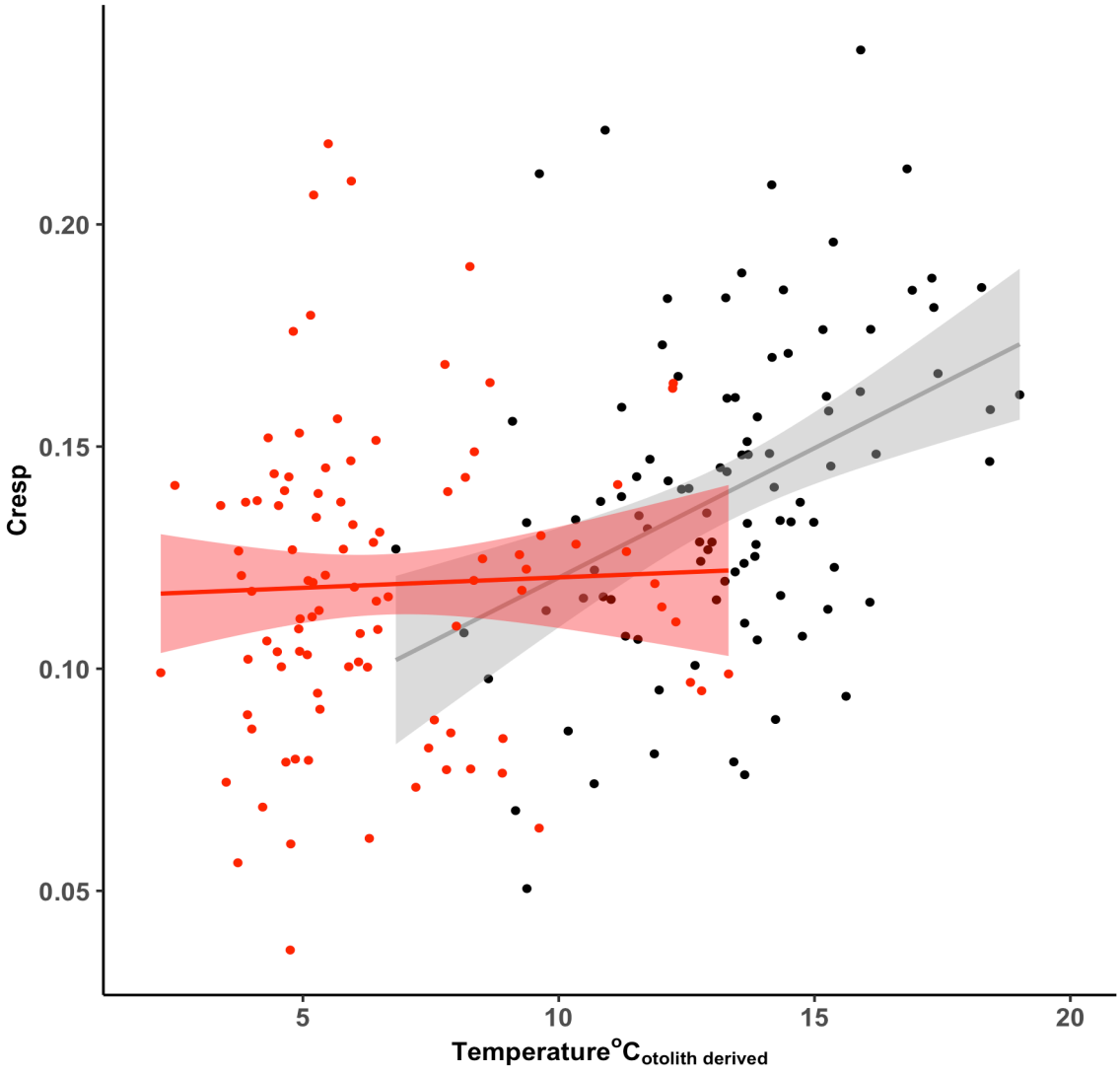


***Figure 23**: Varying metabolic thermal responses over individual life history. Adults represented by the red linear model and red data points, juveniles represented by the black linear model and grey data points*

### 2.4.10 Juveniles

The reconstructed experienced temperature and Cresp relationship for juvenile life stages (one-year post spawning) was examined for 197 randomly selected individuals, irrespective of sex. Condition data during juvenile life stages, and consequently reconstructed SMR, was not predicted, as we are unable to accurately estimate both body mass or length. Cresp values ranged between 0.0505 and 0.239 (an increase of 4.6 times), averaging 0.141 over an experienced temperature range of $6.82^{o}C$ to $24.4^{o}C$ (ranging $17.6^{o}C$). Mixed effects model output results for Cresp vs temperature is summarised in table **5**. There is a significant positive relationship between temperature and Cresp, with higher temperatures resulting in higher $C_{resp}$ alues for juvenile populations, suggesting that metabolic rate is thermally dependent (figure **21** and **23**).

### 2.4.11 Testing for Among Individual Metabolic Effects

To test for consistent metabolic phenotypes (e.g. whether individuals with relatively high Cresp as juveniles also express relatively high Cresp as adults), we first removed temperature effects on $C_{resp}$ by taking the residuals from a Cresp ~ Temperature linear model (lm structure = Cresp ~ Temperature) and mean-centering the residuals for both juvenile and adult populations. We then explored the relationship between mean centered, temperature corrected Cresp between juvenile and adult life stages. We found a positive covariance, implying a consistent among individual relationship between Cresp expressed in year 0 and year 4. As described by figure **24** and table **6**.

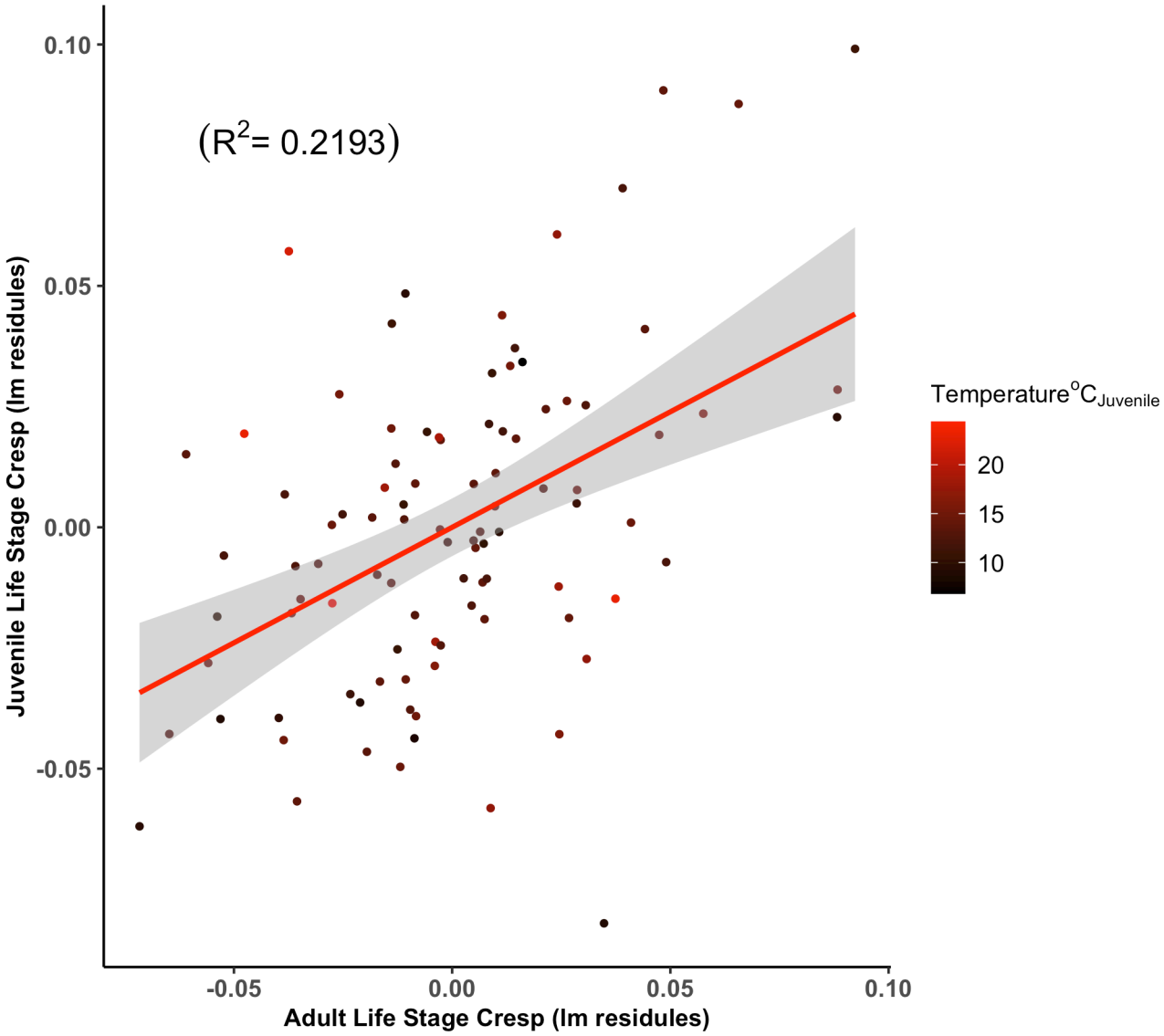


***Figure 24**: Testing for metabolic phenotypic expression. Data presented is extracted metabolic thermal interaction linear model regression residuals for both adult and juvenile life stages. This relationship is described in Table 6. Colour of the data points represented juvenile experienced temperature*

***Table 6**: Linear model output (lm structure = adult Cresp residules ~ juvenile Cresp residules) testing for metabolic phenotypic expression. Data used within model structure is extracted metabolic thermal interaction linear model regression residuals for both adult and juvenile life stages.*

| Variable | Coefficient | standard error | p values |
|---|---|---|---|
| **intercept** | 0.000000000000000005721791 | 0.002944112 | 1 |
| **Adult cresp residuals: Juvenile cresp residuals** | 0.458577458758115064085814 1 | 0.088746876 | **<0.0001*** ** |

Bold values denote significant p values (<0.05) and asterick's define level of significance: p<0.0001 = '<0.0001***'; p< 0.001 = '***'; p < 0.01 = '**'; p<0.05 = '*'

We also attempted to predict the percentage of deviance in metabolic rate at adult stage explained by relative Metabolic rate at juvenile life stage. Adding Cresp at age 0 to the model aiming to explore predictive factors impacting adult Cresp increased model fit, improving AIC values and explaining a higher percentage of deviance (table **7**).

***Table 7**: GLMER model structures, and fitting description used to test the relationship between phenotypic expression and adult Cresp. Model A is represented in equation 2.7, model B includes juvenile Cresp within fixed effects structure, with a lower AIC value of -376.1 compared to -357.1, suggesting a better model fit (and why it is highlighted in bold)*

| Model | Model Structure | AIC | $R^2$ | deviance |
|---|---|---|---|---|
| **Model A** | Otolith derived temperature + Body Mass + (1\|Sex) +(1\|Year) +(1\|month) | -357.1 | 0.193 | -371.09 |
| **Model B** | **Otolith derived temperature + Body Mass + juvenile Cresp +(1\|Sex) +(1\|Year) +(1\|month)** | **-376.1** | **0.318** | **-392.11** |

### 2.4.12 SMR Oxygen Consumption Comparison

We estimated expected individual level SMR using equation **2.6** with body size and temperature data. Temperature dominated predicted variations in SMR, with the total range in estimated SMR (79.88 mg $O_2 kg^{-1} h^{-1}$/24.25 mg $O_2 kg^{-1} h^{-1}$) of 54.44 mg $O_2 kg^{-1} h^{-1}$. While the absolute SMR value is uncertain particularly due to the assumption of common normalisation constant (Bo in equation **2.6**), the difference between oxygen consumption and inferred SMR illustrates the relatively minor realised effect of temperature on oxygen consumption rate, with oxygen consumption /SMR ratio (nominally factorial metabolic rate) apparently decreasing with increasing temperature. (average absolute aerobic difference = 27.72 mg $O_2 kg^{-1} h^{-1}$, maximum = 38.53 mg $O_2 kg^{-1} h^{-1}$, factorial Metabolic rate = 0.61, maximum = 1.78) (figure **25**).

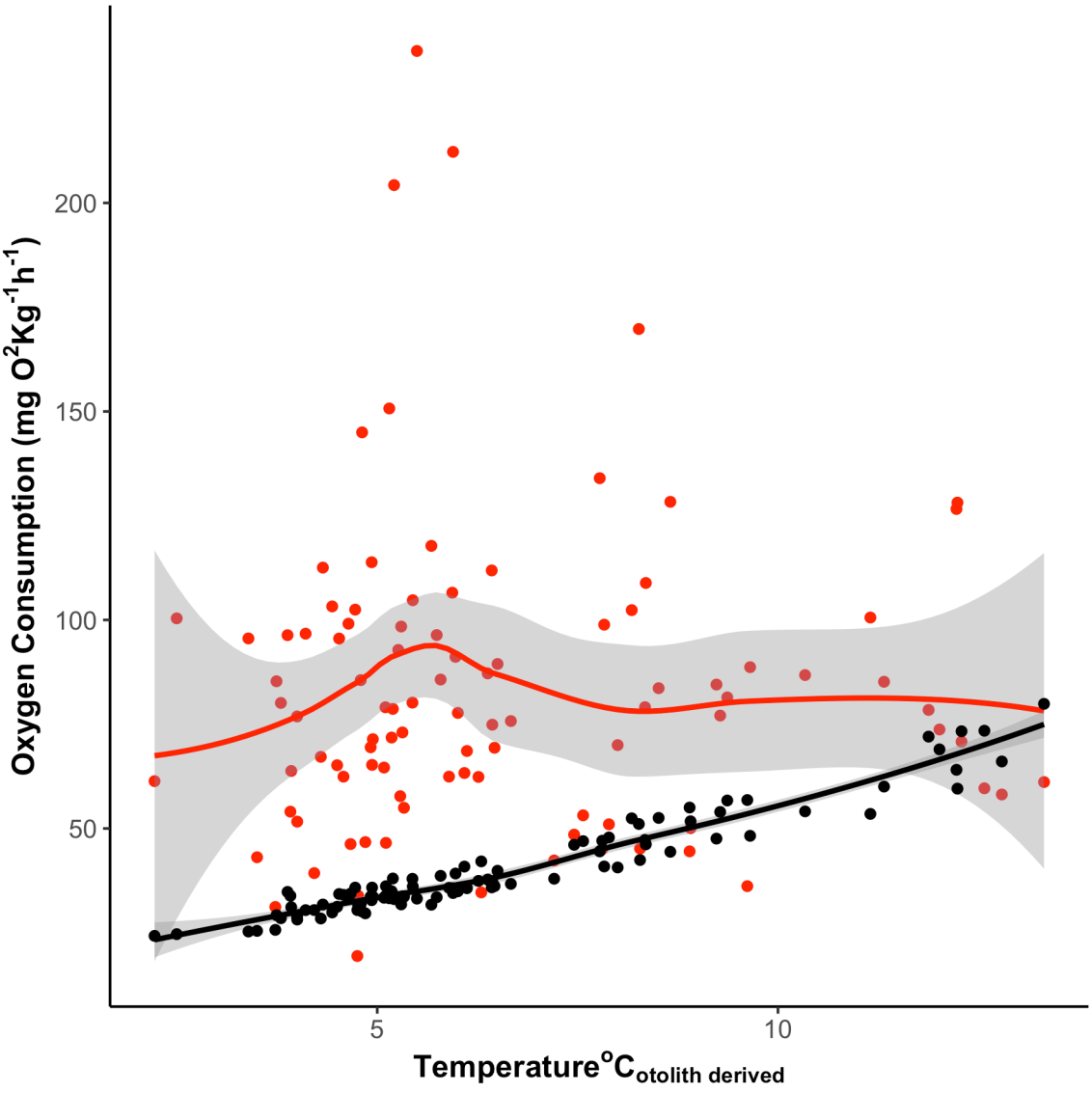


***Figure 25**: Metabolic thermal response curves for otolith derived oxygen consumption (represented by red data points and smoother) and estimated SMR (represented by black data points and smoother)*

When we compare the predicted SMR values over a given temperature gradient to previous studies (fishbase) we find a similar and comparable variability with SMR and temperature. Predicted SMR values from this study expresses a range of 55.6 mg $O_2 kg^{-1} h^{-1}$ with minimum and maximum vales of 24.3 to 79.9 mg $O_2 kg^{-1} h^{-1}$ over a thermal gradient of $13.3^0 C$ to $2.22^0 C$. Fish based studies range between 13 and 202 mg $O_2 kg^{-1} h^{-1}$ with a temperature range of 15 $^0 C$ and maximum and minimum values being 5-$20^0 C$ across a similar body mass range and the common B0 scaling parameter. Therefore, the data within this study predicted SMR values slightly lower than expected (table **8**).

***Table 8**: Otolith estimated and laboratory derived oxygen consumption rate comparison. Laboratory derived data has been collected from FishBase (Froese and Pauly 2000), and represents SMR data from Plaice of varying sizes, both sexes and over a thermal gradients. The data has been split into thermal regimes to allow for more detailed comparison. The oxygen consumption and predicted SMR data is calculated from samples used within this Chapter using equations described above.*

| | 0°C-10°C | | | 10°C-20°C | | |
|---|---|---|---|---|---|---|
| **Mass** | **Fish Base** | **$_{oto}O^2_{consumption}$** | **$SMR_{predicted}$** | **Fish Base** | **$_{oto}O^2_{consumption}$** | **$SMR_{predicted}$** |
| **1- 100g** | 141.47 | - | - | 223.45 | - | - |
| **100 - 200g** | 58.93 | - | 43.62 | 105.86 | - | - |
| **200 - 300g** | 37 | 68.61 | 43.63 | 97.67 | 68.75 | 73.53 |
| **300 - 400g** | 35 | 90.28 | 37.18 | 94 | - | - |
| **400 - 500g** | - | 81.89 | 32.83 | - | 99.53 | 59.41 |
| **500 - 600g** | 21.75 | 101.39 | 35.23 | 59.48 | 58.15 | 66.07 |
| **600 - 700g** | 46 | 79.45 | 31.15 | 124.3 | 114.36 | 56.53 |
| **700 - 800g** | - | 37.14 | 25.57 | - | - | - |

## 2.5 Discussion

Here we used a new indirect respirometry approach to retrospectively infer field metabolic rates from wild living plaice (Chung et al., 2021), and explored the thermal sensitivity of FMR across life stages between and within individuals. Among-individual variations in realised FMR were large and independent of body size and temperature in adult (year 4) life stages, contradicting simplistic assumptions that FMR follows scaling relationships inferred for SMR. We further find strong evidence for the presence of consistent metabolic phenotypes within the sampled population.

When comparing the experienced temperature and FMR presented within this study to modelled environmental temperature, previous studies looking into North Sea plaice and laboratory derived plaice respiratory potential, the range of values within this data set is comparable to previous literature (Darnaude et al., 2014). North Sea sub population A, B and C predicted temperatures have previously been recovered, ranging between $\sim 3^oC$ to $\sim 18^oC$ (Darnaude et al., 2014). Within this study we isolate sub population A, and derive a range of $11.1^oC$ between $2.22^oC$ and $13.3^oC$; with sub population A predicted values from previous studies ranging between $\sim 5^oC$ to $\sim 14^oC$. Oxygen consumption SMR rates from previous literature (such as fish base (Welcomme 1988; Houde and Zastrow 1993;

Froese and Pauly 2000; Rainer et al., 2000)) are slightly higher than the FMR predicted in this study, however the parameters used to convert Cresp values into oxygen consumption are based of Atlantic cod (Chung et al., 2019; Chung et al., 2019b); a species which inhabits a separate environmental niche, has a very different body morphology and is unlikely to express similar physiological trends. As a result, it is unlikely that the plaice oxygen consumption rates presented in this study are accurate, and should not be used to compare with other studies or species; this data is likely to be precise, but inaccurate. This does not negate this study as we are not intending to compare results between species, only at an intraspecific scale, where trends are unlikely to be affected. Each individual has been treated in a similar manner, therefore the oxygen consumption trends over environmental gradients are unlikely to be affected, but we are unable to compare rates of oxygen consumption an intra specific level or between populations of the same species; we are only able to comment on relative shifts between individuals of this specific data set.

Current models attempting to predict fish population distributions and outputs use laboratory-derived respiratory potential to estimate energetic demand supply ratios (Freitas et al., 2010; Kooijman and Kooijman 2010; Kooijman and Troost 2007), in order to quantify the area and geography of habitat suitable for physiological performance. Therefore, the calculation used to derive energetic demand infers that metabolism of wild fish populations scales predictably with body size and temperature (Deutsch et al., 2015a), with the implication that FMR and SMR act in a similar manner (Deutsch et al., 2015a); suggesting that body size and temperature dominate FMR among individual variability. During the time of the formation of fish biogeographical and population models there has been very little data to support this assumption, and as a result this inference has been identified as a source of unknown error within predictions (Nisbet et al., 2012).

In our dataset of 281 wild roaming plaice sampled across 17 years in the North Sea, Cresp values (proxy for FMR) varied by 2-5x among individuals, implying high among-individual variance in FMR across the time frame in this study. Individual body mass varied between approximately 200g and 800g within this study, and experienced temperatures varied over 12 degrees. Despite the relatively large range in body size and experienced temperature, across the sampled individuals, body size and temperature explained very little of the expressed variance in realised FMR in adult (year 4) fish. The lack of any clear relationship between body mass and temperature on expressed Cresp values at year 4 implies that among-individual variations in average energy expenditure are dominated by variation in the extent of

energy consuming processes independent of body size and temperature. Among-individual variations in feeding intensity (including specific dynamic action), activity levels and reproductive investment likely elicit large variations in energy expenditure, and for fishes operating within their aerobic scope, body size and temperature may be poor predictors for daily energy expenditure (Álvarez and Nicieza 2005; Neubauer and Andersen 2019; Rubio-Gracia et al., 2020).

By contrast, in the first year of life, experienced temperature positively co-varied with Cresp values in a predictable manner, and therefore in the first year of life, energy expenditure is more closely related to external temperature. Age 0 fish are under strong selective pressure to grow and are likely to partition a large proportion of available energy into somatic growth (Brown et al., 2005; Liu et al., 2016). The reduced variability in energy trade-offs potentially produces a stronger relationship between experienced temperature and energy expenditure. Consequently, external temperature is likely to be a more reliable predictor of fish performance in early life stages provided fish are operating within their aerobic scope (Dahlke et al., 2020).

### 2.5.1 Phenotypic Variability (Metabolic phenotypes)

Individual variation has been used to measure population stability in previous studies, as a higher degree of phenotypic variation increases the population capacity to absorb environmental instability (Nussey et al., 2007; Rutterford et al., 2015). We drew on the incrementally-grown nature of the otolith to explore the potential for phenotypic effects on among-individual variation in FMR by comparing relative FMR expression at adult and juvenile life stages in the same individuals.

Within the sub-sampled population, we found a significant relationship between relative FMR at age 0 and age 4. Variation in FMR at age 0 explains 0.21% of variation in FMR at age 4 despite uncontrolled effects of year and month of sampling. Additionally, the inclusion of juvenile Cresp when attempting to predict adult metabolic deviance using extrinsic and intrinsic variables improved $R^2$, AIC, model fix and the level of deviance explained, suggesting that trends in adult metabolism is largely controlled by individual physiology and not extrinsic dependency. This relationship potentially implies metabolic phenotypic expression within the population exists.

The consistent relative expression of field metabolic rate level throughout life history is potentially evidence of metabolic phenotypic FMR expression, and between-individual variability in energetic demand preference. The presence of metabolic phenotypes leads us to question if juvenile life stages select thermal conditions to suit their metabolic phenotypic expression, as metabolic rate is thermally dependent, or is adult metabolic expression a result of the environmental conditions experienced by juvenile life stages? If the predictable relationship between juvenile and adult life stage Cresp present within this data set is evidence of metabolic phenotypic expression, and adult's metabolism is not thermally dependent, this potentially implies that adults use a combination of behavioral and environmental drivers to select conditions to better suit their physiological needs. As adult Cresp is not thermally predictable yet juveniles Cresp is, this suggest that adult Cresp is controlled by more factors, and they select environmental conditions to inhabit which suit their physiology at any given point in time. Therefore, the thermal dependence of Cresp is reduced at adult life stages. Ontogenetically-persistent among-individual variation in metabolic rate could arise through genetic differences, or could reflect canalisation of phenotypes based on conditions experienced in early life stages (Metcalfe et al., 2016; Norin et al., 2016; Duncan et al., 2019). In our study we attempted to control for the effect of experienced temperature on early life stage metabolism.

Previous studies have demonstrated the existence of metabolic phenotypes through controlled selective breeding under laboratory conditions, where individuals of elevated or suppressed energetic demand are selected to reproduce (De Verdal et al., 2018; Killen et al., 2021). Here we demonstrate the existence of individual metabolic phenotypes within wild populations, with some individuals expressing elevated and suppressed metabolism persisting throughout individual life history. The difference between this study and previous laboratory experiments is that the individuals within this data set are unlikely to experience similar selective pressures. This allows us to explore the degree of adult metabolic deviance which is explained by juvenile energetic demand.

The inclusion of juvenile Cresp improved both model fit, AIC values and the deviance explained within predicted model values; when incorporated into model structure juvenile Cresp increases $R^2$ values by 12.5%, as well as significantly improving both model fit and deviance explained. These metrics suggest that energetic demand throughout life history is required to further our understanding of *in situ* metabolic trends, and brings us to question the degree of among individual variability in SMR and

MMR studies which can be explained by metabolic phenotypic diversity; which, at this stage in metabolic studies, is rarely accounted for.

Potentially metabolic phenotypic expression could be a measure of the resilience of the population to environmental instability (Killen et al., 2013). The theory of individual variability claims to predict the stability of a population based on the distribution of phenotypes present within a population, with communities where individual level energetic demand is closely centered around the population level mean being more vulnerable to extrinsic variability (Killen et al., 2013). With increased individual level deviance there is a greater chance that a section of a population will survive and be better suited to environmental re-structuring, therefore the population is more stable (Violle et al., 2012). Potentially the theory of individual variability can be applied to this data set, if the distribution of metabolic phenotypic expression is calculated for multiple populations. It may also be possible to predict possibly adult level metabolic phenotypic expression based of juvenile energetic demand distributions, aiding with biogeographical and fisheries output models.

### 2.5.2 Applicability of this Data

It has been suggested that to improve our ability to model population responses we need to measure metabolic (and consequently energetic demand) responses in wild populations (Jager and Zimmer 2012), as the lack of *in situ* data has inhibited model studies when attempting to predict individual energy budgets (Nisbet et al., 2012). There have been attempts to mathematically estimate the amount of oxygen available over that needed to sustain SMR (metabolic index), by comparing the model derived environmental oxygen saturation of population distributions to aerobic scope findings (Deutsch et al, 2020). Using this method, flounder were found to select environments with oxygen concentrations 3 to 4 times greater than the oxygen demand required for SMR, suggesting that sustained FMR is likely to be lower than but approaching 3 to 4 times greater than SMR (Deutsch et al, 2020). It is difficult to identify population energy budgets using this methodology, as fish communities undergo behavioral cycles over annual and individual life history time scales, with each form of behavior likely varying in energetic demand. Relying on modelled oxygen saturation and distribution may not provide enough detail to model how populations are likely to respond on smaller then community levels. The strong dependence on laboratory findings also means the same assumptions which have been used to criticise aerobic scope studies apply, however this data is extremely useful from a physiology perspective, as it

can help identify a how FMR is likely to vary over interspecific scales. Quantifying diversity in population metabolic phenotypic overtime, together with experienced environmental variables, may also provide information on the role of phenotypic expression in modulating population sensitivity to external environmental drivers (Metcalfe et al., 2016).

Marine fish distributions have been suggested to be limited to waters where oxygen availability is sufficient to sustain metabolic rates 3 times SMR (Deutsch et al., 2020). Within this data set individual factorial metabolic scope (FMR/inferred SMR) is estimated to lie between 0.63-7.12 with an average of 2.21. While estimates of factorial FMR are subject to a wide range of assumptions, the estimated values do not contradict inferences drawn from metabolic theory (Deutsch et al., 2020). FMR and factorial metabolic scope clearly varies systematically throughout the annual cycle, with seasonal behavioral cycles, as energetic requirements vary with individual behavioral demands.

## 2.6 Conclusions

- Within this data set there is a significant degree of adult life stage FMR variability between individuals, irrespective of extrinsic or intrinsic variables, such as temperature and body size; as we see no predictable covariance between FMR with body mass or temperature. These results suggest that within this data set FMR does not interact with extrinsic and intrinsic variables in a similar manner as predicted by established metabolic theories of ecology. Indicating that FMR varies independently form laboratory derived SMR, and potentially respiratory potential findings do not capture natural population metabolic trends with enough precision for accurate biogeographical and output model estimations.
- There is no clear evidence for metabolic thermal limitation when assessing FMR thermal response curves within this data. The experienced temperature expressed by individuals suggests that the population is operating near the warmer range of laboratory predicted species limits, yet we see no predictable significant interaction as derived by laboratory derived studies.
- During Juvenile life stages FMR varies predictably with temperature, in a similar manner expressed by SMR studies. This suggests that juvenile FMR is thermally dependable and the interactions between extrinsic variability and energetic demand are inconsistent throughout life stage within this population.
- Due to the lack of thermal and body mass metabolic scaling relationships during adult life stage, we suggest that energetic expenditure is potentially dominated by opportunistic and seasonal variations in food availability and energy partitioning.
- When comparing FMR during juvenile and adult life stages we see a predictable positive co variance. With individuals expressing relatively (to the population average) high or low Cresp

values during juvenile stages maintaining this relative expression during adult life stages. We suggest this is potentially evidence of metabolic phenotypic expression, however we are unable to derive if this predictable interaction is due to the experienced conditions during juvenile life stages or a genetic component.

# 3 Variations in European Plaice Otolith Derived Field Metabolic Rate Over the Seasonal Cycle

## 3.1 Abstract

Basal metabolic rate scales predictably with both temperature and body size under controlled laboratory conditions, and this relationship has been key for the formation of various conceptual frameworks attempting to constrain how diverse environmental factors impact energetic demand. For instance, the predictable interaction between body size, temperature and standard metabolic rate has been used to parameterise biogeographical and population models to predict animal responses to future climate scenarios. However, when attempting to apply these findings to wild fish populations operating within their aerobic scope, variations in realised field metabolic may be larger than laboratory derived respiratory potential, and therefore independent of temperature and body size. Studies have also suggested that intrinsic variables such as behavioral and or phenotypic plastic responses are able to act as an "aerobic buffer", however at this current point in time we lack detailed observations of fine scale variations in individual metabolic rates expressed by fish operating in natural conditions to explore these unknown factors.

Here we describe how field metabolic rates vary seasonally drawing on a dataset of observations from 558 free-roaming European plaice from the North Sea. These samples have previously been used to explore allometric scaling relationships of field metabolic rate (FMR), and show a significant degree of residual FMR variability independent of body size and experienced temperature.

In this current chapter we show that observed seasonal and among-individual variations in FMR far exceed predicted thermal effects on SMR. Estimated FMR peaked in autumn months prior to spawning, and, overall, females displayed higher FMR than males. Estimated time-averaged FMR was lower than 3 times predicted SMR in the overwhelming majority of cases.

These data provide observational context for considering the implications of thermal influences on physiological performance in wild fishes across populations, seasons and sexes.

## 3.2 Introduction

Identifying how external environmental and ecological variables impact the energetic demands of ectotherms is key to understanding biogeographical patterns in marine fish populations (Deutsch et al., 2015b; Verberk et al., 2016; Ern 2019), and predicting how population distributions are likely to respond to future climatic variability (Rutterford et al., 2015). In recent years metabolic frameworks, such as the gill-oxygen limitation theory (GOLT) (Pörtner and Knust 2007) and the oxygen and capacity limited thermal tolerance (OCLTT) (Clark et al., 2013), which aim to explain how environmental conditions limit performance (Farrell et al., 2008), have been applied to future climate scenario models to prediction population distributions and fishery production (Deutsch et al., 2015b).

Environmental temperature is a primary environmental variable driving fish ecophysiology (Brett 1971; Farrell 1997; Lee et al., 2003); due to thermodynamic increases in reaction rates (Clark et al., 2013) and reduction in dissolved oxygen concentrations at higher temperatures (Pörtner and Knust 2007). Chapter 2 suggests that adult populations field metabolic rate is less thermally predictable than previously believed, however from a standard metabolic rate perspective temperature is a controlling variable which we need to consider. Conceptual theories describing fish physiological performance are generally derived from, and supported by, laboratory-based experiments measuring respiratory potential as a function of temperature and body size (McKenzie et al., 2020). Such experiments commonly determine the thermal sensitivity of individual oxygen consumption rates at the extreme ends of the metabolic spectrum, maximum metabolic rate (MMR) and standard metabolic rate (SMR) (Brown et al., 2004). The difference between the MMR and SMR is termed the aerobic scope (Lefrançois and Claireaux 2003), and is assumed to represent the available energetic resources for physiological function (Clark et al., 2013). Variations in aerobic scope throughout a thermal range, and especially the presence of a thermal optima in aerobic scope underpin many predictions of fish physiological performance within the GOLT, OCLTT and other conceptual frameworks (Pörtner and Knust 2007). Recently, studies estimating environmental oxygen concentrations required for sustained metabolic performance and population abundance suggest that oxygen supply must be 3-5 times higher than that required for sustained SMR in order to maintain population abundance (Deutsch et al., 2020), explaining why population distributions are often constrained at temperatures well below the expected

thermal range where maximum physiological performance is negatively impacted (Norin et al., 2014; Holt and Jørgensen 2015).

Fish are therefore expected to seek and persist in waters where oxygen supply/demand ratios remain within the aerobic scope 'buffer', providing energy needed to perform above maintenance levels (Farrell 2016). This implies that marine animals require a significant aerobic buffer (Deutsch et al, 2020). The existence of an aerobic buffer in turn implies that temperature is likely to account for less variance in field metabolic rates of animals, as the aerobic buffer allows energy budgeting among different energy consuming activities.

Very little is known about energy partitioning and thermal sensitivity of metabolic rate in wild fishes because of the difficulty of determining time-integrated field metabolic rate of fishes operating in natural environments (Chung et al., 2021). It is unclear whether external conditions such as water temperature continue to exert a strong influence on fish metabolism within the aerobic scope buffer, or alternatively whether variations in energy demands associated with partitioning energy between feeding, migration, reproduction and other energetic demands outweigh influences of external temperature (Nisbet et al., 2012). This is an important consideration, as if field metabolism of fish is relatively insensitive to thermal variations while operating within the aerobic scope buffer, attempts to predict fish performance based on future water temperature projections may be compromised, especially for populations operating within the core thermal niche. The concept of a critical aerobic scope level of performance, however it does impact our ability to detect how close a population is to the critical level where physiological performance is affected.

In the absence of *in situ* observations of individual-level field metabolic rates, there have been attempts to estimate energetic demands in wild fishes through bioenergetic models such as dynamic energy budget models (DEB) (Kooijman and Troost 2007; Kooijman and Kooijman 2010; Sousa et al., 2010; Nisbet et al., 2012; Kooijman and Lika 2014). DEBs attempt to predict individual performance considering the allocation of available energy to four principle metabolic processes; 1, assimilation (food ingestion to reserved potential energy); 2, dissipation, defined as metabolic expenditure that does not lead to the production of new biological material, dissipation may include natural behavior such as migration (reserve to mineral products); 3, growth (reserve potential energy to somatic growth); and 4, reproduction (reserved potential energy to reproductive reserve) (Nisbet et al., 2012). The sum of these

physiological processes is the field metabolic rate. DEB models are parameterised largely through laboratory-derived physiological measurements and can be used to explore relationships between energy partitioning (e.g. growth or reproductive output) and environmental variables such as dissolved oxygen concentration, temperature and prey availability (Freitas et al., 2010). From an aquaculture perspective, with a theoretically unlimited prey supply and minimal changes to dissipation and reproduction energetic partitioning, an increase in thermal conditions ($+2^{o}C$) results in DEB predictions of an increased individual growth rate, resulting in reduced time period for individuals to reach the required commercial size limit (Mangano et al., 2019). When attempting to explain variations in growth rate (from otolith increment data), it has been suggested that food availability pays a greater role than thermal conditions (Fablet et al., 2009) when attempting to predict standard metabolic rate. Studies attempting to derive the relationship between hypoxic condition and oxygen consumption rates have found an associated reduction in growth and reproduction rates with limited aerobic capacity (Thomas et al., 2019), but state that unknown variables such as the dose effect (Jager and Zimmer 2012) and our lack of understanding of how "wild organisms" have the ability to adapt over individual life histories (Spicer 2014) reduce the applicability of DEB model outputs to *in situ* scenarios. Time and temperature integrated individual level field metabolic rate data has the potential to act as a test of DEB and other bioenergetic model predictions of seasonally varying energy budgets and resource requirements.

Here we apply a newly emerging method of reconstructing the field metabolic rate, termed otolith derived field metabolic rate (Chung et al., 2019; Chung et al., 2019b; Martino et al., 2020; Alewijnse et al., 2021; Chung et al., 2021), to the North Sea European plaice (*Pleuronectes platessa*) population over annual and decadal time scales across the life history of individuals. Otolith derived FMR estimates the proportion of respiratory derived carbonate within otolith aragonite, compared to other carbonate sources (such as dissolved inorganic carbonate) based on their different isotopic signatures (Chung et al., 2019; Chung et al., 2019b). Simultaneously, the stable oxygen isotope of the same otolith samples can be used to infer experienced temperature (Geffen 2012). The FMR thermal responses curves of these samples have previously been analysed, in an attempt to answer if metabolic scaling relationships derived from laboratory SMR studies, used in metabolic theories of ecology and biogeographical model predictions, can be applied to natural populations. Within this data set FMR does not vary systematically with temperature or body mass, indicating that energetic demand cannot be predicted from extrinsic variability alone within this North Sea plaice population, however there is

a large unexplained metabolic deviance within the data set. Therefore, we explore variations in observed field metabolic rate over seasonal, environmental and physiological gradients, to identify if FMR varies systematically across the annual cycle, to identify the degree of variability which can be explained by condition and feeding or reproductive cycles. The aim of this project is to aid with understanding the relationship between environmental drivers and metabolic trends, potentially providing useful data for modelling estimates.

Plaice are a commercially important, benthic, temperately distributed migratory species (Ciotti 2012). Within the North Sea system there are three distinct sub populations (southerly, westerly and easterly populations), with linked complex annual reproductive cycles (Hunter et al., 2004; Hunter et al., 2009). During the summer months each sub population inhabits distinct feeding grounds, and all undergo a migration to more southerly, coastal locations to spawn during winter months, with a subtle distinction between male and female migration timings (Hunter et al., 2004; Hunter et al., 2009). Juvenile plaice reach maturity and reproductive capacity approximately 3 years post spawning, when growth rate reduces. Attempts to model plaice energetic partitioning via DEB models suggest that individual growth rates are largely explained by food selection and less thermally dependent (Van der Veer et al., 2010), however this study standardised food quality between groups, only increasing quantity, when standard metabolic rate is potentially controlled by food quality. Laboratory experiments have been used to determine the optimal thermal range (measured between 1 to $27^{o}C$) of performance for juvenile individuals, finding optimal growth rates at approximately $20^{o}C$ (Fonds et al., 1992).

## 3.3 Methods

### 3.3.1 Sample Selection

Otolith samples analysed within this study were collected during Cefas beam trawl surveys, spanning all four fishing monthly quarters (1 = January-March, 2 = April-June, 3 = July-September, 4= October-December) and North Sea ICES areas IVB and IVC (to minimise potential geographical dependent metabolic variability). All otoliths were pre-aged by Cefas sclerochronologists. To minimise age-dependent metabolic variability we sampled fish with a relatively high growth rate (aiming for individuals of 4 years old) and therefore larger volumes of otolith available for sampling. Otoliths were selected from survey years with high sample coverage. North Sea annual average water temperature

experienced a significant period of warming within ICES areas IVB and IVC from 1980s-2010 (Núñez-Riboni and Akimova 2015), otoliths were therefore selected from years reflecting colder (older) and warmer (more recent) periods as well as periods with relatively high and low place abundance. The sample years selected were 1984, 1985, 1986, 1987, 1990 1993, 1995, 1997, 1998, 1999, 2001 and 2002; The distribution of data throughout sexes, months and years is presented in table **9**. The The distribution of the data within the North Sea is presented in figure **26**.

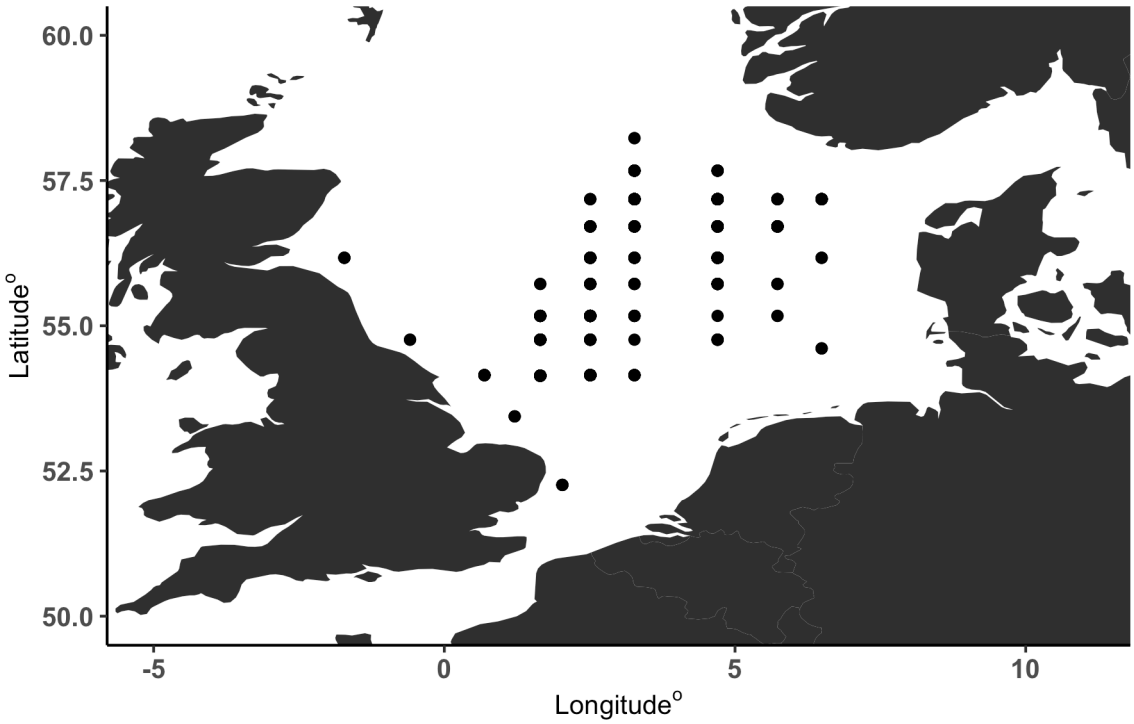


***Figure 26**: Sample capture locations for individuals used within this chapter. Each point representing a trawling station for an ICES rectangle, specifically the "ground fish" survey. Therefore, each point represents multiple individuals, as they were collected from the CEFAS otolith archive were "ground fish" survey samples are stored.*

***Table 9**: Representing the distribution of Samples selected for analysis throughout years, sub populations and sexes, used within this chapter. The data is split by North Sea plaice sub-populations, which individuals have been assigned to using previous tagging, isotopic analysis and experienced extrinsic variability studies (Hunter et al., 2009; Darnaude at al., 2014). Year Regime represents the reason why this year was selected for analysis, as we originally aimed to target specific events, such as a year of high recruitment, and attempt to explain the metabolic variability associated with such events.*

| | | **Males (n)** | | | **Females (n)** | | |
|---|---|---|---|---|---|---|---|
| **Year** | **Year Regime** | **A** $_{\text{sub population}}$ | **B** $_{\text{sub population}}$ | **C** $_{\text{sub population}}$ | **A** $_{\text{sub population}}$ | **B** $_{\text{sub population}}$ | **C** $_{\text{sub population}}$ |
| Year | Cold Year | - | 2 | 1 | - | 1 | 3 |
| 1985 | Cold Year | 13 | 10 | 9 | 11 | 4 | 3 |
| 1986 | High recruitment | 10 | 7 | 8 | 7 | 11 | 8 |
| 1987 | Cold Year | 6 | 4 | 7 | 20 | 6 | 7 |
| 1990 | Warm Year | 13 | 2 | 8 | 13 | 4 | 10 |
| 1993 | Low SSB | 12 | 3 | 7 | 19 | 3 | 6 |
| 1995 | Low SSB | 12 | 2 | 4 | 17 | 5 | 10 |
| 1997 | High recruitment | 12 | 5 | 1 | 26 | 3 | 3 |
| 1998 | Warm Year | 14 | - | 2 | 28 | - | 6 |
| 1999 | Warm Year | 18 | 1 | - | 31 | - | - |
| 2001 | High recruitment | 12 | 6 | 4 | 8 | 11 | 9 |
| 2002 | Warm Year | 10 | 9 | 2 | 19 | 6 | 4 |
| **total** | | **132** | **51** | **53** | **199** | **54** | **69** |

### 3.3.2 Sample Preparation

The otolith preparation protocol followed previous work (Chung et al., 2019; Alewijnse et al., 2021). Initially otoliths were cleaned with fresh water to remove any residue tissue, and fixed to an epoxy (Struers Eopfix resin) mount with the proximal (sulcus) surface uppermost. Otolith sampling was designed to provide sufficient powder averaging fish growth over the smallest time interval possible. The external otolith surface area representing the most recent period of aragonite deposition was then sampled, using a Dremel 4000 rotary engraving tool, with straight sided, cylindrical diamond bits. Sampling was performed with the shaft of the drill bit touching at an incident angle to the otolith surface allowing the most efficient recovery of powder. Aragonite powder was collected from the surface of the resin block containing otoliths by tapping powder into a weigh paper.

Following external edge sampling, a subset of the otoliths were sectioned (to approximately 20 $\mu m$ thickness) at the University of Southampton thin sectioning laboratories. Otolith sections were used to visually estimate the depth of external milling and therefore the time period of sampled otolith growth (and therefore the time period which FMR and temperature is integrated), and to provide access to the first year of growth for analyses of FMR and temperature during juvenile life stages.

Otolith thin sections were photographed and time period represented by the milled sample, individual age and growth and marginal otolith condition (opaque or translucent) was estimated from digital images using ImageJ (Schneider et al., 2012) in combination with the ObjectJ plug-in. Otolith growth representing the second half of the first year of life was sampled using an ESI New Wave Micromill either by milling trenches and/or from multiple drill holes (described in the chapter 4 focusing on growth rate and FMR interactions)

### 3.3.3 Mass Spectrometry

The stable isotope compositions of carbon and oxygen in otolith aragonite were measured at the Stable Isotope Ratio Mass Spectrometry Laboratory (SEAPORT Laboratory, Southampton, UK), with a Kiel IV Carbonate device coupled with a MAT253 isotope ratio mass spectrometer. Approximately 20-70 $\mu g$ of aragonite powder was accurately weighed into borosilicate glass reaction vessels prior to

evolution of $CO_2$ through reaction with phosphoric acid. The calibration standards used were NBS 19 and NBS 18, as well as a quality control GS1 (Carrara marble produced by the SEAPORT laboratory). Results are reported in permil ($‰_o$) (as $\delta^{13}C$ and $\delta^{18}O$ values) relative to Vienna Pee Dee Belemnite. Accuracy and precision determined from long-term analyses of internal standards of known composition is 0.01 $‰_o$ for both $\delta^{13}C$ and $\delta^{18}O$ of otolith aragonite. The standard deviations determined from repeated measures of internal standards in each run are presented in the supplementary materials.

### 3.3.4 Estimation of the Proportion of Metabolic Carbon in Otolith Aragonite

We estimated the proportion of respiratory carbon in otolith aragonite, refered to as Cresp (Chung et al., 2020) from a two-component mixing model as described by Chung et al., 2019:

$$C_{resp} = \frac{(\delta^{13}C_{oto} - \delta^{13}C_{DIC-sw})}{(\delta^{13}C_{diet} - \delta^{13}C_{DIC-sw})} + \epsilon_{total} \qquad (3.1)$$

Where $\delta^{13}C_{oto}$ represents the $\delta^{13}C$ values of the sampled otolith aragonite, $\delta^{13}C_{DIC-sw}$ represents the $\delta^{13}C$ value of dissolved inorganic carbon (DIC), $\delta^{13}C_{diet}$ represents the $\delta^{13}C$ values of individual diet (Chung et al., 2019; Chung et al., 2019b). $\epsilon_{total}$ is the total isotopic fractionation from DIC and diet to blood, blood to endolymph and endolymph to otolith (Chung et al., 2019; Chung et al., 2019b). The absolute value of $\epsilon_{total}$ may vary among species, and requires further laboratory experimentation to calculate. Within this study, we assume that $\epsilon_{total}$ does not vary systematically among individuals of the same species and is set to 0 (Chung et al., 2021). $\delta^{13}C_{diet}$ values were estimated based on a compilation of stable isotope data from plaice from the North Sea provided by Jennings and Cogan (2015) ranging from -19.4$‰_o$ to -14.5$‰_o$ (varying due to geographical distribution). $\delta^{13}C_{DIC}$ values were estimated from Burt et al., 2016, who presented spatially explicit $\delta^{13}C_{DIC}$ values from across the North Sea collected in September 2011 by (Burt et al., 2016) (ranging from 0.5$‰_o$-0.8$‰_o$), and adjusted for the Suess effect (the decrease in $\delta^{13}C_{DIC-sw}$ over time due to anthropogenic carbon emissions since the industrial revolution) (Tagliabue and Bopp 2008). We solved for Cresp and standard deviations using Monte Carlo statistical analysis (see table **19**). In subsequent analyses we take the median of the posterior distribution for Cresp values.

### 3.3.5 Estimating Oxygen Consumption Rate

To assist with comparing this data to alternative measures of metabolic rate (such as aerobic scope), Cresp values were converted into equivalent oxygen consumption rate using a previously calculated statistical calibration, based on juvenile cod (*Gadus morhua*) (Chung et al., 2019; Chung et al., 2019b). The relationship between Cresp values and oxygen consumption rates is best estimated as an exponential model with an upper limit ('C') reflecting the maximum proportion of respired carbon that the fish can maintain in the blood (and thus endolymph and otolith). A similar calibration experiment with the temperate Australian snapper (*Pagrus auratus*) (Martino et al., 2020), returned a calibration with a similar exponential form, but different covariates, reflecting likely species-specific variations in the proportions of respiratory carbon tolerated in the blood. Here we apply both published statistical calibration models to the plaice data, recognising that the estimated mass-specific oxygen consumption rates may require re-assessment as and when calibration experiments are performed for plaice. Due to COVID restrictions we were unable to perform the calibration experiments on Plaice:

$$C_{resp} = C\left(1 - e^{-k(\text{Oxygen Consumption Rate})}\right) \qquad (3.2)$$

$$\text{Oxygen Consumption Rate} = \frac{\ln\left(1 - \frac{C_{resp}}{C}\right)}{-k} \qquad (3.3)$$

Where C is an upper boundary nominally reflecting the maximum proportion of respiratory carbon that the fish can accommodate in blood (and therefore otolith aragonite) fitted as 0.243 and k is a decay constant with a fitted value of $8.88 \times 10^{-3}$. The derived oxygen consumption from equation 3.3 is in the units of $mgO_2kg^{-1}h^{-1}$.

### 3.3.6 Otolith Derived Experienced Temperature

Time averaged otolith derived experienced temperature was reconstructed using a species-specific otolith isotope temperature equation (Geffen 2012).

$$\delta^{18}O_C - \delta^{18}O_W = 3.72 - 0.19T(^oC) \qquad (3.4)$$

$\delta^{18}O$ values of the ambient sea water ($\delta^{18}O_W$) vary largely according to salinity, as freshwater inputs have lower $\delta^{18}O_W$ values than seawater. In the North Sea salinity varies considerably in space and time, complicating the use of oxygen isotope thermometry (see below). $\delta^{18}O$ values of the ambient sea water were initially estimated from the National Aeronautical Space Administration's (NASA) "global seawater oxygen-18 Database" (LeGrande and Schmidt 2006). Otolith derived temperature error deviations values were calculated using Monte Carlo statistical analysis (table **10**). Due to variations in experienced salinity between individuals of the same population (figure **27**) we use modelled temperature estimated from an AHOI model (a physical-statistical model of hydrography for fisheries and ecology studies) described by Núñez-Riboni and Akimova (2015) presented in (figure **28**). The extracted model outputs were subsetted to only include the bottom 5m of the water column, as plaice are a benthic fish species. We aimed to match the otolith aragonite sampling depth with the time period over which model temperature outputs were averaged.

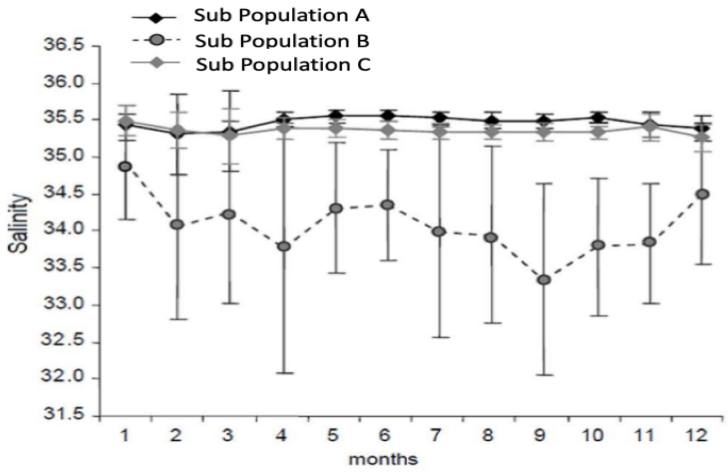


***Figure 27**: Expressing the variations in experienced salinity between North-Sea Plaice sub-populations, based of tagging distribution data, the salinity data has been predicted from the time and location of each individual and the environmental parameters present within each location. Adapted from Darnaude (2014).*

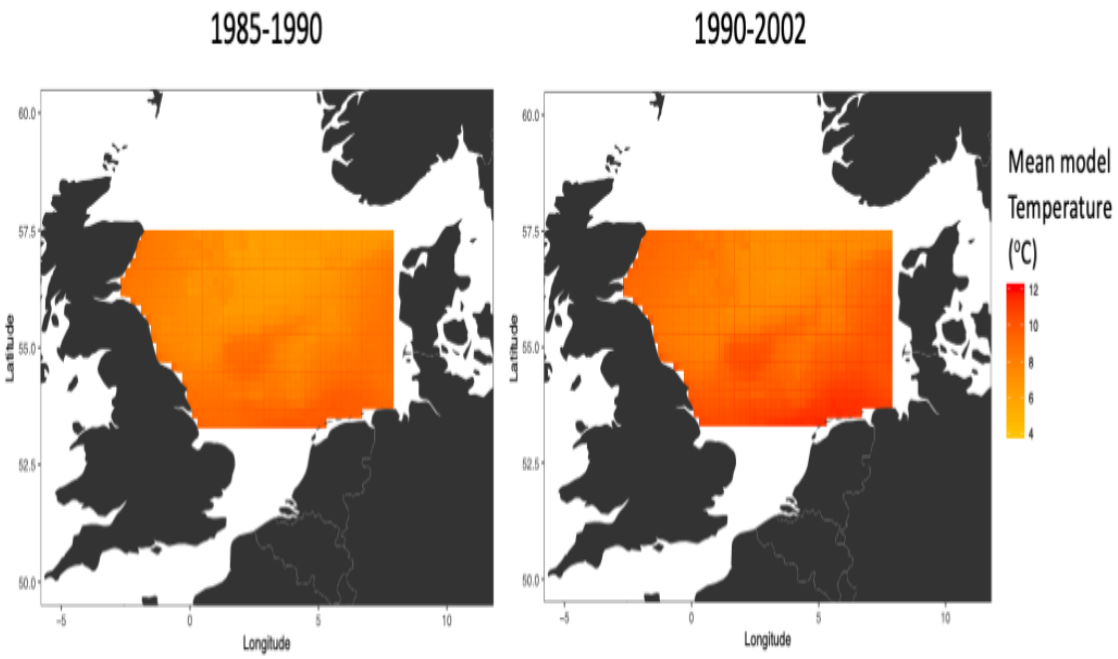


***Figure 28**: AHOI model benthic North Sea temperature estimates outputs (Núñez-Riboni and Akimova 2015). Subsetted to only include the benthic 5m layer (as it is likely this represents the environment Plaice are likely to experience), the sample area and time period. Individual specific temperatures were calculated using unique sample locations and possible movement area (based of tagging studies (Hunter et al., 2003)).*

### 3.3.7 Fish Condition

We estimated condition to identify seasonal variations in energy storage and use, and potentially among-individual variations in performance (Bervoets and Blust 2003). Condition is defined in equation **3.5** (Bervoets and Blust 2003), where weight is in g and length is in cm. The equation used to derive condition is designed for cylindrical fish, therefore the values presented are unusually high, however as we are comparing between a singular plaice population intraspecific trends are unlikely to be affected. During Cefas surveys weight was measured to the nearest 5g, forming a standard deviation of 2.5, and length was measured to the nearest cm, giving a standard deviation of 0.5. To calculate condition incorporating standard deviations of weight and length we used Monte Carlo analysis presented in table **19**.

$$\text{condition (gcm\^-3)} = \frac{\text{weight (g)}}{\text{length (cm)}^3} \qquad (3.5)$$

### 3.3.8 Assigning Plaice to Sub-population

Plaice in the North Sea are divided into three sub-populations, which experience differing salinity environments throughout the seasonal cycle (Darnaude et al., 2014). Sub-population (B) in particular occupies low salinity waters in the German Bight. As oxygen-isotope based temperature estimates require assumptions about the isotopic composition of oxygen in water (which is variable and unpredictable in low salinity environments), we use model temperature estimates presented in figure **28** to reduce unexplained deviance in the data. We developed the following identification pipeline to assign individuals into most likely sub populations:

- Individuals captured north of latitude $56^{o}N$ are assigned to group A.
- Individuals with $\delta^{18}O$ values in excess of $2.3\%_{o}$ are assigned to group A.
- Individuals sampled north of latitude $56^{o}N$ but showing apparent experienced temperature higher than $14^{o}C$, are assigned to group B.
- Individuals sampled in winter months east of $4^{o}E$ where apparent experienced temperature exceeds $11^{o}C$ are assigned to group B.
- Individuals captured west of longitude $2^{o}E$ are assigned to group C.
- Individuals sampled in winter months sampled west of $4^{o}E$ showing apparent individual experienced temperatures > $11^{o}C$ are assigned to group C (Darnaude, 2014).

The resulting experienced temperatures were then compared to seawater temperature estimates from physical ocean modes (Núñez-Riboni and Akimova 2015) over the time integrated period and likely geographical range of movement (Darnaude et al., 2014). Subsequent analyses involving individual estimated temperatures were restricted to population A where experienced salinity fluctuations are limited to less than $1.5\%_{o}$ (Darnaude et al., 2014) figure **27**.

### 3.3.9 Data Analysis Methods

To examine the degree of Cresp variability explained by season, condition, years, sex, location and temperature we applied generalised additive models (GAM). We tested for interactive effects of season (after splitting the data into feeding and breeding time periods based off tagging survey data), months

and environmental variables on both Cresp, and selected the best fitting model from comparison of AIC values. We treated year as a random factor as we are combining data from multiple years in order to form a continual monthly time series (due to sample collection limitations as a result of the pandemic). The Linear models, Wilcoxon signed-rank test and GAM's were performed in R, and figures were produced using the package ggplot2 (Wickham 2009). GAM models were constructed using the mgcv (Wood 2003; Wood 2004; Wood 2011; Wood et al., 2016; Wood 2017) package nlme (Bates et al., 2015). GAM model selection was performed using AIC values and varying levels of model complexity. Firstly, the most complex model was structure was formed, then subsequent possible and favourable model strictures were tested against AIC values, to test model fit.

## 3.4 Results

We determined $\delta^{13}C$ and $\delta^{18}O$ values in a total of 558 otoliths within this study. 250 of these otoliths were thin sectioned to allow an estimate of the amount of time integrated in the external drill sampling. In many cases trenches (made by hand drilling prior to otolith thin sectioning) attributable to external drilling were not clearly visible in sections, however where the drilled proportion of the outer edge was apparent (likely representing the deeper drilled otoliths), the period of time which this area represents was estimated to the nearest month. This is to calculate the period of time (as growth rate is proportional to otolith aragonite deposition) over which adult stage Cresp was calculated over. The time integrated period for the remaining samples (where the milling depth was not clear from the thin section) was estimated from the average of the individuals captured over the growing and spawning season, as the growth rates vary between time periods. Then the average over the two time periods was applied to individuals where we are unable to measure the period which field metabolic rate was calculated over, as the drilling trenches are not visible. All otoliths were pre-aged by Cefas to be four years post spawning; however, we find the age to vary between 3 and 8 (described in more detail in Chapter 4).

### 3.4.1 Assigning Plaice to Sub-Population

The geographical sample distribution over the monthly cycle is presented in table **9** showing that all three North Sea plaice sub populations are represented in this study, 272 samples were assigned to population A, 17 to population B and 108 to population C. $\delta^{13}C_{oto}$ values range between 0.986‰ and

-2.46‰ for population A averaging -0.406‰, for population B the rage is between 0.74‰-1.31‰ averaging -0.359‰, and for population C the range was 0.776‰-1.9‰ averaging -0.496‰; reported below in table **14**.

### 3.4.2 Temperature Reconstruction

Time averaged experienced temperature reconstructed from $\delta^{18}O_{oto}$ values ranged between $1.4^{o}C$ to $13.3^{o}C$, with an average of $1.4^{o}C$ for population A, ranging from $19.5^{o}C$ to $11.3^{o}C$ with an average of $13.5^{o}C$ for population B and $14.6^{o}C$ to $5.08^{o}C$ averaging $10.4^{o}C$ for population C.

Estimates of sea surface temperatures at the location and month of capture were recovered from the AHOI ocean model (Núñez-Riboni and Akimova 2015) described in section **3.3.6**. The relationship between temperatures reconstructed from otolith $\delta^{18}O$ values and model benthic temperature estimates (estimated for each fish over the individual specific time integrated period and the possible migratory geographical area) show a positive covariance, but with large degree of unexplained variance (p value of $3.67 \times 10^{-11}$, $R^2$ of 0.092). The positive intercept and low slope imply that otolith-estimated temperatures are, in general, lower than model benthic temperatures at the point of capture (figure **29**). Both model estimated and otolith derived temperatures are described in table **11**.

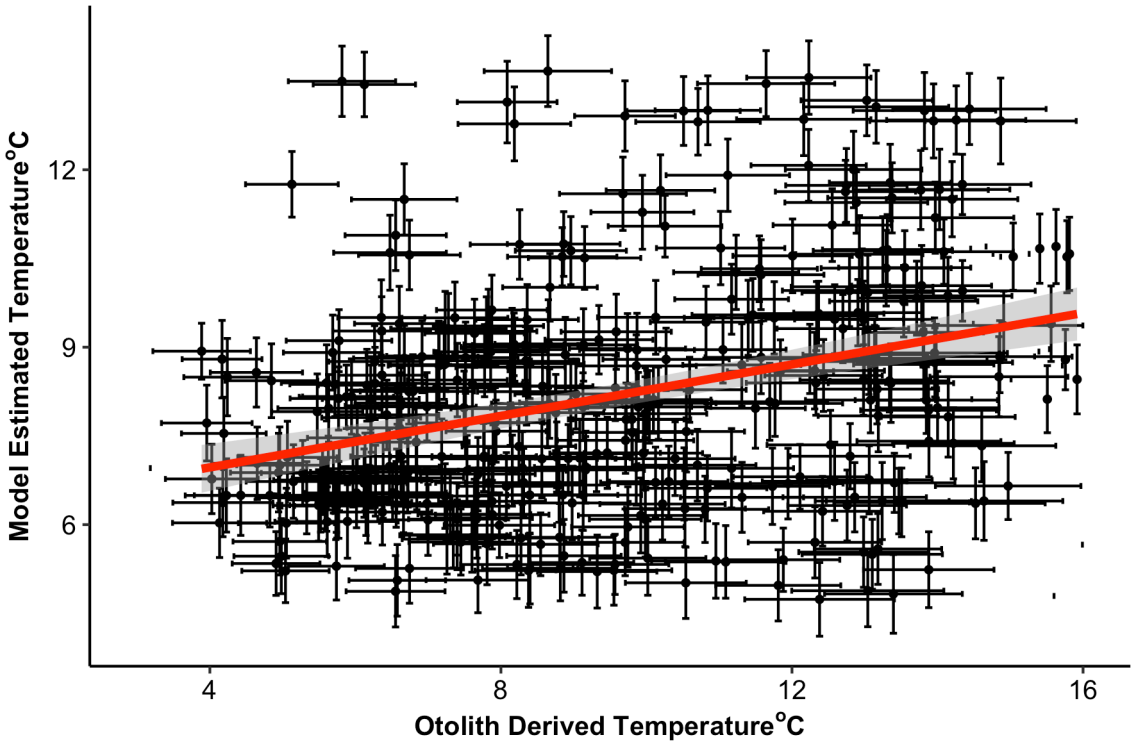


***Figure 29***: *A comparison between otolith derived and model estimated temperature values, each value has been calculated for each individual and error bars are derived using Monte Carlo simulation analysis. There is a weak positive correlation between the two values, as described above, however this figure highlights the degree of variability between the two variables.*

**Table 10**: *Describing the linear model output data, structured to explore the interaction between estimated modelled and otolith derived temperature values. Linear model structure = Model estimated temperature ~ Otolith derived Temperature*

| Term | Coefficient | standard error | p values |
|---|---|---|---|
| **intercept** | 4.767783 | 0.5380046 | **<0.0001*** ** |
| **Model Temperature** | 0.423882 | 0.0624874 | **<0.0001*** ** |

Bold values denote significant p values (<0.05) and asterick's define level of significance: p<0.0001 = '<0.0001***'; p< 0.001 = '***'; p < 0.01 = '**'; p<0.05 = '*'

To model the relationship between Cresp and temperature we chose to use model estimates rather than otolith-derived temperature estimates due to the experienced salinity variability between the separate

plaice sub populations (figure **30**) (Darnaude et al., 2014), potentially reducing the validity of the otolith derived temperature estimates. This allows us to group all three sub populations when examining Cresp trends over the annual cycle (figure **30**). Otolith derived temperature can be applied when studying a singular sub population with minimal potential salinity variability, however in this chapter as we are combining sub populations (described in chapter 2 and 4) the high range of likely experienced salinities which makes mathematically modelled temperature a better option. A direct comparison between otolith derived and model derived temperature is presented within table **11**.

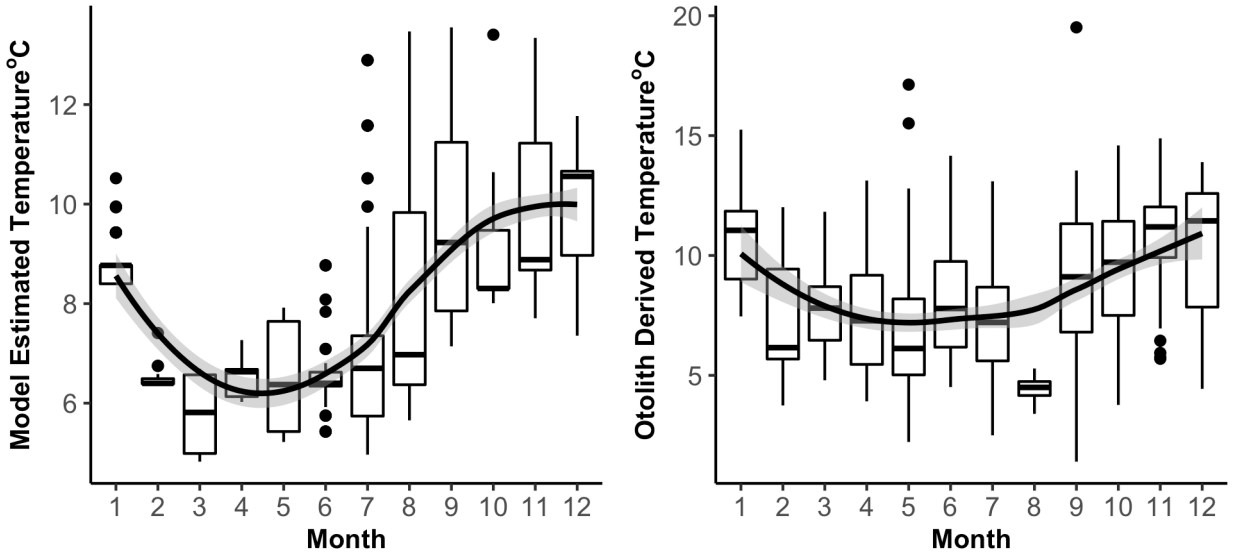


***Figure 30****: Seasonal variations in otolith derived and model temperature over the annual cycle for the same individuals. The Temperature scales for each Y axis should be treated independently as they are different temperature measurements, and should not be compared, therefore the Y axis is not consistent between graphs*

Individual monthly population averaged model temperature estimates express both maximum absolute ($13.6^{o}C$) values and relatively high individual variability (with a total range of $6.41^{o}C$) during the later stages of the growing/feeding season (September to December) (figure **30**). From December through to March, the spawning season when the separate sub populations migrate to their southerly breeding grounds, the monthly model temperature estimates reduce, reaching minimum annual averages ($6.38^{o}C$ during March) accompanied with relatively low individual variability ($4.41^{o}C$). During the early post-spawning season (March to May), as the sub-populations begin their migrations back to northerly feeding grounds, there are no significant changes in model temperature estimates, which remain relatively low with a reduced individual variability. From June through to August (the onset of the

growing season), when each population is believed to inhabit separate biogeographical distributions, model temperature estimates increase ($13.5^{o}C$), with relatively high individual variability. There is a significant variation in model temperature estimates throughout the annual cycle and between sexes, with males on average experiencing higher temperatures (as predicted by best fitted GAM models, aiming to explain model temperature variability using season, individual months and sex as factors, the model structure is described in below in equation **3.6**, figure **31** and figure **32**). This has previously been tested in chapter 2, however that was data focusing on a singular population, and potentially different sub populations of plaice express a different result.

***Table 11**: Presenting the estimated model and otolith derived temperature data, split between months and sexes. To allow for a direct comparison between the two variables.*

| | Male (°C) | | | Female (°C) | | | Male (°C) | | | Female (°C) | | |
|---|---|---|---|---|---|---|---|---|---|---|---|---|
| **Month** | **$Model_{min}$** | **$Model_{max}$** | **$Model_{mean}$** | **$Model_{min}$** | **$Model_{max}$** | **$Model_{mean}$** | **$Otolith_{min}$** | **$Otolith_{max}$** | **$Otolith_{mean}$** | **$Otolith_{min}$** | **$Otolith_{max}$** | **$Otolith_{mean}$** |
| 1 | 8.40 | 10.53 | 8.92 | 8.40 | 9.96 | 9.06 | 5.70 | 14.89 | 10.94 | 6.96 | 14.02 | 11.40 |
| 2 | 6.39 | 7.41 | 6.57 | 6.39 | 6.75 | 6.54 | 8.18 | 13.75 | 11.83 | 4.44 | 13.90 | 8.46 |
| 3 | 4.83 | 6.69 | 5.60 | 4.83 | 6.69 | 5.84 | 9.37 | 15.25 | 12.29 | 7.46 | 11.85 | 10.00 |
| 4 | 6.14 | 7.27 | 6.68 | 6.03 | 6.64 | 6.25 | 4.01 | 6.98 | 5.72 | 3.75 | 12.02 | 6.88 |
| 5 | 5.43 | 7.92 | 7.41 | 5.22 | 7.92 | 6.33 | 6.09 | 11.83 | 8.78 | 4.80 | 10.18 | 7.33 |
| 6 | 5.43 | 8.77 | 6.63 | 5.43 | 8.77 | 6.68 | 3.92 | 13.13 | 8.16 | 3.93 | 10.45 | 6.38 |
| 7 | 4.97 | 9.55 | 6.63 | 4.97 | 10.52 | 6.81 | 3.37 | 17.13 | 7.27 | 2.23 | 9.85 | 5.84 |
| 8 | 5.66 | 9.99 | 7.38 | 5.98 | 13.48 | 8.02 | 6.57 | 11.44 | 9.18 | 4.52 | 14.16 | 6.85 |
| 9 | 7.15 | 13.56 | 8.47 | 7.15 | 13.56 | 9.42 | 4.20 | 12.58 | 7.25 | 2.50 | 13.10 | 7.50 |
| 10 | 8.31 | 8.31 | 8.31 | 8.01 | 8.31 | 8.24 | 4.33 | 5.29 | 4.81 | 3.40 | 4.77 | 4.24 |
| 11 | 7.74 | 13.14 | 9.60 | 7.71 | 13.14 | 9.92 | 1.40 | 19.52 | 9.56 | 3.05 | 13.55 | 8.19 |
| 12 | 7.36 | 11.78 | 9.71 | 7.96 | 11.78 | 9.86 | 3.77 | 13.68 | 9.32 | 4.76 | 14.59 | 9.20 |

### 3.4.3 Seasonal variations in Temperature at Capture

Below is the GAM model structure used to Seasonal variations in temperature at capture (F = treated as factor within model structure), described in equation **3.6** and table **12**. Cresp is included within model structure to explore if individuals select temperatures based on their metabolic expression. Season is a division of the data into feeding and spawning seasons, to explore if individuals select variable temperatures based on behavioral activities, and is treated as a factor because season is linked to temperature variability. Year is included as a factor because we have attempted within this chapter to form a continual annual cycle, and due to covid restrictions this had to be made up of multiple years, therefore it is included as a factor to remove the impact of yearly temperature variability. The Partial effects plots, expressing the effects of Cresp, condition, year, season, and sex, are presented in figure **31** and **32**.

$$\text{Temperature} \sim \text{Cresp} + \text{condition} + \text{F(season)} + \text{F(sex)} + \text{F(year)} \qquad (3.6)$$

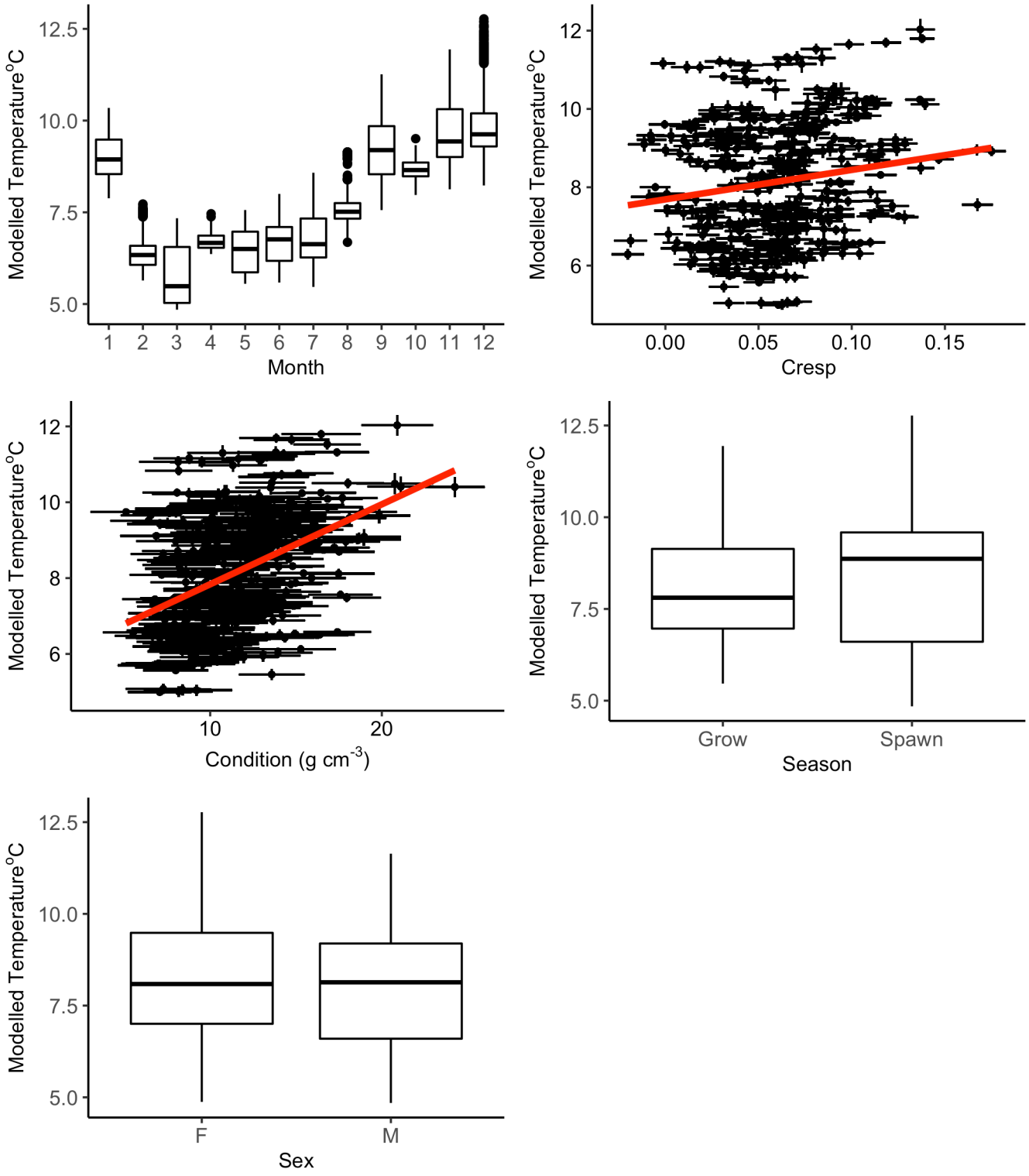


***Figure 31***: *The predicted partial effects plots exploring modelled derived temperature variability over the seasonal cycle. This is simulated data extracted from the best fitted generalised additive model used to explore temperature variability over the seasonal cycle. Model structure is described above in equation 3.6.*

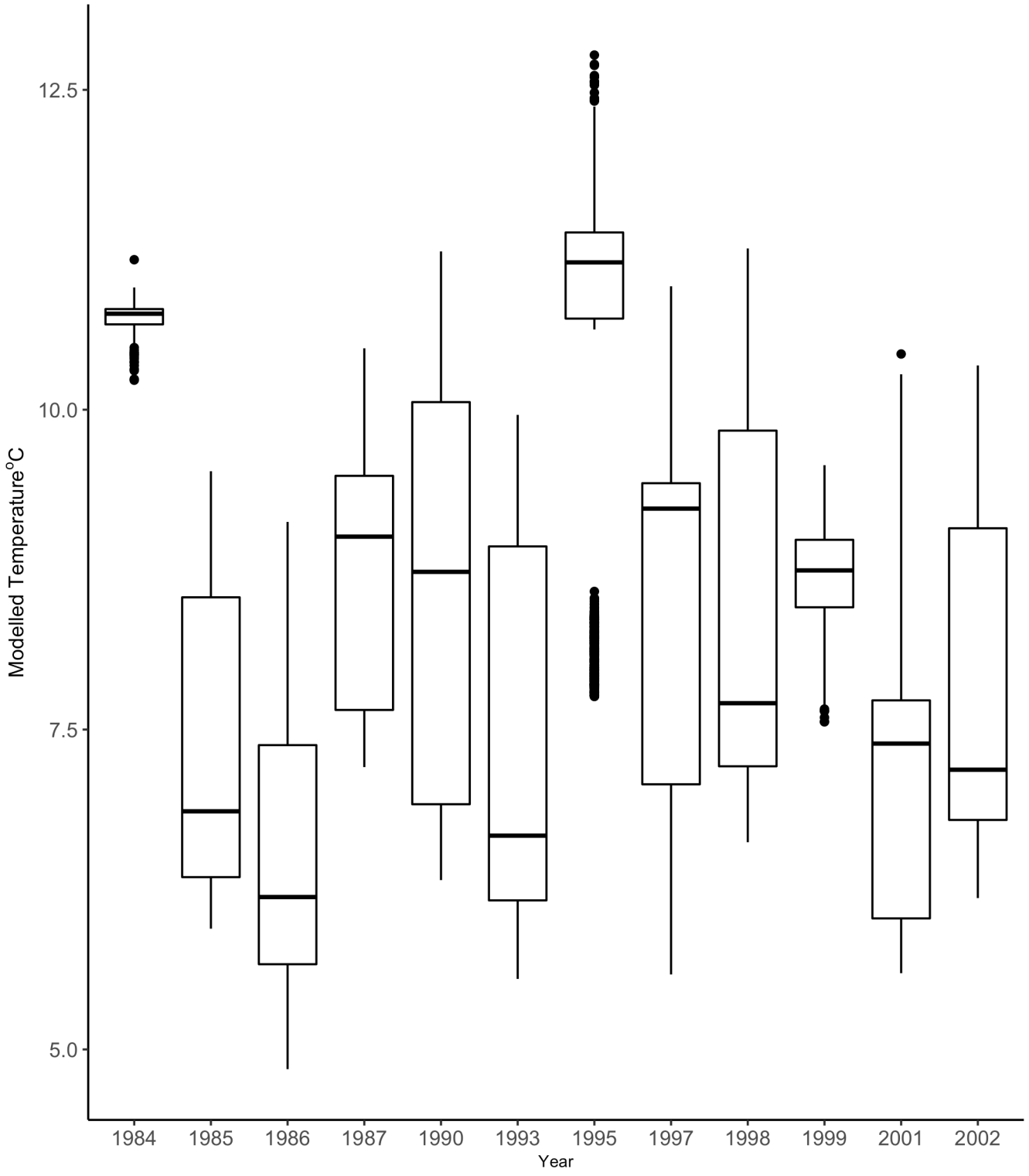


***Figure 32**: The predicted partial effects plots exploring modelled derived temperature variability over the seasonal cycle. This is simulated data which has been extracted from the best fitted generalised additive models, which were used to explore temperature variability over the seasonal cycle. Model structure is described above in equation 3.6.*

***Table 12**: GAM model (described above in equation 3.6) output table, used to explore seasonal variations in model estimated temperature*

| Terms | Coefficient | standard error | p values | effect class |
|---|---|---|---|---|
| **intercept** | 8.9951400 | 1.0068719 | **<0.0001*** ** | Factor |
| **Sex** | 0.5177685 | 0.1906530 | **0.0069** ** | Factor |
| **Season** | 0.7325829 | 0.2088179 | **<0.0001*** ** | Factor |
| **Year (1985)** | -2.0541388 | 1.0255831 | **0.046*** | Factor |
| **Year (1986)** | -2.9957273 | 1.0223872 | **0.0036** ** | Factor |
| **Year (1987)** | -0.6819318 | 1.0335438 | 0.51 | Factor |
| **Year (1990)** | -0.7378970 | 1.0277748 | 0.47 | Factor |
| **Year (1993)** | -1.5381279 | 1.0320443 | 0.14 | Factor |
| **Year (1995)** | 0.9406241 | 1.0479455 | 0.37 | Factor |
| **Year (1997)** | -1.6371381 | 1.0219554 | 0.11 | Factor |
| **Year (1998)** | -1.0563104 | 1.0255101 | 0.3 | Factor |
| **Year (1999)** | -1.0811426 | 1.0276385 | 0.29 | Factor |
| **Year (2001)** | -1.9476701 | 1.0936898 | 0.076 | Factor |
| **Year (2002)** | -1.7395533 | 1.0232469 | 0.09 | Factor |
| **Cresp** | | | 0.44 | smoother term |
| **condition** | | | **<0.0001*** ** | smoother term |

Bold values denote significant p values (<0.05) and asterick's define level of significance: p<0.0001 = '<0.0001***'; p< 0.001 = '***'; p < 0.01 = '**'; p<0.05 = '*'

## 3.4.4 Fish Condition

Condition varies seasonally in a similar manner in males and females, with minimum average monthly values (7.21 g $cm^{-3}$) at the end of the spawning season (April) followed by a gradual increase in

condition with maximum monthly average (21.1 g $cm^{-3}$) values occurring before the spawning season (October), presented in figure **33** and figure **35**. At the onset of the spawning season condition values reduce, reaching minimum values between March to May. The individual variability of monthly condition values is at a minimum from March to May (5.69g $cm^{-3}$ to 6.85 g $cm^{-3}$), and a maximum (17.7 g $cm^{-3}$to 24.2 g $cm^{-3}$) from October to November (figure **33**). When comparing condition between sex regardless of seasonality, females have slightly higher average condition expression (figure **34**). GAM models (aiming to explain condition variability using season, months and sex as factors) suggests a significant variation in condition throughout monthly cycle and sex, with females expressing higher variability and absolute condition values (figure **34**, figure **35**, table **13** and equation **3.7**).

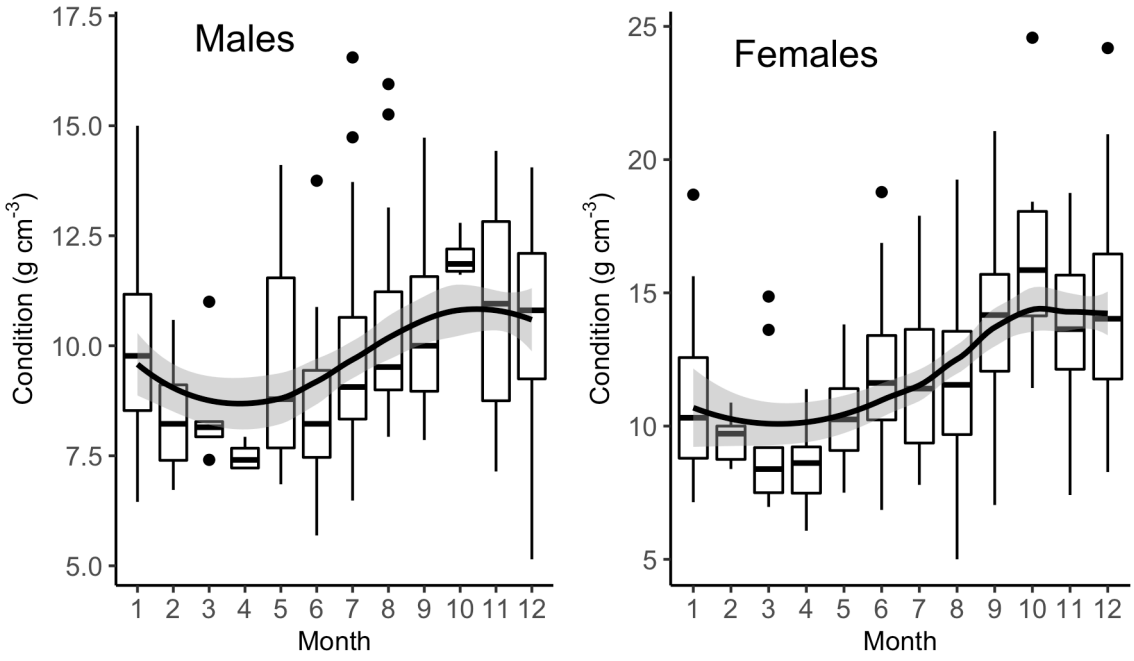


***Figure 33**: Describing the seasonal variations in condition, split between months. The calculation used to derive condition is described in the methods section.*

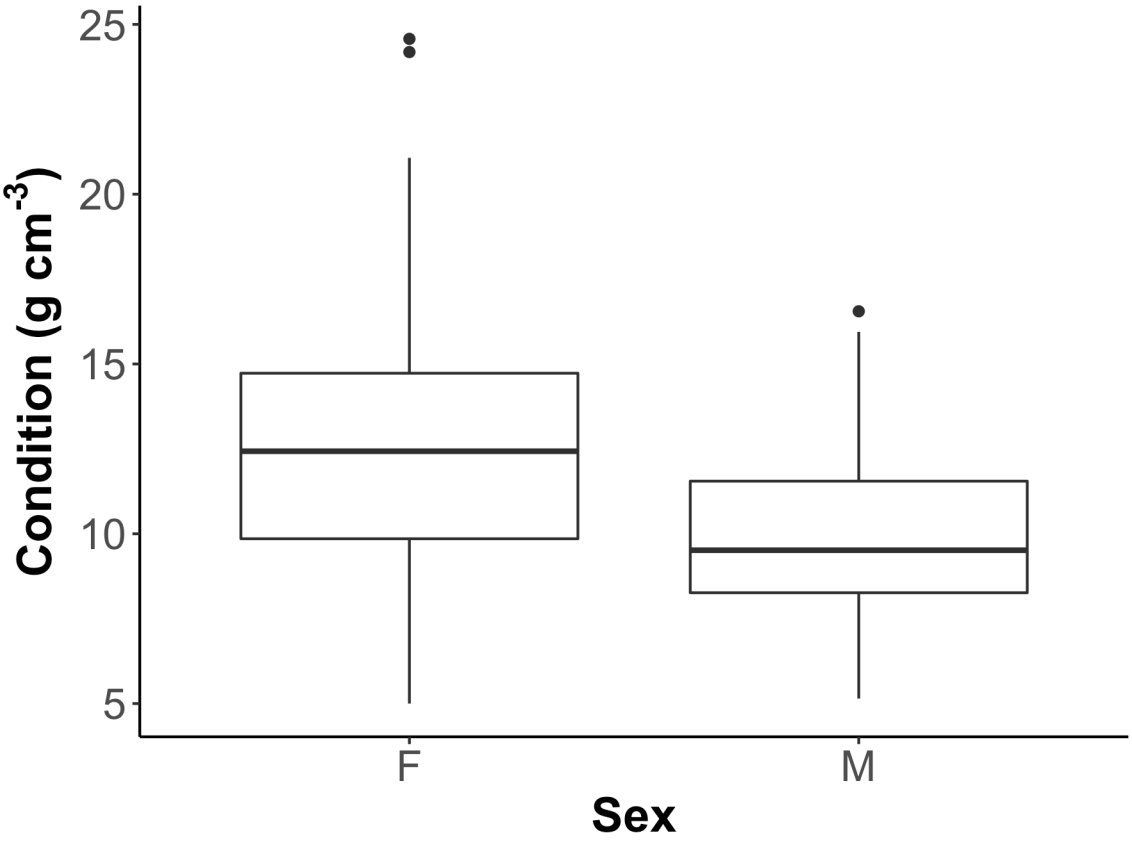


***Figure 34**: Box plots describing the variability in total average condition values when data is grouped by sex, irrespective of seasonal cycle.*

Below is a description of the GAM model structure used to Seasonal variations in condition at capture.

$$\text{condition} \sim \text{Cresp} + \text{Modelled Temperature} + \text{F(sex)} + \text{(month)} + \text{F(Season)} \qquad (3.7)$$

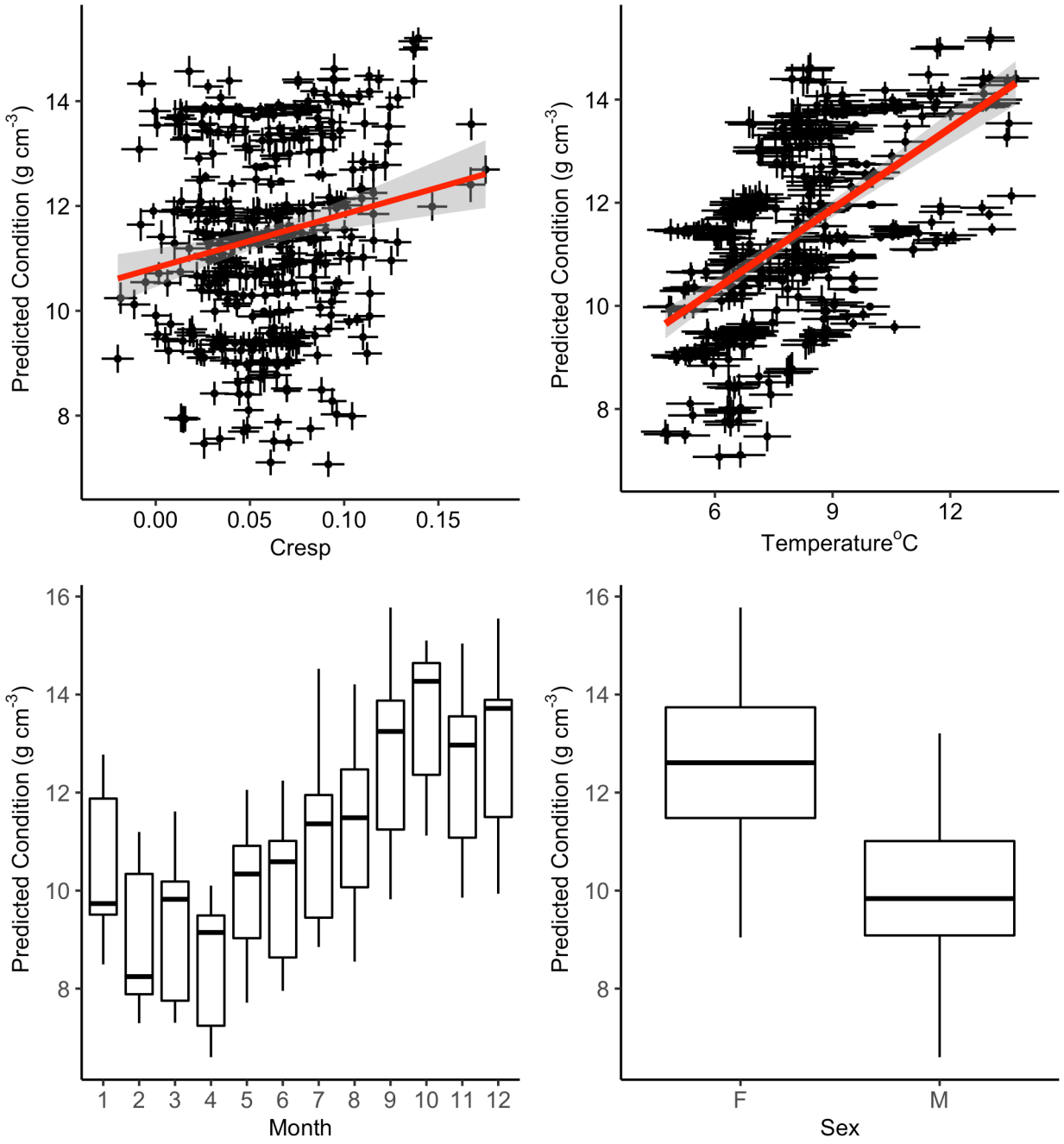


***Figure 35**: Predicted partial effects plots exploring condition variability over the seasonal cycle. This data is simulated extracted generalised additive model data. Model structure is described above in equation 3.7*

***Table 13**: GAM model (described above in equation 3.7) outputs, used to explore seasonal variations in condition*

| Terms | Coefficient | standard error | p values | effect class |
|---|---|---|---|---|
| **intercept** | 12.5624429 | 0.2023287 | **<0.0001*** ** | Factor |
| **Sex** | -2.4372568 | 0.2597385 | **<0.0001*** ** | Factor |
| **Season** | -0.3312832 | 0.3308349 | 0.32 | Factor |
| **Cresp** | | | 0.18 | Smoother Term |
| **Modelled Temperature** | | | **<0.0001*** ** | Smoother term |
| **Month** | | | **<0.0001*** ** | Smoother Term |

Bold values denote significant p values (<0.05) and asterick's define level of significance: p<0.0001 = '<0.0001***'; p< 0.001 = '***'; p < 0.01 = '**'; p<0.05 = '*'

### 3.4.5 Cresp Values

Cresp values range between 0.0194 and 0.218 for population A with an average of 0.11, between 0.0393 and 0.162 with an average of 0.109 for B and between 0.0315 to 0.185 with an average of 0.116 for population C. When comparing overall each sub population, regardless of annual cycle, there is no significant difference in Cresp expression (Kruskal-Wallis p-value = 0.169) between population (figure **36**).

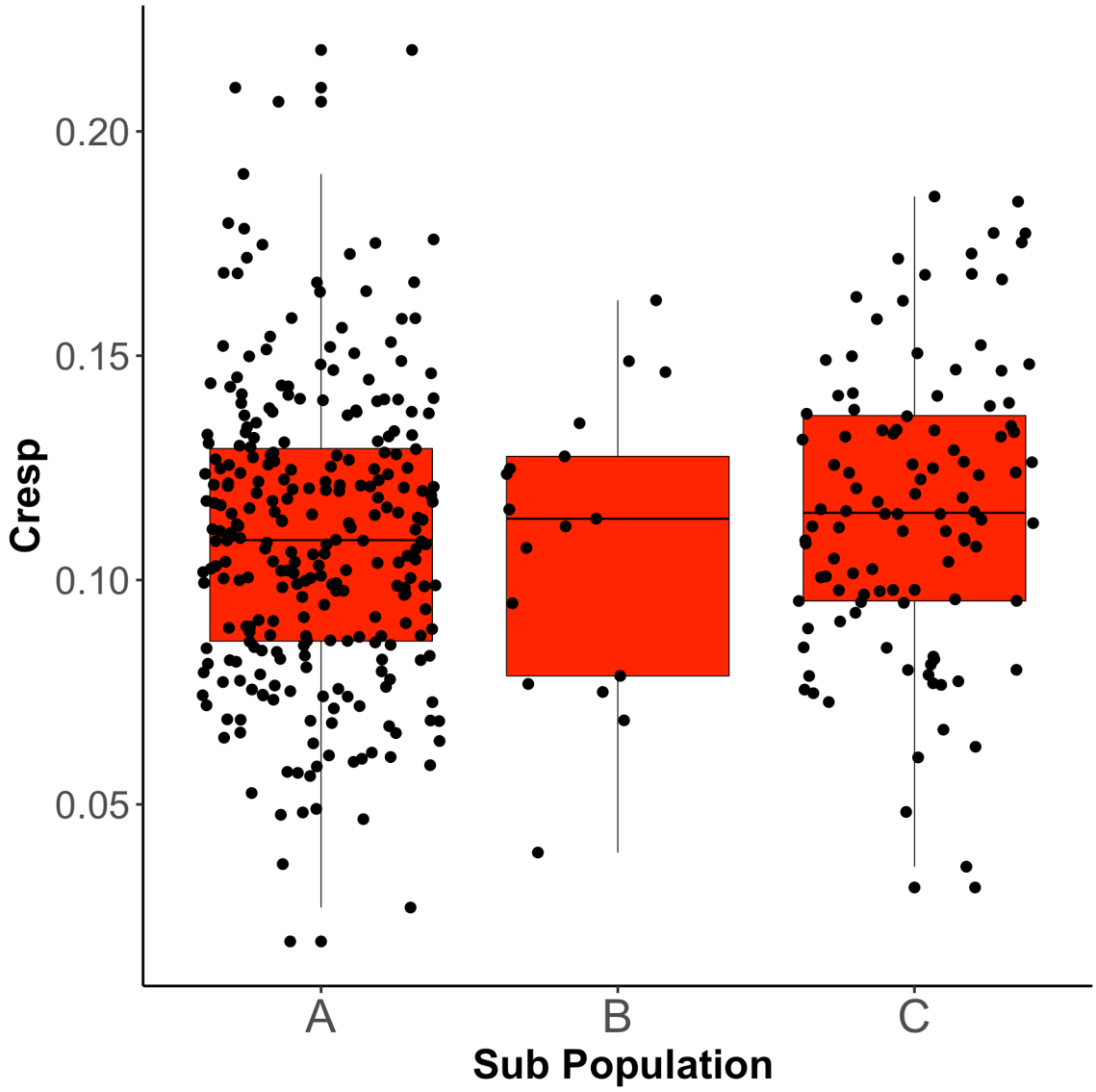


***Figure 36**: Expressing the Cresp variability between North Sea sub-populations. Here sub population are ground and averaged regardless of sex and seasonal cycle. The method used to derive the appropriate sub population for each individual is described above in the methods sections, and is based on previous tagging surveys (Hunter et al., 2003), as well as isotopic and extrinsic variability each sub population has been measured to experience (Darnaude et al., 2014).*

Total population (sub population A, B and C grouped together) Cresp values are at their highest absolute values during the growing season (approximately 0.218) (August to November, figure **38**). With the beginning of the spawning season, when the population begins to migrate to more southerly waters (December to February), monthly population-specific averages of Cresp values begin to reduce (0.0649), accompanied by an increase in individual variability. Population Cresp values reach minimum average values (0.0367) and maximum variances, during the spawning season (March to

April), followed by a gradual rise in average Cresp values, as individuals migrate to the northerly feeding grounds (table **15**, figure **37** and figure **38**).

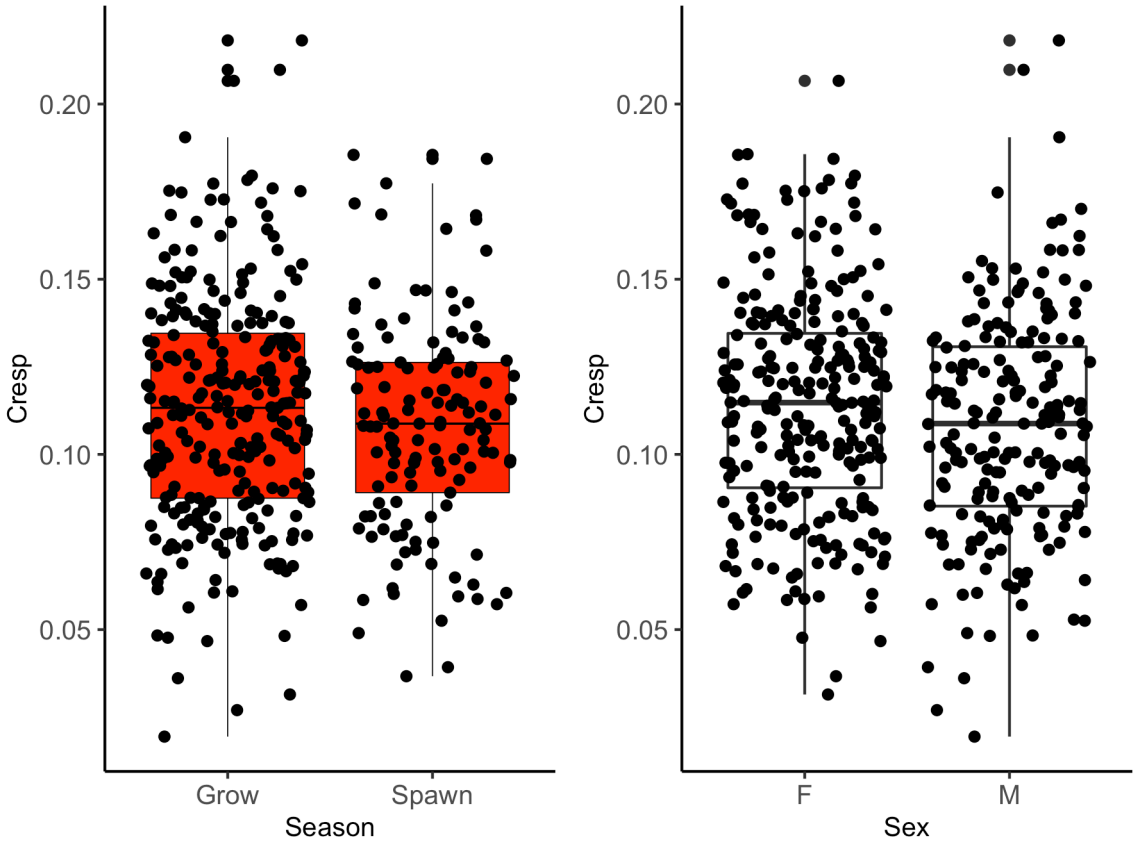


***Figure 37**: Expressing the Cresp variability between seasons (the growing and spawning seasons, split by month using previous tagging data (Hunter et al., 2003)) and sexes.*

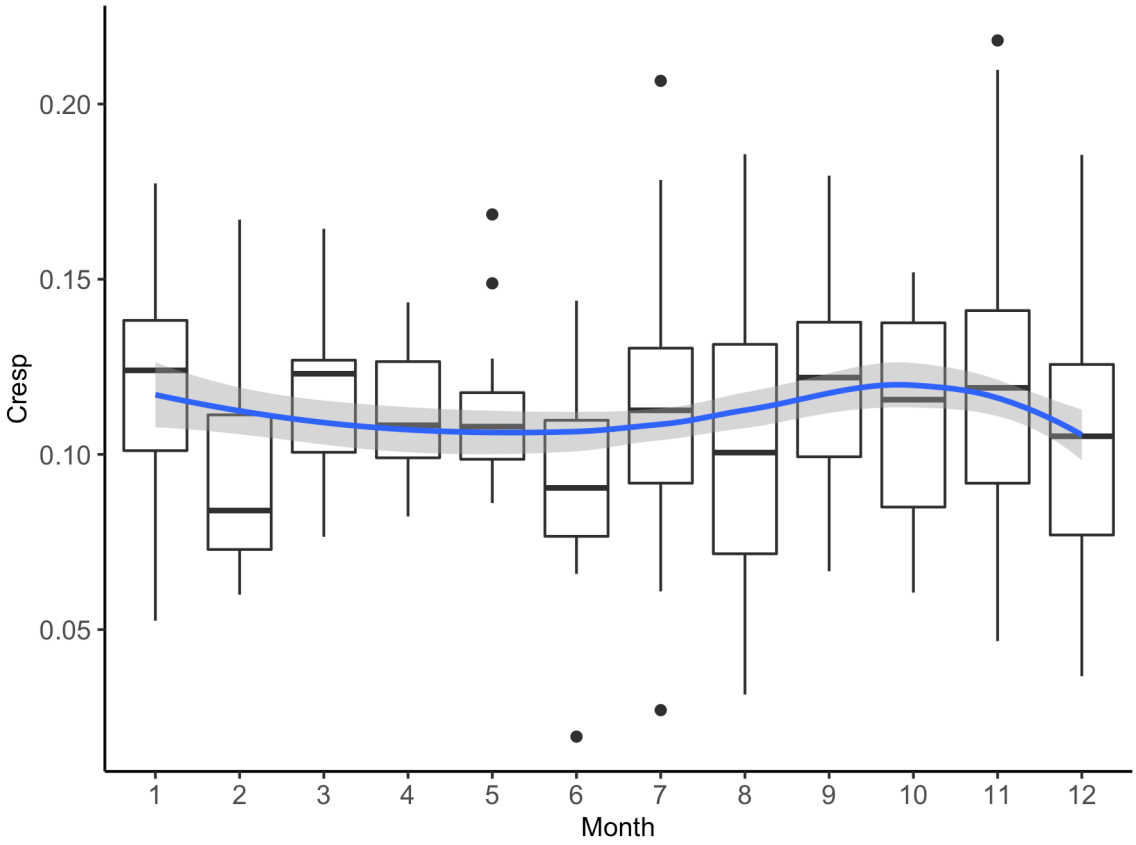


***Figure 38**: Expressing the Cresp variability over the annual cycle, split by month.*

***Table 14**: Description of otolith isotopic measurements, split by carbon and oxygen isotopic values as well as over the monthly cycle and between sexes. Data is arranged to show the minimum, maximum and average values for each month, isotopic elemental value and sex*

| | Male | | | Female | | | Male | | | Female | | |
|---|---|---|---|---|---|---|---|---|---|---|---|---|
| **Month** | $\delta^{18}O_{min}$ | $\delta^{18}O_{max}$ | $\delta^{18}O_{mean}$ | $\delta^{18}O_{min}$ | $\delta^{18}O_{max}$ | $\delta^{18}O_{mean}$ | $\delta^{13}C_{min}$ | $\delta^{13}C_{max}$ | $\delta^{13}C_{mean}$ | $\delta^{13}C_{min}$ | $\delta^{13}C_{max}$ | $\delta^{13}C_{mean}$ |
| 1 | 0.90 | 2.64 | 1.72 | 1.06 | 2.40 | 1.58 | -1.40 | 0.26 | -0.74 | -1.48 | 0.81 | -0.42 |
| 2 | 1.11 | 2.25 | 1.61 | 1.08 | 2.88 | 2.12 | -1.07 | 0.60 | 0.02 | -1.22 | 0.68 | -0.04 |
| 3 | 0.83 | 1.95 | 1.39 | 1.47 | 2.31 | 1.82 | -1.60 | 0.05 | -0.48 | -1.08 | 0.02 | -0.61 |
| 4 | 1.67 | 2.96 | 2.40 | 1.44 | 3.01 | 2.32 | -0.62 | -0.18 | -0.43 | -1.23 | 0.17 | -0.63 |
| 5 | 1.48 | 2.57 | 2.01 | 1.79 | 2.81 | 2.33 | -1.65 | 0.03 | -0.55 | -0.63 | -0.23 | -0.44 |
| 6 | 1.23 | 2.98 | 2.15 | 1.74 | 2.98 | 2.51 | -1.14 | 0.31 | -0.25 | -0.94 | 0.99 | -0.10 |
| 7 | 0.47 | 3.09 | 2.29 | 1.29 | 3.30 | 2.51 | -2.34 | 0.37 | -0.50 | -1.38 | 0.96 | -0.37 |
| 8 | 1.35 | 2.48 | 1.92 | 1.03 | 2.87 | 2.31 | -1.56 | 0.78 | -0.30 | -1.36 | 0.70 | -0.10 |
| 9 | 1.34 | 2.93 | 2.33 | 1.24 | 3.25 | 2.28 | -1.91 | 0.37 | -0.74 | -1.22 | 0.38 | -0.36 |
| 10 | 2.72 | 2.90 | 2.81 | 2.82 | 3.08 | 2.92 | -1.06 | 0.30 | -0.47 | -1.31 | -0.30 | -0.81 |
| 11 | 0.02 | 3.46 | 1.88 | 1.15 | 3.15 | 2.16 | -1.67 | 0.61 | -0.54 | -2.46 | 0.64 | -0.63 |
| 12 | 1.13 | 3.01 | 1.97 | 0.95 | 2.82 | 1.95 | -1.77 | 0.71 | -0.48 | -1.16 | 0.74 | -0.12 |

***Table 15**: Description of Cresp values, calculated using otolith carbon isotopic values described in the text above. Data is arranged to show the minimum, maximum and average values for each month, isotopic elemental value and sex.*

| | | | | | | |
|---|---|---|---|---|---|---|
| | | | **male** | | | **female** |
| **Month** | **$Cresp_{min}$** | **$Cresp_{max}$** | **$Cresp_{mean}$** | **$Cresp_{min}$** | **$Cresp_{max}$** | **$Cresp_{mean}$** |
| 1 | 0.90 | 2.64 | 1.72 | 1.06 | 2.40 | 1.58 |
| 2 | 1.11 | 2.25 | 1.61 | 1.08 | 2.88 | 2.12 |
| 3 | 0.83 | 1.95 | 1.39 | 1.47 | 2.31 | 1.82 |
| 4 | 1.67 | 2.96 | 2.40 | 1.44 | 3.01 | 2.32 |
| 5 | 1.48 | 2.57 | 2.01 | 1.79 | 2.81 | 2.33 |
| 6 | 1.23 | 2.98 | 2.15 | 1.74 | 2.98 | 2.51 |
| 7 | 0.47 | 3.09 | 2.29 | 1.29 | 3.30 | 2.51 |
| 8 | 1.35 | 2.48 | 1.92 | 1.03 | 2.87 | 2.31 |
| 9 | 1.34 | 2.93 | 2.33 | 1.24 | 3.25 | 2.28 |
| 10 | 2.72 | 2.90 | 2.81 | 2.82 | 3.08 | 2.92 |
| 11 | 0.02 | 3.46 | 1.88 | 1.15 | 3.15 | 2.16 |
| 12 | 1.13 | 3.01 | 1.97 | 0.95 | 2.82 | 1.95 |

### 3.4.6 Modeling variation in Cresp values

The best fitting GAM models explaining variation in Cresp values as a function of temperature, condition, year, month, season and sex are described in equations **3.8** and **3.9**. Partial effects plots for each term are shown in figure **39**. The model described in equation **3.8** includes month within GAM structure, where the model described in equation **3.9** includes season. We aimed to test the effect of month and season independently, as they are co-varying predictor factors (because season is dependent upon month), and would potentially impact model outputs.

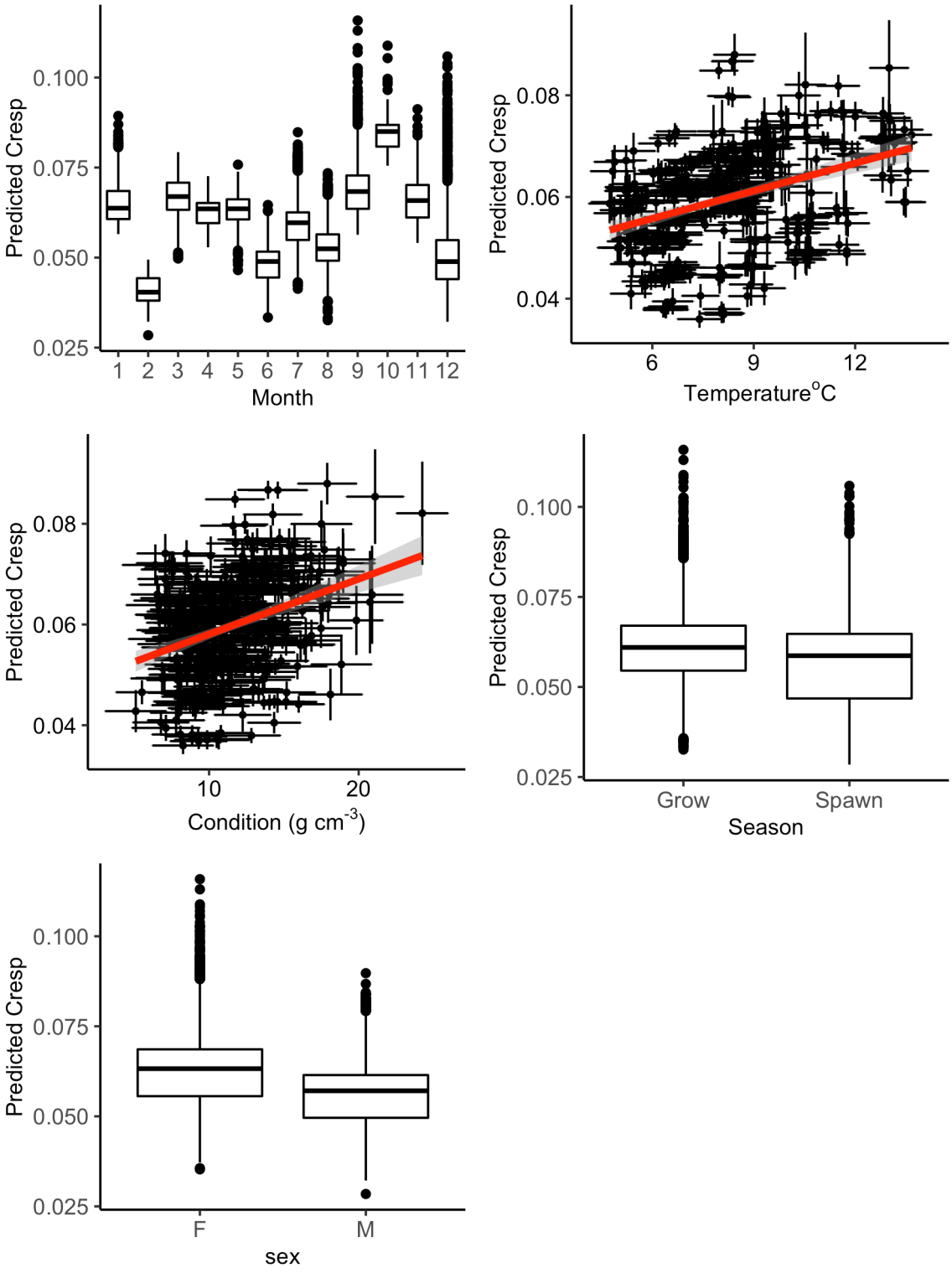


***Figure 39**: Predicted partial effects plots exploring Cresp variability over the seasonal cycle, combining both models described by equations 3.8 and 3.9 below. This data is simulated extracted model data from the model structures described in equations 3.8 and 3.9.*

The effects of temperature and condition on Cresp are small and confidence terms only exceed 0 at edges of the measured range (for temperature). Only month has a strong effect, with highest Cresp values predicted for the end of the growing season around Sept-October (as shown in table **16** and figure **39**).

Best fitted GAM models predict Cresp varies among months (equation **3.8**) as well as between spawning and growing season (equation **3.9**). Cresp expresses no significant interaction with condition or temperature (tables **16** and **17**). The range of predicted modelled experienced temperatures within this data set is below the laboratory-derived optimum thermal range for Plaice growth rates (approximately $20^{o}C$) (Van der Veer et al., 2009), and we see no evidence of thermal limitation, due to a lack of parabolic relationship with Cresp and temperature (figure **39**). When the Cresp thermal response curve (regardless of month) is analysed we see no metabolic thermal dependence (linear model P value = 0.75) (figure **39**). When individuals are grouped by month of capture (model described by equation **3.8**), overall average monthly Cresp values, express no significant relationship with temperature, with a linear model P value of 0.078.

$$\text{Cresp} \sim \text{Temperature} + \text{condition} + \text{F(month)} + \text{F(sex)} + \text{F(year)} \qquad (3.8)$$

***Table 16**: GAM model output table exploring the controlling factors of Cresp expression including month as factor. Model structure is described by equation 3.8 above*

| Terms | Coefficient | standard error | p values | effect class |
|---|---|---|---|---|
| **Intercept** | 0.1097435864 | 0.019828097 | **<0.0001*** ** | Factor |
| **Year (1985)** | 0.0116301227 | 0.019275242 | 0.55 | Factor |
| **Year (1986)** | 0.0164182322 | 0.019501027 | 0.4 | Factor |
| **Year (1987)** | 0.0086842662 | 0.018700767 | 0.64 | Factor |
| **Year (1990)** | -0.0179805636 | 0.018563906 | 0.33 | Factor |
| **Year (1993)** | -0.0029290665 | 0.018717660 | 0.88 | Factor |
| **Year (1995)** | -0.0324474070 | 0.018962384 | 0.088 | Factor |
| **Year (1997)** | -0.0088961204 | 0.018529505 | 0.63 | Factor |
| **Year (1998)** | 0.0072248289 | 0.018818142 | 0.7 | Factor |
| **Year (1999)** | 0.0066473812 | 0.018994691 | 0.73 | Factor |
| **Year (2001)** | -0.0284822349 | 0.019870478 | 0.15 | Factor |
| **Year (2002)** | -0.0021289238 | 0.019252727 | 0.91 | Factor |
| **Month (Febuary)** | -0.0222486590 | 0.011610507 | 0.056 | Factor |
| **Month (March)** | -0.0130246163 | 0.012379371 | 0.29 | Factor |
| **Month (April)** | -0.0047950826 | 0.014766902 | 0.75 | Factor |
| **Month (May)** | 0.0085534721 | 0.011278293 | 0.45 | Factor |
| **Month (June)** | -0.0117576891 | 0.011288321 | 0.3 | Factor |
| **Month (July)** | -0.0086853887 | 0.008848411 | 0.33 | Factor |
| **Month (August)** | 0.0036712965 | 0.008747993 | 0.67 | Factor |
| **Month (September)** | 0.0107025588 | 0.009511018 | 0.26 | Factor |
| **Month (October)** | -0.0042404174 | 0.015972659 | 0.79 | Factor |
| **Month (November)** | 0.0094395070 | 0.009218977 | 0.31 | Factor |
| **Month (December))** | 0.0192577512 | 0.009572195 | **0.045*** | Factor |
| **Sex** | 0.0006004084 | 0.003496873 | 0.86 | Factor |
| **Temperature** | | | 0.082 | Smoother term |
| **condition** | | | 0.42 | Smoother term |

Bold values denote significant p values (<0.05) and asterick's define level of significance: p<0.0001 = '<0.0001***'; p< 0.001 = '***'; p < 0.01 = '**'; p<0.05 = '*'

Below is the GAM model structure used to test for seasonal variations in Cresp at capture, with model outputs described in table **17**. As described above we are using season here to explore the impact of behavior on metabolic expression. We are looking at if feeding and spawning are linked with changes in Cresp expression.

$$\text{Cresp} \sim \text{Temperature} + \text{condition} + \text{F(season)} + \text{F(sex)} + \text{F(year)} \qquad (3.9)$$

***Table 17**: GAM model output exploring the controlling factors of Cresp expression including season as factor. Model structure is described by equation 3.9 above*

| Terms | Coefficient | standard error | p values | effect class |
|---|---|---|---|---|
| **intercept** | 0.10670818945 | 0.018258889 | **<0.0001*** ** | Factor |
| **Season** | 0.00984430397 | 0.003977969 | **0.014*** | Factor |
| **Sex** | 0.00082579150 | 0.003466404 | 0.81 | Factor |
| **Year (1985)** | 0.01244174798 | 0.019078223 | 0.51 | Factor |
| **Year (1986)** | 0.01618391908 | 0.019161239 | 0.4 | Factor |
| **Year (1987)** | 0.01532473492 | 0.018508769 | 0.41 | Factor |
| **Year (1990)** | -0.01828781398 | 0.018506370 | 0.32 | Factor |
| **Year (1993)** | 0.00143152597 | 0.018612312 | 0.94 | Factor |
| **Year (1995)** | -0.03167614954 | 0.018883016 | 0.094 | Factor |
| **Year (1997)** | -0.00872232659 | 0.018550795 | 0.64 | Factor |
| **Year (1998)** | 0.00997943273 | 0.018730615 | 0.59 | Factor |
| **Year (1999)** | 0.00727264091 | 0.018689328 | 0.7 | Factor |
| **Year (2001)** | -0.02543640054 | 0.019701623 | 0.2 | Factor |
| **Year (2002)** | 0.00001674266 | 0.019018685 | 1 | Factor |
| **Temperature** | | | 0.15 | Smoother term |
| **Condition** | | | 0.54 | Smoother term |

Bold values denote significant p values (<0.05) and asterick's define level of significance: p<0.0001 = '<0.0001***'; p< 0.001 = '***'; p < 0.01 = '**'; p<0.05 = '*'

### 3.4.7 Oxygen consumption

As the plaice sampled within this data set are of relatively similar body sizes, reconstructed SMR (calculated using model temperature estimates, described in section **2.3.9**) displays a similar temporal pattern to model temperature throughout the annual cycle, with minimum values (39.18 $mgO_2kg^{-1}h^{-1}$, as described previously in chapter 2) during the spawning season, and a gradual increase from June as temperatures rise. To compare this data set to other laboratory derived SMR studies we converted Cresp values into oxygen consumption, using a previous conversation factor for cod (equation **3.3**), under the assumption that $O_2$ consumption reported within this study is precise yet potentially inaccurate, as intraspecific trends will be unaffected. To calculate absolute oxygen consumption expression, we require further experimentation specific to Plaice. Best fitted GAM models, attempting to explain the variability in oxygen consumption rates using season, condition, temperature and variability over the annual cycle as variables, suggest that there is a correlation with SMR and between seasons; with the growing season expressing higher oxygen consumption rates (figure **40**).

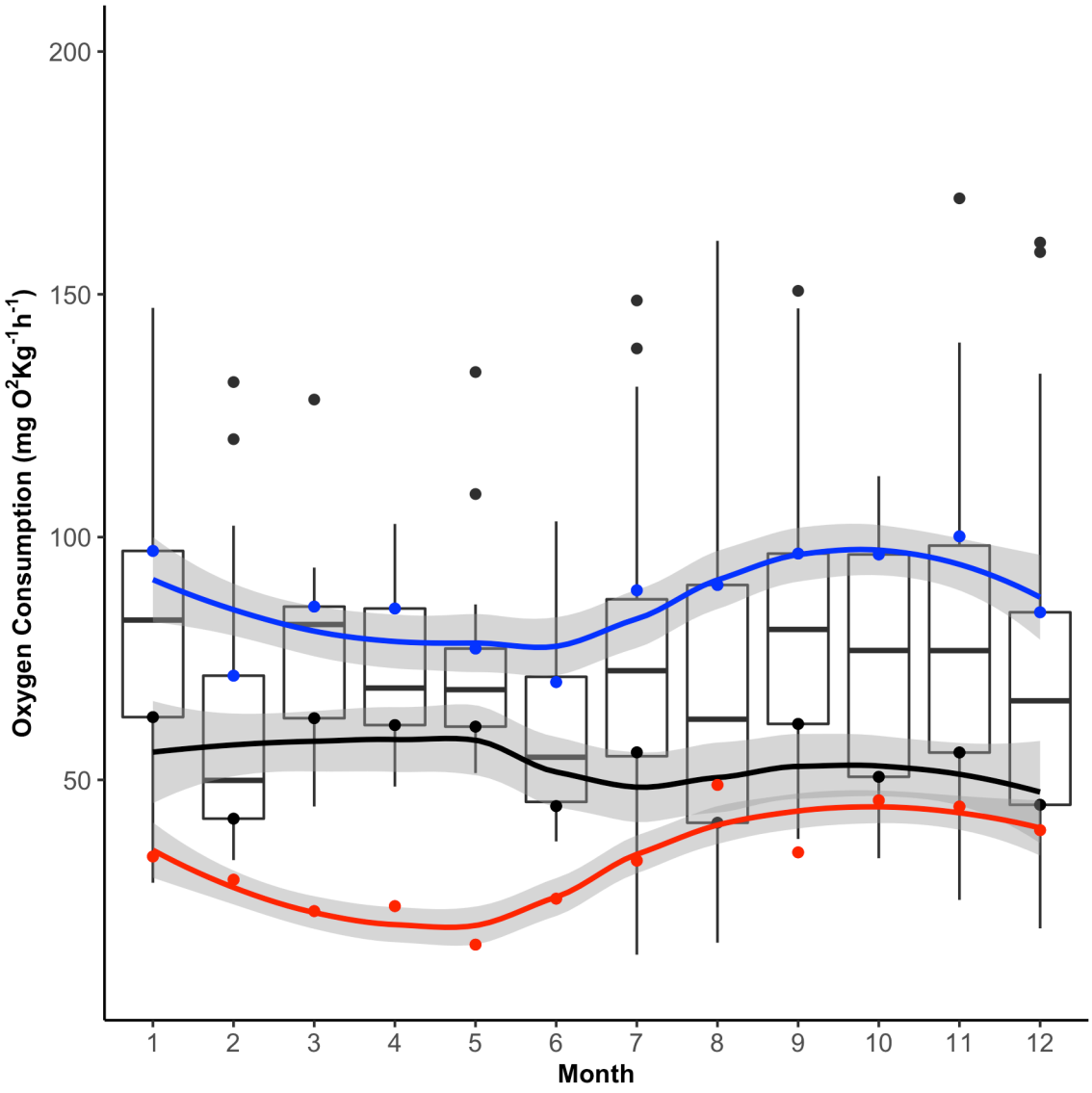


***Figure 40**: Seasonal variations in field aerobic range. Dark blue smoother representing the upper 75th quartile of Cresp expression, red smoother representing the lower 25th quartile of Cresp expression. The black smoother representing the range between the 75th and 25th quartile. This is termed field aerobic range, and is an attempt to compare to laboratory derived aerobic scope findings, and tells us the range of field metabolic rate expression over a population, and how the higher and lower levels of metabolic expression interact with temperature*

Monthly population average oxygen consumption rates estimated from carbon isotope data were higher than estimated SMR values throughout the annual cycle, but we saw no systematic seasonal effects on the difference between SMR and oxygen consumption estimates. Periods of high oxygen consumption also represent highest predicted SMR.

To relate this data to aerobic scope findings we estimated the minimum observed field aerobic range (FAR) (in units of mg$O_2 kg^{-1} h^{-1}$). To do this we calculated the monthly upper quartile (highest 75%) and lower quartile (bottom 25%) of population oxygen consumption rates over the annual cycle, the difference between the two representing field aerobic range (figure **40**). Best fitted GAM models, attempting to explain the variability in field aerobic range over the annual cycle (using season and months as factors), predict that field aerobic range is higher during the growing season relative to spawning season. Indicating that the population is expressing a higher energetic demand during the growing season relative to the spawning season (equation **3.10** and table **18**).

$$FAR \sim F(season) + Temperature \qquad (3.10)$$

***Table 18****: GAM model (structure described above in equation 3.10) outputs exploring the factors impacting field aerobic range over the seasonal cycle*

| Terms | Coefficient | standard error | p values | effect class |
|---|---|---|---|---|
| intercept | 36.207569 | 1.519889 | **<0.0001*** ** | Factor |
| Season | -5.808931 | 2.404513 | **0.027*** | Factor |
| Temperature | | | **<0.0001*** ** | Smoother term |

Bold values denote significant p values (<0.05) and asterick's define level of significance: p<0.0001 = '<0.0001***'; p< 0.001 = '***'; p < 0.01 = '**'; p<0.05 = '*'

***Table 19**: Description of fixed effects variables, used within varying iterations of model structure, between sexes and seasonal cycles*

| | males | | | | Females | | | |
|---|---|---|---|---|---|---|---|---|
| | | | | Growing season | | | | |
| | min | max | range | SD | min | max | range | SD |
| Cresp | 0.02 | 0.22 | 0.12 | 0.04 | 0.04 | 0.21 | 0.12 | 0.04 |
| $O_2$Consumption (mg $O_2kg^{-1}hr^{-1}$) | 9.93 | 236.45 | 74.61 | 34.35 | 16.47 | 204.28 | 78.12 | 31.69 |
| SMR (mg $O_2kg^{-1}hr^{-1}$) | 34.91 | 76.68 | 46.55 | 8.96 | 31.07 | 71.7 | 45.49 | 9.38 |
| Condition (g $cm^{-3}$) | 5.69 | 16.56 | 10.17 | 2.13 | 6.86 | 21.08 | 12.67 | 2.93 |
| Temperature $(^oC)_{Model}$ | 3.42 | 15.01 | 7.83 | 2.01 | 2.94 | 15.32 | 8.25 | 2.25 |
| Temperature $(^oC)_{Otolith}$ | 1.3 | 24.37 | 9.58 | 3.25 | 1.32 | 25.85 | 8.64 | 3.5 |
| | | | | Spawning season | | | | |
| Cresp | 0.04 | 0.17 | 0.11 | 0.03 | 0.04 | 0.19 | 0.12 | 0.04 |
| $O_2$Consumption (mg $O_2kg^{-1}hr^{-1}$) | 20.9 | 131.94 | 68.72 | 23.64 | 19.42 | 160.68 | 74.51 | 29.87 |
| SMR (mg $O_2kg^{-1}hr^{-1}$) | 36.34 | 68.69 | 49.47 | 7.48 | 52146 | 61.64 | 45.75 | 7.8 |
| Condition (g $cm^{-3}$) | 5.15 | 15 | 9.66 | 2.31 | 7.15 | 24.19 | 12.17 | 3.75 |
| Temperature $(^oC)_{Model}$ | 3.31 | 13.2 | 8.37 | 1.8 | 3.03 | 13.75 | 8.2 | 2.11 |
| Temperature $(^oC)_{Otolith}$ | 3.91 | 25.18 | 12.15 | 3.41 | 2.58 | 24.69 | 10.96 | 3.51 |

# 3.5 Discussion

## 3.5.1 Annual Cycle

Field metabolic rates (expressed as Cresp values) varied systematically throughout the annual cycle, with higher metabolic rates expressed during late spring and late summer, associated with post spawning recovery and pre-spawning increases in condition respectively. Spawning periods and early summer, by contrast were characterised by relatively low field metabolic rates. Individual estimated median factorial metabolic rate varied throughout the season, with peaks around 2-3 times SMR and a maximum monthly factorial metabolic rate average of 1.98, consistent with estimates of environmental limits on population persistence (e.g. the 'metabolic index' of Deutsch et al., (2020)).

Over the annual cycle, plaice experienced temperature ranges in excess of $10^oC$, which would be expected to more than double metabolic costs based on estimates of $Q_{10}$ values for standard metabolic rates on fishes between 2 and 3 (Gauldie 1996). Despite this, we found no systematic relationship between experienced temperature and field metabolic rate in young adult (Age 3-6) plaice. This strongly implies that while operating within the thermal niche, variations in expressed field metabolic rate are more strongly influenced by individual differences and behavioral energy expenditure (See also chapter 2). We see no consistent relationship between experienced temperature and Cresp values within months or within years (as predicted from best fitted GAM models). Experienced temperatures do not reach experimentally derived temperatures for optimal growth (maximum individual experienced temperature of $13.52^oC$, when optimum growth rates occur at approximately $20^oC$), and we do not see evidence for temperature limitation of Cresp values (e.g. parabolic patterns in temp Cresp relationships) when examining the total population. If individuals are split into sub populations, such as the highest 75th and lowest 25th quartiles of FMR expression, the highest FMR observed in any month did covary positively with temperature, implying that highest performances were limited by (low) temperatures.

To explain time periods when the population expresses maximum energetic expenditure, we examine the annual migratory and breeding cycle of North Sea plaice (Darnaude et al., 2014). From June till November (feeding season) the three distinct North Sea sub populations are separated into their

associated higher latitude feeding grounds (Darnaude et al., 2014), and it is believed that individuals primarily focus on feeding, increasing (or optimising) their condition (Hunter et al., 2009). Within the feeding season, individuals do not undertake large migratory movements over wide habitat areas within short time periods, as apparent from tagging surveys (Hunter et al., 2004). From June to August, at the beginning of the feeding season (Hunter et al., 2009), population FMR and SMR expression is at a comparable range as they start to feed, evident from the gradual rise in condition values yet still relatively low absolute condition. As the feeding season progresses from September to November, the elevation of population FMR from SMR rapidly increases, peaking during October, and condition values reach a maximum. During this time period the population is feeding at a maximum rate, apparent from condition rapidly increasing to the annual peak, and previous tagging surveys (Hunter et al., 2004). This elevation in energetic expenditure coinciding with increased feeding activity suggests that feeding and growth of gonads represents a high net energetic input, consistent with DEB study findings (Fablet et al., 2009), either through increase in foraging movement (the "constant station" hypothesis) (Andersen and Beyer 2006; Breck 1993) or the energetic demand of digestion (the "constant activity" hypothesis) (Cruz-Font et al., 2019; Deslauriers et al., 2017). During the feeding season experienced temperature values are relatively low. Field aerobic range also expresses maximum values between September to November, as it is during this time period where population FMR individual variability is at a maximum. Individual variability has previously been used as a measure of population stability, with a high range of metabolic phenotypic expression suggested to result in the population being more adaptable to environmental variability (Killen 2014). Here an increase in the range of metabolic expression potentially suggests that some individuals elevate their FMR whilst others are able to gain condition at a lower level of energetic expenditure.

From December to January, each sub population migrates to shallower waters, usually in lower latitudes, to spawn, accompanied with a decreased modelled experienced temperature and predicted SMR. This migration coincides with a reduction in population FMR, and consequently the elevation from SMR also decreases, suggesting that individuals reduce energy expenditure. Condition values also begin to sharply reduce from December, indicating that individuals are no longer feeding and rely on reserved fat stores for the energetic requirement of migration and spawning (Jobling 1980). Previous works looking into the impact of food deprivation on population SMR expression have reported a reduction in overall population SMR expression and individual variability (Killen et al., 2013), similar to FMR expression within this study as feeding activity reduces. The reduction of FMR elevation from

SMR, implies that spawning has a comparatively low energetic cost when compared to feeding and storing potential energy as fat reserves, presumably maximising the efficiency of stored energy. Field aerobic range is also at a minimum during spawning time periods, potentially suggesting minimum individual metabolic expression. This result is comparable to laboratory-based studies during time periods when the population is not feeding (Killen et al., 2013).

From February to April the sub populations migrate north to return to separate feeding grounds. During this time experienced temperature reduces once more, similar to previous works (Darnaude et al., 2014), and condition values reach the minimum. Population FMR and SMR are at a similar range, representing a small energetic demand close to SMR. From March onwards FMR increases, and subsequently the elevation from SMR is again increased. This trend coincides with the end of migratory behavior, when individual's potential energy fat stores are at a minimum, with low conditional values. This data suggests that, although environmental drivers must contribute to metabolic expression, primary metabolic controllers are likely to be a combination of prey availability and behavioral cycles.

Previous works focusing on plaice physiology have found that laboratory derived oxygen consumption (SMR) and growth rates scale predictably with temperature and body mass (Priede and Holliday 1980). Optimum growth rates have found to peak at approximately $20^{o}C$ when prey availability is an unlimited factor, with higher temperatures resulting in thermally limiting conditions (Fonds et al., 1992). Studies with controlled food availability, find that above 18 degrees SMR reduces, as prey abundance becomes a limiting factor (Van der Veer et al., 2009). The data presented within this study does not show any clear temperature or body mass scaling with FMR, however previous laboratory studies derive metabolic relationships using one aspect of metabolism, SMR, when as DEB models point out there are multiple energetic drivers contributing the total energetic demand, FMR (Van der Veer et al., 2010). The individuals presented within this study also do not experience similar conditions as individuals of previous works, as they are wild individuals who inhabit an ecological niche they are adapted to, and do not exist within environments where their physiological functionality is limited. There is however some debate as to what environmental conditions suit plaice, and how they may change over the life history of an individual. For example, there is an observed shift to a lower optimal temperature with increasing fish size, which is potentially related to a reduction in the rate of food intake with increasing fish size due to the lack of suitably-sized (large) prey (Van der Veer et al., 2009). Stomach contents analysis also suggests that some plaice chose to inhabit sub-optimal foraging grounds, as is the case

for various large North Sea fish species (Van der Veer et al., 2009; Daan 1973; Rijnsdorp and Vingerhoed 2001). DEB models studies state that some aspects need addressing to explain temperature tolerance, such as food deprivation and oxygen starvation and despite the evidence suggesting an inverse relationship between body size/volume and optimal temperatures for growth in flatfish (Yamashita et al., 2001; Van der Veer et al., 2009), the underlying processes remain unclear. It is likely that many unique factors make up each individuals optimal conditions, which are consistently changing over time as priorities change, and this data represents how individuals each chose the ecological niche best suited for their needs, therefore clear FMR environmental trends are unlikely and we require more detailed data (such as specific location prey availability) to form clearer conclusions.

### 3.5.2 Summarising the Broader Implications of the Findings

Otolith based FMR estimates are sensitive enough to record seasonal variations in expressed FMR within populations. In a population operating within its thermal niche, individual level FMR does not covary with temperature, however at a population level, seasonal variations in energetic costs of feeding, migrating and spawning have a stronger effect on expressed FMR than the observed 10-degree variation in temperature. Periods of highest expressed FMR (and highest inferred factorial SMR) likely reflect periods where individuals are most vulnerable to increased temperatures and/or reduced oxygen availability. For instance, marine heatwave conditions during April-May and September-October may be more detrimental to performance of North Sea plaice than equivalent temperature excursions experienced during June-August or December-March.

Field metabolic rates (and consequently daily energy and oxygen requirements) in North Sea plaice peak around October, coincident with peak condition. Plaice therefore potentially operate closer to MMR in October, maximising storage of energy resources. Plaice may therefore be more sensitive to decreases in water oxygen content or marine heat waves, both acting to lower MMR, in late summer or early autumn.

This data set implies that as variables such as temperature and condition do not appear to be the main drivers of FMR expression, to increase the accuracy or population distribution and output models we need to improve our understanding of the controlling factors of metabolic expression. As temperature must impact *in situ* population SMR (Pörtner 2010), yet reconstructed SMR and FMR appear to show

no interaction, this implies that either individual behavior or physiology acts as an “aerobic buffer” allowing the elevation or suppression of FMR expression in response to the needs of the individual over the annual cycle. To improve our abilities to predict population energetic demands, and consequently model biogeography, we need a more detailed understanding of how environmental conditions and ecological variables impact the energetic demand of behavior (Rutterford et al., 2015; Senina et al., 2020). Such as the impact of reduced prey abundance during feeding months and anomalous thermal conditions post spawning during periods of high juvenile growth. Potentially as the energetic response to the environment changes throughout life history, we need to model population outputs as sub populations, such as juveniles and adults, rather than treating the whole population; to capture responses to environmental changes in more detail. If population FMR is reconstructed over the annual cycle during multiple life stages on a consistent basis, this will improve our understanding of how the energetic demands of the population are controlled, potentially improving our ability to predict and respond to shifts in biogeography and abundance (Chung et al., 2021).

# 4 Relationships between Individual Level Field Metabolic Rate and Growth Rate in Wild Living Plaice

## 4.1 Abstract

Growth rate is a fundamental variable used as a measure of fish population performance and varies with multiple sources of extrinsic and intrinsic variability, including temperature, predation pressure, metabolic performance, population genotype and phenotype, prey availability and many more. Individual and population level growth rates are critical metrics in fisheries science and management and have also been used to assess the impact of climate change on wild populations.

However, mechanisms or processes controlling fish growth rate remain unclear, particularly regarding the relative importance of intrinsic physiological traits compared to extrinsic conditions (e.g. temperature, food availability). Observations of *in situ* field metabolic rate may improve our understanding of factors influencing individual growth rate, particularly if somatic growth accounts for a large proportion of energy costs.

Here we combine otolith derived field metabolic rate and otolith increment analyses to quantify the level of among-individual variation in growth rate than can attributed to intrinsic or extrinsic drivers in the context of juvenile and adult life stages, experienced temperature, body mass, condition, sex and cohort. We also define a new variable for thermal habitat selection, termed temperature anomaly, based on the temperature experienced by the fish compared to the potential thermal habitats available (this is based on the idea that fish can select the habitats based on environmental conditions which suit their physiology) within the timeframe of sampling.

We find that among individual variation in somatic growth rate is strongly related to body condition. Within the data set we find no strong relationship between growth rate and experienced temperature or expressed field Metabolic rate. However, in juvenile life stages we identify a weak negative relationship between somatic growth rate and temperature whilst in the same individuals at adult life stages, growth and temperature shows a weakly positive correlation. Among different measures of

thermal experience available within this study (otolith derived, model derived and temperature anomaly) temperature anomaly had the strongest influence on growth rate, implying individuals employ behavioral thermoregulation to maximise growth potential within a given experienced habitat. All growth models contained a large residual variance, and it is likely that variables unmeasurable in this study (such as food availability) have strong influence on attained growth, but, surprisingly, independently of individual-level field metabolic rate.

# 4.2 Introduction

## 4.2.1 The Importance of Growth Rate

Growth is a fundamental parameter in ecology (Ciotti 2012): individual growth rate reflects the ability of the individual to capture sufficient resources to sustain somatic growth (Arendt 1997; Post and Parkinson 2001; Huss et al., 2008; Ciotti 2012; Ciotti et al., 2014), and in a fisheries context, the mean growth rate of individuals within the population defines fishery potential (Björndal et al., 2004). The proportion and rate at which a fish population grows or reduces in abundance, body mass, body length and geographical distribution are key variables used to assess population stability in response to climatic variability and the level of anthropogenic exploitation a fishery stock can sustain (Quinn 2003; Björndal, et al 2004; Plagányi 2007; Sippel et al., 2015;).

Population growth rate measures changes in abundance (or biomass) within the community, and is the combination of individual growth rate, reproductive rate and mortality rate (Gedamke et al., 2007). As such, changes in individual growth rate are of key importance for understanding a population (or stock) response to ecological and environmental change (Heino and Godø 2002; Rolland et al., 2009; Brown et al., 2012; Kuparinen and Hutchings 2012), and the consequences for harvesting management. Individual growth rate is itself the realised product of metabolic costs and resource acquisition (Gedamke et al., 2007), and therefore growth rate responds to intrinsic (metabolic demand) and extrinsic (resource supply) terms (Hessenauer et al., 2015). Bioenergetic models of fish production typically model growth as a function of metabolic rate (Fonds et al., 1992; Humston et al., 2004; Van Denderen et al., 2020;), however while many studies have investigated linkages between standard metabolic rate and growth rate in fishes (Dutil et al., 1997; Cutts and Metcalfe 1998; McCarthy 2000) the relationship between realised field metabolic rate and growth rate among individuals within a population of marine fish has not (to our knowledge) been explicitly demonstrated.

Studies attempting to explain the relationship between SMR, MMR, individual variability and growth rate produce conflicting results, with similar environmental variables (such as temperature) showing both positive and negative correlations with growth over comparable small-scale geographical ranges (Ellis and Gibson 1995; Davey et al., 2006; Ciotti 2012; Killen 2014; Auer et al., 2015; Zeng et al.,

2018). Laboratory derived respiratory potential (aerobic scope and SMR) findings report a positive relationship between SMR and growth when individuals are exposed to cooler thermal ranges, yet a negative correlation at higher temperatures (Jobling 1996; Auer et al., 2015), with maximum metabolic rate producing contradictory results (positive interaction under warm conditions and negative in the cooler regimes) (Jobling 1996). Other studies exploring relationships between metabolic rate and growth rate in salmonids have found differences between geographically connected and unconnected sub populations (Morita et al., 2014); with either no relationship between SMR and growth or a negative correlation, both irrespective of extrinsic parameters such as temperature (Railsback 2022). Such observations contradict inferences drawn from SMR as under laboratory conditions salmonids express a consistent positive correlation between SMR and somatic growth. The inconsistent nature between studies highlights the importance of context, field-based observation and individual variation when assessing relationships between metabolism and expressed growth (Ciotti et al., 2014).

Within this study we explore the extent to which among-individual variation in growth rates within wild North Sea plaice can be explained by intrinsic and extrinsic factors, specifically variations in experienced temperature, population size and metabolic rate.

### 4.2.2 How Growth Rate is Measured: Final Growth Trajectory

Individual-level growth in fishes can be measured in several ways with no standard unit of assessment between studies, resulting in each survey tailoring their methods to suit the questions they are asking (Lugert et al., 2016). The most universally applied estimate of mean individual growth rate within a population draws on fitting von Bertalanffy type growth models (Sainsbury 1980; Pilling et al., 2002; Essington et al., 2001) to summaries population-level age-length data, deriving fitted estimates of theoretical maximum size and the rate (age) at which it is reached (Pilling and Kirkwood 2002). Studies relying on age-length relationships, termed “final state”, have been criticised for failing to capture the potentially high degree of inter and intra individual variability of growth trajectories, as energetic resources acquired by individuals are thought to be distributed between basal metabolism, reproduction, growth and other life processes which fluctuate over the life history of each individual (Denechaud et al., 2020). It has also been suggested that as growth processes are linked to both intrinsic and extrinsic factors, age-length index growth patterns may not be able to identify which variables

impact energetic allocation, potentially reducing the validity of model predictions using “final state” measurements (Morrongiello and Thresher 2015).

### 4.2.3 How Growth Rate is Measured: Otolith Growth Rate

As discussed in chapter 2 the relationship between environmental variables and intrinsic expression (specifically metabolism) changes over the life history of the individual (Denechaud et al., 2020). The evidence of metabolic phenotypes potentially suggests that to assess fish population health we need to measure juvenile and adult populations independently, rather than assuming extrinsic environmental variables impact both juveniles and adults in a similar manner. This evidence coupled with previous studies which report a correlation between growth rate and metabolism (Fonds et al., 1992; Van Humston et al., 2004; Denderen et al., 2020;) suggests that the extrinsic and intrinsic variables impacting growth rate potentially change throughout the life history of an individual. Therefore, to identify how intrinsic and extrinsic variables impact individual and population growth rates we need to measure somatic growth over the life history of the individual, as it is likely that the growth rate relationships with environmental conditions vary between juvenile and adult life stages (Denechaud et al., 2020). An easy, simple and widely used method is measuring growth chronologies found in calcified tissues, such a bivalve shells and fish otoliths, as they have proven to provide long term ecological data at a fine scale, including daily growth increments (Morrongiello, et al., 2012). Incremental growth of these hard structures is typically closely related to somatic growth (Doubleday et al., 2015; Black et al., 2019; Denechaud et al., 2020) and often identifiable at fixed temporal scales (i.e., daily, seasonal or yearly), thus providing continuous time-resolved growth histories of individuals and populations (Morrongiello et al., 2011; Black et al., 2013).

The linear distance between successive otolith annuli (increment width) is a commonly used proxy for growth rate in studies focusing on wild populations, with data sets allowing the identification of time periods of elevated or suppressed growth rates, which may be statistically linked to extrinsic variables such as temperature and population density (Morrongiello et al., 2011; Morrongiello et al., 2014; Morrongiello and Thresher 2015; Morrongiello, et al., 2019). Recently time series of otolith growth rate trajectory data have been used in combination with mixed effects modelling to attempt to attribute deviance in the data to both extrinsic (environmental) and intrinsic (physiological) factors (Morrongiello and Thresher 2015; Denechaud et al., 2020). Such studies highlight the benefits of

applying otolith derived growth rate, as they have found interactive impacts of multiple variables such as elevated growth rates during periods of high prey abundance with a small proportion of the variation in growth explained by temperature, however interpretations of mutually-interdependent variables may be complicated in this case by strong co-variation between prey abundance and thermal conditions (Denechaud et al., 2020). The relationship between temperature and growth becomes increasingly complex when examining sub populations, with examples of suppressed growth rates for individuals inhabiting the warmer range of a single species geographical distribution when compared to fish which select cooler thermal conditions (Pörtner 2010), further indicating that growth rates (and drivers of among-individual variation in growth) are likely to be context-dependent, influenced by the interactive effect of physiological, external conditions and energetic availability (Killen 2014).

### 4.2.4 Growth Data are used to inform Fishing Quotas

From a fisheries science perspective, length-age relationships (relationship between age and size is determined through examining multiple individuals of a species where the age and length can be accurately determined and compared) are a quick and reliable method of predicting the reproductive capacity of a population and the level of exploitation which can be sustained (Stoeven, et al 2021). This method has been used to determine broad level changes in growth per unit time within populations and/or single stocks which in turn influences the economic value of the fishery, as faster growing fish populations have a greater imputed asset price per unit (Edwards 1990; Huang et al., 2021). Length-age index variations between sub populations have been used to identify growth patterns over geographical distributions, such as for *Gadus morhua* between the southern North Sea and the Arctic North Atlantic displaying different separate optimal thermal ranges for growth (Pörtner and Farrell 2008), which in turn impacts the exploitation rate and economic value of each sub population, as it has been suggested that growth rate can directly link to the recovery of a population and can sustain a higher exploitation rate (Stoeven et al., 2021), with more individuals reaching maturity quicker, and a higher stock spawning biomass. Some studies suggest that from a commercial perspective, length-age measurements can be used to accurately predict the exploitation limit of population during current and past time frames (Conover and Present 1990; Weatherley 1990), but are potentially unable to predict future trends or how adaptable fishing quotes should be (Denechaud et al., 2020); as there are historic examples when a fish population experiencing over exploitation has only been identified after the stock has collapsed (Myers et al., 1996; Myers and Hutchings 1997).

Studies assessing current fishing quotas point out that juvenile life stages are thought to be more sensitive to environmental instability (Jonassen and Imsland 1999; Sogard 1992), therefore climate change is expected to have a major effect on the distribution and abundance of fishes through its influence on recruitment, which is hard to predict from "final state" analysis (Thresher et al., 2007).

### 4.2.5 Environmental Factors Controlling Growth

Length-age observations from wild communities and laboratory studies have also been used to assess the impact of climatic variability on individual level growth rate, identifying ecological trends associated with extrinsic variability (Brandt et al., 1992; Pinsky et al., 2021). When examining the impact of temperature one consistent trend between studies is thermal niche separation of sub populations, with separate optimal thermal windows for growth (Neill et al., 2004; Reid et al., 2012). Observational studies have also shown that fish can respond to changes in prey availability by modifying their distribution over broad spatial scales (Perry et al., 2005; Pinsky et al., 2013), vertically in the water column in lakes or the ocean (Dulvy et al., 2008; Pinsky et al., 2013), within stream networks, or by varying prey selection (Comte and Grenouillet 2013). This is likely to be related to a consistent theme between studies: the relationship between experienced temperature and food availability, with laboratory studies showing that when groups of fish experience a predictable food supply, individual growth rate covaries with temperature, and that limited prey availability at higher temperatures results in suppressed growth (Jobling 1982). This trend has been linked to aerobic scope and metabolic theory, with warmer thermal conditions resulting in higher metabolic rates, which, if matched with unlimited prey resource results in more energy available for growth (Blier et al., 1997; Clark et al 2013; Gräns et al., 2014; Jutfelt et al., 2021). However, where prey availability does not match thermally-induced increases in metabolic rate (or if aerobic scope is limited by oxygen availability), the energy availability for intrinsic physiological processes in reduced (Blier et al., 1997). As energetic demand is an intrinsic variable with prey availably and thermal conditions being extrinsic factors this potentially suggests that to fully understand and model growth rate trends we need to measure and account for energetic supply and demand ratios.

Critically, the observations described above indicate that among-individual variation in growth rate is likely to vary with conditions experienced by individuals. Consequently, attempts to quantify environmental effects on growth require information on the conditions experienced by fish operating in wild conditions (and the energetic response of the fish) at the scale of the individual (Nisbet et al., 2000; Chung et al., 2019; Chung et al., 2019b).

Within this study we concentrate on individual-level observations, combining estimates of field metabolic rate, experienced temperature and growth rate all inferred retrospectively from otoliths of the same individual fish. We draw on these observations to quantify the degree of among-individual variability in growth rate that can be explained by individual level field metabolic rate and individual-specific sources of extrinsic variability, particularly temperature. Unexplained variation in growth rate may then be attributed to factors that we could not measure at individual level, such as feeding availability and energy partitioning.

### 4.2.6 Otolith Derived Metabolic Rate

We apply otolith derived field metabolic rate (Chung et al., 2019; Chung et al., 2019b; Alewijnse et al., 2021; Chung et al., 2021), otolith derived temperature, model sea floor temperature, otolith growth chronology and time of capture physiology (such as age, length, mass) to explore both intrinsic and extrinsic factors affecting individual and population growth rate (Chung et al., 2019; Chung et al., 2019b; Alewijnse et al., 2021; Chung et al., 2021). The inclusion of both individual specific temperature paired with metabolism allows us to study growth without using environmental averages of large and diverse water bodies, which are unlikely to fully recover variations experienced at the level of the individual. Otolith-derived FMR measurements allow us to test if growth rate scales predictably with energetic demand, or if there is a more complex balance between energy supply and demand. We aim to identify how the factors impacting growth rate change during juvenile and adult life stages, in an attempt to provide useful data which can potentially be applied to future community dynamics and biogeographical model studies.

## 4.3 Hypotheses

Initially we model size as a function of age at the individual level to summaries individual level growth rate. We then add additional variables to models to test specific hypotheses:

- Inclusion of field metabolic rate will increase the explained deviance in age-size growth models (i.e. among-individual variation in Cresp at the point of sampling or in year 0 accounts for some of the among individual variation in whole life growth rate)
- Intrinsic variables coding for energy demand such as sex, body size and condition at capture explain less among-individual variation in growth rate than extrinsic variables coding for resource availability such as temperature, or year of capture.
- We expect juvenile growth rate to vary positively with temperature
- We expect extrinsic variables to explain a greater proportion of among-individual variation in growth in juvenile compared to adult life stages (because of increasingly complex energetic trade-off potential in adult stages).

## 4.4 Methods

### 4.4.1 Data Collection

Otolith samples analysed within this study were collected during Cefas beam trawl surveys, spanning all four fishing monthly quarters (1 = January-March, 2 = April-June, 3 = July-September, 4= October-December) and North Sea ICES areas IVB and IVC (to minimise potential geographical dependent metabolic variability). All otoliths were pre-aged by Cefas sclerochronologists to have been spawned 4 years prior to capture. We selected this age class to minimise age-dependent metabolic variability whilst sampling fish with a relatively high growth rate and therefore larger volumes of aragonite available for collection. North Sea annual average water temperature experienced a significant period

of warming within ICES areas IVB and IVC from 1980s-2010 (Núñez-Riboni and Akimova, 2015), otoliths were therefore selected from years reflecting colder (more historic) and warmer (more recent) periods as well as periods with relatively high and low place abundance. The sample years selected were 1984, 1985, 1986, 1987, 1990 1993, 1995, 1997, 1998, 1999, 2001 and 2002; The distribution of data throughout sexes, months and years is presented in table **20** and figure **41**.

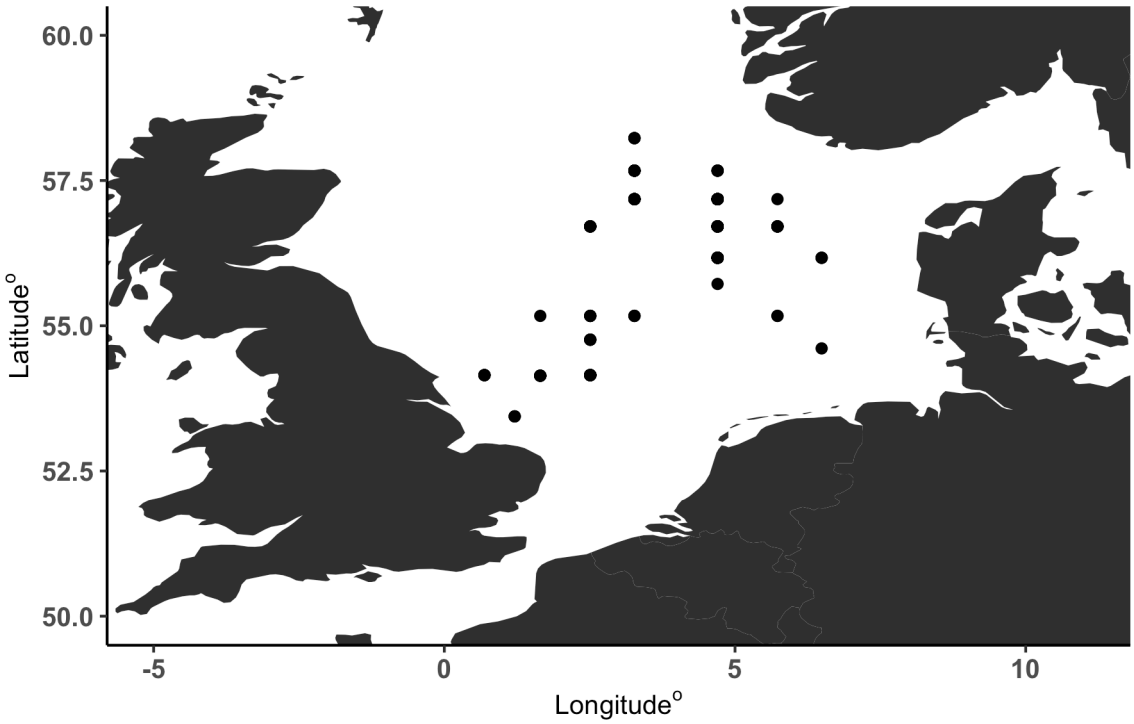


***Figure 41****: Displaying the capture distributions for samples analysed within this chapter. These are displayed in singular trawling locations for individual ICES rectangles, as part of the "ground fish" Cefa survey. Therefore, each trawling location represents multiple individuals caught during trawling.*

***Table 20**: Representing the distribution of Samples selected for analysis within this chapter throughout years, sub populations and sexes, used within this chapter. The data is split by North Sea plaice sub-populations, which individuals have been assigned to using previous tagging, isotopic analysis and experienced extrinsic variability studies (Hunter et al., 2009; Darnaude at al., 2014). Year Regime represents the reason why this year was selected for analysis.*

| | | **Males (n)** | | | **Females (n)** | | |
|---|---|---|---|---|---|---|---|
| **Year** | **Year Regime** | **A** $_{\text{sub population}}$ | **B** $_{\text{sub population}}$ | **C** $_{\text{sub population}}$ | **A** $_{\text{sub population}}$ | **B** $_{\text{sub population}}$ | **C** $_{\text{sub population}}$ |
| Year | Cold Year | - | 2 | 1 | - | 1 | 3 |
| 1985 | Cold Year | 13 | 10 | 9 | 11 | 4 | 3 |
| 1986 | High recruitment | 10 | 7 | 8 | 7 | 11 | 8 |
| 1987 | Cold Year | 6 | 4 | 7 | 20 | 6 | 7 |
| 1990 | Warm Year | 13 | 2 | 8 | 13 | 4 | 10 |
| 1993 | Low SSB | 12 | 3 | 7 | 19 | 3 | 6 |
| 1995 | Low SSB | 12 | 2 | 4 | 17 | 5 | 10 |
| 1997 | High recruitment | 12 | 5 | 1 | 26 | 3 | 3 |
| 1998 | Warm Year | 14 | - | 2 | 28 | - | 6 |
| 1999 | Warm Year | 18 | 1 | - | 31 | - | - |
| 2001 | High recruitment | 12 | 6 | 4 | 8 | 11 | 9 |
| 2002 | Warm Year | 10 | 9 | 2 | 19 | 6 | 4 |
| **total** | | **132** | **51** | **53** | **199** | **54** | **69** |

### 4.4.2 Age and Growth Analysis

A shallow tray of strewers epoxy resin (a brand of epoxy) was allowed to set, and otoliths were mounted to the strewers, sulcus side up, using epofix epoxy resin; providing a strong base for otolith drilling and later sectioning.

Prior to sampling, several randomly-selected samples were drilled and sectioned to ensure the drilling depth was shallow and not including a large time scale (aiming for 2 weeks). The otolith aragonite powder was produced by using a hand held dremmel with a small drill bit at a low drill speed on the outside edge of the otolith. The amount of aragonite powder produced preferably weighted between 30 and 50 $\mu g$. Once the aragonite powder is extracted from the otolith then the sample is sectioned in half to revealing the core; providing the drilling depth (measured after dremmel sampling once otolith was sectioned and photographed. Image analysis was performed using image J), growth data and allowing the opportunity to calculate field metabolic rate throughout the life history of the individual. To section the otolith each sample is fully imbedded in strewers epoxy resin, removed from the mold, then the resin is then ground back, in the transverse orientation to allow better quality resolution for aragonite sampling, using a diamond plate until the core is revealed. Using carborundum powder, the sample was hand ground to remove large scratches from the diamond plate and ensure the section is flat then glued to a slide using epofix resin. Then using a "Petro Thin" and a micrometer the sample is thinned to 30-50 $\mu m$ depending on the sample. Samples are then polished, with a 15-minute cycle with saturated aluminum oxide solution and a turning plate. This provides ample visual acuity to identify yearly and monthly growth rings, allowing for growth rate measurements and potential future drilling over monthly time scales (figure **43**).

### 4.4.3 Image analysis

Otolith sections were photographed with Image Pro Plus (Schneider et al., 2012) software using reflected light, as we found with this data set reflected light produced an image with clear annual growth rings. Multiple images were combined using a photomosaic collage in photoshop CS6 without allowing the software to adapt images for smoother blending fit. Images were analysed using the Object J plug

in of ImageJ software, which has been used by multiple studies to rapidly analyse multiple images including otoliths. All images were taken at a common magnification (0.5664 $\mu m$ per pixel).

Otolith annuli were identified as combination of an opaque and translucent zone. Plaice spawn in winter and birth/hatch date is arbitrarily assigned to the 1st of January of the birth year.

The measurement of yearly growth rates was standardised between each individual sample, as demonstrated by figure **43**. We measured annual growth ring increment width over both the ventral and dorsal axis. Each measurement was z-scored (a statistical measurement that describes a value's relationship to the mean of the group of values). Z-score is measured in terms of standard deviations from the mean. If a Z-score is 0, it indicates that the data point's score is identical to the mean score (Ciotti 2012) and the data from the two axes compared to identify if either axis can be used interchangeably to recover relative growth between years. The otolith core measurement was standardised as the edge of the first opaque band for each individual, as this is thought to be the end of the first year (figure **42**). All otoliths were independently measured by two people on separate occasions and statistically compared, to ensure there are no major discrepancies in age of increment width between readers. Adult (individual at time of capture, approximately 4 years of age) increment width was treated firstly as raw size per pixel data then standardised by dividing the increment width by individual mass$^{1/3}$ as described in equation **4.4**. This conversion was performed because if a large and small individual express similar increment widths, then smaller individual grew comparatively more in relation to its size (and dedicated a greater proportion of metabolic potential to somatic growth), therefore if we treat the two raw individuals raw increment width without a comparison to size it is possible to miss physiological effects.

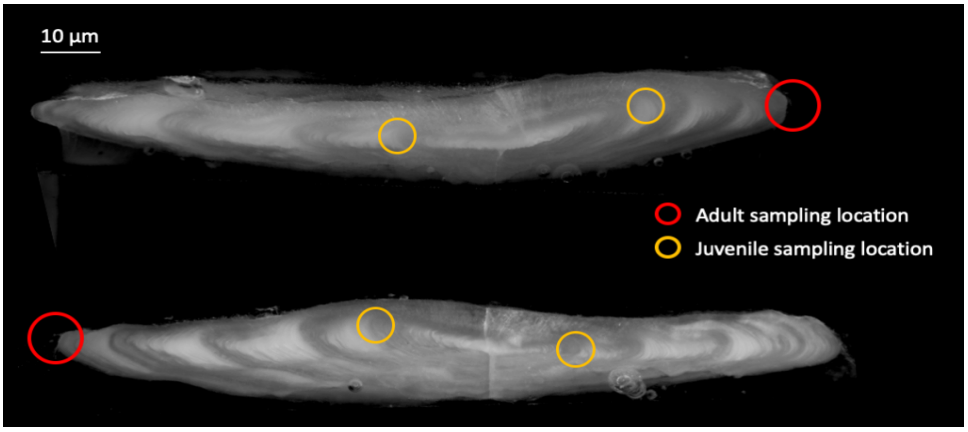


***Figure 42***: *Description of otolith aragonite sampling. The figure displayed a thin sectioned otolith, photographed with reflected light and the adult and juvenile life stage sampling locations.*

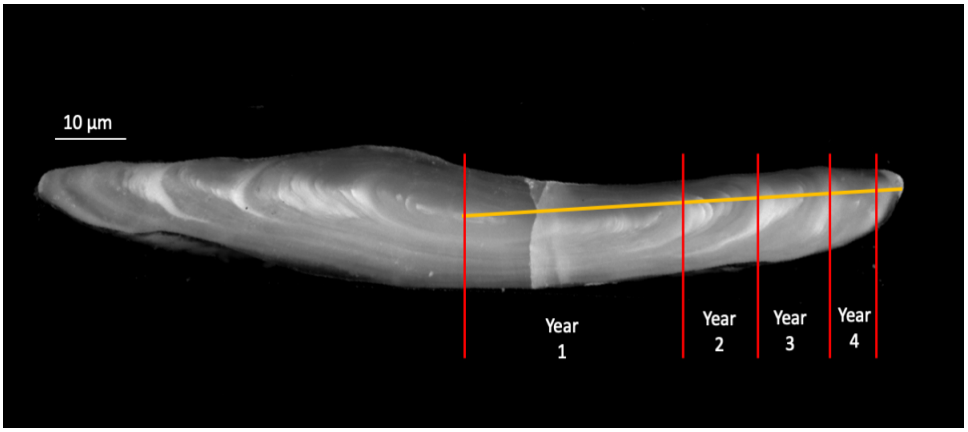


***Figure 43***: *Describing otolith ageing process, with otolith Annuli measurement highlighted, with identification and measurement method. This figure is describing how we aged the individuals presented within this chapter.*

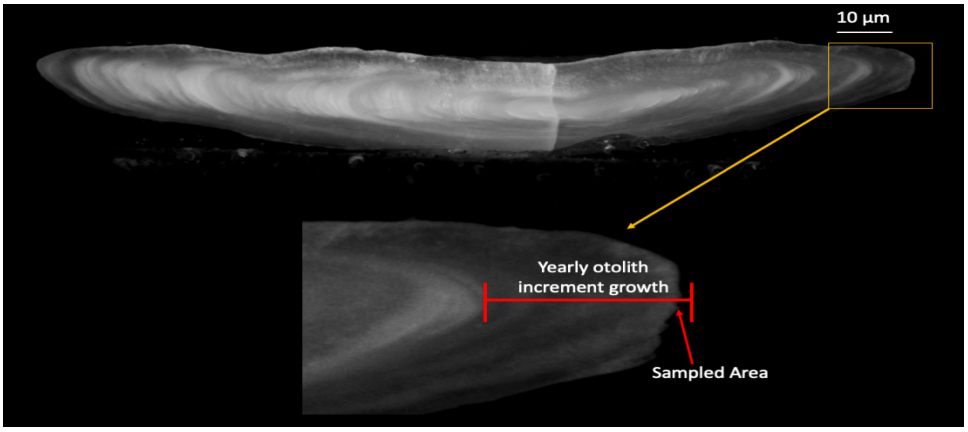


***Figure 44**: Description of how the otolith aragonite sampling time integration estimation was calculated. Highlighting the dremmel sampling depth, and the proportion of which that section contributes to the total year of growth represents the number of months sampled.*

### 4.4.4 Stable isotope analyses

The otolith aragonite isotopic carbonate signature was measured twice per individual, outer edge sampling occurred before sectioning when the otolith was mounted into a resin block before being imbedded. Outer edge sampling occurred using a Dremel hand engraving tool with a diamond bit operating a low rotation speed. Sampling was focused on the sulcal edge section of the otolith. Drilling depth was kept to a minimum to reduce the time period over which metabolic rate and temperature is averaged. When the area of drilled aragonite material is visible in the otolith thin section the time period represented was averaged to the nearest month. For otolith thin sections where the outer edge sample period is not present is was estimated by averaging the sample time period (of the toatal data set) over the month which the sample was captured, as growth rate varies through the season (Lincoln 1981; Hovenkamp 1989; Nash et al., 1994) it is likely that the sample time period also varies. The average sampled time period per individual is estimated at approximately one month for outer edge sampling (Figure **44**). Each sectioned otolith time integration period was estimated independently (Figure **44**). Juvenile otolith aragonite sampling was performed on thin sectioned otoliths, targeting the first annual band, in the first opaque to translucent boundary of otolith aragonite (Figure **42**). The time period over which otolith aragonite was measured was kept to a minimum, and was estimated to represent a maximum of one month. Samples were drilled using a Merchanteck Micromill with conical diamond-embedded dental drill bits. The area to be drilled was pre-selected from digital images with ImageJ

software (Schneider et al., 2012). Otolith aragonite was stored in glass vials for as short a time period as possible before the isotopic signatures were measured.

### 4.4.5 Mass spectrometry

The stable isotope compositions of carbon and oxygen in otolith aragonite were measured at the Stable Isotope Ratio Mass Spectrometry Laboratory (SEAPORT Laboratory, Southampton, UK), with a Kiel IV Carbonate device coupled with a MAT253 isotope ratio mass spectrometer. Approximately 30-50 $\mu g$ of aragonite powder was accurately weighed into borosilicate glass reaction vessels prior to evolution of $CO_2$ through reaction with phosphoric acid. The calibration standards used were NBS 19 and NBS 18, as well as a quality control GS1 (Carrara marble produced by the SEAPORT laboratory). Results are reported in permil (‰) (as $\delta^{13}C$ and $\delta^{18}O$ values) relative to Vienna Pee Dee Belemnite. Accuracy and precision determined from long-term analyses of internal standards of known composition is 0.01 ‰ for both $\delta^{13}C$ and $\delta^{18}O$ of otolith aragonite. The standard deviations determined from repeated measures of internal standards in each run are presented in the supplementary materials.

### 4.4.6 Otolith-derived experienced temperature

Time averaged experienced temperature was reconstructed using a species-specific otolith isotope temperature equation (Geffen 2012).

$$\delta^{18}O_C - \delta^{18}O_W = 3.72 - 0.19T(^oC) \qquad (4.1)$$

$\delta^{18}O$ values of the ambient sea water ($\delta^{18}O_W$) vary according to salinity, as freshwater inputs have lower $\delta^{18}O_W$ values than seawater. In the North Sea, salinity varies considerably in space and time, complicating the use of oxygen isotope thermometry (see Figure **45**). To reduce salinity bias within $\delta^{18}O$ values we only analysed sub population A experienced temperature values with minimal salinity variability (see Figure **45**). $\delta^{18}O$ values of the ambient sea water were initially estimated from the National Aeronautical Space Administration's (NASA) "global seawater oxygen-18 Database" (LeGrande and Schmidt 2006) (Figure **46**).

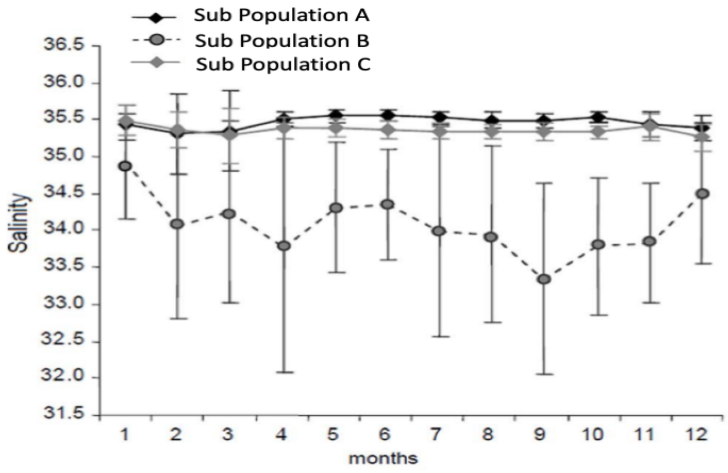


***Figure 45**: Sub population variations in experienced salinity, based of tagging distribution data. Adapted from Darnaude (2014)*

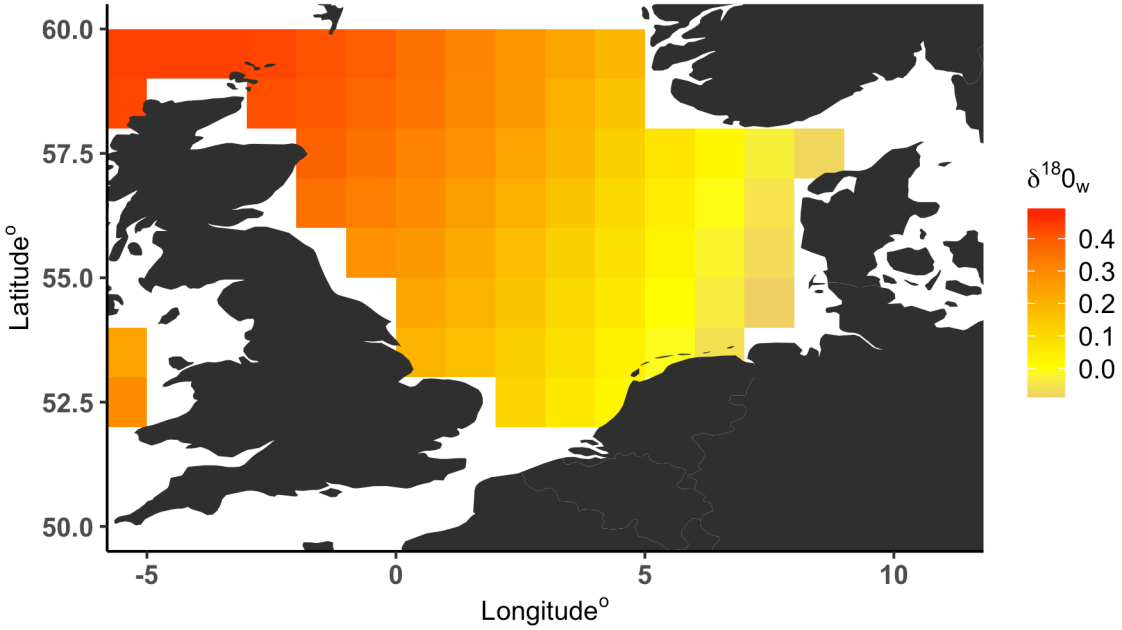


***Figure 46**: NASA global seawater oxygen-18 Database model outputs (LeGrande and Schmidt 2006). Subsetted to include only include benthic environments (bottom 5m) over the total 17-year range of data collection. Individual specific values were calculated from sample locations during adult life stages" output*

### 4.4.7 Estimating habitat temperature

To estimate the experienced temperature at the point of capture, individual-specific estimated water temperatures (based of trawling locations and otolith aragonite integrated time period) were recovered from the AHOI model (a physical-statistical model of hydrography for fisheries and ecology studies) (Núñez-Riboni and Akimova 2015) for each sample independently. The formation of this model is described by Van der Sleen (2018). As plaice are benthic fish we subsetted the water column to only include the deepest 5 metres of water at each latitude and longitude. Individual experienced water temperatures were estimated using the time, latitude and longitude when the individual was captured and averaged over the time period which the otolith derived temperature was calculated to be averaged over. The geographical range over which the model temperature was calculated was set as the theoretical area which the individual potentially could have travelled, based on data from electronic tagging of individual free roaming plaice in the North Sea (Hunter, et al., 2003). Therefore, each individual has a unique time, location, period and area which model temperature was averaged over. For example, swimming speeds are reported to be elevated from October to March during times of migration/spawning and be highest for the western sub-population (Darnaude et al., 2014), however the maximum area travelled is unaffected by swimming speed during feeding and spawning time periods (Buckley and Arnold 2001). During spawning and feeding time periods the area over which the individual potential inhabited is fixed to its sub-population geographical range (Hunter et al., 2009), and during migration periods the area is increased to include possible migratory routes described by Hunter (2003). This is described below in figure **47**

### 4.4.8 Temperature anomaly

We derive a measure of the degree to which each individual expresses thermal selection, termed ‘temperature anomaly’, which describes the difference between the absolute temperature inferred from otolith oxygen isotope thermometry and the water temperature in the location and time of sampling as predicted from the AHOI model (Núñez-Riboni and Akimova 2015):

$$\text{Temperature anomaly}^{o}C = Temp_{oto}{}^{o}C - Temp_{model}{}^{o}C \qquad (4.2)$$

Model temperature ($Temp_{model}$) within this method represents the average temperature of all the environments the individual could have experienced (described in section **4.4.7** and figure **47**), and otolith derived temperature ($Temp_{oto}$) provides the thermal average of the habitats the individual chose to experience. Therefore, the individual temperature anomaly indicates whether the individual chose warmer or cooler conditions than the average which it could have experienced (if the assumption of constant $\delta^{18}O_W$ values is valid). Positive values indicate fish that chose warmer conditions. The temperature anomaly is therefore intended as a proxy for thermal habitat selection.

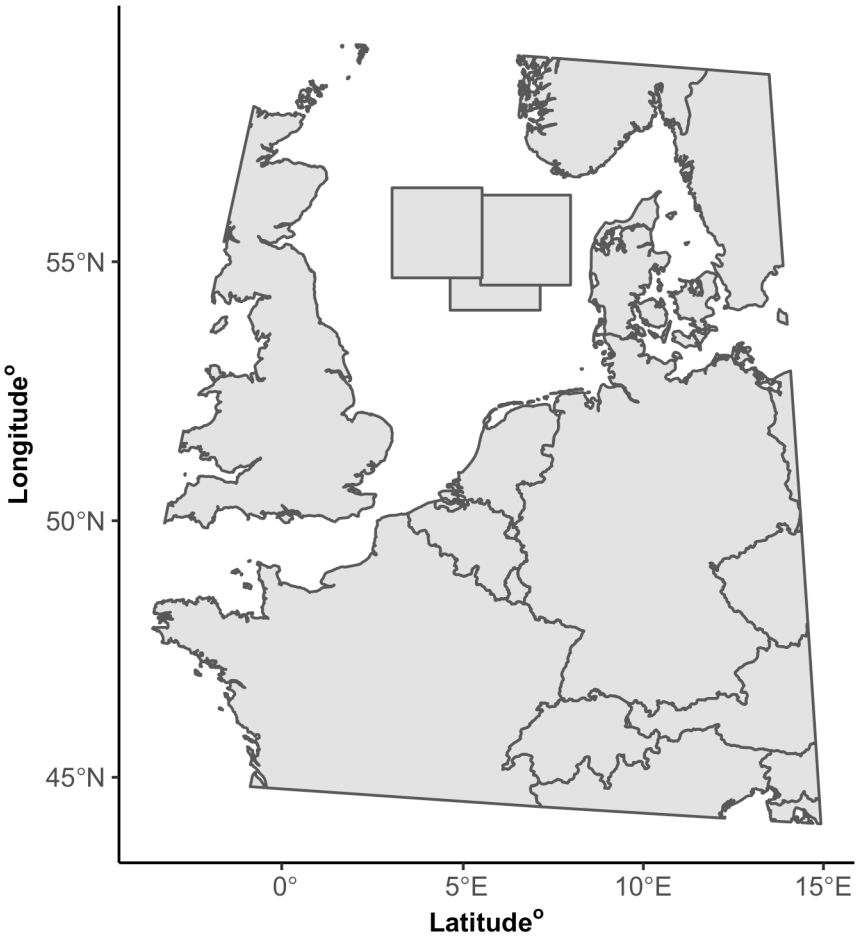


***Figure 47**: Example of the methodology for estimating individual specific modelled experienced temperature. Grey rectangles represent the area over which benthic water temperatures are calculated. This area is estimated using Plaice tagging survey data performed by CEFAS (Hunter et al., 2003). We have calculated this area in a rectangle to allow for comparison to ICES rectangles.*

Figure **47** demonstrates the area for 3 individuals over which the model temperature (section **4.4.7**) was calculated (and used in equation **4.2**). These theoretical areas are calculated from Cefas plaice tagging data over the entire seasonal cycle, tracking their movements throughout the migratory, feeding and breeding cycles, with small scale population migrations up to 20km (Hunter, et al., 2003). From this data, using time of year and the period over which experienced temperature was estimated we formed a theoretical maximum area the fish could have migrated. The area over which temperature is averaged is a rectangle, partly to match ICES rectangles and partly for simplicity to match the data set which the samples were collected from.

### 4.4.9 Otolith Metabolic rate

We estimated the proportion of respiratory carbon in otolith aragonite (Cresp) from a two-component mixing model as described by Chung et al., 2019 and Chung et al., 2019b:

$$C_{resp} = \frac{(\delta^{13}C_{oto} - \delta^{13}C_{DIC-sw})}{(\delta^{13}C_{diet} - \delta^{13}C_{DIC-sw})} + \epsilon_{total} \qquad (4.3)$$

Where $\delta^{13}C_{oto}$ represents the $\delta^{13}C$ values of the sampled otolith aragonite, $\delta^{13}C_{DIC-sw}$ represents the $\delta^{13}C$ value of dissolved inorganic carbon (DIC), $\delta^{13}C_{diet}$ represents the $\delta^{13}C$ values of individual diet (Alewijnse et al., 2021). $\epsilon_{total}$ is the total isotopic fractionation from DIC and diet to blood, blood to endolymph and endolymph to otolith (Chung et al., 2021). The absolute value of $\epsilon_{total}$ may vary among species, and requires further laboratory experimentation to calculate. Within this study, we assume that $^{\varepsilon}$total does not vary systematically among individuals of the same species and is set to 0 (Chung et al., 2019; Chung et al., 2019b). $\delta^{13}C_{diet}$ values were estimated based on a compilation of stable isotope data from plaice from the North Sea provided by Jenning and Cogan (2015) ranging from -15.95‰ to -18.22‰ (varying due to geographical distribution). $\delta^{13}C_{DIC}$ values were estimated from Burt et al., 2016, who presented spatially-explicit $\delta^{13}C$ DIC values from across the North Sea collected in September 2011 (Burt et al., 2016) (ranging from 0.5‰-0.8‰), and adjusted for the Suess effect (the decrease in $\delta^{13}C_{DIC-sw}$ over time due to anthropogenic carbon emissions since the industrial revolution) (Tagliabue and Bopp 2008). We solved for Cresp using Monte Carlo resampling with 100 random draws of a mean-centered normal distribution for each sampled or estimated variable, with the standard deviations of variables presented in tables **21**, **28** and **30**. In subsequent analyses we take the median of the posterior distribution for Cresp values

***Table 21**: Describing the equation parameters used for all calculations within this chapter, split by adult and juvenile life stage. The source of the parameter value is also provided.*

## Adult Populations

| parameter | value | source | sD | source |
|---|---|---|---|---|
| $\delta^{18}O_w$ | 0.0135 (minimum) 0.294 (maximum) | (LeGrande and Schmidt 2006) | 0.1 | 95% CI range = 0.4 per mill (Trueman 2019) |
| $\delta^{18}O_{oto}$ | 0.0122 (minimum) 3.297 (maximum) | (SEAPORT Laboratory, Southampton, UK) | 0.05 | 95% CI range = 0.2 per mill (Trueman 2019) |
| $\delta^{13}C_{diet}$ | -16.82 (average) | (Jennings and Cogan 2015) | 0.25 | 95% CI range = 1 per mill (Trueman 2019) |
| $\delta^{13}C_{DIC}$ | 0.623 (average) | (Burt et al., 2016) | 0.1 | 95% CI range = 0.4 per mill (Trueman 2019) |
| $\delta^{13}C_{oto}$ | -2.45 (minimum) 0.7 (maximum) | (SEAPORT Laboratory, Southampton, UK) | 0.1 | 95% CI range = 0.4 per mill (Trueman 2019) |
| $Temp^{Slope}$ | -0.190 (average) | - | 0.01 | (Geffen 2012). |
| $Temp^{INT}$ | 3.72 (average) | - | 0.01 | (Geffen 2012). |

## Juvenile Populations

| | | | | |
|---|---|---|---|---|
| $\delta^{18}O_w$ | 0.1 (singular estimation) | (LeGrande and Schmidt 2006) | 0.15 | estimation from likely location (Hunter 2009) |
| $\delta^{18}O_{oto}$ | 2.081 (maximum) -0.917 (minimum) | (SEAPORT Laboratory, Southampton, UK) | 0.08 | estimation from likely location (Hunter 2009) |
| $\delta^{13}C_{diet}$ | -16.82 (average) | (Jennings and Cogan 2015) | 0.8 | estimation from likely location (Hunter 2009) |
| $\delta^{13}C_{DIC}$ | 0.623 (average) | (Burt et al., 2016) | 0.15 | estimation from likely location (Hunter 2009) |
| $\delta^{13}C_{oto}$ | -2.877 (minimum) 0.468 (maximum) | (SEAPORT Laboratory, Southampton, UK) | 0.15 | estimation from likely location (Hunter 2009) |

### 4.4.10 Fish Mass

This data set has previously been analysed to investigate the relationship between metabolic rate and temperature and condition through the annual cycle (Chapters 2 and 3). To identify body size metabolic rate relationships during juvenile years we use otolith size, as this has been shown to directly correlate with growth, and has been used by previous studies as a proxy for body size. We also define a new variable, mass corrected growth (described by equation **4.4**), to compare measurements between individuals of different masses. If two individuals, one of large body size and another of a relatively smaller body size express the same linear incremental growth over the same time period, the individual with a smaller body size (mass) grew comparatively more in relation to its size, and therefore contributed a greater proportion of total energy to growth. We use $mass^{1/3}$ to infer mass as a function of inferred length, in a similar manner to the conditional calculation below. We use $mass^{1/3}$ not otolith length as not every otolith within this data set is a complete, some have previously been cracked by Cefas sclerologists for aging populations for management purposes and we were unable to collect specific samples due to covid restrictions.

$$\text{mass corrected growth } (\mu m/yr/g) = \frac{\text{Increment width } (\mu m)}{mass_g^{1/3}} \qquad (4.4)$$

### 4.4.11 Condition

We estimated condition at capture to identify seasonal variations in energy storage and use, and potentially among-individual variations in performance (Bervoets and Blust 2003). Condition is defined in equation **4.5** (Bervoets and Blust 2003), where weight is in g and length is in cm. Weight is measured to the nearest 5g, giving a standard deviation of 2.5g, and length is measured to the nearest cm, giving a standard deviation of 0.5. Condition standard deviations were calculated using Monte Carlo resampling.

$$\text{Condition (g cm}^{-3}) = \frac{Weight(g)}{Length^3(cm)} \qquad (4.5)$$

## 4.4.12 Data Analysis Approaches

Hierarchical linear mixed-effects modelling (Zuur et al., 2009) was used to estimate the degree of increment width variability explained by extrinsic variables including temperature, year of spawning, year of capture and intrinsic variables such as metabolism (represented by Cresp within this chapter), body length, condition, age and sex. Prior to analysis all intrinsic and extrinsic factors were z-scored (previously described in section **4.4.3**) to aid model convergence and interpretation (Morrongiello and Thresher 2015; Morrongiello et al., 2014). Initially model structure involved forming simplistic GLM models for age and sex, with growth rate as a predictor variable. These models were then extended to incorporate the effects of calendar year of spawning, year of birth, metabolism and the effects of temperature (tables **22** and **23**). In order to predict the varying sources of growth throughout life history of an individual we formulated several mixed effects models to explain both adult increment growth and juvenile growth (tables **22** and **23**). Model selection, including AIC values and deviance explained is detailed below, with models selected to perform statistical analysis with (sections **4.4.12.1**- **4.5.2.5**).

### 4.4.12.1 Juveniles

As the data displays a gaussian distribution we are able to apply a linear mixed effects model. Table **22** displays $R^2$ and AIC values of the models used to explain juvenile increment growth, with increasing complexity of model structure. Fixed effects within these models include temperature during juvenile life stages and Cresp during juvenile life stages, as it is believed that these factors may impact growth rate. The year of birth and is definged as a random effect. Initially a combination of multiple factors were tested to optimize base model structure (table **22**), including year of birth, temperature, Cresp and sex. Models were then ranked using Akaike's information criterion corrected for small sample sizes (AICc) and the optimal model was selected (Burnham and Anderson 2004). If the difference in AICc (ΔAICc) between the highest and a second highest ranked model was < 2, the two were considered to be equally supported (Burnham and Anderson 2004). Models were fit using the LNME4 package (Bates et al., 2015). Model "Juv_4" was selected due to favourable $R^2$ and AIC values, suggesting optimal model fit. Due to the findings of chapters 2 and 3, suggesting that in juvenile populations metabolism is impacted by temperature in a predictable manner, and Cresp varies between sexes, for models "juv_4" and "juv_5" we include interactive effects of temperature, Cresp and sex

when attempting to explain growth rate variability. This increases the model fit, with more favourable AIC values and higher degree of deviance in the data explained. Year of birth is treated as a random factor as we do not have a large enough data set, including enough years to from reliable statistical inference, the inclusion of more years was prevented due to COVID, and we are working on collecting more samples.

***Table 22**: Juvenile model structure selection methodology description, the response variable is otolith derived growth during the first year of life. Providing AIC and variance explained selection criteria. Model "juv_4" was selected for statistical inference due to favourable model fit criteria.*

| Model ID | Model Structure | Marginal $R^2$ | Conditional $R^2$ | AIC |
|---|---|---|---|---|
| Juv_1 | Juvenile Growth ~ Temperature + Sex + (1\|Year of birth) | 0.03760740 | 0.3779039 | 1,540.265 |
| Juv_2 | Juvenile Growth ~ Temperature + (1\|Year of birth) | 0.02945634 | 0.3443394 | 1,539.535 |
| Juv_3 | Juvenile Growth ~ Temperature + Cresp + Sex + (1\|Year of birth) | 0.05515400 | 0.4016066 | 1,548.437 |
| **Juv_4** | **Juvenile Growth ~ Temperature * Cresp * Sex + (1\|Year of birth)** | **0.07807233** | **0.4367303** | **1,539.511** |
| Juv_5 | Juvenile Growth ~ Temperature * Cresp * Sex + (sex\|Year of birth) | 0.05759573 | 0.4108447 | 1,539.514 |

#### 4.4.12.2 Adults

Adult increment width data expressed a gamma distribution, therefore the a generalised mixed effects model (GLMER) was applied to the data. Table **23** presents the various model structures used during the optimization process. In our analysis, we focused on modeling the mass-corrected increment width (as described in Equation **4.4**). Additionally, we modelled raw otolith-derived temperature, model extracted temperature and the previously described temperature anomaly data (within section **4.4.8** and equation **4.2**). This analysis was conducted to determine which temperature measurement explains the greatest level of deviance in mas corrected growth rate data. The results of each model structure, including $R^2$ and AIC values, are summarized in Table **23.** Other intrinsic variables used within model structures include condition, age, Cresp, juvenile Cresp, total otolith width (as adult growth is a measure of otolith growth during last year of life) and sex. Random factors include the year of spawning (YOS), sex and year of capture (YOC). YOS and YOC are both treated as random factors as we are unable to account for the reasons for the deviance they might explain, and we do not have a large enough data set to accurately test these effects, sampling was prevented due to COVID. We have not included interactive affects as previously described because we do not find a significant interaction between adult Cresp and temperature. "Total growth - final year of growth" is used as a proximation

for growth rate over individual life history compared to the final year growth rate. If two individuals express the same “total growth - final year of growth” yet differing final year of growth rate this could potentially represent a variation in energetic partitioning. Models of increasing complexity were tested, with AIC and deviance explained compared. Model “G” was selected for statistical inference due to the most favourable AIC and deviance explained values (model selection occurred in a similar manner to previous studies (Burnham and Anderson 2004)), despite not being the most complex model. Model checks were performed with the R package “Utilities.Package”, AIC values were calculated with AICodavg (Mazerolle 2020), mixed effects modelling was performed in lme4 and bootpredictlme4 (Bates et al., 2015).

***Table 23**: Adult model structure selection methodology description, the response variable is otolith derived mass corrected growth during the first year of life. Providing AIC and variance explained selection criteria. Model G was selected for statistical inference due to favourable model fit criteria.*

| Model | Model structure | Conditional $R^2$ | AIC |
|---|---|---|---|
| A | Adult otolith growth ~ Temperature anomaly + (1\|YOC) + (1\|sex) + (1\|YOS) | 0.347 | 403.27 |
| B | Adult otolith growth ~ Temperature anomaly + Cresp + (1\|YOC) + (1\|sex) + (1\|YOS) | 0.360 | 403.45 |
| C | Adult otolith growth ~ Temperature anomaly + Cresp + condition + (1\|YOC) + (1\|sex) + (1\|YOS) | 0.524 | 363.38 |
| D | Adult otolith growth ~ Temperature anomaly + Cresp + condition + (1\|YOC) + (1\|sex) + (1\|YOS) + (1\|Age) | 0.684 | 341.59 |
| E | Adult otolith growth ~ Model Temperature + Cresp + condition + (1\|YOC) + (1\|sex) + (1\|YOS) + (1\|Age) | 0.695 | 338.90 |
| F | Adult otolith growth ~ otolith experienced Temperature + Cresp + condition + (1\|YOC) + (1\|sex) + (1\|YOS) + (1\|Age) | 0.708 | 348.85 |
| **G** | **Adult otolith growth ~ Temperature anomaly + Cresp + condition + (total growth - final year) + (1\|YOC) + (1\|sex) + (1\|YOS)** | **0.722** | **307.86** |
| H | Adult otolith growth ~ Model Temperature + Cresp + condition + (total growth - final year) + (1\|YOC) + (1\|sex) + (1\|YOS) | 0.665 | 309.98 |
| I | Adult otolith growth ~ otolith experienced Temperature + Cresp + condition + (total growth - final year) + (1\|YOC) + (1\|sex) + (1\|YOS) + (1\|Age) | 0.653 | 315.39 |
| J | Adult otolith growth ~ Temperature anomaly + Cresp + Juvenile Cresp + condition + (total growth - final year) + (1\|YOC) + (1\|sex) + (1\|YOS) | 0.710 | 308.88 |

# 4.5 Results

## 4.5.1 Growth Rate Increments Through Years

Yearly growth increments, defined as the distance between annulus lines (defined in section **4.4.2** and figure **43**), were measured for 188 individuals spanning from 1980-2002, yielding a dataset of 1133 individual increment measurements. As the distribution of data is relatively uneven over temporal and spatial scales, this data set cannot be treated as a time series, as previous otolith derived growth rate studies have been structured, therefore we have grouped all the data to examine relationships between eco-physiological factors and growth rate, therefore we include year as a random factor.

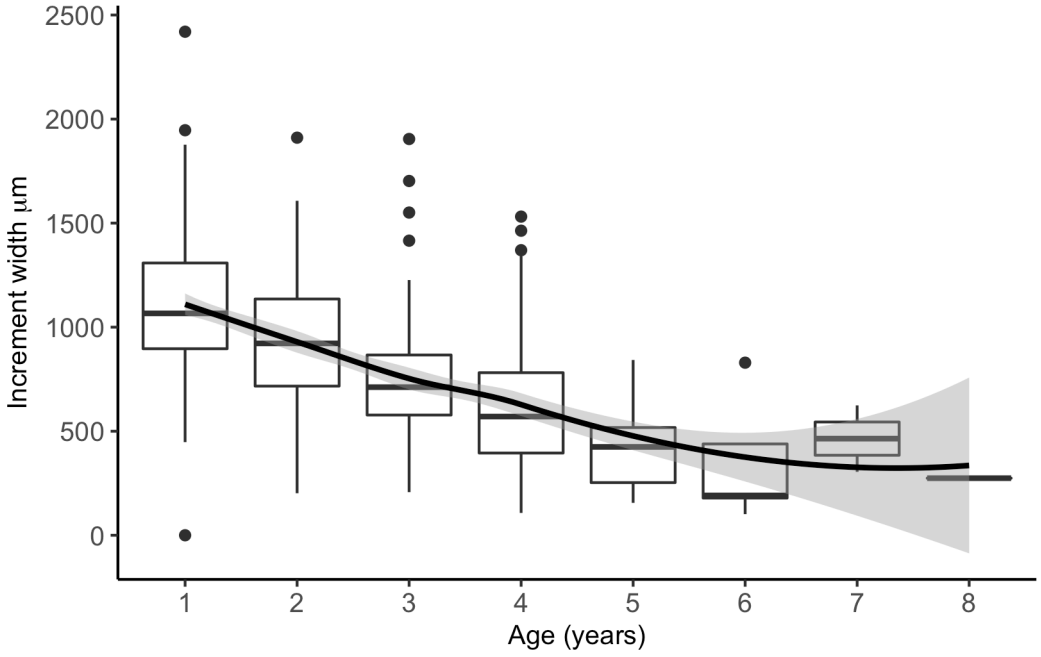


***Figure 48**: Showing the average increment width growth within the population split by age class.*

As expected, median yearly increment width decreases with age in a predictable manner, similar to previous studies and age-length growth indices studies (figure **48**). However, among individuals, there is a high degree of variability, with widest increments (and therefore highest lifetime highest growth rate) seen in the second and even third year of life in many cases. Age at capture within this sample set ranged from 3 to 8 years old, but the majority of the data comes from individuals between 3-4 years old. Increment width within the first year of life averaged 1118.5$\mu m$ with a maximum of 2419.8$\mu m$ and minimum of 447.5$\mu m$. During year two the average fell to 929.3$\mu m$, 752.9$\mu m$ during year 4, 627.9$\mu m$ during year 5, 406.4$\mu m$ during year 6 and beyond this age class the sample size is too small to form a meaningful average (Table **24**). The distribution of the number of individuals, average, minimum and maximum growth rates at throughout age class is summarized in (Table **24**).

***Table 24**: Describing the minimum, maximum and average otolith annuli width for each age class between sexes*

| | Male Increment width (μm) | | | | Female Increment width (μm) | | | |
|---|---|---|---|---|---|---|---|---|
| **Age** | **N** | **Min** | **Max** | **Mean** | **N** | **Min** | **Max** | **Mean** |
| 1 | 47 | 247.5 | 1877 | 1077.566 | 80 | 447.5 | 2,419.8 | 1,129.2875 |
| 2 | 47 | 201.9 | 1388.1 | 868.8894 | 80 | 510.7 | 1,910.6 | 969.6237 |
| 3 | 46 | 370.7 | 1060.8 | 719.45 | 80 | 207.2 | 1,904.3 | 774.3863 |
| 4 | 41 | 251.1 | 1328.5 | 545.4439 | 73 | 107.2 | 1,531.3 | 672.8562 |
| 5 | 12 | 155.6 | 842.4 | 406.625 | 16 | 168.0 | 646.2 | 406.1750 |
| 6 | 1 | 829.4 | 829.4 | 829.4 | 4 | 101.4 | 438.9 | 227.6250 |
| 7 | 1 | 624.2 | 624.2 | 624.2 | 1 | 304.6 | 304.6 | 304.6000 |
| 8 | - | - | - | - | 1 | 274.3 | 274.3 | 274.3000 |

## 4.5.2 Mixed Effects Model Output Description

### 4.5.2.1 Juveniles

To explore the interactive effect of multiple variables on growth rate during several stages of life we use mixed effects modelling. The models are described in tables **22** and **23** accompanied with the intrinsic and extrinsic model effects outputs below (Table **25** and **26**). Table **22** compares the proportion of explained variance and AIC criteria of each of the models structures used for juvenile life stages. Each of the mixed effects model listed in table **22** explained more of the total variance witin the data when compared to simple linear models that do not include random effects within model structure. The model within this series which presented the most favourable AIC and deviance explained values overall was "Juv_4", despite not being the most complex. "Juv_4" expresses the most effective partitioning of the sources of variance within the data and thus provides usable information as to why individuals differ in their mass specific growth rates (Denechaud et al., 2020). These models suggest that Cresp, temperature and year of birth explain the greatest degree of among individual variation in juvenile growth in the data set, as when these variables are not included as fixed effects the degree of variance explained and $R^2$ reduces. Table **25** describes the model outputs from the best fitted model "Juv_4". Tables **25** and **26** are used to identify variables which co-vary significantly with predictor variables (being otolith growth rate during adult and juvenile life stages), then predicted data is

extracted and plotted to explore interactions, in a similar manner to previous studies (Denechaud et al., 2020). The predicted data from "Juv_4" has been extracted and used to inturpret interactions within figures **49**, **52**, **53**, **54** and **55**.

***Table 25**: Best fitted selected model (Juv_4) output tables descripting juvenile otolith increment width fixed and random effects*

| Variable | Coefficient | standard error | p values | effects class | group |
|---|---|---|---|---|---|
| **intercept** | 2,750.1 | 3,040.6 | 0.37 | fixed | |
| **Temperature** | -648.1 | 1,197.8 | 0.59 | fixed | |
| **Cresp** | 266.2 | 1,496.6 | 0.86 | fixed | |
| **sex (males)** | 1,882.1 | 10,634.9 | 0.86 | fixed | |
| **Temperature:Cresp** | -106.6 | 599.1 | 0.86 | fixed | |
| **Temperature:sex (males)** | -1,118.2 | 4,181.7 | 0.79 | fixed | |
| **Cresp:sex (males)** | 1,682.4 | 5,554.5 | 0.76 | fixed | |
| **Temperature:Cresp:sex(males)** | -828.9 | 2,183.8 | 0.71 | fixed | |
| **intercept** | 217.3 | | - | random | Year of Birth |
| **Observations** | 311.6 | | - | random | Residual |

Bold values denote significant p values (<0.05) and asterick's define level of significance: p<0.0001 = '<0.0001***'; p< 0.001 = '***'; p < 0.01 = '**' ; p<0.05 = '*'

#### 4.5.2.2 Adults

Table **23** compares the $R^2$ and AIC criteria of each model used to explore the interactive effects of intrinsic and extrinsic variables on adult mass specific increment growth, in a series of increasingly complex mixed model structures. Within the models described in table **23** we have used a variety of temperature variables, with the intention of exploring which temperature measurement explains the highest degree of mass specific growth rate variability. From the effect of including/excluding predictor variables on model fit and AIC values, we can attribute the level of deviance explained to each variable.

We then extract the predicted data to plot interactions, in a similar manner to previous studies (Denechaud et al., 2020).

#### 4.5.2.3 Models Including Raw Otolith Derived Experienced Temperature

Models "F" and "I" both include raw otolith derived temperature (described by equation **4.1**). They therefore are attempting to explained the deviance within mass spcific increment width data using otolith derived temperature, condition and cresp as fixed effects. Model "F" and "I" include YOC, sex, YOS and Age as random effects (table **23**). Model "I" includes "total growth rate - final year" of growth, which represents growth rate throughout individual life history, and as a result model "I" expresses more favorable AIC values however the $R^2$ is not significantly affected. This indicates that the inclusion of total growth of the individual improved model fit; however, all fixed and random effects included within both model structure "F" and "I" improved model fit, and therefore are thought to contribute to (or covary with) among-individual variation in growth rate.

#### 4.5.2.4 Models Including Raw Model Derived Experienced Temperature

Models E and H express the same model structure as F (same structure as E) and I (same structure as H) with the inclusion of raw modelled temperature instead of otolith derived temperature (table **23**). When examining $R^2$ values there is no significant difference between model "E" or "H" outputs or between models "F" and "I", however AIC values are significantly lower for modelled temperature (models "E" and "H"). This suggests that using modelled temperature produced a better model fit when compared to otolith derived temperature (table **23**).

#### 4.5.2.5 Models Including Temperature Anomaly Data

When applying the same model structure as "F", "E" , "I" and "H" but using temperature anomaly dataaner to explain deviance within mass specific growth rate the AIC and $R^2$ were both significantly improved; suggesting that temperature anomaly data has the greatest explanatory power of the three temperature values (table **23**). Within this series of models (A-J) the most complex structure was not preferred (most complex being model J, and the difference between G, H and I being the temperature variables used), with AIC values not significantly improve beyond model G and $R^2$ values showing no

significant increase beyond 0.675. Therefore, model G was used to explain the fixed and random effects impacting mass specific growth rate deviance, as it expresses the highest $R^2$ and most favorable AIC values with the most simplistic model structure. This model suggests that when sex, YOC and YOS are treated as random factors then Cresp, condition, temperature anomaly and "toatal growth – final year" all significantly contributed to the explanation of mass specific growth rate variability. This is also apparent from the more simplistic models used during the model testing phase which do not include Cresp, condition, temperature anomaly or otolith width (excluding final year growth), with AIC and $R^2$ values being significantly higher (for AIC) and lower ($R^2$) (table **23**); suggesting reduced model fit and lower explanatory power. Condition appears to be the only variable with a negative relationship (high condition values corresponding to low growth rates) (table **23**). Without subsequent further data collection, we are unable to predict the remaining sources of variance within the data, however it is likely that an inclusion of the prey availability, predation pressure, the degree of energetic input to reproduction and maintenance will improve the model estimation of variance. Below in table **26** we display the model output for model "G", which after model selection (by comparing AIC and deviance explained) has been selected for the statistical interpretation of the data.

***Table 26**: Best fitted selected model (G) output tables descripting adult mass corrected growth fixed and random effects*

| Terms | Coefficient | standard error | p values | group | Group |
|---|---|---|---|---|---|
| **intercept** | -1.0458105 | 0.004546 | **<0.0001*** ** | fixed | |
| **Temperature anomaly** | 0.0290304 | 0.004367 | **<0.0001*** ** | fixed | |
| **Cresp** | 0.0247962 | 0.004493 | **<0.0001*** ** | fixed | |
| **condition** | -0.3292656 | 0.004360 | **<0.0001*** ** | fixed | |
| **Total growth - final year** | 0.1828200 | 0.004366 | **<0.0001*** ** | fixed | |
| **intercept** | 0.0004061 | | - | random | YOC |
| **intercept** | 0.0948663 | | - | random | YOS |
| **intercept** | 0.0604995 | | - | random | sex |
| **observations** | 0.3800299 | | - | random | Residual |

Bold values denote significant p values (<0.05) and asterick's define level of significance: p<0.0001 = '<0.0001***'; p< 0.001 = '***'; p < 0.01 = '**' ; p<0.05 = '*'

### 4.5.3 Otolith Derived Temperature

Otolith derived temperature is previously described by Table **27** and by equation **4.1** with a range between $2.22^{o}C$ and $19.51^{o}C$ for adult population, and between $8.62^{o}C$ and $24.40^{o}C$ for juvenile populations (table **28**). The otolith derived temperature was the only temperature variable used for both year one and four life stages as we cannot estimate modelled temperature for juvenile life stages (as we do not know the location during otolith sampling), with the potential for future studies looking into more life stages for a more in-depth relationship between physiology and temperature over the entire life history of an individual. Year one increment width growth covaried weakly with temperature, with higher temperatures associated with lower individual growth rates. Raw temperature shows no significant interaction with adult increment width (as predicted from best fitted mixed effects models, table **25**), as shown from figure **49**.

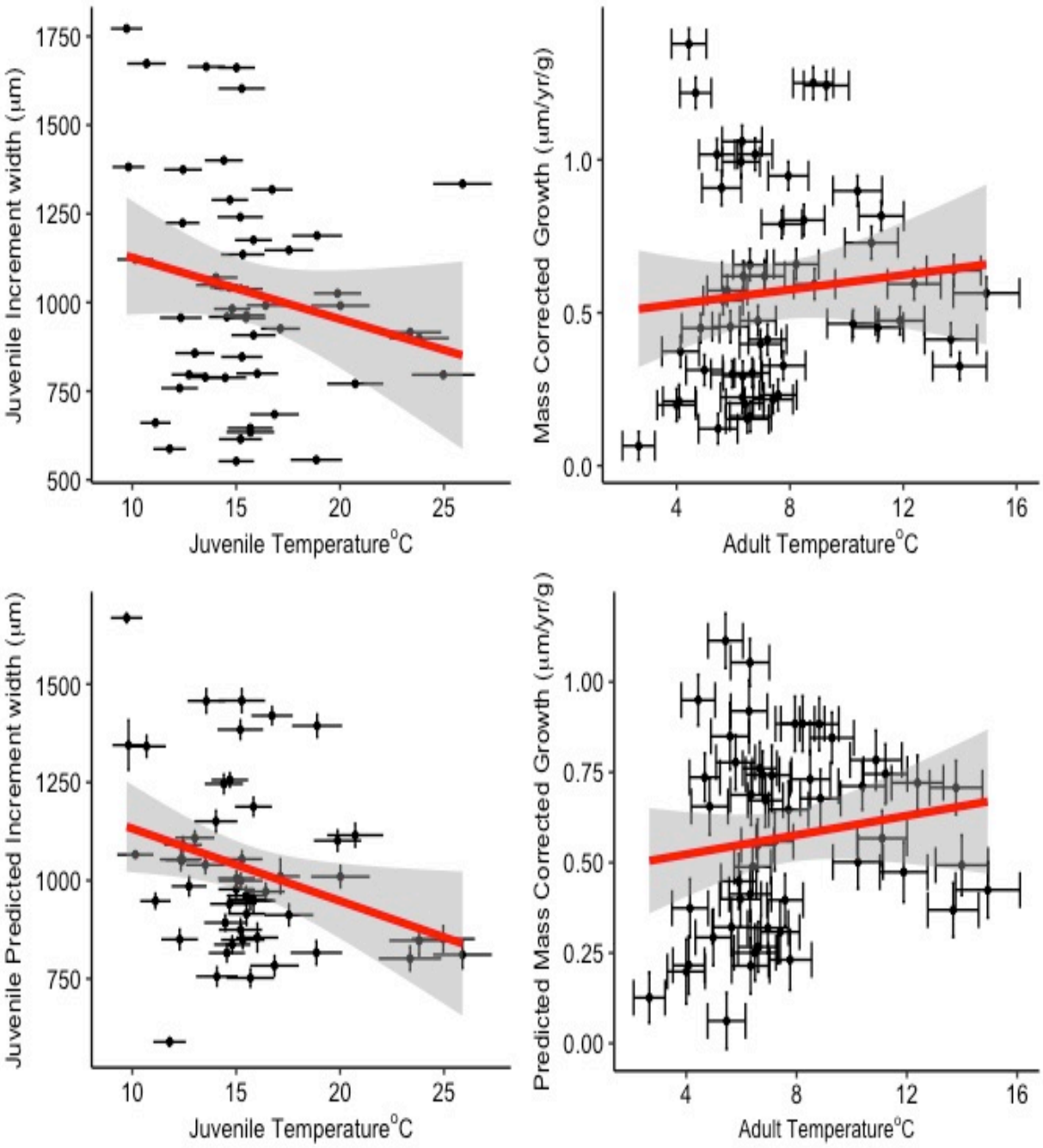


***Figure 49****: For adult population we are demonstrating the growth and thermal interaction for simulated extracted model output data and raw mass corrected growth comparison, using otolith derived experienced temperature. For juvenile life stages we are comparing the thermal (otolith derived experienced temperature) interaction with both simulated extracted model output data with raw increment width.*

### 4.5.4 Model Temperature

We estimated modelled water temperature for each individual fish (during adult life stage) at time of capture from model output averages (Núñez-Riboni and Akimova., 2015) (the benthic habitat temperature model is described and section **4.4.7**) by sub setting the benthic layer of sea temperature (as plaice are a benthic species) over the time frame which we estimate the metabolic rate was averaged (from thin sectioned otoliths) across a theoretical rectangular area which it is possible for an individual to have inhabited (according to north sea plaice tagging studies (Figure **47**)). Model derived water temperature ranged from $6.0^{o}C$ to $13.6^{o}C$ with an average of $9.25^{o}C$. The range and average for model derived temperature is similar to otolith derived temperature, and when compared there is a significant positive linear interaction (lm (model structure = Otolith derived temperature ~ Model Temperature Output) t value = 4.198 and p value of $8.604 \times 10^{-05}$, $R^2$ = 0.2062), however there is a large degree of variability between the two values from an individual perspective (Figure **50**), which potentially implies the presence of thermal microhabitats. Otolith derived values and standard deviations were calculated using Monte Carlo resampling, with equation parameters presented in table **21**. A comparison of model derived and otolith derived temperatures, divided between months and sexes is presented in table **27** and figure **50**.

***Table 27**: Adult life stage model estimated and otolith derived experienced temperature description, showing minimum, maximum and average values split between sex and temperature measurement.*

| | Male (°C) | | | Female (°C) | | | Male (°C) | | | Female (°C) | | |
|---|---|---|---|---|---|---|---|---|---|---|---|---|
| **Month** | **$Model_{min}$** | **$Model_{max}$** | **$Model_{mean}$** | **$Model_{min}$** | **$Model_{max}$** | **$Model_{mean}$** | **$Otolith_{min}$** | **$Otolith_{max}$** | **$Otolith_{mean}$** | **$Otolith_{min}$** | **$Otolith_{max}$** | **$Otolith_{mean}$** |
| 1 | 6.77 | 10.41 | 8.76 | - | - | - | 5.86 | 9.12 | 7.21 | - | - | - |
| 2 | - | - | - | - | - | - | - | - | - | - | - | - |
| 3 | 5.07 | 7.93 | 6.38 | 4.67 | 8.19 | 6.54 | 8.61 | 13.42 | 10.88 | 6.36 | 13.34 | 9.07 |
| 4 | - | - | - | 4.73 | 7.63 | 6.13 | - | - | - | 2.4 | 15.16 | 8.26 |
| 5 | 6.44 | 9.58 | 7.92 | 4.72 | 8.35 | 6.42 | 11.04 | 15.97 | 13.79 | 6.18 | 10.6 | 8.11 |
| 6 | 5.19 | 8.01 | 6.53 | 4.75 | 8.3 | 6.45 | 2.73 | 5.72 | 4.44 | 3.55 | 7.38 | 5.32 |
| 7 | 5.35 | 10.33 | 7.27 | 5.13 | 9.4 | 7.19 | 4.61 | 13.58 | 7.72 | 1.38 | 13.4 | 6.49 |
| 8 | - | - | - | 4.25 | 8.2 | 6.33 | - | - | - | 4.13 | 8.35 | 5.79 |
| 9 | 6.39 | 10.87 | 8.4 | 6.28 | 11.7 | 8.78 | 5.39 | 15.86 | 9.62 | 3.93 | 16.2 | 8 |
| 10 | - | - | - | 6.69 | 9.72 | 8.13 | - | - | - | 3.12 | 7.6 | 5.31 |
| 11 | 7.16 | 10.47 | 8.57 | 6.95 | 12.32 | 9.4 | 4.73 | 18.61 | 10.03 | 2.36 | 7.97 | 4.9 |
| 12 | 7.86 | 10.75 | 9.32 | 7.28 | 13.22 | 9.72 | 6.06 | 9.01 | 7.41 | 4.19 | 9.64 | 6.89 |

***Table 28**: Juvenile life stage Cresp and otolith derived temperature description. Showing minimum, maximum and mean values, with standard deviations calculated using Monte Carlo simulation analysis. This data is split between sex.*

| | | | | | | | | |
|---|---|---|---|---|---|---|---|---|
| | | | | male | | | | female |
| **variable** | **min** | **max** | **mean** | **SD** | **min** | **max** | **mean** | **SD** |
| Cresp | 0.034 | 0.196 | 0.097 | 0.034 | 0.013 | 0.22 | 0.087 | 0.039 |
| Temperature ($^{o}C$)$_{otolith}$ | 9.413 | 24.126 | 15.645 | 2.953 | 7.597 | 26.94 | 15.530 | 4.023 |

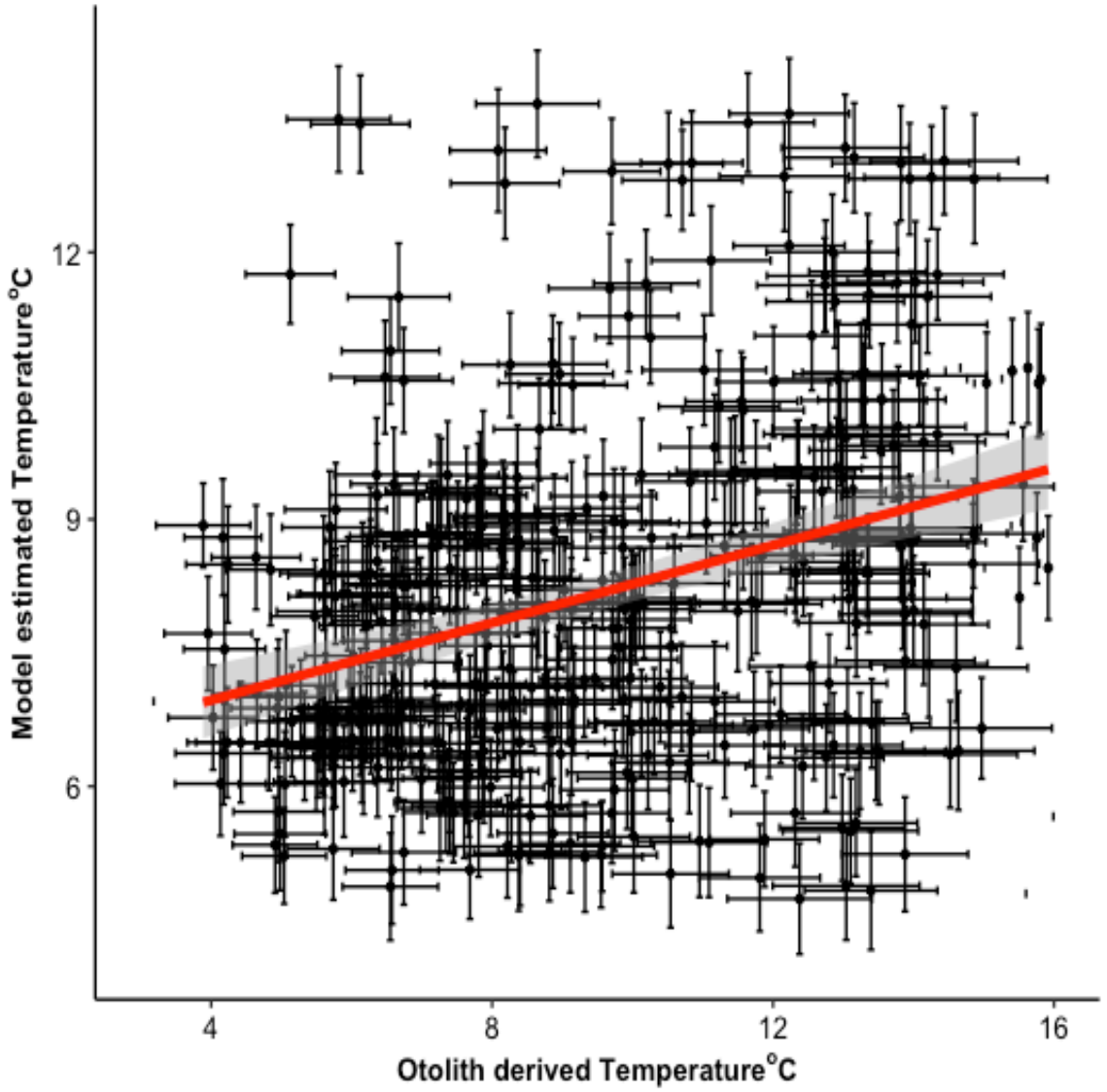


***Figure 50**: Estimated Model and otolith derived experienced temperature comparison (all raw data presented). The error bars are calculated using Monte Carlo simulation analysis.*

### 4.5.5 Temperature Anomaly

Temperature anomaly ($^{o}C$), described in section **4.4.8** and equation **4.2,** covaried non-linearly with condition (g $cm^{-3}$), as shown by figure **51**. Higher temperature anomaly values indicate than an individual selected warmer habitats relative to those available in the surrounding environment. Within this data set individuals with high temperature anomaly values typically express lower condition, which is a trend that is not explained by seasonal variations in condition (i.e. temperature anomaly values are relatively well distributed across months of capture). Otolith derived temperature generally expresses

lower values than modelled outputs, suggesting that individuals usually select cooler thermal regimes within the area of habitat presented to them, but this potentially varies systematically across month and sex (table **29**). Temperature anomaly also shows a predictable relationship with mass corrected increment width at time of capture (apparent form fitted linear and mixed effect models, table **26**). Low temperature anomaly values are associated with reduced mass specific growth (figure **52**). There is a positive covariance between the two variables until an inflection at temperature anomaly values around 3 (figure **52**). Selection of cooler temperatures within the available habitat therefore appears to be associated with reduced somatic growth and increased condition.

***Table 29**: Description of temperature anomaly data distribution between months and sexes. Showing minimum, maximum and average values*

| | Male (°C) | | | Female (°C) | | |
|---|---|---|---|---|---|---|
| **Month** | **Temp anomaly$_{min}$** | **Temp anomaly$_{max}$** | **Temp anomaly$_{mean}$** | **Temp anomaly$_{min}$** | **Temp anomaly$_{max}$** | **Temp anomaly$_{mean}$** |
| 1 | -4.91 | -0.95 | -2.77 | - | - | - |
| 2 | - | - | - | - | - | - |
| 3 | 0.16 | 5.39 | 2.88 | -0.98 | 4.87 | 1.82 |
| 4 | - | - | - | -5.02 | 8.21 | 1.74 |
| 5 | -4.55 | 0.61 | -1.89 | -0.35 | 3.91 | 1.67 |
| 6 | -5.53 | -0.32 | -2.62 | -4.72 | 0.57 | -1.55 |
| 7 | -5.46 | 4.39 | -0.85 | -7.02 | 4.31 | -1.55 |
| 8 | - | - | - | -3.72 | 0.89 | -1.3 |
| 9 | -5.11 | 6.87 | -0.36 | -7.3 | 5.32 | -2.18 |
| 10 | - | - | - | -6.61 | -1.79 | -4.26 |
| 11 | -4.69 | 7.16 | 0.18 | -7.9 | -2.32 | -5.15 |
| 12 | -5.43 | -1.25 | -3.34 | -8.23 | -1.13 | -4.38 |

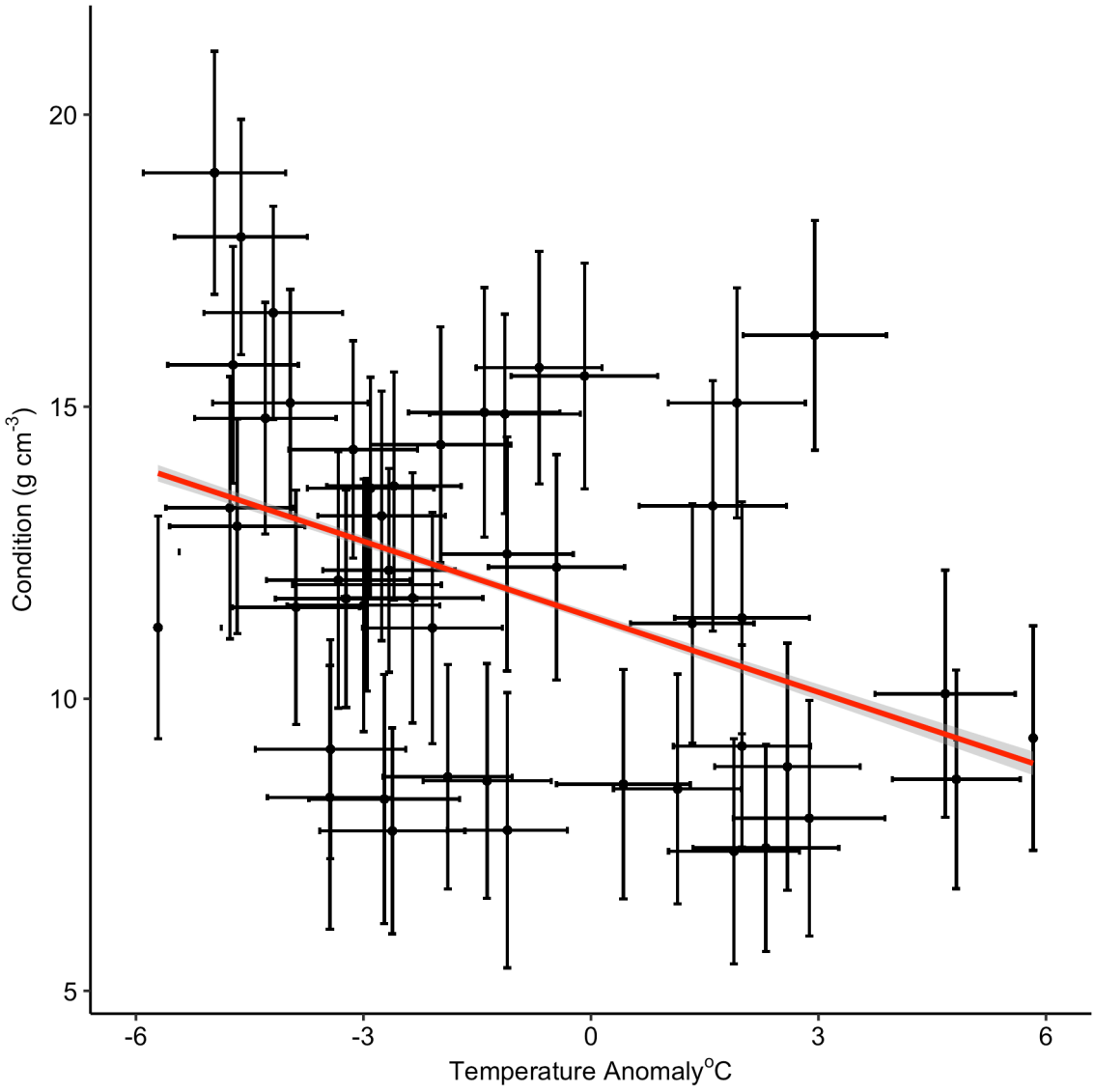


***Figure 51**: Displaying the expressed temperature anomaly and fish condition interaction. Error bars are calculated using Monte Carlo simulation analysis*

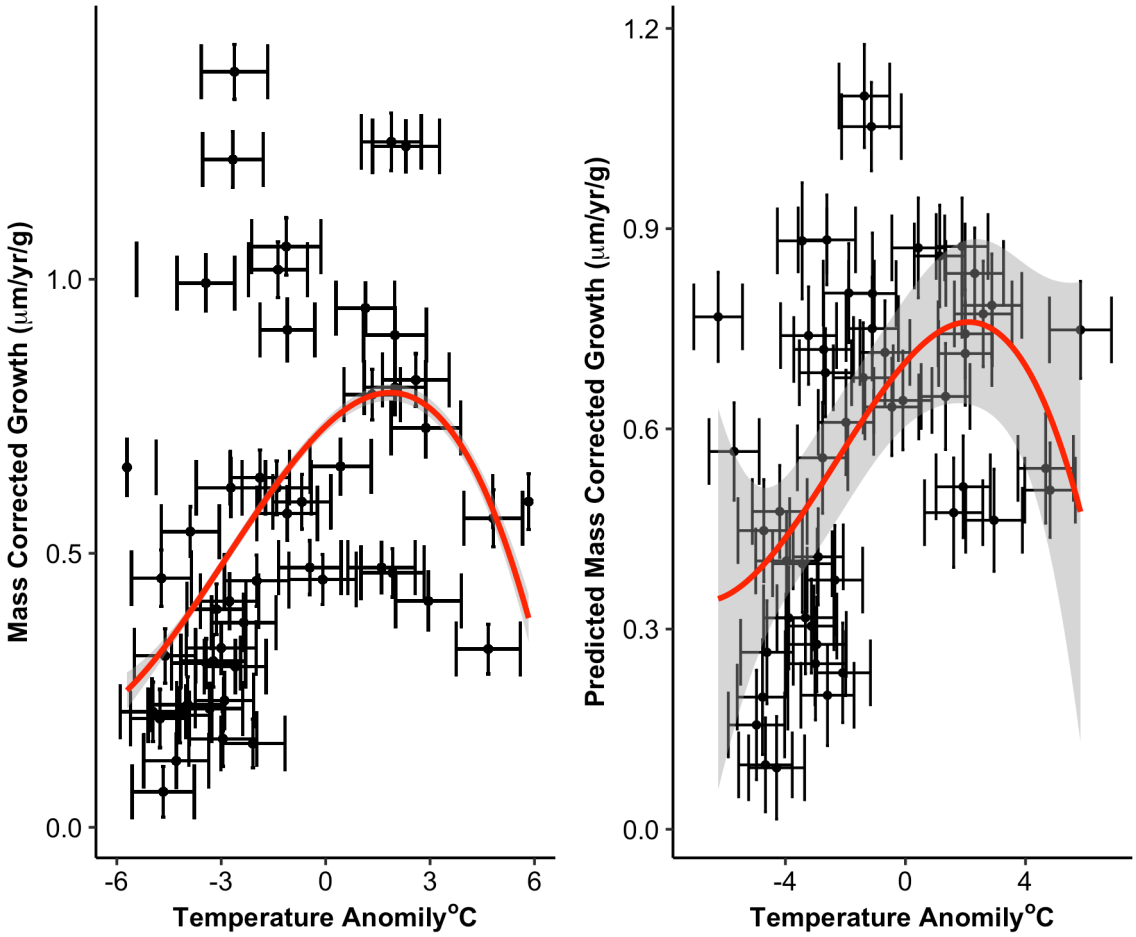


***Figure 52**: Simulated extracted model predicted mass corrected growth data (B) and raw mass corrected growth rate (A) and temperature anomaly interaction. Error bars are calculated using Monte Carlo simulation analysis*

### 4.5.6 Condition

Condition (described by section **4.4.11** and equation **4.5**) of the individuals at the time of capture ranged between 6.48g $cm^{-3}$ and 19.31g $cm^{-3}$. Condition values co-vary negatively with mass corrected growth (described in section **4.4.10** and equation **4.4**) in the last year of life, with higher condition values associated with lower mass specific growth rates (displayed in figure **53**, predicted from partial effects outputs within linear and mixed effects models in table **23** and **26**). As fish mass is a variable

within both condition and mass corrected growth the covariance here is potentially confounded by the common effect of body size. Mass is used to calculate both condition and mass corrected increment width, which potentially explains the correction between the two variables. When we compare condition with raw increment width we see no relationship between the two variables.

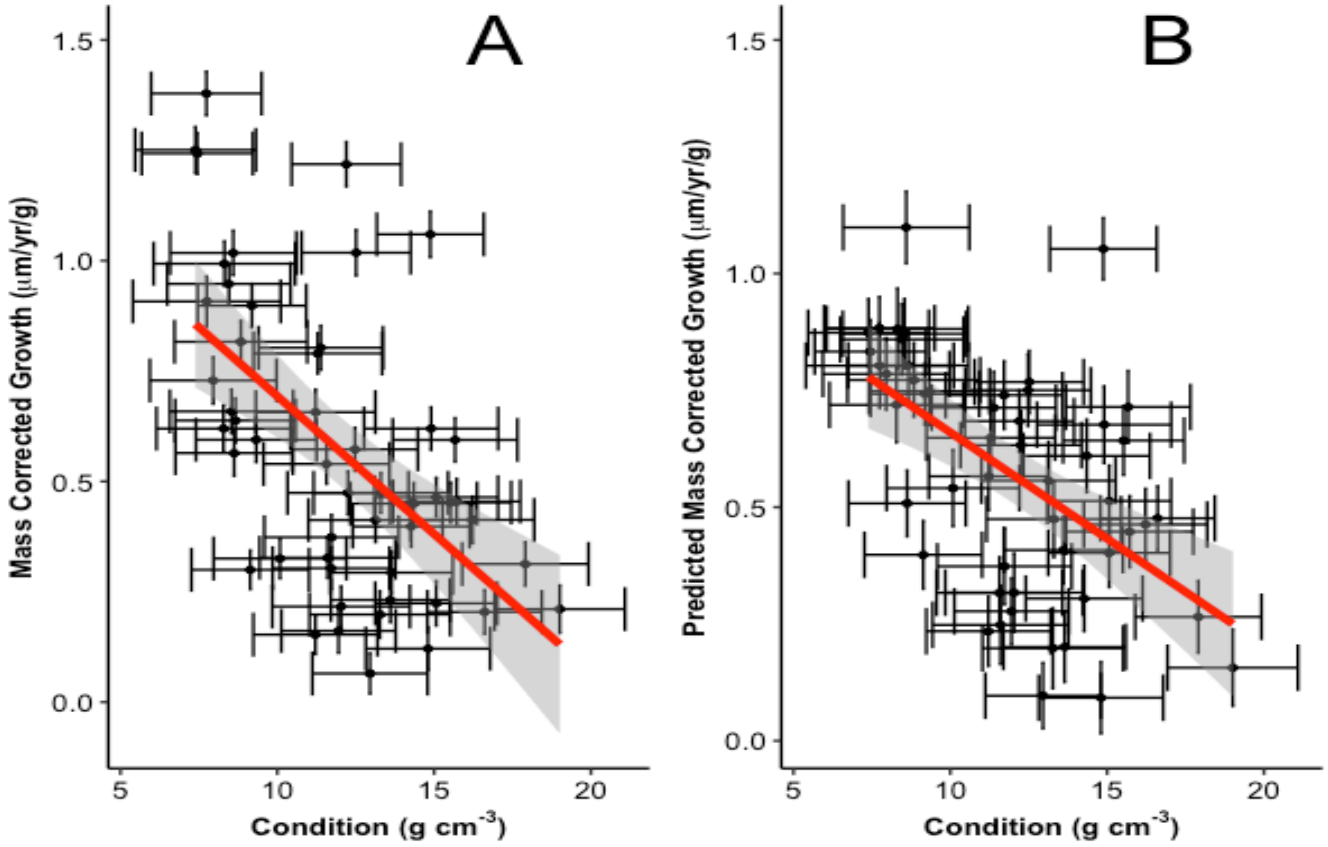


***Figure 53**: Simulated extracted model predicted (B) and raw (A) mass corrected growth and condition interaction. Error bars are calculated using Monte Carlo analysis, as previously described.*

### 4.5.7 Metabolic Rate

The otolith-derived metabolic rate (Cresp used in this chapter, described in section **4.4.9** and equation **4.3**) of these individuals has previously been described by chapters **2** and **3**. Here we group all sub populations of North Sea plaice into one data set as we are interested in exploring total population growth trends, and require a lager data set than can be achived from analysing each sub population individually. Cresp ranged between 0.0366 and 0.21 for adult populations with an average of 0.116 (table **30**). For juvenile populations the range is between 0.050 and 0.239 with an average of 0.134

(table **28**, and figure **54**). Both adult and juvenile Cresp values show a slight negative covariance with mass specific increment width (figure **54**, displaying model predicted data), and shown in model predicted output data and tables **25** and **26**). This could potentially indicate that higher energetic demand suppresses growth rate.

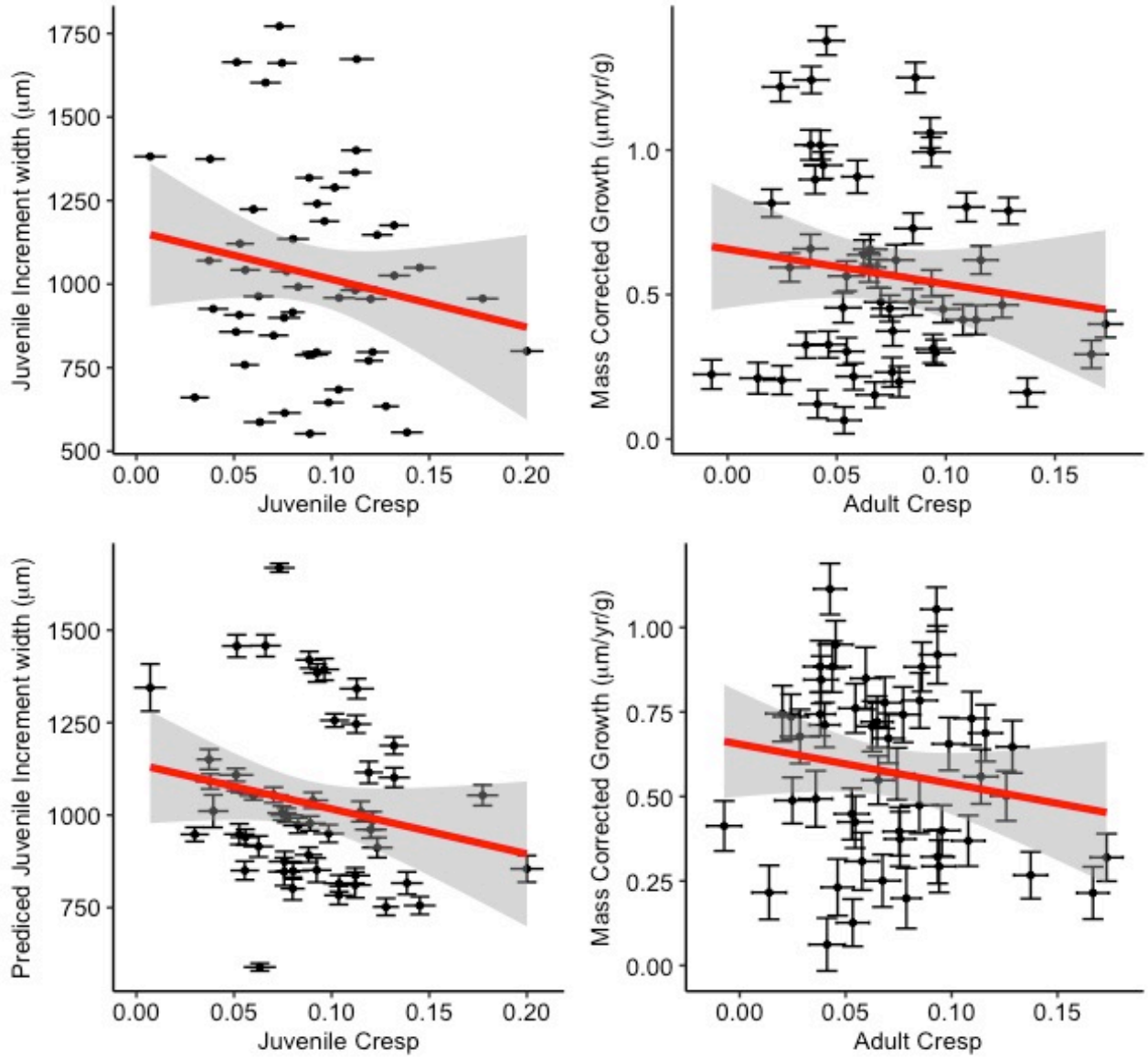


***Figure 54****: For adult population we are demonstrating the growth and Cresp interaction for simulated extracted model output data and raw mass corrected growth comparison. For juvenile life stages we are comparing Cresp with both simulated extracted model output data with raw increment width. Error bars are calculated with Monte Carlo analysis.*

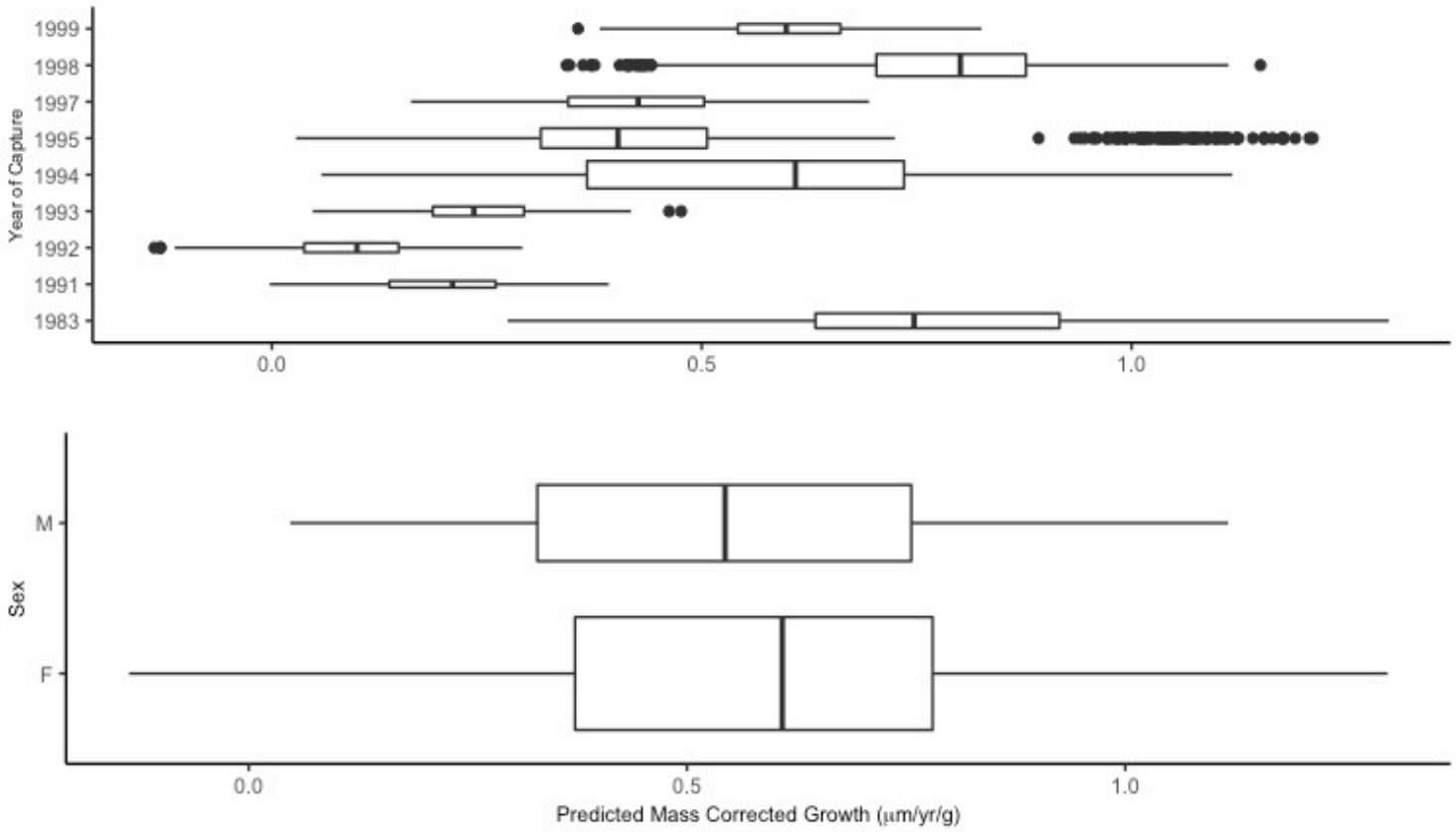


***Figure 55**: Adult life stage Cresp and growth interaction model predicted random effects plots, using best fitted model G simulated and extracted data.*

***Table 30**: Adult life stage Cresp distribution between months and sexes. Showing minimum, maximum and average values*

| | male | | | female | | |
|---|---|---|---|---|---|---|
| **Month** | **$Cresp_{min}$** | **$Cresp_{max}$** | **$Cresp_{mean}$** | **$Cresp_{min}$** | **$Cresp_{max}$** | **$Cresp_{mean}$** |
| 1 | 0.086 | 0.13 | 0.114 | - | - | - |
| 2 | - | - | - | - | - | - |
| 3 | 0.066 | 0.107 | 0.085 | 0.017 | 0.14 | 0.074 |
| 4 | - | - | - | 0.048 | 0.092 | 0.071 |
| 5 | 0.048 | 0.082 | 0.063 | 0.085 | 0.147 | 0.12 |
| 6 | 0.028 | 0.071 | 0.046 | 0.05 | 0.115 | 0.084 |
| 7 | 0.002 | 0.115 | 0.063 | 0.005 | 0.108 | 0.051 |
| 8 | - | - | - | 0.019 | 0.141 | 0.073 |
| 9 | 0.016 | 0.096 | 0.054 | 0.003 | 0.162 | 0.071 |
| 10 | - | - | - | 0.074 | 0.113 | 0.094 |
| 11 | 0.034 | 0.189 | 0.12 | -0.006 | 0.093 | 0.053 |
| 12 | 0.04 | 0.079 | 0.058 | -0.026 | 0.094 | 0.036 |

# 4.6 Discussion

## 4.6.1 Intrinsic vs Extrinsic Variability

When comparing the levels of variance explained within this data set by varying model structures it becomes clear that the models with intrinsic factors included within their structure explain a higher level of variance within the data; and are therefore more effective at predicting among-individual variance in otolith increment width (tables **23** and **22**). A greater proportion of the variance in growth

rates could be explained for adult life stages compared to age 0 life stages, probably because the retrospective sampling meant that there were more intrinsic variables available to model adult growth.

The importance of intrinsic variables in explaining variance in growth (and the high proportion of total variance explained by the available variables) implies that adult growth rate is potentially less directly influenced by environmental drivers. Adult growth is slower, and therefore less variable, but this still is useful information.

Previous studies attempting to explain the factors impacting fish growth in laboratory studies have focused on temperature and aerobic scope (Gräns et al., 2014; Farrell 2016; Jutfelt et al., 2021), asking if variations in aerobic capacity relating to temperature variability can predict the length at age class of a fish stock. Such studies have produced varying results with no unifying conclusions (Blier, et al., 1997; Jutfelt et al., 2014; Scheuffele et al., 2021). Studies which have observed changes in fish length and mass under wild conditions, using fishing trawl data have reported a shift in phenotypic expression (Perry et al., 2005; Killen et al., 2015), with populations now expressing a reduced length at age of maturity, implying reduced population level growth rates (Perry et al., 2005; Killen et al., 2015), however this is related to fisheries induced evolution; a trend which has been correlated to increased average summer and winter water temperatures, reducing individual aerobic capacity and therefore the amount of energetic partitioning towards growth (Perry et al., 2005).

Among individual variation in growth was not strongly related to either modelled or experienced temperature. Previous studies have produced contradictory findings regarding the relationship between temperature and growth rate, with wild fish surveys suggesting positive, negative and no interactions with increased winter and summer temperatures (Huang et al., 2021; Attrill and Power 2002; Murdoch and Power 2013). Some surveys have found evidence of sub-population thermal preference (Ciotti 2012), however we are measuring the thermal interaction within a single population so such trends are unlikely to be identifiable. From a laboratory-derived SMR perspective there are again contradictory findings regarding thermally-controlled growth, with somatic growth being largely explained by extrinsic conditions the individuals are exposed to, such as food availability (Russell et al., 1996). In theory, when food availability is unlimited, growth rate is expected to covary positively with temperature at least until optimum temperatures are reached (Jobling 1980; Rowe and Thorpe 1990; Jobling 1996), however within this study as each individual experienced different environmental

conditions we are unable to measure or control dietary input. It is therefore possible that any direct relationship between temperature and growth is overwhelmed by variations associated with individual feeding rate and/or energy partitioning. The random effect of year of sampling was informative, potentially suggesting that resource availability is a stronger driver of among individual variation in growth rate than variations in experienced temperature in the sampled population (figure **55** and table **26**). Without more specific meta data (such as food availability, which is unavailable) for each year we are unable to statistically suggest a reason for this interaction between growth and year, however we hypothesis that the inclusion of variables such as food availability may potentially improve mixed effects model outputs

What is of interest is how the relationship between temperature and growth rate changes over the life history of the individual, similarly to metabolic thermal responses (Dahlke et al., 2020). This again potentially suggests there are different factors impacting juvenile and adult growth, with juvenile physiology being more closely linked to external environmental factors and adults being likely more closely linked to behavior. Juvenile growth rate is faster, however as previously mentioned the level of variability between adult and juvenile populations is still useful data. An implication of this finding is that it may be difficult to predict future plaice growth based on climate model (temperature) projections. Similarly, inferring temporal variation in environmental drivers based on time series of growth rate data may also be more complex than previously recognised.

RNA-based estimates of the individual level daily growth rates (G, day−1, measured using white muscle RNA and DNA concentration), coupled with experienced water temperatures (calculated at the time of capture), and fresh body mass have been used to examine the extrinsic parameters impacting *in situ* plaice growth rates (Ciotti et al., 2010); aiming to test the effects of temperature on growth over small scale (25km) gradients (Ciotti et al., 2010; Ciotti 2012). Laboratory derived growth rate studies (such as aerobic scope findings) predict that population level somatic growth is likely to be temperature dependent and vary over small scale spatial gradients; however, such ecological trends are not present within RNA derived *in situ* growth data (Ciotti et al., 2010). This indicates that *in situ* RNA derived growth rate data does not agree with laboratory aerobic scope studies, and we are potentially unable predicted *in situ* growth trends from extrinsic variables alone (Ciotti et al., 2010). The same studies find that growth is predictable from total growth, food availability and condition, suggesting that plaice growth might be closely linked to growth phenology and individual physiology. However, with the

inclusion of Cresp and experienced temperature we hope to aid with explaining more of the deviance within the data (Ciotti et al., 2010).

The inclusion of sex as a random factor did not improve model fit, having no significant impact on AIC or $R^2$ values, and we see no significant difference in otolith increment width between sexes, suggesting that within this data set sex is not a good predictor of growth rate. Condition expresses a predictable negative relationship with mass corrected increment width, with high condition values corresponding with reduced growth. This relationship potentially represents either individual physiological phenotypic differentiation (with some individuals growing in length quicker than condition), energetic partitioning or different habitats (as Plaice are migratory) promoting either growth or condition. We are unable within this data set to form conclusions explaining these trends, however their individual physiological needs shift over the annual cycle correlated to the breeding and migratory cycles, with condition promotion during certain seasons (Rijnsdorp 1990; Hunter, et al., 2003; Teal et al., 2012), which potentially explains the trends within this data set.

Temperature anomaly, which we suggest is a measure of thermal selection (and habitat preference by inference), showed a systematic relationship with mass corrected increment width. Individuals selecting cooler conditions (temp anomaly < 3) show a positive relationship between temperature anomaly and growth until values greater than 3, above which reduced growth rates are seen. As low growth rates are associated with increases in condition (and pre-spawning life periods) it appears that individuals select relatively cool waters compared to the local habitat average during periods of intense feeding supporting gonad development. Somatic growth is elevated in fish that occupy waters close to the local habitat average, perhaps implying differential behavioral thermoregulation associated with high intensity feeding.

### 4.6.2 Adult life stage Field Metabolic Rate and Age-Size Growth Relationship

Theory and laboratory experimentation suggest that somatic growth is maximised at temperatures below the thermal optimum with unlimiting oxygen and food resources (Jobling 1997; Blier, et al., 1997; Jutfelt et al., 2021). Under these conditions, data from previous studies suggest there should be a positive covariation between growth and field metabolic rate (Blier, et al., 1997; Jutfelt et al., 2021). The inclusion of Cresp within adult mixed effects model structure did reduce model AIC scores and

increased the overall proportion of deviance in growth rate explained. However, the relationship between Cresp values and growth is relatively weak (Figure **54**).

When using raw Cresp values it is unlikely that statistical models capture the full relationship between energetic demand and growth rate, as we are not accounting for the physiological expression of FMR, like aerobic scope studies do. Aerobic scope studies quantify the degree of available energetic resources by comparing the maximum and minimum respiratory potential of an individual (Clark et al., 2013), therefore linking extrinsic variability with an intrinsic individual specific form of physiology. When examining the relationship between raw SMR or MMR values with environmental parameters aerobic scope studies report a 3-fold level of unexplained deviance within the data (Clark et al., 2013). Here we are reporting individual FMR expression with no measure of SMR or MMR; and in chapter 2 we derive the presence of metabolic phenotypes expressed within wild populations. Therefore, we are unable to measure the relative nature of FMR between individuals, meaning that we are unable to tell how close an individual's Cresp value is close to its maximum value. It is likely that the two fish which express a similar Cresp are operating at different levels within their aerobic scope . We are unable to tell from one Cresp value the proportion of its aerobic scope which is available to the individual; therefore, we are unable to calculate the percentage of available energetic resources are partitioned towards growth rate. The inclusion of a measure of individual specific metabolic capacity has the potential to improve mixed effects model fit and degree of growth rate deviance within the data.

### 4.6.3 Extrinsic Interaction with Growth Rate Over Life Stage

Juvenile and adult life stages express a different relationship between growth rate and temperature. Adults express elevated growth rates with higher experienced raw temperature, resulting in a predicted positive interaction, whilst juvenile growth is suppressed with increasing thermal conditions (producing a negative correlation). We are unable to explain this difference in growth dependence with temperature between life stages only using the variables presented within this study. However, we suggest that it is behavioral differences and physiological drivers which explain this interaction. Due to size-based predation pressure smaller individuals more susceptible to predation, and this creates a stronger selection pressure for fast growth (Sasaki et al., 2002; Dorenbosch et al., 2009; Aikio et al., 2013). Adults potentially have the ability to select extrinsic conditions to optimize energetic demand to suit their physiological and behavioral needs more than juveniles (Hunter, et al., 2003; Hunter et

al., 2009). However, due to the interactive relationship between predictive variables within the model structure it is difficult for us to suggest the reason behind juvenile suppressed increment width with higher experienced temperatures.

Form a theoretical perspective, when looking at aerobic scope studies, this population is operating below its maximum capacity as the FMR thermal response does not show an arrhinias interaction as seen in laboratory studies (Clark et al., 2013), therefore as temperature increases so does the available energetic resources for the individual (Farrell 2016), if laboratory data is applicable to natural scenarios. Previous studies have suggested that when the aerobic scope is high it is likely to promote growth as there is more energy availability left over after physiological maintenance (Farrell 2013), however in juvenile life stages we do not see this relationship, with higher metabolic rates and experienced temperatures resulting in reduced growth rates. This potentially suggests that growth rate is not only controlled by temperature and that there are multiple extrinsic variables (which we are unable to measure) limiting individual's energetic production (Nisbet et al., 2000), as experienced temperature is below the optimum thermal range for performance. Alternatively, this could indicate that an increased FMR does not indicate higher available energetic resources, and individuals are operating with a reduced aerobic scope, with less energetic partitioning going towards growth rate promotion. From the single FMR value without a varied and controlled environmental gradient it is very difficult to relate this data to aerobic scope findings, as metabolism expresses a high degree of variability between individuals under standardised extrinsic parameters (Clark et al., 2013), and it is only when compared to an individual's unique base line metabolism we see physiological interaction (Farrell 2016). As a result, there might be a thermal maximum present within this data set, but we are unable to measure it without accompanied individual specific aerobic scope data.

Laboratory studies which have experimented with daily somatic growth in response to food availability have found that when individuals experience unlimited food supply daily growth rate scales predictably temperatures in a linear manner, however when food availability is limited growth rate is suppressed at higher temperatures (Nicieza and Metcalfe 1997; Donelson et al., 2010). This relationship is theoretically explained by higher temperatures requiring a large energetic input to sustain a linear relationship with growth compared to the energetic supply (Pörtner and Peck 2010). This is potentially the case within this data set with higher temperatures during juvenile life stages resulting in elevated FMR, therefore a higher energetic demand and the available energetic resources of the individual are

not devoted toward somatic growth but towards other physiological intrinsic variables. Studies have also found metabolic suppression when individuals food availability is limited in relation to their demand (Norin and Malte 2011; Killen 2014; Metcalfe et al., 2016). That fact juvenile growth is a reduced at higher temperatures here potentially suggests that food availability at the higher temperatures limited growth rate as in laboratory studies. The trends present within this data set are relatable to laboratory-based findings, which potentially indicates that the reason for the decline in juvenile growth rate at higher experienced temperatures is due to a higher energetic demand than supply at warmer water temperatures, limiting aerobic scope. Therefore, leading to a reduced energetic availability and growth rate (Clark, et al 2013). Fundamentally, within this data set we see strong support for the view that individual variation in growth rate (within a single population) is highly context-dependent. Variations in individual energy supply-demand is likely to overwhelm common external effects such as temperature making predicting growth rate at the scale of individuals is likely to remain problematic.

### 4.6.4 Issue with this data

When applying *in situ* data trends to laboratory study findings a we encounter a few issues with comparability, as controlled experiments have the ability to isolate the relationship with temperature, metabolism and multiple other factors (Nisbet et al., 2000). *In situ* data is unable to isolate variables, and is therefore the combination of multiple predictor variables, potentially with interactive responses. Insitu wild growth rate and metabolic data is likely to be impacted by multiple sources uncertainty which we are unable to control, such as behavioral. When suggesting explanations for *in situ* data trends, we are comparing this data to laboratory studies such as aerobic scope theories. Therefore, we are applying population averages (Cresp and growth rate) which are the result of multiple predictor variables to a controlled independent relationship between a singular external variable and an individual specific intrinsic variable (for example SMR) (Farrell 2013); and this could lead to miss interpretation. If we examine raw SMR data independent from MMR or aerobic scope there is an unexplained three-fold level of variability when extrinsic variables are controlled and standardised (Clark, et al., 2013), and population trends are only apparent when compared to MMR and aerobic scope. Therefore, to properly interpret FMR data we need to pair FMR with associated SMR data.

### 4.6.5 Predicting Growth Rate Beyond Linear Interactions

This data is aiming to explore the relationship between in situ measured extrinsic and intrinsic variables with growth rate and compare the findings to model and laboratory study findings predicting the variables which impact population growth rate. Here we find that thermal conditions, metabolism and other intrinsic variables do impact growth in a predictable manner as theorised by previous studies, however the key finding is the degree of unexplained deviance within the data when such previously mentioned factors are accounted for and what factors we suggest are responsible. Some studies have suggested extrinsic variables we are unable to measure within this data set such as food availability, population complexity, predation and other factors are likely to impact population growth rate (Thorson 2020); but to test this theory we need more environmental meta data specific to small scale geographical areas. Another finding of interest within this data set is how the relationship with growth rate and temperature changes throughout life history of individuals, suggesting that the driving forces of metabolism change with the maturity.

### 4.6.6 The Importance of Habitat Selection

This data set does lead up to question the causes of ecological trends previously published which report strong population correlations with temperature, as we do not see such a dependable relationship here. There is the potential that the trends reported are not due to temperature but environmental warming is a secondary cause leading to further extrinsic variable adaptation, which is responsible for growth rate deviance. This may potentially explain the inconsistent relationship with temperature between studies, as warming impacts some habitats at a faster rate than others, and to properly assess growth rate trends we need to look into habitat adaptation.

# 5 Conclusion

## 5.1 FMR Thermal Interactions

The impact of elevated thermal conditions on marine ecosystems has become a highly debated topic (Clarke and Johnston 1999a; Farrell et al., 2008; Farrell 2013; Clark et al., 2013; Sandblom et al., 2014; Jutfelt 2020), due to recent rapid warming of summer and winter water temperatures (Núñez-Riboni and Akimova 2015) and our lack of knowledge about the adaptive capacity of marine communities (Brander 2007). Laboratory studies which isolate thermal and physiological interactions, find that fish SMR and MMR are thermal predictable (Froese and Pauly 2000; Clark et al., 2013; Pauly 2021), and use the difference between the two, termed aerobic scope (Clark et al., 2013), to estimate the individual energetic resource availability used for growth, maintenance and other physiological and behavioral processes (Rombough 1994; Guderley and Pörtner 2010). Studies have used the predicted maximum thermal range where fish energetic supply demand ratios allow for optimum physiological performance, according to lab studies, to predict changes in population biogeography, based on future climate scenario models (Deutsch et al., 2015a). However, there are multiple theories which attempt to explain the causes for metabolic thermal dependence, from oxygen supply and demand ratios to enzymatic thermal dependence (Ern 2019; Pauly 2021). As a result, marine population responses to predict climate conditions are a highly debated topic, with model studies which aim to predict population biogeography producing contradictory estimations (Nisbet et al., 2012). There have also been questions regarding the application of laboratory derived studies to *in situ* situations, with case studies examining the similar extrinsic intrinsic interactions producing varied outputs (Baird et al., 2007).

There are some issues with previously used methods which attempt to use aerobic scope findings to model fish population outputs and movements. Laboratory studies attempt to identify the relationship between an isolated intrinsic and environmental factor (Clark et al.2013), when natural communities experience multiple extrinsic sources of variability (Nisbet et al., 2012), and potentially adapt their behavior to suit physiological needs. This has led to studies attempting to predict field metabolic rate, for example using oxygen supply and demand ratios, as a method to estimate the elevation of FMR from SMR in an attempt to aid with model predictions . Here we utilise the varying isotopic sources of

carbonate contributing to otolith aragonite to estimate the relative proportion of respired carbonate contribution, and therefore metabolic rate (Chung et al., 2021). We use this technique in an attempt to measure metabolic interactions with extrinsic variables, and compare to laboratory studies and theoretical predictions (Deutsch et al, 2020).

## 5.1.1 FMR Thermal Response Findings

### 5.1.1.1 Adult Thermal Dependence

We examine how body mass and temperature scales with FMR. As we are not controlling the conditions experienced by individuals presented within this study it is unlikely that we are measuring energetic demand at the maximum thermal range of performance, therefore we do not expect to see an Arrhenius relationship as present with SMR data (Clark et al.2013); because wild populations potentially select habitats which suit their individual physiology (Railsback and Harvey 2002; Shepherd and Litvak 2004; Lindberg et al., 2006). FMR is therefore unlikely to express as strong predictable relationship with temperature and we do not expect FMR to covary in a similar manner as SMR, as we do not know prior to isotopic sampling the thermal range we are measuring.

Within this data set individual level adult FMR does not scale predictably with either temperature or body mass, suggesting that the relationship between FMR and extrinsic variability or intrinsic factors differs from SMR. This potentially disagrees with metabolic theory studies (Clarke and Johnston 1999a; Farrell et al., 2008; Clark et al.2013; Farrell 2013; Sandblom et al., 2014; Ern 2019; Jutfelt 2020; Pauly 2021), and leads us to question the validity of applying SMR studies to natural populations.

However, there are multiple sources of unknown extrinsic and intrinsic variability that are potentially suppressing thermal interactions, such as habitat selection and food availability. We also do not know if we are measuring the total FMR spectrum of the population, or if we are subsetting FMR data without knowing. Potentially with more FMR measurements we will find that this data only represents a small section of total population FMR expression. However, this lack of thermal or body mass dependence does make us question the applicability of SMR data, and we require more FMR measurements paired with lab studies to fully understand the trends presented within this adult population.

#### 5.1.1.2 Juvenile Thermal Dependence

We measured the juvenile metabolic thermal dependence, for the same individuals as adults, by sampling otolith aragonite deposited one-year post spawning, therefore one year of age. Body mass, length, location is unknown for juvenile life stages, therefore we have not calculated condition or body as there would be a high degree of unexplainable variability with the data. As a result of unknown sources of isotopic variability, it is unlikely that we are reporting the full FMR thermal dependence within this study. However, there is a strong predictable relationship present between juvenile FMR and experienced temperature, with higher temperatures correlating with FMR elevation. This data is similar to laboratory derived SMR (Ott et al., 1980; Clark et al., 2013). However, as with the adult population, we are unable to tell how close juveniles are to the thermal maximum of performance. This variable thermal dependence over life stage implies that to assess the impact of changing climates on a singular population we need to treat adults and juveniles as sub populations and model their biogeography and population output separately.

We are also unable to accurately derive if this is interactions is the result of thermal metabolic dependence or behavioral thermal habitat selection, to suit variable metabolic phenotypic expression; which we will only be able to distinguish with FMR paired with measured aerobic scope data.

The inconsistent relationship between extrinsic factors and energetic demand throughout the life history of the individual, we suggest is likely behavioral based. The primary physiological driver of juvenile populations is believed to be predation pressure (Marras et al., 2011); therefore, they are believed to focus on foraging to increase body mass and length with minimal social or behavioral factors, when adult ecological pressures are related to breeding pressure and less body size predation pressure. During juvenile life stages individuals do not undergo complex annual breeding and feeding cycles (Hunter et al., 2009), so it is likely that the inclusion of feeding and spawning seasonal cycles reduces the thermal dependence of metabolism when the primary objective of the individual is no longer increasing in size.

#### 5.1.1.3 Phenotypic Expression

When comparing FMR expression over the different life stages (once the temperature and body mass covariance is removed) we see a predictable linear relationship, with individuals which express

relatively high or low metabolic rates compared to the population average during juvenile life stages maintaining this relationship during adult life stages. This is irrespective of metabolic expression, as both absolute Cresp and extrinsic interactions are inconsistent with life stage, but the relative distribution of FMR within the population remains consistent. This is potentially evidence of metabolic phenotypic expression in natural settings.

Metabolic phenotypic expression has previously been reported in laboratory settings, with studies successfully selectively breeding individuals with certain metabolic traits in order to either raise or reduce community metabolism (Metcalfe et al., 2016). This is useful from a fisheries modelling and management perspective, as if we can monitor the changes in the distribution of metabolic phenotypic expression we can potentially suggest if the population is being impacted by changing climates and the vulnerability of the population.

## 5.1.2 Future study development

### 5.1.2.1 Inclusion of Multiple Species

Plaice express complex annual cycles, including specific breeding and spawning geographical areas with seasonally timed migrations (Hunter et al., 2009). Other species which inhabit similar habitats and water bodies express very different behavioral, breeding and life cycles, and it is likely that metabolic expression changes with physiology, functionality and behavior between species (Deutsch et al., 2015a). To improve our understanding of ecosystem metabolic thermal interaction we need to measure multiple species from separate habitats; as metabolic thermal dependence is likely to vary between species and functionality.

At this stage in field metabolic rate studies we do not know which functional groups (benthic, pelagic ect) are likely to present higher population averages or greater variability of metabolic expression. This information could potentially identify which functional groups have the capacity to adapt their behavior or distributions in response to environmental instability, which is useful data for predictive model studies. By measuring thermal sensitivity over environmental niches and interspecies gradients we will potentially be able to model marine community interactions in response to environmental shifts with

more precision. With further study, and combined with laboratory derived SMR, this otolith derived metabolic rate method could potentially be used to answer such questions.

#### 5.1.2.2 Metabolic Thermal Dependence Through Life History

Within this data set we are unable to measure if the expressed change in metabolic thermal interaction over the life history of the individual is due to thermal selection or metabolic dependence. Do the environmental conditions the individual is exposed to at juvenile life stages impact adult metabolic expression or do juveniles select environments to suit their metabolic phenotypic expression?

An experiment measuring SMR paired with FMR field studies would potentially provide an answer, which is useful from a modelling perspective, as it will provide information about ecosystem stability and likely future biogeographical distributions. Measuring the age at which this thermal dependency breaks down is interesting from a fisheries management and an academic perspective, as this data set potentially suggests that juveniles are more susceptible to climatic variation. With a measure of sub population venerability, we may be able to form more targeted fishing stocks exploitation techniques (Galland 2017), which is a popular method used by governmental bodies responsible for policy formation and fishing quota calculations.

#### 5.1.2.3 FMR Phenotypic Expression uses

As we can identify metabolic phenotypic expression within the population we can potentially measure which phenotypes are more likely to survive in response to varying climatic scenarios. From an ecosystem functionality perspective this would provide information regarding how environmental conditions during juvenile life stages impacts population structure over annual and generational time scales. To achieve this, we need to consistently sample a small proportion of juvenile and adult populations over annual cycles and measure metabolic trends, then see how the distribution of phenotypic diversity changes.

#### 5.1.2.4 SMR and FMR Comparisons

The paring of both juvenile and adult SMR and FMR data would provide evidence regarding the interaction between the two measurements; data representing the elevation of FMR from SMR will potentially increase the variance explained in FMR trends from a statistical model perspective. FMR thermal dependence curves produced within this study cannot be used to predict of how close an individual is to their maximum metabolic rate or thermal range of performance. This is because we are unable to measure individual metabolic trends at their maximum aerobic capacity as we cannot control the extrinsic variables they are subjected to in the wild. Therefore, even though juveniles metabolic expression varies predictably with temperature, we are unable to estimate their aerobic scope, and it is possible that individuals at varying levels of FMR expression are operating within the same range of their aerobic scope of performance. If this is the case then this data is less applicable for model studies, as we are unable to calculate the energetic maximum capacity of the individuals, which is required to estimate biogeography and population outputs (Deutsch et al., 2015a). This FMR data, paired with aerobic scope data will tell us if individuals attempt to select environments to optimise their aerobic scope, and again inform us how applicable laboratory studies are to *in situ* scenarios.

## 5.2 Seasonal Variations in FMR

The third chapter of this PhD focused on measuring metabolic elevation and suppression throughout the annual cycle, in an attempt to identify how much variance within metabolic data is explained by extrinsic variables, such as temperature and behavioral patterns. Previous studies have attempted to identify how metabolic rate in responds to multiple behavioral and external variables in the laboratory (Killen et al., 2013). As a result, it is difficult to directly apply such findings real life scenarios, however there are advantages of laboratory-based studies which field metabolic rate (FMR) data is unable to replicate.

For example, aerobic scope data measures the elevation in energetic demand from an individual baseline perspective (standard metabolic rate) (Clark et al., 2013), therefore each measurement accounts for phenotypic expression. Current FMR data relies on relative variability between population averages over uncontrolled environmental gradients, and does not account for individual phenotypic

expression. Standard metabolic rate (SMR) also expresses a high degree of intraspecific variability over standardised environmental and physiological conditions when studied from a population average perspective (Clark et al., 2013). Therefore, it is likely that SMR populations averages (singular measurements) significantly vary regardless of extrinsic factors, potentially in a similar manner to FMR measurements presented within this study.

SMR studies also have the ability to isolate the interaction between specific predictor and response variables, when FMR expression is the combinative interaction of multiple factors, many of which we are unaware of and unable to measure. However, identifying SMR trends related to seasonal patterns is difficult, as it is hard to replicate behavioral cycles, such as migration, under laboratory settings. One popular method used to assess population health and stability is individual variability (Killen et al., 2013), therefore measuring the range of expression within the data rather than the mean. Individual variability theory suggest that a higher range of phenotypes expressed within a population implies that it is more stable and less susceptible to environmental instability, as it is more likely that a proportion of the population are able to survive (Killen et al., 2013). With this method you do not require a baseline level of individual metabolic expression, to account for individual specific phenotype. Therefore, to measure FMR trends throughout the annual cycle, we assess both population means and individual variability, to understand how each behavioral or environmental variable impacts energetic demand.

### 5.2.1 Seasonal Fluctuations in FMR findings

Field metabolic rate over than annual cycle shows periods of both population average elevation, suppression and fluctuations of individual variability. This suggests that otolith derived FMR is able to detect trends in energetic demand with enough sensitivity to identify time periods when the metabolic rate of the population is elevated, and potentially time periods when the population is more susceptible to environmental instability. This allows us to explore the environmental, physiological and behavioral factors which impact energetic demand over the annual cycle.

Metabolic theories of ecology suggest that energetic demand is primary controlled by oxygen availability, body mass and temperature (Pörtner 2010; Clark et al., 2013), however the data used to derive such theories originate from isolated extrinsic and intrinsic variables responses under laboratory studies. When in natural scenarios there are multiple environmental controlling factors for

physiological or phenotypic expression (Nisbet et al., 2012). Here we find that neither temperature or body mass are the primary drivers of metabolic expression, as periods of energetic demand elevation and suppression are not significantly predicted by thermal interactions or individual body mass.

Periods of metabolic elevation coincide with increased fish conditional values, feeding periods and times when the population inhabits northerly cooler waters. Lower Population metabolic rate levels occur during southerly breeding time periods, with minimum values just prior to the feeding season. Therefore, it is likely that metabolic trends are more closely linked to behavior cycles than extrinsic factors, and individual energetic demand varies with the needs of the individual at any given time. As metabolic elevation and increased individual variability occurs during feeding it is hard to identify if the act of foraging for food or the energetic demand associated with digestion are the primary divers of metabolic elevation.

During spawning time periods (when individuals do not feed) after migration when the entire North Sea community (all sub populations) gather in the southern North Sea to breed the population experiences a reduction in FMR expression and individual variability (Hunter et al., 2009). This would suggest that it is the increased effort of digestion which is responsible for metabolic elevation, as it is unlikely that individual movements are reduced to a significant extent when compared to the feeding season.

There are studies which attempt to identify if gaining body mass or using fat reserve is more energetically demanding, with results suggesting that production of potential energetic stores is a costlier process, with higher associated energetic demand (Fonds et al., 1992). This could potentially explain the results presented within this data set, as when fish are feeding their energetic demand is greater, however without further targeted field surveys this is speculation. Chapter 3 of this thesis however, aims to describe how population level metabolic rate is inconsistent throughout the seasonal cycle and cannot be predicted from extrinsic variability alone, and then suggest potential reasons for these trends; we are not aiming to explain population trends in metabolic rate, as we require more individual specific meta data for statistical model analysis. As laboratory derived SMR is predictable from thermal conditions and body mass (Clark et al., 2013), this suggests that SMR does not act in a similar manner to FMR under natural scenarios; FMR is likely controlled by multiple unmeasurable

factors (such as individual behavior or potentially food availability), and potentially it is these unknown variables account for the discrepancy between the two measurements.

Potentially the inclusion of *in situ* FMR data can aid with improving the accuracy of biogeographical and population output models, as the inconsistency between FMR and SMR trends indicate that laboratory derived SMR data may not be directly applicable to *in situ* scenarios; therefore, leading to higher error vales in predictive models than previously believed

## 5.2.2 Future Study Development

There are several directions in which you could develop this research chapter, with the aim of further understanding ecosystem functionality, improving biogeographical model estimates and identifying key time periods and areas where the community is potentially more venerable.

### 5.2.2.1 Inclusion of Multiple Species

The primary issue with applying this data to ecosystem functionality studies is that we are only measuring one species from a very specific ecological niche, when marine ecosystems are three-dimensional systems. The biological drivers which species experience are largely due to ecological interactions between multiple species of the community, such as predation pressure, prey availability, habitat competition and many more (Killen et al., 2013). The metabolic effect of ecological interactions has previously been studied from an individual variance perspective under controlled conditions, with each factor producing a significant energetic demand response. With the incorporation of multiple species metabolic interactions over the annual cycle we could potentially identify metabolic niches, which species experience higher feeding pressure, which species is likely to be more vulnerable to environmental instability and many more; which is important data for predictive model studies and policy formation.

From an academic and ecosystem functionality perspective tracking species movements with associated energetic demand will answer/compliment several studies which attempt to predict individual growth rates and stress levels in response to population dynamics; with model studies suggesting higher stress levels and increased energetic cost of maintenance with elevated population

density. The combination of FMR and locational data (from fish tagging studies) will enable studies to test such hypothesis, which again will aid in the development of improving sustainable fishing techniques, the formation of limited catch areas which aim to improve fisheries output without an increase in fishing effort.

#### 5.2.2.2 Data Coverage

A simpler improvement to this study would be a greater data coverage over monthly time scales over a singular annual cycle. The main issue with this study was that it was designed to be a time series over a yearly cycle, with the intention of gaining enough monthly coverage over each year to identify years of higher average FMR expression, as we were not expecting otolith aragonite to identify FMR trends with enough precision to identify annual cycles. After initial sample collection we were unable to collect more due to the COVID-19 pandemic. As a result, we combined months from several years to measure annual trends in metabolic deviance. Therefore, as the year of sampling spans approximately 17 years, with different fishing and otolith processing techniques this potentially is incorporating a level of unexplained variance. The addition of multiple samples spanning a wide geographical range over each month might help identify metabolic trends with more certainty.

#### 5.2.2.3 Multiple Sources of Extrinsic Variability

One of the key findings of this work is the degree of unexplained variance within the data once FMR, body mass, temperature, sex, year, month and condition are accounted for. This brings to question which extrinsic and intrinsic variables are responsible for this unexplained variance. The inclusion of more variables, such as food availability, would likely help improve model estimates and model fit, as previously discussed in chapter 2 and 4 food availability has been suggested to be a controlling factor of aerobic scope. From literature studies it is likely that variables such as prey availability and predation pressure (Killen et al., 2013), which should be possible to estimate form current trawl survey data, will aid with the FMR variability estimations.

The incorporation of more targeted sample distribution and density, more levels of species interactions and more extrinsic variables will aid with our understanding of ecosystem functionality, how close species are to their maximum energetic capacity and the level of exploitation a population can likely

sustain. It is likely that with some development this project can successfully aid with improving model fisheries output and biogeographical predictions.

## 5.3 Growth Rate and FMR

Growth rate is a diverse and directly applicable measurement to marine communities, used in multiple ecological disciplines to draw conclusions about ecosystem services, the economic value given to a population, the impact of climatic variation and anthropogenic disturbances on populations (Ciotti 2012). There have been multiple methods for measuring growth rate of fish populations, from size length relationships, scale growth and otolith somatic growth rings (Deutsch et al., 2020). However, the environmental conditions of which many previous studies have correlated to somatic growth trends have been externally measured averages, calculated over large geographical ranges which are not specific to the individual of which they are studying (Deutsch et al., 2020).

There are both positives and negatives to this approach, with total population averages being useful from a fisheries management perspective, as broad scale trends in ecosystem functionality can be paired with extrinsic variables calculated over wide geographical ranges (Maunder and Punt 2013). However, this approach is unlikely to identify individual level growth rate trends, such as behavioral responses or the interactive relationship between multiple intrinsic and extrinsic variables.

Here we combine otolith derived growth rates with experienced temperature, modelled temperature, FMR and multiple other intrinsic variables paired with mixed effects modelling techniques to explore the controlling factors on growth rate. Previous lab studies have proposed that individual growth rate variability can partially be explained by aerobic scope expression, with higher energetic availability leading to more energetic partitioning and quicker growth rates (Blier, et al., 1997). As FMR data is not directly comparable to aerobic scope it is unlikely that we will see such trends, especially as we are unable to control unknown extrinsic variables such as prey availability and predation pressure, which both potentially impact individual growth rate. What we aim to answer is if an individual who experienced higher temperatures or expresses relatively higher FMR is more prone to faster growth rates or prioritises differing intrinsic physiological characteristics.

### 5.3.1 Growth Rate FMR Relationship Findings

We used varying mixed effects modelling techniques to examine the intrinsic and extrinsic variables impacting growth rate over life history for both juveniles and adult populations separately.

For juvenile populations the variables with the strongest explanatory power are temperature, metabolism and year of spawning, however the year of spawning might be thermally dependent. Due to minimal juvenile intrinsic physiological information we are unable to include variables such as body mass, and are therefore potentially increasing the level of unexplained growth rate variance within this data set, however we are able to say there is a predictable relationship with experienced temperature. When extracting the fixed effects of the model there is a clear relationship with juveniles which experience lower temperatures expressing higher growth rates, and suppressed growth with higher thermal conditions.

This is similar to laboratory findings, where an increased temperature regime paired with a consistent energetic input results in reduced growth rates (Norin et al., 2014); therefore, potentially we are measuring supply and demand ratios in relation to energetic input, and with increased temperature the demand increases relative to the supply. This is comparable to a reduced aerobic scope, resulting in less available energy partitioning for growth when other physiological processes take priority (Clark et al., 2013).

When examining adult growth rate raw experienced temperature and model estimated temperature does not show a significant relationship with growth rate. This again suggests a significant different to juvenile populations (comparable to thermal dependency).

Adult growth rate, according to mixed effects modelling, is impacted by metabolism, condition, total individual growth throughout the life history and temperature anomaly data. Condition appears to be the only variable expressing a negative predictable relationship with growth. Higher condition values result in lower growth rates, this might represent energetic partitioning between individuals, with some favoring growth and others condition, or individuals which express a lower resting energetic demand (due to lower experienced temperature) allowing condition values to increase. The inclusion of intrinsic sources of variability within adult populations increases the model fit and variance explained within

this data set, with a higher proportion of predicted growth rate variability attributed to intrinsic sources relative to extrinsic sources. This could potentially suggest that intrinsic physiological factors control the degree of energetic partitioning diverted towards growth; and the inclusion of more intrinsic variables might improve population model growth rate predictions.

Temperature anomaly shows a predictable relationship with mass corrected increment width at time of capture (apparent form fitted linear and mixed effect models), with an increase in increment width form a temperature anomaly from -5 to 3, followed by a reduction.

This apparent optimal range for mass corrected increment width, which may suggest that individuals that selected warmer conditions promoted growth rate until a thermal maximum range followed by a reduction, is comparable to previous growth rate and metabolic studies.

Temperature anomaly expresses a predictable relationship with condition values. With higher temperature anomaly values, indicating individuals that selected warmer habitats relative to the available in the surrounding environment, resulting in lower conditional values. Here we hypothesis that temperature anomaly is a proxy for thermal habitat selection, with individuals selecting environments which suit physiological need at any given point of the feeding/spawning cycles.

### 5.3.2 Future study development

Similarly, to the other chapters the most useful addition to this study is data form multiple species from separate niches. Understanding which functional groups are impacted by different extrinsic variables, and if food availability or temperature changes the growth patterns of one group how this impacts the whole community structure is useful from a biographical and fisheries output modelling perspective.

The comparison between experienced and modelled temperature within this study shows a strong predictable relationship with growth rate, condition and FMR. This data potentially suggests that habitat selection is a strong predictor of physiology and individuals select environments that suit their physiological needs. Therefore, to improve models attempting to predict population dynamics we need to measure the diversity of the available habitats to a population and how they change over time. Potentially habitat diversity is a good predictor of which metabolic and growth phenotypes will be

more prevalent with changing climates. Exploring this relationship with different species might potentially reveal the territorial nature of separate functional groups, as benthic species are likely to be more habitat dependent. This data will likely aid with the development of ecosystem functionality models.

## 5.4 Take home message

This study aims to develop a newly emerging method used to measure field metabolic rate of marine fisheries. Here we have aimed to address simple questions, formed from literature which could benefit from the addition of field metabolic rate.

The first question centralised around if SMR, aerobic scope and MMR studies are comparable to FMR data, and if they are consistent with their relationship with environmental variables. To answer this, we looked at field metabolic rate from both adult and juvenile life stages. We find that juveniles metabolism is predictable from experienced temperature, in a comparable manner to SMR, aerobic scope and MMR findings. The same relationship is not present with adult populations, suggesting that metabolic thermal dependence is not consistent throughout life stage. We also found evidence of the presence of metabolic rate phenotypes, as individuals who express relatively high of low metabolic rates compared to the population average maintain this relationship throughout life history. This Chapter (chapter 1) highlights the importance of field metabolic rate studies, as we can begin to test how established metabolic theories of ecology are applicable to natural settings.

The second question is if metabolic expression is consistent throughout the annual cycle, and if environmental or behavioral variables can explain the highest degree of metabolic variance in the data. To answer this, we turn the data into a time series, regardless of year of capture (due to COVID restrictions we are unable to sample a complete annual cycle from a singular year), and divide the data into spawning and growing seasons. We display evidence of higher and lower levels of population metabolic rate average expression at varying times of year, with the growing/feeding season responsible for higher metabolic rate expression. This could suggest that the act of foraging requires a greater energetic input than spawning. Metabolic rate when plotted over the annual cycle shows no correlation with temperature, which also suggest that a higher level of individual metabolic expression variability is explained by behavioral cycles when compared to environmental variability.

The final data chapter (chapter 5) attempts to answer how much growth rate deviance can be explained by metabolic rate and experienced temperature. To do this we combine otolith derived field metabolic rate and otolith increment analyses to quantify the level of among-individual variation in growth rate than can attributed to intrinsic or extrinsic drivers. We also define a new variable for thermal habitat selection, termed temperature anomaly, based on the temperature experienced by the fish compared to the potential thermal habitats available (this is based on the idea that fish can select the habitats based on environmental conditions which suit their physiology).We find that among individual variation in somatic growth rate is strongly related to body condition. We find no strong relationship between growth rate and experienced temperature or expressed field Metabolic rate. However, in juvenile life stages we identify a weak negative relationship between somatic growth rate and temperature whilst in the same individuals at adult life stages, growth and temperature shows a weakly positive correlation. Among different measures of thermal experience available within this study (otolith derived, model derived and temperature anomaly) temperature anomaly had the strongest influence on growth rate, implying individuals employ behavioral thermoregulation to maximise growth potential within a given experienced habitat.

# References

Agüera, A., Ahn, I.-Y., Guillaumot, C., and Danis, B. (2017). A Dynamic Energy Budget (DEB) model to describe Laternula elliptica (King, 1832) seasonal feeding and metabolism. *PLoS One* 12, e0183848.

Aikio, S., Herczeg, G., Kuparinen, A., and Merilä, J. (2013). Optimal growth strategies under divergent predation pressure. *Journal of Fish Biology* 82, 318–331.

Albert, C. H., Thuiller, W., Yoccoz, N. G., Douzet, R., Aubert, S., and Lavorel, S. (2010). A multi-trait approach reveals the structure and the relative importance of intra-vs. interspecific variability in plant traits. *Functional Ecology* 24, 1192–1201.

Albouy, C., Guilhaumon, F., Leprieur, F., Lasram, F. B. R., Somot, S., Aznar, R., (2013). Projected climate change and the changing biogeography of coastal Mediterranean fishes. *Journal of Biogeography* 40, 534–547.

Alewijnse, S. R., Stowasser, G., Saunders, R. A., Belcher, A., Crimmen, O. A., Cooper, N., (2021). Otolith-derived field metabolic rates of myctophids (Family Myctophidae) from the Scotia Sea (Southern Ocean). *Marine Ecology Progress Series* 675, 113–131.

Al-Hossaini, M., Liu, Q., and Pitcher, T. J. (1989). Otolith microstructure indicating growth and mortality among plaice, Pleuronectes platessa L., post-larval sub-cohorts. *Journal of Fish Biology* 35, 81–90.

Allen, B. M., Brophy, D., McGrath, D., and King, P. A. (2008). Hatching times, larval duration, settlement and larval growth of plaice (*Pleuronectes platessa*) in Galway Bay determined using otolith microstructure. in *Biology and Environment: Proceedings of the Royal Irish Academy*, 127–134.

Álvarez, D., and Nicieza, A. G. (2005a). Is metabolic rate a reliable predictor of growth and survival of brown trout (Salmo trutta) in the wild? *Canadian Journal of Fisheries and Aquatic Sciences* 62, 643–649.

Amara, Laffargue, P., Dewarumez, J. M., Maryniak, C., Lagardère, F., and Luzac, C. (2001). Feeding ecology and growth of O-group flatfish (sole, dab and plaice) on a nursery ground (Southern Bight of the North Sea). *Journal of Fish Biology* 58, 788–803.

Andersen, K. H., and Beyer, J. E. (2006). Asymptotic size determines species abundance in the marine size spectrum. *The American Naturalist* 168, 54–61.

Angilletta Jr, M. J., (2009). Thermal adaptation: a theoretical and empirical synthesis.

Arendt, J. D. (1997). Adaptive intrinsic growth rates: an integration across taxa. *Q Rev Biol* 72, 149–177.

Armstrong, M. J., and Witthames, P. R. (2012). Developments in understanding of fecundity of fish stocks in relation to egg production methods for estimating spawning stock biomass. *Fisheries Research* 117, 35–47.

Arnold, G. P., and Cook, P. H. (1984). "Fish migration by selective tidal stream transport: first results with a computer simulation model for the European continental shelf," in *Mechanisms of migration in fishes* 14, 227–261.

Attrill, M. J., and Power, M. (2002). Climatic influence on a marine fish assemblage. *Nature* 417, 275–278.

Auer, S. K., Salin, K., Rudolf, A. M., Anderson, G. J., and Metcalfe, N. B. (2015). The optimal combination of standard metabolic rate and aerobic scope for somatic growth depends on food availability. *Functional Ecology* 29, 479–486.

Bach, C., and Hazlett, B. (2010). Individuality in the predator defense behaviour of the crab Heterozius rotundifrons. *Behaviour* 147, 587–597.

Baird, D. J., Brown, S. S., Lagadic, L., Liess, M., Maltby, L., Moreira-Santos, M., (2007). In situ-based effects measures: Determining the ecological relevance of measured responses. *Integrated Environmental Assessment and Management: An International Journal* 3, 259–267.

Bates, Mächler, M., Bolker, B., and Walker, S. (2015). Fitting Linear Mixed-Effects Models Using lme4. *The Journal of Statistical Software* 67, 1–48. doi: 10.18637/jss.v067.i01.

Bates, A. E., Barrett, N. S., Stuart-Smith, R. D., Holbrook, N. J., Thompson, P. A. and Edgar, G. J., (2014). Resilience and signatures of tropicalization in protected reef fish communities. *Nature Climate Change* 4, 62–67.

Baudron, A. R., Needle, C. L., Rijnsdorp, A. D., and Marshall, T. C., (2014). Warming temperatures and smaller body sizes: synchronous changes in growth of North Sea fishes. *Global Change Biology* 20, 1023–1031.

Beauregard, D., Enders, E., and Boisclair, D. (2013). Consequences of circadian fluctuations in water temperature on the standard metabolic rate of Atlantic salmon parr (Salmo salar). *Canadian Journal of Fisheries and Aquatic Sciences* 70, 1072–1081.

Bernhardt, and Leslie (2013). Resilience to climate change in coastal marine ecosystems. *Annual Review of Marine Science* 5, 371–392.

Bervoets, L., and Blust, R. (2003). Metal concentrations in water, sediment and gudgeon (Gobio gobio) from a pollution gradient: relationship with fish condition factor. *Environmental Pollution* 126, 9–19.

Binning, S. A., Ros, A. F. H., Nusbaumer, D., and Roche, D. G. (2015). Physiological plasticity to water flow habitat in the damselfish, Acanthochromis polyacanthus: linking phenotype to performance. *PLoS One* 10, e0121983.

Biro, P. A., Beckmann, C., and Stamps, J. A. (2010). Small within-day increases in temperature affects boldness and alters personality in coral reef fish. *Proceedings of the Royal Society B: Biological Sciences* 277, 71–77.

Björndal, T., Lane, D. E., and Weintraub, A. (2004a). Operational research models and the management of fisheries and aquaculture: A review. *European Journal of Operational Research* 156, 533–540.

Björndal, T., Lane, D. E., and Weintraub, A. (2004b). Operational research models and the management of fisheries and aquaculture: a review. *European Journal of Operational Research* 156, 533–540.

Black, Andersson, C., Butler, P. G., Carroll, M. L., DeLong, K. L., Reynolds, D. J., (2019). The revolution of crossdating in marine palaeoecology and palaeoclimatology. *Biological Letters*15, 20180665.

Black, von Biela, V. R., Zimmerman, C. E., and Brown, R. J. (2013). Lake trout otolith chronologies as multidecadal indicators of high-latitude freshwater ecosystems. *Polar Biology* 36, 147–153.

Blier, P. U., Pelletier, D., and Dutil, J. (1997). Does aerobic capacity set a limit on fish growth rate? *Reviews in Fisheries Science* 5, 323–340.

Bœuf, G., and Payan, P. (2001). How should salinity influence fish growth? *Comparative Biochemistry and Physiology Part C: Toxicology & Pharmacology* 130, 411–423.

Bokma, F. (2004). Evidence against universal metabolic allometry. *Functional Ecology* 18, 184–187.

Bolger, T., and Connolly, P. L. (1989). The selection of suitable indices for the measurement and analysis of fish condition. *Journal of Fish Biology* 34, 171–182.

Bolnick, D. I., Amarasekare, P., Araújo, M. S., Bürger, R., Levine, J. M., Novak, M., (2011). Why intraspecific trait variation matters in community ecology. *Trends in Ecological Evolution* 26, 183–192.

Brander (2010). Impacts of climate change on fisheries. *Journal of Marine Systems* 79, 389–402.

Brander, K. M. (1995). The effect of temperature on growth of Atlantic cod (*Gadus morhua*). *ICES Journal of Marine Science* 52, 1–10.

Brander, K. M. (2007). Global fish production and climate change. *Proceedings of the National Academy of Sciences* 104, 19709–19714.

Brandt, S. B., Mason, D. M., and Patrick, E. V. (1992). Spatially-explicit models of fish growth rate. *Fisheries (Bethesda)* 17, 23–35.

Breck, J. E. (1993). Foraging theory and piscivorous fish: are forage fish just big zooplankton? *Transactions of the American Fisheries Society* 122, 902–911.

Brett, J. R. (1971). Energetic responses of salmon to temperature. A study of some thermal relations in the physiology and freshwater ecology of sockeye salmon (Oncorhynchus nerkd). *American zoologist* 11, 99–113.

Brody, S., and Lardy, H. A. (1946). Bioenergetics and growth. *The Journal of Physical Chemistry A* 50, 168–169.

Brown, C., Gardner, C., and Braithwaite, V. A. (2005). Differential stress responses in fish from areas of high-and low-predation pressure. *Journal of Comparative Physiology B* 175, 305–312.

Brown, C. J., Fulton, E. A., Possingham, H. P., and Richardson, A. J. (2012). How long can fisheries management delay action in response to ecosystem and climate change? *Ecological Applications* 22, 298–310.

Brown, J. H., Allen, A. P., and Gillooly, J. F. (2007). The metabolic theory of ecology and the role of body size in marine and freshwater ecosystems. *Body Size: The Structure and Function of Aquatic Ecosystems*, 1–15.

Brugère, C., and Young, C. De (2015). Assessing climate change vulnerability in fisheries and aquaculture: available methodologies and their relevance for the sector. *FAO Fisheries and Aquaculture Technical Paper*, (597)

Bruno, J. F., Carr, L. A., and O'Connor, M. I. (2015). Exploring the role of temperature in the ocean through metabolic scaling. *Ecology* 96, 3126–3140.

Buckley, and Arnold, G. (2001). Orientation and swimming speed of plaice migrating by selective tidal stream transport: Preliminary Results from Acoustic Tracking and ADCP Measurments. *Electronic Tagging and Tracking in Marine Fisheries with Electronic Devices* 20, 263–277.

Buckley, Y. M., Ramula, S., Blomberg, S. P., Burns, J. H., Crone, E. E., Ehrlén, J., (2010). Causes and consequences of variation in plant population growth rate: a synthesis of matrix population models in a phylogenetic context. *Ecological Letters* 13, 1182–1197.

Burnham, K. P., and Anderson, D. R. (2004). Multimodel inference: understanding AIC and BIC in model selection. *Sociological Methods and Research* 33, 261–304.

Burrows, M. T., Schoeman, D. S., Buckley, L. B., Moore, P., Poloczanska, E. S., Brander, K. M., (2011). The pace of shifting climate in marine and terrestrial ecosystems. *Science* 334, 652–655.

Burt, W. J., Thomas, H., Hagens, M., Pätsch, J., Clargo, N. M., Salt, L. A., (2016). Carbon sources in the North Sea evaluated by means of radium and stable carbon isotope tracers. *Limnology and Oceanography* 61, 666–683.

Carbonara, P., and Follesa, M. C. (2019). Handbook on fish age determination: a Mediterranean experience. *General Fisheries Commission for the Mediterranean. Studies and Reviews*, I–179.

Cavender-Bares, J., Kozak, K. H., Fine, P. V. A., and Kembel, S. W. (2009). The merging of community ecology and phylogenetic biology. *Ecological Letters* 12, 693–715.

Chabot, D., Steffensen, J. F., and Farrell, A. P. (2016). The determination of standard metabolic rate in fishes. *Journal of Fish Biology* 88, 81–121.

Chapelle, G., and Peck, L. S. (1999). Polar gigantism dictated by oxygen availability. *Nature* 399, 114–115.

Cheung, W. W. L., Close, C., Lam, V., Watson, R., and Pauly, D. (2008). Application of macroecological theory to predict effects of climate change on global fisheries potential. *Marine Ecology Progress Series* 365, 187–197.

Cheung, W. W. L., Lam, V. W. Y., Sarmiento, J. L., Kearney, K., Watson, R. E. G., Zeller, D., (2010). Large-scale redistribution of maximum fisheries catch potential in the global ocean under climate change. *Global Change Biology* 16, 24–35.

Chown, S. L., and Gaston, K. J. (1999). Exploring links between physiology and ecology at macro-scales: the role of respiratory metabolism in insects. *Biological Reviews* 74, 87–120.

Christensen, R. H. B. (2019). ordinal—Regression Models for Ordinal Data. *R package version* 10, p.54

Chung, Jørgensen, K. M., Trueman, C. N., Knutsen, H., Jorde, P. E., and Grønkjær, P. (2021). First measurements of field metabolic rate in wild juvenile fishes show strong thermal sensitivity but variations between sympatric ecotypes. *Oikos* 130, 287–299.

Chung, Trueman, C. N., Godiksen, J. A., and Grønkjær, P. (2019a). Otolith δ13C values as a metabolic proxy: approaches and mechanical underpinnings. *Marine and Freshwater Research* 70, 1747–1756.

Chung, Trueman, C. N., Godiksen, J. A., and Grønkjær, P. (2020). Otolith δ13C values as a metabolic proxy: approaches and mechanical underpinnings. *Marine and Freshwater Research* 70, 1747–1756.

Chung, Trueman, C. N., Godiksen, J. A., Holmstrup, M. E., and Grønkjær, P. (2019b). Field metabolic rates of teleost fishes are recorded in otolith carbonate. *Communications Biology* 2, 1–10.

Ciotti, B. J. (2012). *Patterns and causes of spatial and temporal variation in growth rates of early juvenile European plaice Pleuronectes platessa*. University of Delaware.

Ciotti, B. J., Targett, T. E., Nash, Batty, R. S., Burrows, M. T., and Geffen, A. J. (2010). Development, validation and field application of an RNA-based growth index in juvenile plaice Pleuronectes platessa. *Journal of Fish Biology* 77, 2181–2209.

Ciotti, B. J., Targett, T. E., Nash, and Geffen, A. J. (2014). Growth dynamics of European plaice Pleuronectes platessa L. in nursery areas: a review. *Journal of Sea Research* 90, 64–82.

Ciotti, B. J., Targett, T. E., and Burrows, M. T. (2013). Spatial variation in growth rate of early juvenile European plaice Pleuronectes platessa. *Marine Ecology Progress Series* 475, 213–232.

Clark, R. A., Fox, C. J., Viner, D., and Livermore, M. (2003). North Sea cod and climate change–modelling the effects of temperature on population dynamics. *Global Change Biology* 9, 1669–1680.

Clark, Sandblom, and Jutfelt (2013). Aerobic scope measurements of fishes in an era of climate change: respirometry, relevance and recommendations. *Journal of Experimental Biology* 216, 2771–2782.

Clarke, A. (2006). Temperature and the metabolic theory of ecology. *Functional Ecology* 20, 405–412.

Clarke, A., and Johnston, N. M. (1999). Scaling of metabolic rate with body mass and temperature in teleost fish. *Journal of Animal Ecology* 68, 893–905.

Collie, J. S., Botsford, L. W., Hastings, A., Kaplan, I. C., Largier, J. L., Livingston, P. A., (2016). Ecosystem models for fisheries management: finding the sweet spot. *Fish and Fisheries* 17, 101–125.

Comte, L., and Grenouillet, G. (2013). Do stream fish track climate change? Assessing distribution shifts in recent decades. *Ecography* 36, 1236–1246.

Conover, D. O., and Present, T. (1990). Countergradient variation in growth rate: compensation for length of the growing season among Atlantic silversides from different latitudes. *Oecologia* 83, 316–324.

Cook, D. G., Wells, R. M. G., and Herbert, N. A. (2011). Anaemia adjusts the aerobic physiology of snapper (Pagrus auratus) and modulates hypoxia avoidance behaviour during oxygen choice presentations. *Journal of Experimental Biology* 214, 2927–2934.

Craig, J. K., and Crowder, L. B. (2005). Hypoxia-induced habitat shifts and energetic consequences in Atlantic croaker and brown shrimp on the Gulf of Mexico shelf. *Marine Ecology Progress Series* 294, 79–94.

Creutzberg, Eltink, A. T. G. W., and Van Noort, G. J. (1978). "The migration of plaice larvae Pleuronectes platessa into the western Wadden Sea," in *Physiology and Behaviour of Marine Organisms* 12, 243–251.

Criscuolo, F., Monaghan, P., Nasir, L., and Metcalfe, N. B. (2008). Early nutrition and phenotypic development:'catch-up'growth leads to elevated metabolic rate in adulthood. *Proceedings of the Royal Society B: Biological Sciences* 275, 1565–1570.

Crowder, L. B., McDonald, M. E., and Rice, J. A. (1987). Understanding Recruitment of Lake Michigan Fishes: The Importance of Size-Based Interactions Between Fish and Zoopiankton. *Canadian Journal of Fisheries and Aquatic Sciences* 44, s141–s147.

Crozier, L. G., and Hutchings, J. A. (2014). Plastic and evolutionary responses to climate change in fish. *Evolutionary Applications* 7, 68–87.

Cruz-Font, L., Shuter, B. J., Blanchfield, P. J., Minns, C. K., and Rennie, M. D. (2019a). Life at the top: Lake ecotype influences the foraging pattern, metabolic costs and life history of an apex fish predator. *Journal of Animal Ecology* 88, 702–716.

Cruz-Font, L., Shuter, B. J., Blanchfield, P. J., Minns, C. K., and Rennie, M. D. (2019b). Life at the top: Lake ecotype influences the foraging pattern, metabolic costs and life history of an apex fish predator. *Journal of Animal Ecology* 88, 702–716.

Cruz-Neto, A. P., and Bozinovic, F. (2004). The relationship between diet quality and basal metabolic rate in endotherms: insights from intraspecific analysis. *Physiological and Biochemical Zoology* 77, 877–889.

Cui, Y., and Wootton, R. J. (1988). Effects of ration, temperature and body size on the body composition, energy content and condition of the minnow, *Phoxinus phoxinus*. *Journal of Fish Biology* 32, 749–764.

Cury, P. M., Fromentin, J.-M., Figuet, S., and Bonhommeau, S. (2014). Resolving Hjort's dilemma: how is recruitment related to spawning stock biomass in marine fish? *Oceanography* 27, 42–47.

Cutts, and Metcalfe, T. (1998). Aggression and growth depression in juvenile Atlantic salmon: the consequences of individual variation in standard metabolic rate. *Journal of Fish Biology* 52, 1026–1037.

Cutts, Metcalfe, and Taylor (1998). Aggression and growth depression in juvenile Atlantic salmon: the consequences of individual variation in standard metabolic rate. *Journal of Fish Biology* 52, 1026–1037.

Daan (1973). A quantitative analysis of the food intake of North Sea cod, Gadus morhua. *Netherlands Journal of Sea Research* 6, 479–517.

Daan, N., Bromley, P. J., Hislop, J. R. G., and Nielsen, N. A. (1990). Ecology of North Sea fish. *Netherlands Journal of Sea Research* 26, 343–386.

Dahlke, F. T., Wohlrab, S., Butzin, M., and Pörtner, H.-O. (2020). Thermal bottlenecks in the life cycle define climate vulnerability of fish. *Science* 369, 65–70.

Darnaude, A. M., Sturrock, A., Trueman, C. N., Mouillot, D., Campana, S. E., and Hunter, E. (2014). Listening in on the past: what can otolith δ18O values really tell us about the environmental history of fishes? *PLoS One* 9, 108539.

Darveau, C.-A., Suarez, R. K., Andrews, R. D., and Hochachka, P. W. (2002). Allometric cascade as a unifying principle of body mass effects on metabolism. *Nature* 417, 166–170.

Daskalov, G. M., Grishin, A. N., Rodionov, S., and Mihneva, V. (2007). Trophic cascades triggered by overfishing reveal possible mechanisms of ecosystem regime shifts. *Proceedings of the National Academy of Sciences* 104, 10518–10523.

Davey, A. J. H., Turner, G. F., Hawkins, S. J., and Doncaster, C. P. (2006). Mechanisms of density dependence in stream fish: exploitation competition for food reduces growth of adult European bullheads (Cottus gobio). *Canadian Journal of Fisheries and Aquatic Sciences* 63, 597–606.

De Verdal, H., Komen, H., Quillet, E., Chatain, B., Allal, F., Benzie, J. A. H., (2018). Improving feed efficiency in fish using selective breeding: a review. *Reviews in Fisheries Science and Aquaculture* 10, 833–851.

Degens, E. T., Deuser, W. G., and Haedrich, R. L. (1969). Molecular structure and composition of fish otoliths. *Marine Biology* 2, 105–113.

Del Raye, G., and Weng, K. C. (2015). An aerobic scope-based habitat suitability index for predicting the effects of multi-dimensional climate change stressors on marine teleosts. *Deep Sea Research Part II: Topical Studies in Oceanography* 113, 280–290.

Denechaud, C., Smoliński, S., Geffen, A. J., Godiksen, J. A., and Campana, S. E. (2020). A century of fish growth in relation to climate change, population dynamics and exploitation. *Global Change Biology* 26, 5661–5678.

Der Veer, V., and Witte, J. I., (1993). The ‘maximum growth/optimal food condition’hypothesis: a test for 0-group plaice Pleuronectes platessa in the Dutch Wadden Sea. *Marine Ecology Progress Series* 101, 81–90.

Deslauriers, D., Chipps, S. R., Breck, J. E., Rice, J. A., and Madenjian, C. P. (2017). Fish bioenergetics 4.0: an R-based modeling application. *Fisheries (Bethesda)* 42, 586–596.

Deutsch, C., Ferrel, A., Seibel, B., Pörtner, H.-O., and Huey, R. B. (2015a). Climate change tightens a metabolic constraint on marine habitats. *Science* 348, 1132–1135.

Deutsch, C., Ferrel, A., Seibel, B., Pörtner, H.-O., and Huey, R. B. (2015b). Climate change tightens a metabolic constraint on marine habitats. *Science (1979)* 348, 1132–1135.

Deutsch, C., Penn, J. L., and Seibel, B. (2020). Metabolic trait diversity shapes marine biogeography. *Nature* 585, 557–562.

Devlin, R. H., Leggatt, R. A., and Benfey, T. J. (2020). "Genetic modification of growth in fish species used in aquaculture: phenotypic and physiological responses," in *Fish Physiology* 38, 237–272.

Dingemanse, N. J., and Dochtermann, N. A. (2013). Quantifying individual variation in behaviour: mixed-effect modelling approaches. *Journal of Animal Ecology* 82, 39–54.

Donelson, J. M., Munday, P. L., McCormick, M. I., Pankhurst, N. W., and Pankhurst, P. M. (2010). Effects of elevated water temperature and food availability on the reproductive performance of a coral reef fish. *Marine Ecology Progress Series* 401, 233–243.

Donelson, J. M., Munday, P. L., McCormick, M. I., and Pitcher, C. R. (2012). Rapid transgenerational acclimation of a tropical reef fish to climate change. *Nature Climate Change* 2, 30–32.

Dorenbosch, M., Grol, M. G. G., de Groene, A., van der Velde, G., and Nagelkerken, I. (2009). Piscivore assemblages and predation pressure affect relative safety of some back-reef habitats for juvenile fish in a Caribbean bay. *Marine Ecology Progress Series* 379, 181–196.

Doubleday, Z. A., Izzo, C., Haddy, J. A., Lyle, J. M., Ye, Q., and Gillanders, B. M. (2015). Long-term patterns in estuarine fish growth across two climatically divergent regions. *Oecologia* 179, 1079–1090.

Dulvy, N. K., Rogers, S. I., Jennings, S., Stelzenmüller, V., Dye, S. R., and Skjoldal, H. R. (2008). Climate change and deepening of the North Sea fish assemblage: a biotic indicator of warming seas. *Journal of Applied Ecology* 45, 1029–1039.

Dumas, A., France, J., and Bureau, D. (2010). Modelling growth and body composition in fish nutrition: where have we been and where are we going? *Aquactic Resources* 41, 161–181.

Duncan, I.M., Bates, A. E., James, N. C., and Potts, W. M. (2019). Exploitation may influence the climate resilience of fish populations through removing high performance metabolic phenotypes. *Scientific Reports* 9(1), 11437.

Duncan, R.P., Forsyth, D. M., and Hone, J. (2007). Testing the metabolic theory of ecology: allometric scaling exponents in mammals. *Ecology* 88(2), 324–333.

Dupont-Prinet, A., Chatain, B., Grima, L., Vandeputte, M., Claireaux, G., and McKenzie, D. J. (2010). Physiological mechanisms underlying a trade-off between growth rate and tolerance of feed deprivation in the European sea bass (Dicentrarchus labrax). *Journal of Experimental Biology* 213, 1143–1152.

Dutil, J.-D., Lambert, Y., and Boucher, E. (1997). Does higher growth rate in Atlantic cod (Gadus morhua) at low salinity result from lower standard metabolic rate or increased protein digestibility? *Canadian Journal of Fisheries and Aquatic Sciences* 54, 99–103.

Edwards, Blaxter, J. H. S., Gopalan, U. K., and Mathew, C. V (1970). A comparison of standard oxygen consumption of temperate and tropical bottom-living marine fish. *Comparative Biochemistry and Physiology* 34, 491–495.

Edwards, S. F. (1990). An economics guide to allocation of fish stocks between commercial and recreational fisheries.

Edwards, and Steele, J. H. (1968). The ecology of 0-group plaice and common dabs at Loch Ewe I. Population and food. *Journal of Experimental Marine Biology and Ecology* 2, 215–238.

Ejbye-Ernst, R., Michaelsen, T. Y., Tirsgaard, B., Wilson, J. M., Jensen, L. F., Steffensen, J. F., Pertoldi, C., Aarestrup, K. and Svendsen, J.C., (2016). Partitioning the metabolic scope: the importance of anaerobic metabolism and implications for the oxygen-and capacity-limited thermal tolerance (OCLTT) hypothesis. *Conservation Physiology,* 4(1), P.cow019.

Ellis, T., and Gibson, R. N. (1995). Size-selective predation of 0-group flatfishes on a Scottish coastal nursery ground. *Marine Ecology Progress Series* 127, 27–37.

Ern, R. (2019). A mechanistic oxygen-and temperature-limited metabolic niche framework. *Philosophical Transactions of the Royal Society B* 374, 20180540.

Essington, T. E., Kitchell, J. F., and Walters, C. J. (2001). The von Bertalanffy growth function, bioenergetics, and the consumption rates of fish. *Canadian Journal of Fisheries and Aquatic Sciences* 58, 2129–2138.

Evans, S., (1983). Production, predation and food niche segregation in a marine shallow soft-bottom community. *Marine Ecology Progress Series. Oldendorf* 10(2), 147–157.

Fablet, R., Pecquerie, L., Hoie, H., Jolivet, A., Millner, R., Mosegaard, H., (2009). Can we model otolith growth and opacity patterns as a response to environmental factors and fish metabolism? A DEB-based framework. (Doctoral Dissertation, University of California)

Farrell, A., (2013). Aerobic scope and its optimum temperature: clarifying their usefulness and limitations–correspondence on J. Exp. Biol. 216, 2771-2782. *Journal of Experimental Biology* 216, 4493–4494.

Farrell, A. (1997). Effects of temperature on cardiovascular performance. In Seminar Series-Society for Experimental Biology (Vol. 61, pp.135–158). Cambridge University Press.

Farrell, A. (2016). Pragmatic perspective on aerobic scope: peaking, plummeting, pejus and apportioning. *Journal of Fish Biology* 88, 322–343.

Farrell, E. J., Sandblom, E., and Clark, T. D. (2009). Fish cardiorespiratory physiology in an era of climate change. *The Canadian Journal of Zoology* 87, 835–851.

Farrell, S. G., Cooke, S. J., Patterson, D. A., Crossin, G. T., Lapointe, M., (2008). Pacific salmon in hot water: applying aerobic scope models and biotelemetry to predict the success of spawning migrations. *Physiological and Biochemical Zoology* 81, 697–708.

Field, C. B., and Barros, V. R. (2014). *Climate change 2014–Impacts, Adaptation and Vulnerability: Regional Aspects*. Cambridge University Press.

Fogarty, M. P., and Cohen, E. B. (1991). Recruitment variability and the dynamics of exploited marine populations. *Trends in Ecological Evolution* 6, 241–246.

Fonds, M., Cronie, R., Vethaak, A. D., and der Puyl, P. Van (1992). Metabolism, food consumption and growth of plaice (Pleuronectes platessa) and flounder (Platichthys flesus) in relation to fish size and temperature. *Netherlands Journal of Sea Research* 29, 127–143.

Forster, J., Hirst, A. G., and Atkinson, D. (2012). Warming-induced reductions in body size are greater in aquatic than terrestrial species. *Proceedings of the National Academy of Sciences* 109, 19310–19314.

Frank, K. T., Petrie, B., Choi, J. S., and Leggett, W. C. (2005). Trophic cascades in a formerly cod-dominated ecosystem. *Science* 308, 1621–1623.

Freitas, V., Cardoso, J. F. M. F., Lika, K., Peck, M. A., Campos, J., Kooijman, S. A. L. M., (2010). Temperature tolerance and energetics: a dynamic energy budget-based comparison of North Atlantic marine species. *Philosophical Transactions of the Royal Society B: Biological Sciences* 365, 3553–3565.

Froese, R., and Pauly, D. (2000). *FishBase 2000: Concepts Designs and Data Sources*. WorldFish.

Froese, R., Gascuel, D., Sumaila, U. R., and Pauly, D. (2016). Minimizing the impact of fishing. *Fish and fisheries* 17(3), 785–802.

Galland, G. R. (2017). Fishing responsibly and sustainably. *Science (1979)* 357, 558.

Gamito, S. (1998). Growth models and their use in ecological modelling: an application to a fish population. *Ecological Modell*ing. 113, 83–94.

Gandar, A., Laffaille, P., Marty-Gasset, N., Viala, D., Molette, C., and Jean, S. (2017). Proteome response of fish under multiple stress exposure: effects of pesticide mixtures and temperature increase. *Aquatic Toxicology* 184, 61–77.

Gauldie, R. W., (1996). Biological factors controlling the carbon isotope record in fish otoliths: principles and evidence. *Comparative Biochemistry and Physiology B.* 115, 201–208.

Gedamke, T., Hoenig, J. M., Musick, J. A., DuPaul, W. D., and Gruber, S. H. (2007). Using demographic models to determine intrinsic rate of increase and sustainable fishing for elasmobranchs: pitfalls, advances, and applications. *North American Journal of Fisheries Managment* 27, 605–618.

Geffen, A. J. (2012). Otolith oxygen and carbon stable isotopes in wild and laboratory-reared plaice (Pleuronectes platessa). *Environmental Biology of Fishes* 95, 419–430.

Gibson, R.N., (1980). A quantitative description of the behaviour of wild juvenile plaice (*Pleuronectes platessa*). *Animal Behaviour* 28, 1202–1216.

Gibson, R. N., Robb, L., Wennhage, H., and Burrows, M. T. (2002). Ontogenetic changes in depth distribution of juvenile flatfishes in relation to predation risk and temperature on a shallow-water nursery ground. *Marine Ecology Progress Series* 229, 233–244.

Gienapp, P., Teplitsky, C., Alho, J. S., Mills, J. A., and Merilä, J. (2008). Climate change and evolution: disentangling environmental and genetic responses. *Molecular Ecology.* 17, 167–178.

Gillooly, J. H., West, S., and Charnov, M., (2001). Effects of size and temperature on metabolic rate. *Science (1979)* 293, 2248–2251.

Gingerich, A. J., Philipp, D. P., and Suski, C. D. (2010). Effects of nutritional status on metabolic rate, exercise and recovery in a freshwater fish. *Journal of Comparative Physiology B* 180, 371–384.

Glazier, D. S. (2005). Beyond the '3/4-power law': variation in the intra-and interspecific scaling of metabolic rate in animals. *Biological reviews* 80, 611–662.

Glazier, D. S. (2010). A unifying explanation for diverse metabolic scaling in animals and plants. *Biological Reviews* 85, 111–138.

Glazier, D. S. (2014). Metabolic scaling in complex living systems. *Systems* 2, 451–540.

Goldspink, C. R. (1979). The population density, growth rate and production of roach *Rutilus mtilus* in Tjeukemeer, The Netherlands. *Journal of Fish Biology* 15, 473–498.

Gräns, A., Jutfelt, F., Sandblom, E., Jönsson, E., Wiklander, K., Seth, H.,(2014). Aerobic scope fails to explain the detrimental effects on growth resulting from warming and elevated CO2 in Atlantic halibut. *Journal of Experimental Biology* 217, 711–717.

Grønkjær, P., Pedersen, J. B., Ankjærø, T. T., Kjeldsen, H., Heinemeier, J., Steingrund, P., (2013). Stable N and C isotopes in the organic matrix of fish otoliths: validation of a new approach for studying spatial and temporal changes in the trophic structure of aquatic ecosystems. *Canadian Journal of Fisheries and Aquatic Sciences* 70, 143–146.

Guderley, H., and Pörtner, H. O. (2010). Metabolic power budgeting and adaptive strategies in zoology: examples from scallops and fish. *The Canadian Journal of Zoology* 88, 753–763.

Harrison, J. F. (2017). Do performance–safety tradeoffs cause hypometric metabolic scaling in animals? *Trends in Ecological Evolution* 32, 653–664.

Hatton, I. A., Dobson, A. P., Storch, D., Galbraith, E. D., and Loreau, M. (2019). Linking scaling laws across eukaryotes. *Proceedings of the National Academy of Sciences* 116, 21616–21622.

Hazel, J. R. (1984). Effects of temperature on the structure and metabolism of cell membranes in fish. *American Journal of Physiology-Regulatory, Integrative and Comparative Physiology* 246, R460–R470.

Healy, T. M., and Schulte, P. M. (2012). Thermal acclimation is not necessary to maintain a wide thermal breadth of aerobic scope in the common killifish (Fundulus heteroclitus). *Physiological and Biochemical Zoology* 85, 107–119.

Heather, F. J., Childs, D. Z., Darnaude, A. M., and Blanchard, J. L. (2018). Using an integral projection model to assess the effect of temperature on the growth of gilthead seabream Sparus aurata. *PLoS One* 13, e0196092.

Hefford, A. E., (1916). *Report on sexual differentiation in the biology and distribution of plaice in the North Sea*. HM Stationery Office.

Heino, M., and Godø, O. R. (2002). Fisheries-induced selection pressures in the context of sustainable fisheries. *Bulletin of Marine Science* 70, 639–656.

Hessenauer, J.M., Vokoun, J. C., Suski, C. D., Davis, J., Jacobs, R., and O'Donnell, E. (2015). Differences in the metabolic rates of exploited and unexploited fish populations: a signature of recreational fisheries induced evolution? *PLoS One* 10, e0128336.

Hiddink, J. G., Burrows, M. T., and Garcia M, J. (2015). Temperature tracking by North Sea benthic invertebrates in response to climate change. *Global Change Biology* 21, 117–129.

Hiddink, J. G., Rijnsdorp, A. D., and Piet, G. (2008). Can bottom trawling disturbance increase food production for a commercial fish species? *Canadian Journal of Fisheries and Aquatic Sciences* 65, 1393–1401.

Hirst, A. G., Glazier, D. S., and Atkinson, D. (2014). Body shape shifting during growth permits tests that distinguish between competing geometric theories of metabolic scaling. *Ecological Letters* 17, 1274–1281.

Hofmann, G. E., and Todgham, A. E. (2010). Living in the now: physiological mechanisms to tolerate a rapidly changing environment. *Annual Review of Physiology* 72, 127–145.

Holt, R. E., and Jørgensen, C. (2015). Climate change in fish: effects of respiratory constraints on optimal life history and behaviour. *Biological Letters* 11, 20141032.

Hopkins, K. D. (1992). Reporting fish growth: A review of the basics 1. *Journal of World Aquatic Society* 23, 173–179.

Houde, E. D., and Zastrow, C. E. (1993). Ecosystem-and taxon-specific dynamic and energetics properties of larval fish assemblages. *Bulletin of Marine Science* 53, 290–335.

Hovenkamp, F. (1989). Within-season variation in growth of larval plaice (*Pleuronectes platessa*). *Rapp. P.-v. Réun. Cons. int. Explor. Mer* 191, 248–257.

Hovenkamp, F. (1992). Growth-dependent mortality of larval plaice Pleuronectes platessa in the North Sea. *Marine Ecology Progress Series.* 82, 95–101.

Huang, M., Ding, L., Wang, J., Ding, C., and Tao, J. (2021). The impacts of climate change on fish growth: A summary of conducted studies and current knowledge. *Ecological Indicators* 121, 106976.

Hulshof, C. M., Violle, C., Spasojevic, M. J., McGill, B., Damschen, E., Harrison, S., (2013). Intra-specific and inter-specific variation in specific leaf area reveal the importance of abiotic and biotic drivers of species diversity across elevation and latitude. *Journal of Vegetation Science* 24, 921–931.

Humston, R., Olson, D. B., and Ault, J. S. (2004). Behavioral assumptions in models of fish movement and their influence on population dynamics. *Transactions of the American Fisheries Society* 133, 1304–1328.

Hunter, E., Cotton, R. J., Metcalfe, J. D., and Reynolds, J. D. (2009). Large-scale variation in seasonal swimming patterns of plaice in the North Sea. *Marine Ecology Progress Series* 392, 167–178.

Hunter, E., Metcalfe, J. D., Arnold, G. P., and Reynolds, J. D. (2004). Impacts of migratory behaviour on population structure in North Sea plaice. *Journal of Animal Ecology* 73, 377–385.

Hunter, E., Metcalfe, J. D., and Reynolds, J. D. (2003). Migration route and spawning area fidelity by North Sea plaice. *Proceedings of the Royal Society of London Series B: Biological Sciences* 270, 2097–2103.

Huss, M., Byström, P., and Persson, L. (2008). Resource heterogeneity, diet shifts and intra-cohort competition: effects on size divergence in YOY fish. *Oecologia* 158, 249–257.

Huss, M., Lindmark, M., Jacobson, P., van Dorst, R. M., and Gårdmark, A. (2019). Experimental evidence of gradual size-dependent shifts in body size and growth of fish in response to warming. *Global Change Biology* 25, 2285–2295.

Hutchings, J. A. (2000). Collapse and recovery of marine fishes. *Nature* 406, 882–885.

Hutchinson, W. F., Van Oosterhout, C., Rogers, S. I., and Carvalho, G. R. (2003). Temporal analysis of archived samples indicates marked genetic changes in declining North Sea cod (Gadus morhua). *Proceedings of the Royal Society of London. Series B: Biological Sciences* 270, 2125–2132.

Ivandic, V., Thomas, W. T. B., Nevo, E., Zhang, Z., and Forster, B. P. (2003). Associations of simple sequence repeats with quantitative trait variation including biotic and abiotic stress tolerance in Hordeum spontaneum. *Plant breeding* 122, 300–304.

Jackson, J. B. C., Kirby, M. X., Berger, W. H., Bjorndal, K. A., Botsford, L. W., Bourque, B. J.,(2001). Historical overfishing and the recent collapse of coastal ecosystems. *Science (1979)* 293, 629–637.

Jager, T., and Zimmer, E. I. (2012). Simplified dynamic energy budget model for analysing ecotoxicity data. *Ecological Modelling* 225, 74–81.

Jakoby, O., Grimm, V., and Frank, K. (2014). Pattern-oriented parameterization of general models for ecological application: towards realistic evaluations of management approaches. *Ecological Modelling* 275, 78–88.

Jennings, S., and Cogan, S. M. (2015). Nitrogen and carbon stable isotope variation in northeast Atlantic fishes and squids: Ecological Archives E096-226. *Ecology* 96, 2568.

Jerde, C. L., Kraskura, K., Eliason, E. J., Csik, S. R., Stier, A. C., and Taper, M. L. (2019). Strong evidence for an intraspecific metabolic scaling coefficient near 0.89 in fish. *Frontiers in Physiology*, 1166.

Jobling, M., (1980). Effects of starvation on proximate chemical composition and energy utilization of plaice, Pleuronectes platessa L. *Journal of Fish Biology*17, 325–334.

Jobling, M., (1981). The influences of feeding on the metabolic rate of fishes: a short review. *Journal of Fish Biology* 18, 385–400.

Jobling, M., (1982). A study of some factors affecting rates of oxygen consumption of plaice, Pleuronectes platessa L. *Journal of Fish Biology* 20, 501–516.

Jobling, M., (1996). Temperature and growth: modulation of growth rate via temperature change. *In Seminar series-society for experimental biology.(Vol.61 pp.*225–254). Cambridge University Press.

Jobling, M., (1997). Temperature and growth: modulation of growth rate via temperature. in *Global Warming: Implication for Freshwater and Marine Fish. Society for Experimental Biology, Seminar Series*, 225–253.

Johnston, I. A., and Dunn, J. (1987). Temperature acclimation and metabolism in ectotherms with particular reference to teleost fish. in *Symposia of the Society for Experimental Biology* 41, pp.67–93).

Jonassen, T. M., Imsland, A. K., and Stefansson, S. O. (1999). The interaction of temperature and fish size on growth of juvenile halibut. *Journal of Fish Biology* 54, 556–572.

Jones, F. R. H., Arnold, G. P., Walker, M. G., and Scholes, P. (1979). Selective tidal stream transport and the migration of plaice (*Pleuronectes platessa*) in the southern North Sea. *ICES Journal of Marine Science* 38, 331–337.

Jones, M. C., Dye, S. R., Pinnegar, J. K., Warren, R., and Cheung, W. W. L. (2012). Modelling commercial fish distributions: Prediction and assessment using different approaches. *Ecological Modelling* 225, 133–145.

Jutfelt, F., (2020). Metabolic adaptation to warm water in fish. *Functional Ecology* 34, 1138–1141.

Jutfelt, F., Gräns, A., Jönsson, E., Wiklander, K., Seth, H., Olsson, C., (2014). Response to 'How and how not to investigate the oxygen and capacity limitation of thermal tolerance (OCLTT) and aerobic scope–remarks on the article by Gräns et al.' *Journal of Experimental Biology* 217, 4433–4435.

Jutfelt, F., Norin, T., Åsheim, E. R., Rowsey, L. E., Andreassen, A. H., Morgan, R., (2021). 'Aerobic scope protection'reduces ectotherm growth under warming. *Functional Ecology* 35, 1397–1407.

Jutfelt, F., Norin, T., Ern, R., Overgaard, J., Wang, T., McKenzie, D. J., (2018). Oxygen-and capacity-limited thermal tolerance: blurring ecology and physiology. *Journal of Experimental Biology* 221, jeb169615.

Kalish, J. M. (1991). 13C and 18O isotopic disequilibria in fish otoliths: metabolic and kinetic effects. *Marine Ecological Progression Series* 75, 191–203.

Katsanevakis, S., and Maravelias, C. D. (2008). Modelling fish growth: multi-model inference as a better alternative to a priori using von Bertalanffy equation. *Fish and Fisheries* 9, 178–187.

Kearney, M. R., and White, C. R. (2012). Testing metabolic theories. *The American Naturalist* 180, 546–565.

Keyombe, J. L., Waithaka, E., and Obegi, B. (2015). Length–weight relationship and condition factor of Clarias gariepinus in Lake Naivasha, Kenya. *International Journal of Fisheries Aquatic Studies* 2, 382–385.

Kieffer, J. D. (2000). Limits to exhaustive exercise in fish. *Comparative Biochemistry and Physiology A Molecular and Integrative Physiology* 126, 161–179.

Killen, S. S., (2014). Growth trajectory influences temperature preference in fish through an effect on metabolic rate. *Journal of Animal Ecology* 83, 1513–1522.

Killen, S. S., Costa, I., Brown, J. A., and Gamperl, A. K. (2007). Little left in the tank: metabolic scaling in marine teleosts and its implications for aerobic scope. *Proceedings of the Royal Society B: Biological Sciences* 274, 431–438.

Killen, S. S and Halsey, N. (2017). Do method and species lifestyle affect measures of maximum metabolic rate in fishes? *Journal of Fish Biology* 90, 1037–1046.

Killen, S. S., Marras, S., Metcalfe, N. B., McKenzie, D. J., and Domenici, P. (2013). Environmental stressors alter relationships between physiology and behaviour. *Trends in Ecological Evolution* 28, 651–658.

Killen, S. S., Marras, S., Nadler, L., and Domenici, P. (2017). The role of physiological traits in assortment among and within fish shoals. *Philosophical Transactions of the Royal Society B: Biological Sciences* 372, 20160233.

Killen, S. S., Nadler, L. E., Grazioso, K., Cox, A., and McCormick, M. I. (2021). The effect of metabolic phenotype on sociability and social group size preference in a coral reef fish. *Ecology and Evolution*11, 8585–8594.

Killen, S. S., Atkinson, D., and Glazier, D. S. (2010). The intraspecific scaling of metabolic rate with body mass in fishes depends on lifestyle and temperature. *Ecological Letters* 13, 184–193.

Killen, S. S., Marras, S., and McKenzie, D. J. (2011). Fuel, fasting, fear: routine metabolic rate and food deprivation exert synergistic effects on risk-taking in individual juvenile European sea bass. *Journal of Animal Ecology* 80, 1024–1033.

Killen, S. S., Marras, S., Ryan, M. R., Domenici, P., and McKenzie, D. J. (2012). A relationship between metabolic rate and risk-taking behaviour is revealed during hypoxia in juvenile European sea bass. *Functional Ecology* 26, 134–143.

Killen, S. S., Nati, J. J. H., and Suski, C. D. (2015). Vulnerability of individual fish to capture by trawling is influenced by capacity for anaerobic metabolism. *Proceedings of the Royal Society B: Biological Sciences* 282, 20150603.

Kleiber, M., and others (1932). Body size and metabolism. *Hilgardia* 6, 315–353.

Kleiber, and others (1961). The fire of life. An introduction to animal energetics. *The fire of life. An introduction to animal energetics.*

Kolok, A. S., Hartman, M. M., and Sershan, J. (2002). The physiology of copper tolerance in fathead minnows: insight from an intraspecific, correlative analysis. *Environmental Toxicology and Chemistry: An International Journal* 21, 1730–1735.

Komoroske, L. M., Connon, R. E., Lindberg, J., Cheng, B. S., Castillo, G., Hasenbein, M., Fangue, N.A., (2014). Ontogeny influences sensitivity to climate change stressors in an endangered fish. *Conservation Physiology,* 2(1), pp.cou008.

Kooijman, B., and Kooijman, S. (2010). *Dynamic energy budget theory for metabolic organisation*. Cambridge university press.

Kooijman, B., and Lika, K. (2014). Comparative energetics of the 5 fish classes on the basis of dynamic energy budgets. *Journal of Sea Research* 94, 19–28.

Kooijman, B., and Troost, T. A. (2007). Quantitative steps in the evolution of metabolic organisation as specified by the dynamic energy budget theory. *Biological Reviews* 82, 113–142.

Kozlowski, J., and Konarzewski, M. (2005). West, Brown and Enquist's model of allometric scaling again: the same questions remain. *Functional Ecology* 19, 739–743.

Krause, J., Loader, S. P., McDermott, J., and Ruxton, G. D. (1998). Refuge use by fish as a function of body length–related metabolic expenditure and predation risks. *Proceedings of the Royal Society of London. Series B: Biological Sciences* 265, 2373–2379.

Kuipers (1977). On the ecology of juvenile plaice on a tidal flat in the Wadden Sea. *Netherlands Journal of Sea Research* 11, 56–91.

Kuparinen, A., and Hutchings, J. A. (2012). Consequences of fisheries-induced evolution for population productivity and recovery potential. *Proceedings of the Royal Society B: Biological Sciences* 279, 2571–2579.

Kushnir, Y. (1994). Interdecadal variations in North Atlantic sea surface temperature and associated atmospheric conditions. *Journal of Climate* 7, 141–157.

Laohmus, M., and Björklund, M. (2015). Climate change: what will it do to fish—parasite interactions? *Biological Journal of the Linnean Society* 116, 397–411.

Lande, R., (1973). Food and feeding habits of plaice (*Pleuronectes platessa*) in Borgenfjorden, North-Trondelag, Norway. *Norwegian journal of Zoology* 21, 91–100.

Lara, M. De, Doyen, L., Guilbaud, T., and Rochet, M.J. (2007). Is a management framework based on spawning-stock biomass indicators sustainable? A viability approach. *ICES Journal of Marine Science* 64, 761–767.

Last, P. R., White, W. T., Gledhill, D. C., Hobday, A. J., Brown, R., Edgar, G. J., (2011). Long-term shifts in abundance and distribution of a temperate fish fauna: a response to climate change and fishing practices. *Global Ecology and Biogeography* 20, 58–72.

Leach, G. J., and Taylor, M. H. (1980). The role of cortisol in stress-induced metabolic changes in Fundulus heteroclitus. *General and Comparative Endocrinology* 42, 219–227.

Lee, C. G., Farrell, A. P., Lotto, A., Hinch, S. G., and Healey, M. C. (2003). Excess post-exercise oxygen consumption in adult sockeye (Oncorhynchus nerka) and coho (O. kisutch) salmon following critical speed swimming. *Journal of Experimental Biology* 206, 3253–3260.

Lefrançois, C., and Claireaux, G. (2003a). Influence of ambient oxygenation and temperature on metabolic scope and scope for heart rate in the common sole Solea solea. *Marine Ecology Progress Series* 259, 273–284.

Lefrançois, C., and Claireaux, G. (2003b). Influence of ambient oxygenation and temperature on metabolic scope and scope for heart rate in the common sole Solea solea. *Marine Ecology Progress Series* 259, 273–284.

LeGrande, A. N., and Schmidt, G. A. (2006). Global gridded data set of the oxygen isotopic composition in seawater. *Geophysical Research Letters,* 33(12).

Lincoln, R. F. (1981). The growth of female diploid and triploid plaice (Pleuronectes platessa)× flounder (Platichthys flesus) hybrids over one spawning season. *Aquaculture* 25, 259–268.

Lindberg, W. J., Frazer, T. K., Portier, K. M., Vose, F., Loftin, J., Murie, D. J., (2006). Density-dependent habitat selection and performance by a large mobile reef fish. *Ecological Applications* 16, 731–746.

Lindmark, M., Audzijonyte, A., Blanchard, J. L., and Gårdmark, A. (2022). Temperature impacts on fish physiology and resource abundance lead to faster growth but smaller fish sizes and yields under warming. *Global Changange Biology,* 28(21), pp.6239-6253.

Little, A. G., Dressler, T., Kraskura, K., Hardison, E., Hendriks, B., Prystay, T. (2020). Maxed out: optimizing accuracy, precision, and power for field measures of maximum metabolic rate in fishes. *Physiological and Biochemical Zoology* 93, 243–254.

Little, A. G., Loughland, I., and Seebacher, F. (2020b). What do warming waters mean for fish physiology and fisheries? *Journal of Fish Biology* 97, 328–340.

Liu, H., Zeng, L., Cao, Z., and Fu, S. (2016). Effects of different predator stress on vulnerability to predation and the underlying physiological and behavioral mechanisms of this vulnerability in juvenile qingbo (Spinibarbus sinensis). *Acta Ecologica Sinica* 36, 85–90.

Long, R. (2011). The Marine Strategy Framework Directive: a new European approach to the regulation of the marine environment, marine natural resources and marine ecological services. *Journal of Energy & Natural Resources Law* 29, 1–44.

Loreau, M., Naeem, S., Inchausti, P., Bengtsson, J., Grime, J. P., Hector, A. (2001). Biodiversity and ecosystem functioning: current knowledge and future challenges. *Science (1979)* 294, 804–808.

Lugert, V., Thaller, G., Tetens, J., Schulz, C., and Krieter, J. (2016). A review on fish growth calculation: multiple functions in fish production and their specific application. *Reviews in Fisheries Science and Aquaculture* 8, 30–42.

Lusardi, R. A., and Moyle, P. B. (2017). Two-way trap and haul as a conservation strategy for anadromous salmonids. *Fisheries (Bethesda)* 42, 478–487.

Lynam, C. P., Gibbons, M. J., Axelsen, B. E., Sparks, C. A. J., Coetzee, J., Heywood, B. G., and Brierley, A.S., (2006). Jellyfish overtake fish in a heavily fished ecosystem. *Current biology* 13, pp.R492–R493.

MacDonald, A., Speirs, D. C., Greenstreet, S. P. R., and Heath, M. R. (2018). Exploring the influence of food and temperature on North Sea sandeels using a new dynamic energy budget model. *Frontiers in Marine Science* 5, p.339.

Mace, P. M. (2001). A new role for MSY in single-species and ecosystem approchaes to fisheries stock assessment and management. *Fish and fisheries* 2, pp.2–32.

Macer, P. M. (1967). The food web in Red Wharf Bay (North Wales) with particular reference to young plaice (Pleuronectes platessa). *Helgoland Marine Research* 15, pp.560–573.

MacKenzie, B. R., Gislason, H., Möllmann, C., and Köster, F. W. (2007). Impact of 21st century climate change on the Baltic Sea fish community and fisheries. *Global Change Biology* 13, 1348–1367.

Malloy, K. D., and Targett, T. E. (1994). Effects of ration limitation and low temperature on growth, biochemical condition, and survival of juvenile summer flounder from two Atlantic coast nurseries. *Transactions of the American Fisheries Society.* 123, 182–193.

Mangano, M. C., Giacoletti, A., and Sarà, G. (2019). Dynamic Energy Budget provides mechanistic derived quantities to implement the ecosystem based management approach. *Journal of Sea Research* 143, 272–279.

Marras, S., Claireaux, G., McKenzie, D. J., and Nelson, J. A. (2010). Individual variation and repeatability in aerobic and anaerobic swimming performance of European sea bass, Dicentrarchus labrax. *Journal of Experimental Biology* 213, 26–32.

Marras, S., Cucco, A., Antognarelli, F., Azzurro, E., Milazzo, M., Bariche, M., Butenschon, M., Kay,S., Di Bitetto, M., Quattrocchi, G and Sinerchia, M., (2015). Predicting future thermal habitat suitability of competing native and invasive fish species: from metabolic scope to oceanographic modelling. *Conservation Physiology* 3, p.cou059.

Marras, S., Killen, S., Claireaux, G., Domenici, P., and McKenzie, D. J. (2011). Behavioural and kinematic components of the fast-start escape response in fish: individual variation and temporal repeatability. *Journal of Experimental Biology* 214, 3102–3110.

Martino, J. C., Doubleday, Z. A., Chung, M.-T., and Gillanders, B. M. (2020). Experimental support towards a metabolic proxy in fish using otolith carbon isotopes. *Journal of Experimental Biology* 223, jeb217091.

Martino, J. C., Doubleday, Z. A., and Gillanders, B. M. (2019). Metabolic effects on carbon isotope biomarkers in fish. *Ecological Indicators* 97, pp.10–16.

Mason, D. M., and Brandt, S. B. (1996). Effects of spatial scale and foraging efficiency on the predictions made by spatially-explicit models of fish growth rate potential. *Environmental Biology of Fishes* 45, 283–298.

Maunder, M. N., and Punt, A. E. (2013). A review of integrated analysis in fisheries stock assessment. *Fisheries Research* 142, 61–74.

Mazerolle, M. J. (2020). AICcmodavg: Model selection and multimodel inference based on (Q)AIC(c). Available at: https://cran.r-project.org/package=AICcmodavg.

McAngus, C., Huggins, C., Connolly, J., and Zwet, A. Van Der (2018). The politics and governance of UK Fisheries after Brexit. *Political Insight* 9, 8–11.

McCarthy, I. D. (2000). Temporal repeatability of relative standard metabolic rate in juvenile Atlantic salmon and its relation to life history variation. *Journal of Fish Biology* 57, 224–238.

McCauley, D. J., Pinsky, M. L., Palumbi, S. R., Estes, J. A., Joyce, F. H., and Warner, R. R. (2015). Marine defaunation: animal loss in the global ocean. *Science* 347, 1255641.

McConnaughey, T. A., Burdett, J., Whelan, J. F., and Paull, C. K. (1997). Carbon isotopes in biological carbonates: respiration and photosynthesis. *Geochimica et Cosmochimica Acta* 61, 611–622.

McKenzie, D. J., Zhang, Y., Eliason, E. J., Schulte, P. M., Claireaux, G., Blasco, F. R. (2020). Intraspecific variation in tolerance of warming in fishes. *Journal of Fish Biology 98*. 1536-1555.

Merilä, J., and Hendry, A. P. (2014). Climate change, adaptation, and phenotypic plasticity: the problem and the evidence. *Evolutionary Applications* 7, 1–14.

Messier, J., McGill, B. J., and Lechowicz, M. J. (2010). How do traits vary across ecological scales? A case for trait-based ecology. *Ecological Letters* 13, 838–848.

Metcalfe, Leeuwen, T. E. Van, and Killen (2016). Does individual variation in metabolic phenotype predict fish behaviour and performance? *Journal of Fish Biology* 88, 298–321.

Metcalfe, Taylor, A. C., and Thorpe, J. E. (1995). Metabolic rate, social status and life-history strategies in Atlantic salmon. *Animal Behaviour* 49, 431–436.

Mieszkowska, N., Genner, M. J., Hawkins, S. J., and Sims, D. W. (2009). Effects of climate change and commercial fishing on Atlantic cod Gadus morhua. *Advances in Marine Biology* 56, 213–273.

Monaco, C. J., and McQuaid, C. D. (2018). Applicability of Dynamic Energy Budget (DEB) models across steep environmental gradients. *Scientific Reports* 8, 1–14.

Morgan, M. J. (1993). Ration level and temperature preference of American plaice. *Marine & Freshwater Behaviour & Physiology* 24, 117–122.

Morita, K., Fukuwaka, M., Tanimata, N., and Yamamura, O. (2010). Size-dependent thermal preferences in a pelagic fish. *Oikos* 119, 1265–1272.

Morita, K., Tamate, T., Kuroki, M., and Nagasawa, T. (2014). Temperature-dependent variation in alternative migratory tactics and its implications for fitness and population dynamics in a salmonid fish. *Journal of Animal Ecology* 83, 1268–1278.

Morrongiello, J. R., Crook, D. A., King, A. J., Ramsey, D. S. L., and Brown, P. (2011). Impacts of drought and predicted effects of climate change on fish growth in temperate Australian lakes. *Global Change Biology* 17, 745–755.

Morrongiello, J. R., Sweetman, P. C., and Thresher, R. E. (2019). Fishing constrains phenotypic responses of marine fish to climate variability. *Journal of Animal Ecology* 88, 1645–1656.

Morrongiello, J. R., and Thresher, R. E. (2015). A statistical framework to explore ontogenetic growth variation among individuals and populations: a marine fish example. *Ecological Monographs* 85, 93–115.

Morrongiello, J. R., Thresher, R. E., and Smith, D. C. (2012). Aquatic biochronologies and climate change. *Nature Climate Change* 2, 849–857.

Morrongiello, J. R., Walsh, C. T., Gray, C. A., Stocks, J. R., and Crook, D. A. (2014). Environmental change drives long-term recruitment and growth variation in an estuarine fish. *Global Change Biology* 20, 1844–1860.

Mousseau, T. A., and Fox, C. W. (1998). The adaptive significance of maternal effects. *Trends in Ecological Evolution*13, 403–407.

Murawski, S. A. (1993). Climate change and marine fish distributions: forecasting from historical analogy. *Transactions of the American Fisheries Society* 122, 647–658.

Murdoch, A., and Power, M. (2013). The effect of lake morphometry on thermal habitat use and growth in Arctic charr populations: implications for understanding climate-change impacts. *Ecology of Freshwater Fish* 22, 453–466.

Myers, R. A., Hutchings, J. A., and Barrowman, N. J. (1996). Hypotheses for the decline of cod in the North Atlantic. *Marine Ecology Progress Series* 138, 293–308.

Myers, R. A., Hutchings, J. A., and Barrowman, N. J. (1997). Why do fish stocks collapse? The example of cod in Atlantic Canada. *Ecological Applications* 7, 91–106.

Myers, R. A., and Worm, B. (2005). Extinction, survival or recovery of large predatory fishes. *Philosophical Transactions of the Royal Society B: Biological Sciences* 360, 13–20.

Nash, R. D., and Geffen, A. J., (1999). Variability in stage I egg production and settlement of plaice Pleuronectes platessa on the west side of the Isle of Man, Irish Sea. *Marine Ecology Progress Series* 189, 241–250.

Nash, R. D., Geffen, A. J., and Hughes, G. (1994). Individual growth of juvenile plaice (*Pleuronectes platessa*) on a small Irish Sea nursery ground (Port Erin Bay, Isle of Man, UK). *Netherlands Journal of Sea Research* 32, 369–378.

Natugonza, V., Nyamweya, C., Sturludóttir, E., Musinguzi, L., Ogutu-Ohwayo, R., Bassa, S. (2022). Spatiotemporal variation in fishing patterns and fishing pressure in Lake Victoria (East Africa) in relation to balanced harvest. *Fisheries Research* 252, 106355.

Neat, F., and Righton, D. (2007). Warm water occupancy by North Sea cod. *Proceedings of the Royal Society B: Biological Sciences* 274, 789–798.

Neill, W. H., Brandes, T. S., Burke, B. J., Craig, S. R., Dimichele, L. V, Duchon, K. (2004). Ecophys. Fish: a simulation model of fish growth in time-varying environmental regimes. *Reviews in Fisheries Science* 12, 233–288.

Neubauer, P., and Andersen, K. H. (2019). Thermal performance of fish is explained by an interplay between physiology, behaviour and ecology. *Conservation Physiology* 7, coz025.

Neuheimer, A. B., Thresher, R. E., Lyle, J. M., and Semmens, J. M. (2011). Tolerance limit for fish growth exceeded by warming waters. *Nature Climate Change* 1, 110–113.

Nicholson, G., Jenkins, G. P., Sherwood, J., and Longmore, A. (2008). Physical environmental conditions, spawning and early-life stages of an estuarine fish: climate change implications for recruitment in intermittently open estuaries. *Marine and Freshwater Research* 59, 735–749.

Nicieza, A. G., and Metcalfe, N. B. (1997). Growth compensation in juvenile Atlantic salmon: responses to depressed temperature and food availability. *Ecology* 78, 2385–2400.

Nieland, D. L., and Wilson, C. A. (1993). Reproductive biology and annual variation of reproductive variables of black drum in the northern Gulf of Mexico. *Transactions of the American Fisheries Society* 122, 318–327.

Nielsen, J. L., Ruggerone, G. T., and Zimmerman, C. E. (2013). Adaptive strategies and life history characteristics in a warming climate: Salmon in the Arctic? *Environmental Biology of Fishes* 96, 1187–1226.

Niloshini, S. R., Dempson, B. J., Reist, J. D., and Power, M. (2015). Latitudinal variation in growth and otolith-inferred field metabolic rates of Canadian young-of-the-year Arctic charr. *Ecology of Freshwater Fish* 24, 478–488.

Nisbet, R. M., Jusup, M., Klanjscek, T., and Pecquerie, L. (2012). Integrating dynamic energy budget (DEB) theory with traditional bioenergetic models. *Journal of Experimental Biology* 215, 892–902.

Nisbet, R. M., Muller, E. B., Lika, K., and Kooijman, S. (2000). From molecules to ecosystems through dynamic energy budget models. *Journal of Animal Ecology*, 913–926.

Norin, T., and Clark, T. D. (2017). Fish face a trade-off between ‘eating big’for growth efficiency and ‘eating small’to retain aerobic capacity. *Biological Letters* 13, 20170298.

Norin, T., and Malte, H. (2011). Repeatability of standard metabolic rate, active metabolic rate and aerobic scope in young brown trout during a period of moderate food availability. *Journal of Experimental Biology* 214, 1668–1675.

Norin, T., Malte, H., and Clark, T. D. (2014). Aerobic scope does not predict the performance of a tropical eurythermal fish at elevated temperatures. *Journal of Experimental Biology* 217, 244–251.

Norin, T., Malte, H., and Clark, T. D. (2016). Differential plasticity of metabolic rate phenotypes in a tropical fish facing environmental change. *Functional Ecology* 30, 369–378.

Núñez-Riboni, I., and Akimova, A. (2015a). Monthly maps of optimally interpolated in situ hydrography in the North Sea from 1948 to 2013. *Journal of Marine Systems* 151, 15–34.

Núñez-Riboni, I., and Akimova, A. (2015b). Monthly maps of optimally interpolated in situ hydrography in the North Sea from 1948 to 2013. *Journal of Marine Systems* 151, 15–34.

Nussey, D. H., Wilson, A. J., and Brommer, J. E. (2007). The evolutionary ecology of individual phenotypic plasticity in wild populations. *Journal of Evolutionary Biology* 20, 831–844.

Ohlberger, J., Staaks, G., and Hölker, F. (2007). Estimating the active metabolic rate (AMR) in fish based on tail beat frequency (TBF) and body mass. J*ournal of Experimental Zoology Part A* 307, 296–300.

Ono, K., Licandeo, R., Muradian, M. L., Cunningham, C. J., Anderson, S. C., Hurtado-Ferro, F. (2015). The importance of length and age composition data in statistical age-structured models for marine species. *ICES Journal of Marine Science* 72, 31–43.

Ott, M. E., Heisler, N., and Ultsch, G. R. (1980). A re-evaluation of the relationship between temperature and the critical oxygen tension in freshwater fishes. *Comparative Biochemistry and Physiology A Physiol* 67, 337–340.

Pachauri, R. K., and Reisinger, A. (2008). Climate change 2007. Synthesis report. *Contribution of Working Groups I, II and III to the fourth assessment report of the Intergovernmental Panel on Climate Change. IPCC.*

Pauly, D., (2021). The gill-oxygen limitation theory (GOLT) and its critics. *Science Advances,* 7(2), p.eabc6050.

Perry, A. L., Low, P. J., Ellis, J. R., and Reynolds, J. D. (2005). Climate change and distribution shifts in marine fishes. *Science (1979)* 308, 1912–1915.

Pilling, G. M., Kirkwood, G. P., and Walker, S. G. (2002). An improved method for estimating individual growth variability in fish, and the correlation between von Bertalanffy growth parameters. *Canadian Journal of Fisheries and Aquatic Sciences* 59, 424–432.

Pinsky, M. L., Fenichel, E., Fogarty, M., Levin, S., McCay, B., Martin, K. St. (2021). Fish and fisheries in hot water: What is happening and how do we adapt? *Population Ecology* 63, 17–26.

Pinsky, M. L., Worm, B., Fogarty, M. J., Sarmiento, J. L., and Levin, S. A. (2013). Marine taxa track local climate velocities. *Science (1979)* 341, 1239–1242.

Plagányi, É. E. "Models for an ecosystem approach to fisheries". (2007).

Plaut, I. (2001). Critical swimming speed: its ecological relevance. *Comparative Biochemistry and Physiology A Molecular and Integrative Physiology* 131, 41–50.

Poloczanska, E. S., Brown, C. J., Sydeman, W. J., Kiessling, W., Schoeman, D. S., Moore, P. J. (2013). Global imprint of climate change on marine life. *Nature Climate Change* 3, 919–925.

Pörtner, H. O., (2010). Oxygen-and capacity-limitation of thermal tolerance: a matrix for integrating climate-related stressor effects in marine ecosystems. *Journal of Experimental Biology* 213, 881–893.

Pörtner, H. O., (2021). Climate impacts on organisms, ecosystems and human societies: integrating OCLTT into a wider context. *Journal of Experimental Biology* 224, jeb238360.

Pörtner, H. O., and Farrell, A. P. (2008). Physiology and climate change. *Science (1979)* 322, 690–692.

Pörtner, H. O., and Knust, R. (2007). Climate change affects marine fishes through the oxygen limitation of thermal tolerance. *Science (1979)* 315, 95–97.

Pörtner, H. O., and Peck, M. A. (2010). Climate change effects on fishes and fisheries: towards a cause-and-effect understanding. *Journal of Fish Biology* 77, 1745–1779.

Post, J. R., and Parkinson, E. A. (2001). Energy allocation strategy in young fish: allometry and survival. *Ecology* 82, 1040–1051.

Priede, I. G., and Holliday, F. G. T. (1980). The use of a new tilting tunnel respirometer to investigate some aspects of metabolism and swimming activity of the plaice (*Pleuronectes platessa*). *Journal of Experimental Biology* 85, 295–309.

Quinn, T. J. (2003). Ruminations on the development and future of population dynamics models in fisheries. *Natural Resource Modeling* 16, 341–392.

Rahel, F. J. (2002.). Using current biogeographic limits to predict fish distributions following climate change. *American Fisheries Society Symposium* 62, (pp.99–112).

Railsback, S. F. (2022). What We Don't Know About the Effects of Temperature on Salmonid Growth. *Transactions of the American Fisheries Society* 151, 3–12.

Railsback, S. F., and Harvey, B. C. (2002). Analysis of habitat-selection rules using anindividual-based model. *Ecology* 83, 1817–1830.

Rall, B. C., Brose, U., Hartvig, M., Kalinkat, G., Schwarzmüller, F., Vucic-Pestic, O., (2012). Universal temperature and body-mass scaling of feeding rates. *Philosophical Transactions of the Royal Society B: Biological Sciences* 367, 2923–2934.

Rätz, H.-J., and Lloret, J. (2003). Variation in fish condition between Atlantic cod (Gadus morhua) stocks, the effect on their productivity and management implications. *Fisheries Research* 60, 369–380.

Rauck, G., and Zijlstra, J. J. (1976). On the nursery-aspects of the Waddensea for some commercial fish-species and possible long-term changes (Plaice, Sole, Cod, Whiting, Herring). *Rapports et Proces Verbaux des Reunions,* 172.

Raye, G. Del, and Weng, K. C. (2015). An aerobic scope-based habitat suitability index for predicting the effects of multi-dimensional climate change stressors on marine teleosts. *Deep Sea Research Part II: Topical Studies in Oceanography* 113, 280–290.

Redpath, T. D., Cooke, S. J., Suski, C. D., Arlinghaus, R., Couture, P., Wahl, D. H. (2010). The metabolic and biochemical basis of vulnerability to recreational angling after three generations of angling-induced selection in a teleost fish. *Canadian Journal of Fisheries and Aquatic Sciences* 67, 1983–1992.

Reid, D., Armstrong, J. D., and Metcalfe, N. B. (2011). Estimated standard metabolic rate interacts with territory quality and density to determine the growth rates of juvenile Atlantic salmon. *Functional Ecology* 25, 1360–1367.

Reid, D., Armstrong, J. D., and Metcalfe, N. B. (2012). The performance advantage of a high resting metabolic rate in juvenile salmon is habitat dependent. *Journal of Animal Ecology* 81, 868–875.

Reiss, H., Birchenough, S., Borja, A., Buhl-Mortensen, L., Craeymeersch, J., Dannheim, J., (2015). Benthos distribution modelling and its relevance for marine ecosystem management. *ICES Journal of Marine Science* 72, 297–315.

Reist, J. D., Wrona, F. J., Prowse, T. D., Power, M., Dempson, J. B., Beamish, R. J., (2006). General effects of climate change on Arctic fishes and fish populations. *AMBIO: A Journal of the Human Environment* 35, 370–380.

Rengstorf, A. M., Yesson, C., Brown, C., and Grehan, A. J. (2013). High-resolution habitat suitability modelling can improve conservation of vulnerable marine ecosystems in the deep sea. *Journal of Biogeography* 40, 1702–1714.

Richards, J. G., Heigenhauser, G. J. F., and Wood, C. M. (2002). Lipid oxidation fuels recovery from exhaustive exercise in white muscle of rainbow trout. *American Journal of Physiology-Regulatory, Integrative and Comparative Physiology* 282, R89–R99.

Richards, S. E., Dumas, M.E., Fonville, J. M., Ebbels, T. M. D., Holmes, E., and Nicholson, J. K. (2010). Intra-and inter-omic fusion of metabolic profiling data in a systems biology framework. *Chemometrics and Intelligent Laboratory Systems* 104, 121–131.

Rijnsdorp, A. D., (1989). Maturation of male and female North Sea plaice (*Pleuronectes platessa*). *ICES Journal of Marine Science* 46, 35–51.

Rijnsdorp, A. D., (1990). The mechanism of energy allocation over reproduction and somatic growth in female North Sea plaice, Pleuronectes platessa L. *Netherlands Journal of Sea Research* 25, 279–289.

Rijnsdorp, A. D., Peck, M. A., Engelhard, G. H., Möllmann, C., and Pinnegar, J. K. (2009). Resolving the effect of climate change on fish populations. *ICES Journal of Marine Science* 66, 1570–1583.

Rijnsdorp, A. D., Stralen, V., (1985). Selective tidal transport of North Sea plaice larvae Pleuronectes platessa in coastal nursery areas. *Transactions of the American Fisheries Society* 114, 461–470.

Rijnsdorp, A. D., and Van Leeuwen, P. I. (1996). Changes in growth of North Sea plaice since 1950 in relation to density, eutrophication, beam-trawl effort, and temperature. *ICES Journal of Marine Science* 53, 1199–1213.

Rijnsdorp, A. D., and van Vingerhoed, B. (2001). Feeding of plaice *Pleuronectes platessa* and sole *Solea solea* in relation to the effects of bottom trawling. *Journal of Sea Research* 45, 219–229.

Roessig, J. M., Woodley, C. M., Cech, J. J., and Hansen, L. J. (2004). Effects of global climate change on marine and estuarine fishes and fisheries. *Reviews in Fish Biology and Fisheries* 14, 251–275.

Rolland, V., Nevoux, M., Barbraud, C., and Weimerskirch, H. (2009). Respective impact of climate and fisheries on the growth of an albatross population. *Ecological Applications* 19, 1336–1346.

Rombough, P. J. (1994). Energy partitioning during fish development: additive or compensatory allocation of energy to support growth? *Functional Ecology*, 178–186.

Rowe, D. K., and Thorpe, J. E. (1990). Suppression of maturation in male Atlantic salmon (*Salmo salar*) parr by reduction in feeding and growth during spring months. *Aquaculture* 86, 291–313.

Rubio-Gracia, F., Garcia-Berthou, E., Guasch, H., Zamora, L., and Vila-Gispert, A. (2020). Size-related effects and the influence of metabolic traits and morphology on swimming performance in fish. *Current Zoology* 66, 493–503.

Rummer, J. L., Stecyk, J. A. W., Couturier, C. S., Watson, S.-A., Nilsson, G. E., and Munday, P. L. (2013). Elevated CO2 enhances aerobic scope of a coral reef fish. *Conservation Physiology* 1, cot023.

Russell, N. R., Fish, J. D., and Wootton, R. J. (1996). Feeding and growth of juvenile sea bass: the effect of ration and temperature on growth rate and efficiency. *Journal of Fish Biology* 49, 206–220.

Rutterford, L. A., Simpson, S. D., Jennings, S., Johnson, M. P., Blanchard, J. L., Schön, P.-J. (2015). Future fish distributions constrained by depth in warming seas. *Nature Climate Change* 5, 569–573.

Sainsbury, K. J. (1980). Effect of individual variability on the von Bertalanffy growth equation. *Canadian Journal of Fisheries and Aquatic Sciences* 37, 241–247.

Sanchirico, J. N., Holland, D., Quigley, K., and Fina, M. (2006). Catch-quota balancing in multispecies individual fishing quotas. *Marine Policy* 30, 767–785.

Sandblom, E., Gräns, A., Axelsson, M., and Seth, H. (2014). Temperature acclimation rate of aerobic scope and feeding metabolism in fishes: implications in a thermally extreme future. *Proceedings of the Royal Society B: Biological Sciences* 281, 20141490.

Sasaki, K., Kudo, M., Tomiyama, T., Ito, K., and Omori, M. (2002). Predation pressure on the siphons of the bivalve Nuttallia olivacea by the juvenile stone flounder Platichthys bicoloratus in the Natori River estuary, northeastern Japan. *Fisheries Science* 68, 104–116.

Scheuffele, H., Rubio-Gracia, F., and Clark, T. D. (2021). Thermal performance curves for aerobic scope in a tropical fish (Lates calcarifer): flexible in amplitude but not breadth. *Journal of Experimental Biology* 224(24), jeb243504.

Schmittner, A., Gruber, N., Mix, A. C., Key, R. M., Tagliabue, A., and Westberry, T. K. (2013). Biology and air–sea gas exchange controls on the distribution of carbon isotope ratios (δ 13 C) in the ocean. *Biogeosciences* 10, 5793–5816.

Schneider, C. A., Rasband, W. S., and Eliceiri, K. W. (2012). NIH Image to ImageJ: 25 years of image analysis. *Nature Methods* 9, 671–675.

Schrum, C., Lowe, J., Meier, H. E., Grabemann, I., Holt, J., Mathis, M., Pohlmann, T., Skogen, M.D., and Wakelin, S., (2016). Projected change—North sea. *North Sea region climate change assessment*, 175–217.

Scott, G. R., and Dalziel, A. C. (2021). Physiological insight into the evolution of complex phenotypes: aerobic performance and the O2 transport pathway of vertebrates. *Journal of Experimental Biology* 224(16).

Seebacher, F. (2005). A review of thermoregulation and physiological performance in reptiles: what is the role of phenotypic flexibility? *Journal of Comparative Physiology B* 175, 453–461.

Seidl, M. D., Pirow, R., and Paul, R. J. (2005). Acclimation of the microcrustacean Daphnia magna to warm temperatures is dependent on haemoglobin expression. *Journal of Thermal Biology* 30, 532–544.

Senina, I., Lehodey, P., Sibert, J., and Hampton, J. (2020). Integrating tagging and fisheries data into a spatial population dynamics model to improve its predictive skills. *Canadian Journal of Fisheries and Aquatic Sciences* 77, 576–593.

Shepherd, T. D., and Litvak, M. K. (2004). Density-dependent habitat selection and the ideal free distribution in marine fish spatial dynamics: considerations and cautions. *Fish and Fisheries* 5, 141–152.

Sherwood, G. D., and Rose, G. A. (2003). Influence of swimming form on otolith δ13C in marine fish. *Marine Ecology Progress Series* 258, 283–289.

Simpson, S. D., Jennings, S., Johnson, M. P., Blanchard, J. L., Schön, P.-J., Sims, D. W. (2011). Continental shelf-wide response of a fish assemblage to rapid warming of the sea. *Current Biology* 21, 1565–1570.

Sinnatamby, R. N., Dempson, J. B., Reist, J. D., and Power, M. (2015). Latitudinal variation in growth and otolith-inferred field metabolic rates of Canadian young-of-the-year Arctic charr. *Ecology of Freshwater Fish* 24, 478–488.

Sippel, T., Eveson, J. P., Galuardi, B., Lam, C., Hoyle, S., Maunder, M. (2015). Using movement data from electronic tags in fisheries stock assessment: a review of models, technology and experimental design. *Fisheries Research* 163, 152–160.

Skelly, D. K., Joseph, L. N., Possingham, H. P., Freidenburg, L. K., Farrugia, T. J., Kinnison, M. T. (2007). Evolutionary responses to climate change. *Conservation Biology* 21, 1353–1355.

Sloman, K. A., Morgan, T. P., McDonald, D. G., and Wood, C. M. (2003). Socially-induced changes in sodium regulation affect the uptake of water-borne copper and silver in the rainbow trout, Oncorhynchus mykiss. *Comparative Biochemistry and Physiology Part C: Toxicology & Pharmacology* 135, 393–403.

Sloman, K. A., Motherwell, G., O'connor, K. I., and Taylor, A. C. (2000). The effect of social stress on the standard metabolic rate (SMR) of brown trout, Salmo trutta. *Fish Physiology and Biochemistry* 23, 49–53.

Smalås, A., Strøm, J. F., Amundsen, P., Dieckmann, U., and Primicerio, R. (2020). Climate warming is predicted to enhance the negative effects of harvesting on high-latitude lake fish. *Journal of Applied Ecology* 57, 270–282.

Sogard, S. M. (1992). Variability in growth rates of juvenile fishes in different estuarine habitats. *Marine Ecology Progress Series* 85, 35–53.

Solomon, C. T., Weber, P. K., Cech, J. J. J., Ingram, B. L., Conrad, M. E., Machavaram, M. V. (2006). Experimental determination of the sources of otolith carbon and associated isotopic fractionation. *Canadian Journal of Fisheries and Aquatic Sciences* 63, 79–89.

Sousa, T., Domingos, T., Poggiale, J. C., and Kooijman, S. (2010). Dynamic energy budget theory restores coherence in biology. *Philosophical Transactions of the Royal Society B: Biological Sciences* 365, 3413–3428.

Spicer, J. I. (2014). What can an ecophysiological approach tell us about the physiological responses of marine invertebrates to hypoxia? *Journal of Experimental Biology* 217, 46–56.

Spurgeon, J. J., Pegg, M. A., Pope, K. L., and Xie, L. (2020). Ecosystem-specific growth responses to climate pattern by a temperate freshwater fish. *Ecological Indicators* 112, 106130.

St. John Glew, K., Graham, L. J., McGill, R. A. R., and Trueman, C. N. (2019). Spatial models of carbon, nitrogen and sulphur stable isotope distributions (isoscapes) across a shelf sea: An INLA approach. *Methods Ecology and Evolution*10, 518–531.

Stock, B. C., and Semmens, B. X. (2016). MixSIAR GUI user manual v3. 1. *Scripps Institution of Oceanography, UC San Diego, San Diego, California, USA*.

Stocker, T. F., Qin, D., Plattner, G. K., Alexander, L. V, Allen, S. K., Bindoff, N. L., (2013). Technical summary. *Climate change 2013: the physical science basis. Contribution of Working Group I to the Fifth Assessment Report of the Intergovernmental Panel on Climate Change*, 33–115.

Stoeven, M. T., Diekert, F. K., and Quaas, M. F. (2021). Should Fishing Quotas Be Measured in Terms of Numbers? *Marine Resource Economics* 36, 133–153.

Storch, D., Santelices, P., Barria, J., Cabeza, K., Pörtner, H.-O., and Fernández, M. (2009). Thermal tolerance of crustacean larvae (zoea I) in two different populations of the kelp crab Taliepus dentatus (Milne-Edwards). *Journal of Experimental Biology* 212, 1371–1376.

Tagliabue, A., and Bopp, L. (2008). Towards understanding global variability in ocean carbon-13. *Global Biogeochem Cycles* 22.

Tagliapietra, D., and Sigovini, M. (2010). Biological diversity and habitat diversity: a matter of Science and perception. *Terre et Environnement* 88, 147–155.

Teal, L. R., van Hal, R., van Kooten, T., Ruardij, P., and Rijnsdorp, A. D. (2012). Bio-energetics underpins the spatial response of North Sea plaice (*Pleuronectes platessa*) and sole (*Solea solea*) to climate change. *Global Change Biology* 18, 3291–3305.

Thomas, Y., Flye-Sainte-Marie, J., Chabot, D., Aguirre-Velarde, A., Marques, G. M., and Pecquerie, L. (2019). Effects of hypoxia on metabolic functions in marine organisms: Observed patterns and modelling assumptions within the context of Dynamic Energy Budget (DEB) theory. *Journal of Sea Research* 143, 231–242.

Thorson, J. T. (2020). Predicting recruitment density dependence and intrinsic growth rate for all fishes worldwide using a data-integrated life-history model. *Fish and Fisheries* 21, 237–251.

Thresher, R. E., Koslow, J. A., Morison, A. K., and Smith, D. C. (2007). Depth-mediated reversal of the effects of climate change on long-term growth rates of exploited marine fish. *Proceedings of the National Academy of Sciences* 104, 7461–7465.

Thurstan, R. H., Brockington, S., and Roberts, C. M. (2010). The effects of 118 years of industrial fishing on UK bottom trawl fisheries. *Nature Communications* 1, 1–6.

Tilman, D., HilleRisLambers, J., Harpole, S., Dybzinski, R., Fargione, J., Clark, C. (2004). Does metabolic theory apply to community ecology? It's a matter of scale. *Ecology* 85, 1797–1799.

Todd, C. D., Hughes, S. L., Marshall, C. T., MacLean, J. C., Lonergan, M. E., and Biuw, E. M. (2008). Detrimental effects of recent ocean surface warming on growth condition of Atlantic salmon. *Global Change Biology* 14, 958–970.

Tohse, H., and Mugiya, Y. (2008). Sources of otolith carbonate: experimental determination of carbon incorporation rates from water and metabolic CO2, and their diel variations. *Aquat Biol* 1, 259–268.

Tonn, W. M. (1990). Climate change and fish communities: a conceptual framework. *Transactions of the American Fisheries Society* 119, 337–352.

Treberg, J. R., Killen, S., MacCormack, T. J., Lamarre, S. G., and Enders, E. C. (2016). Estimates of metabolic rate and major constituents of metabolic demand in fishes under field conditions: methods, proxies, and new perspectives. *Comparative Biochemistry and Physiology A Molecular and Integrative Physiology* 202, 10–22.

Trueman, C. N., and Glew, K. S. J. (2019). "Isotopic tracking of marine animal movement," in *Tracking animal migration with stable isotopes* (Elsevier), 137–172.

Trueman, MacKenzie, and Glew, S. J. (2017). Stable isotope-based location in a shelf sea setting: accuracy and precision are comparable to light-based location methods. *Methods Ecology and Evolution* 8, 232–240.

Tyler, J. A., and Brandt, S. B. (2001). Do spatial models of growth rate potential reflect fish growth in a heterogeneous environment? A comparison of model results. *Ecology of Freshwater Fish* 10, 43–56.

Van Denderen, D., Gislason, H., van den Heuvel, J., and Andersen, K. H. (2020). Global analysis of fish growth rates shows weaker responses to temperature than metabolic predictions. *Global Ecology and Biogeography* 29, 2203–2213.

Van Denderen, P. D., Petrik, C. M., Stock, C. A., and Andersen, K. H. (2021). Emergent global biogeography of marine fish food webs. *Global Ecology and Biogeography* 30, 1822–1834.

Van der Sleen, P., Stransky, C., Morrongiello, J. R., Haslob, H., Peharda, M., and Black, B. A. (2018a). Otolith increments in European plaice (*Pleuronectes platessa*) reveal temperature and density-dependent effects on growth 2. *Management* 33, 34.

Van der Sleen, S. C., Morrongiello, J. R., Haslob, H., Peharda, M., and Black, B. A. (2018b). Otolith increments in European plaice (*Pleuronectes platessa*) reveal temperature and density-dependent effects on growth. *ICES Journal of Marine Science* 75, 1655–1663.

Van der Veer, C. J., Peck, M. A., and Kooijman, S.(2009). Physiological performance of plaice *Pleuronectes platessa*: a comparison of static and dynamic energy budgets. *Journal of Sea Research* 62, 83–92.

Van der Veer, Freitas, V., Koot, J., Witte, J. I. J., and Zuur, A. F. (2010). Food limitation in epibenthic species in temperate intertidal systems in summer: analysis of 0-group plaice Pleuronectes platessa. *Marine Ecology Progress Series* 416, 215–227.

Van Winkle, W., Rose, K. A., and Chambers, R. C. (1993). Individual-based approach to fish population dynamics: an overview. *Transactions of the American Fisheries Society* 122, 397–403.

Verberk, W., Durance, I., Vaughan, I. P., and Ormerod, S. J. (2016). Field and laboratory studies reveal interacting effects of stream oxygenation and warming on aquatic ectotherms. *Global Change Biology* 22, 1769–1778.

Vezza, P., Muñoz-Mas, R., Martinez-Capel, F., and Mouton, A. (2015). Random forests to evaluate biotic interactions in fish distribution models. *Environmental Modelling & Software* 67, 173–183.

Vilhunen, S., Tiira, K., Laurila, A., and Hirvonen, H. (2008). The bold and the variable: fish with high heterozygosity act recklessly in the vicinity of predators. *Ethology* 114, 7–15.

Vinton, A. C., and Vasseur, D. A. (2022). Resource limitation determines realized thermal performance of consumers in trophodynamic models. *Ecology Letters 25*. 2142-2155

Violle, C., Enquist, B. J., McGill, B. J., Jiang, L. I. N., Albert, C. H., Hulshof, C. (2012). The return of the variance: intraspecific variability in community ecology. *Trends in Ecological Evolution* 27, 244–252.

Volkoff, H., and Rønnestad, I. (2020). Effects of temperature on feeding and digestive processes in fish. *Temperature* 7, 307–320.

Von herbging, ione hunt (2006). The physiological basis for metabolic scaling in animals: a developing perspective. *Comparative Developmental Physiology: Contributions, Tools, and Trends*, 83.

Von Herbing, I. H., and White, L. (2002). The effects of body mass and feeding on metabolic rate in small juvenile Atlantic cod. *Journal of Fish Biology* 61, 945–958.

Weatherley, A. H. (1990). Approaches to understanding fish growth. *Transactions of the American Fisheries Society* 119, 662–672.

Weerd, J. H. Van, and Komen, J. (1998). The effects of chronic stress on growth in fish: a critical appraisal. *Comparative Biochemistry and Physiology A Molecular and Integrative Physiology* 120, 107–112.

Weibel, E. R., Bacigalupe, L. D., Schmitt, B., and Hoppeler, H. (2004). Allometric scaling of maximal metabolic rate in mammals: muscle aerobic capacity as determinant factor. *Respir Physiol Neurobiol* 140, 115–132.

Weiher, E., Freund, D., Bunton, T., Stefanski, A., Lee, T., and Bentivenga, S. (2011). Advances, challenges and a developing synthesis of ecological community assembly theory. *Philosophical Transactions of the Royal Society B: Biological Sciences* 366, 2403–2413.

Welcomme, R. L. (1988). *International introductions of inland aquatic species*. Food & Agriculture Org.

Wickham, H. (2009). Elegant graphics for data analysis. *Media* 35, 10–1007.

Winberg (1956). Rate of metabolism and food requirements of fishes. *Fish. Res. Bd. Canada Trans. Ser.* 433, 1–251.

Winger, P. D. (2004). Effect of environmental conditions on the natural activity rhythms and bottom trawl catchability of Atlantic cod (*Gadus morhua*) (Doctoral dissertation, Memorial University of Newfoundland).

Wood, A. l., Probert, P. K., Rowden, A. A., and Smith, A. M., (2012). Complex habitat generated by marine bryozoans: a review of its distribution, structure, diversity, threats and conservation. *Aquatic Conservation: Marine and Freshwater Ecosystems* 22, 547–563.

Wood, S. N. (2003). Thin-plate regression splines. *Journal of the Royal Statistical Society (B)* 65, 95–114.

Wood, S. N. (2004). Stable and efficient multiple smoothing parameter estimation for generalized additive models. *Journal of the American Statistical Association* 99, 673–686.

Wood, S. N. (2011). Fast stable restricted maximum likelihood and marginal likelihood estimation of semiparametric generalized linear models. *Journal of the Royal Statistical Society (B)* 73, 3–36.

Wood, S. N. (2017). *Generalized Additive Models: An Introduction with R*. 2nd ed. Chapman and Hall/CRC.

Wood, S. N., Pya, and S"afken, B. (2016). Smoothing parameter and model selection for general smooth models (with discussion). *Journal of the American Statistical Association* 111, 1548–1575.

Woods, S. N., and Weber, R. E. (1975). Effects of ambient PO on hemoglobin-oxygen affinity and red cell ATP concentrations in a belthic fish. *Respiration Physiology* 25, 259–267.

Wootton, H. F., Audzijonyte, A., and Morrongiello, J. (2021). Multigenerational exposure to warming and fishing causes recruitment collapse, but size diversity and periodic cooling can aid recovery. *Proceedings of the National Academy of Sciences* 118, e2100300118.

Wootton, H. F., Morrongiello, J. R., Schmitt, T., and Audzijonyte, A. (2022). Smaller adult fish size in warmer water is not explained by elevated metabolism. *Ecological Letters* 25, 1177–1188.

Wright, P. J., Talbot, C., and Thorpe, J. E. (1992). Otolith calcification in Atlantic salmon parr, Salmo salar L. and its relation to photoperiod and calcium metabolism. *Journal of Fish Biology*40, 779–790.

Wurster, C. M., and Patterson, W. P. (2003). Metabolic rate of late Holocene freshwater fish: evidence from δ13C values of otoliths. *Paleobiology* 29, 492–505.

Yamashita, Y., Tanaka, M., and Miller, J. M. (2001). Ecophysiology of juvenile flatfish in nursery grounds. *Journal of Sea Research* 45, 205–218.

Yang, T.-H., and Somero, G. N. (1993). Effects of feeding and food deprivation on oxygen consumption, muscle protein concentration and activities of energy metabolism enzymes in muscle and brain of shallow-living (Scorpaena guttata) and deep-living (Sebastolobus alascanus) scorpaenid fishes. *Journal of Experimental Biology* 181, 213–232.

Yasuda, T., Komeyama, K., Kato, K., and Mitsunaga, Y. (2012). Use of acceleration loggers in aquaculture to determine net-cage use and field metabolic rates in red sea bream *Pagrus major*. *Fisheries Science* 78, 229–235.

Zakhartsev, M. V, Wachter, B. De, Sartoris, F.-J., Pörtner, H.-O., and Blust, R. (2003). Thermal physiology of the common eelpout (Zoarces viviparus). *Journal of Comparative Physiology B* 173, 365–378.

Zeng, L.-Q., Fu, C., and Fu, S.-J. (2018). The effects of temperature and food availability on growth, flexibility in metabolic rates and their relationships in juvenile common carp. *Comparative Biochemistry and Physiology A Molecular and Integrative Physiology* 217, 26–34.

Zuur, A. F., Ieno, E. N., Walker, N. J., Saveliev, A. A., and Smith, G. M. (2009). "Mixed effects modelling for nested data," in *Mixed effects models and extensions in ecology with R* (Springer), 101–142.